# The Synthesis and Sensing Capabilities of New Amide, Urea and Nitrile Calix[4]arenes

**Benjamin Schazmann B.Sc. M.Sc.**

**Thesis submitted for the Degree of Doctor of Philosophy**

**Supervisor: Professor Dermot Diamond**

**Dublin City University** **August 2006**

## Declaration

I hereby certify that this material, which I now submit for assessment on the programme of study leading to the award of Doctor of Philosophy is entirely my own work and has not been taken from the work of others save and to the extent that such work has been cited and acknowledged within the text of my work.

**Signed:** Benjamin Schazmann
**Benjamin Schazmann**

**ID No.:** 51173166

**Date:** 25/9/2006

## Dedication

Ich widme diese Arbeit an meine lieben Großeltern Walter und Käthe Bühler und Robert und Lene Schazmann. Ich sehne mich nach Euch.

I dedicate this work to my dear grandparents Walter and Kate Bühler and Robert and Lene Schazmann. I miss you all.

## Acknowledgements

I want to thank Professor Dermot Diamond for allowing me great freedom in pursuing my research ideas and giving me an insight into the workings of academia.

Thanks also to all the members of the Adaptive Sensors Group and the staff in the School of Chemistry at DCU for support. In particular, thanks to Ambrose, Damien and Mary.

Thanks to all my fellow PhD students at DCU for collaboration and distraction, in particular to Sarah K., Eoin and Leon (and Damien) for the jamming sessions. Thank you Ciaran for the squash matches. Thank you Sarah B. and Martina for good conversation, craic and IT support.

I will not forget the good times shared: From Friday pints in the slipper to Surf 'n Turf in Galway.

I would like to acknowledge the support I take for granted from my mum Helgard, dad Walter and brothers Jakob and Balthasar as we grow up together. Thank you to my closest companion and friend, Trish. Will you marry me?

## Publications

- Benjamin Schazmann, Nameer Alhashimy and Dermot Diamond. *A Chloride Selective Calix[4]arene Optical Sensor Combining Urea Functionality With Pyrene Excimer Transduction.* **Journal of the American Chemical Society, full article, 2006, *128*, 8607-8614**. (Chapter 4)

- Benjamin Schazmann, Shane O'Malley, Kieran Nolan and Dermot Diamond. *Development of a calix[4]arene sensor for soft metals based on nitrile functionality: relating structural tuning to an Ion Selective Electrode response*. **Supramolecular Chemistry, 2006, 18, 515-522**. (Chapter 5)

- Martina O' Toole, King Tong Lau, Benjamin Schazmann, Roderick Shepherd, PavelN. Nesterenko, Brett Paull and Dermot Diamond. *Novel Integrated PEDD as a Miniaturized Photometric Detector in HPLC.* **The Analyst, 2006, 131, 938-943**.

- Benjamin Schazmann, Gillian McMahon, Kieran Nolan and Dermot Diamond. *Identification and recovery of an asymmetric calix[4]arene tetranitrile derivative using liquid chromatography and mass spectrometry.* **Supramolecular Chemistry, 2005, *17*, 393-399**. (Chapter 6)

- Benjamin Schazmann and Dermot Diamond. *Improved nitrate sensing using Ion Selective Electrodes based on urea-calixarene ionophores.* **New Journal of Chemistry, Submitted**. (Chapter 3)

- Shane O'Malley, Benjamin Schazmann, Dermot Diamond and Kieran Nolan. *The synthesis and analytical potential of a series of phthalocyanine calixarenes and their precursors.* **Chemical Communications, In preparation**.

## Conference contributions

- Ben Schazmann, Shane O'Malley, Kieran Nolan and Dermot Diamond. Using ISEs to monitor changing metal affinities of a series of calix[4]arene nitriles (poster). *11th International Conference on Electroanalysis, Bordeaux,* June 2006.

- Ben Schazmann and Dermot Diamond. Purification by LC-MS for organic chemists: A calixarene case study (poster). *Second World Congress on Synthetic Receptors, Salzburg,* 2005.

- Ben Schazmann and Dermot Diamond. The electrochemical properties of novel calixarene amide Supramolecular hosts (poster). *First World Congress on Synthetic Receptors, Lisbon,* 2003.

- Ben Schazmann and Dermot Diamond. Anion Binding Studies: Calix[4]arene Amide ISEs (poster). *Analytical Research Forum, Sunderland,* 2003.

## Abstract

The synthesis and host-guest chemistry of new structures based on neutral calix[4]arene supramolecular platforms is investigated. Hosts are substituted to varying degrees with functionalised appendages to form cavities for selectively complexing guests. Functional groups include ureas, amides and nitriles, targeting cations and anions as guest species. The main methods used for transducing complexation events are potentiometry and fluorescence. The various hosts and guests investigated attempt to reflect the versatility and ongoing evolution of state-of- the-art calixarene chemistry within the field of supramolecular chemistry. Throughout the thesis there is particular emphasis on relating host structural changes to changing analytical signal upon complexation with a particular guest. This is the link between the sensing signal and chemistry at a molecular level, the heart of every chemical sensor.

The main achievements of this work are a) the development of a urea based chloride selective host with ratiometric fluorescence transduction using pyrenes, b) nitrile based mercury(II) and silver(I) selective hosts using potentiometric transduction, c) the investigation of an amide-calix[4]arene bromide selective host based on potentiometric transduction, d) the developmet of urea-calix[4]arene ionophores showing potential for improved electrochemical aqueous nitrate sensing and e) a contribution to supramolecular synthesis techniques is made by way of a new semi-preparative liquid chromatographic method for the efficient isolation of pure target compounds.

# Abbreviations

LOD Limit Of Detection

ISE Ion Selective Electrode

LC Liquid Chromatography

LC-DAD Liquid Chromatography-Diode Array Detector

TLC Thin Layer Chromatography

MS Mass Spectrometry

DI-MS Direct Injection-Mass Spectrometry

ESI-MS Electrospray Ionisation-Mass Spectrometry

MALDI-MS Matrix-Assisted Laser Desorption/Ionization-Mass Spectrometry

HPLC High Performance Liquid Chromatography

SP-HPLC Semi Preparative High Performance Liquid Chromatography

DMSO Dimethyl Sulfoxide

DMF Dimethyl Formamide

PVC Poly Vinyl Chloride

NMR Nuclear Magnetic Resonance

H:G Host:Guest

UV-Vis UltraViolet-Visible

FIM Fixed Interference Method

SSM Separate Solutions Method

MPM Matched Potentials Method

PET Photoinduced Electron Transfer

EET Electronic Energy Transfer

ICT Internal Charge Transfer

# 1. Chapter 1 Theory and Background

## 1.1 Introduction

This thesis draws on the skills and techniques, spanning the fields of analytical, organic and sensor chemistry in particular. The discipline of chemistry itself is also transgressed by scientific applications such as molecular modelling, electronics, physics and engineering. This is necessary due to the interdisciplinary nature of chemical sensor conception as made clear below.

The milestones in the life of several illustrative examples of chemical sensors are discussed by way of direct experimental observations presented in this thesis. The life cycle of a chemical sensor include the following stages:

1. The conceptual design of a molecular host structure backed up by molecular modelling to predict interaction with a guest.
2. The synthesis, isolation and structural characterisation of the host.
3. Applying a technique(s) for evaluating the selectivity of the host for particular analytes amongst a series of guest species. The manifested selectivity is the single most important characteristic of a chemical sensor.
4. Optimisation: Performing molecular structural changes and/or changing other sensor components to tune the selectivity of the sensor.
5. The full evaluation of a chemical sensor including establishing the selectivity, reproducibility, response range and time, LOD, lifetime and robustness.
6. The incorporation of the above into a practical real life device for the analysis of samples containing target analyte and interferants.

7. The sensor device becomes redundant when an improved device is developed perhaps containing a more selective or sensitive molecular host or a different transduction mechanism. For this, the above steps are repeated.

The synthesis and host-guest chemistry of new structures based on neutral calix[4]arene supramolecular platforms is investigated. Hosts are substituted to varying degrees with functionalised appendages to form cavities for selectively complexing guests. Functional groups include ureas, amides and nitriles. Both cations and anions are analysed as guest species. The main approaches used for transducing complexation events are based on electrochemistry and spectroscopy. The wide variety of hosts and guests investigated reflects the versatility and ongoing evolution of state-of-the-art calixarene chemistry within the field of supramolecular chemistry. Anion complexation is a particularly important for research in this area, as it is less developed than cation sensing. With respect to cation sensing, calixarene chemistry has reached considerable maturity when it comes to group I and II cations, and in particular sodium selective hosts. Therefore, in attempting to work as closely to the current state of the art of cation sensor chemistry, another chapter focuses on transition metals and cations of continued environmental concern like mercury(II).

Regarding the modes of transduction reported, the main methods chosen in this thesis are potentiometric and optical methods, as they clearly have potential for real life applications and devices at a later stage. In potentiometry, the host structure must ideally be immobilised in some way (e.g within a PVC membrane). In addition, this technique recognises that many real life samples are aqueous based, such as in medicine (human body) and the environment. A potentiometric signal may be due to the host and additional characteristics of the sensor such as membrane polarity, ion exchange salts etc. This in turn often leads to selectivities dominated by solvent effects, not host

preorganisation, particularly when aqueous sample phases are involved. Optical transduction methods, most notably fluorescence based signals, are selective, sensitive and practical. They can be specifically assigned to a molecular event such as a particular complexation process and are perhaps less subject to other ambient parameters as described for potentiometric methods above.

Throughout the thesis there is particular emphasis on relating host structural changes to changing analytical signal upon complexation with a particular guest. This is the link between the sensing signal and chemistry at a molecular level, the heart of every chemical sensor. The link is investigated using techniques such as NMR, spectroscopy, electrochemistry and molecular modelling.

The main achievements of this work are a) the development of a urea based chloride selective host with ratiometric fluorescence transduction using a pyrene based calixarene, b) nitrile based calixarene derived mercury(II) and silver(I) selective hosts using potentiometric transduction and c) the discovery of an amide calixarene based bromide selective host also based on potentiometric transduction. A contribution to supramolecular synthesis techniques is made by way of a new semi-preparative Liquid Chromatographic method for the efficient isolation of pure target compounds.

Chapter 1 makes reference to the literature in the context of the work described in the thesis. The theory behind determining the selectivity pattern of a molecular host is discussed. Considerations leading to the choice of instrumental technique to determine selectivity are then revealed. Some background to the specific topics of the thesis is then described as well as unifying themes such as on general calixarene chemistry. Chapter 2 investigates the response of some amide-calix[4]arenes towards a series of cations and anions using potentiometry. Some response towards sodium and calcium is

seen. The same host later reveals bromide selectivity in ISEs configured for anion response. Chapter 3 is similar but describes the synthesis of some urea-calix[4]arenes and investigates their potentiometric response towards both anions and cations. A generally strong response towards anions is revealed in sharp contrast to very little cation interaction. One ionophore shows promising properties for nitrate analysis in water. A margin of nitrate selectivity over chloride (main interferant of nitrate in freshwater samples) 1 order of magnitude better than commercially available materials is achieved. In chapter 4 an alternative optical mode of transduction is investigated with a urea calix[4]arene. This chapter describes the synthesis of a urea based calix[4]arene host with fluorescent pyrene transduction. Dramatic and exclusive chloride selectivity is revealed in solution based studies. Chapter 5 describes the synthesis and mercury(II)/silver(I) selectivity of a number of nitrile functionalised calix[4]arenes. An initially overwhelming mercury(II) response is subdued by deliberate structural intervention as relayed by potentiometric results. Chapter 6 discusses the development of an instrumental LC-MS purification method for calix[4]arenes. This method is of particular use for complex mixtures of low target yield where high separation efficiency is required. It complements the existing organic tools used in calix[4]arene synthesis.

## *1.2 The Selectivity of a molecular host compound towards guests*

When the synthetic chemist designs and synthesises a novel host/receptor compound, the most important parameter to be ascertained is the selectivity of the Host towards a series of competing analytes or guests. This information must be known as it indicates whether the new host should be developed and improved further or if it shows suitable characteristics it can be incorporated directly into a real life sensor application, pollution extraction method, chromatographic material etc.

The two main types of selectivity are kinetic and thermodynamic selectivity[1]. Kinetic selectivity is difficult to achieve and measure for artificial host systems. This type of selectivity depends on which analyte is transformed the fastest for a given host, not which one is bound the strongest. These systems often lack rigidity and elaborate preorganisation as these parameters are more associated with thermodynamic control and would slow down the kinetics. Nature is more adept at producing such kinetically controlled systems than science at present. Enzymatic catalysis of biochemical reactions is an example of a mechanism reliant on kinetic selectivity.

The main focus of this thesis is on the more common thermodynamic based selectivity of complex formation processes, which is easier to rationalise and manipulate in artificial systems to the advantage of science. Key terms such as the 'lock and key' model, complementarity and preorganisation are associated with the study of thermodynamic selectivity. The interaction between a host and guest is first considered without and then with a solvent term, to highlight the strong influence the solvent has on the complexation process.

*Host-Guest complexation without considering the solvent*

When a host (H) and a particular guest (G) form a non-covalent bond(s) between them, a complex is formed and typically an equilibrium situation exists as shown in Equation 1.1:

$$H + G \rightleftharpoons HG \qquad \text{(Eqn 1.1)}$$

The thermodynamic equilibrium constant or binding constant, K, is a measure of how strong the interaction between H and G is (Equation 1.2):

$$K = \frac{[HG]}{[H][G]} \qquad \text{(Eqn 1.2)}$$

The selectivity for of one guest over another is then simply (Equation 1.3):

$$Selectivity = \frac{K(Guest1)}{K(Guest2)} \qquad \text{(Eqn 1.3)}$$

Another way of expressing complexation is in terms of the Gibbs free energy (ΔG), which is related to the binding constant (Equation 1.4):

$$\Delta G = -RT \ln K \qquad \text{(Eqn 1.4)}$$

The overall free energy has an enthalpy (ΔH) and an entropy (ΔS) term (Equation 1.5):

$$\Delta G = \Delta H - T\Delta S \qquad \text{(Eqn 1.5)}$$

When a host and guest form a complex, the host may have to rearrange to bind the guest and the guests may be held rigidly within a host cavity. There is generally a loss of entropy (disorder) for such an arrangement which lowers the free energy term and ΔS is negative. If the host cavity has the right dimensions for a particular guest, the rearrangement necessary (and so entropy loss) is minimised by the 'lock and key' or 'best fit' principle for the ideal guest.

In addition to the entropic term, there is a favourable enthalpy term (negative) due to the formation of non-covalent bonds within the complex. The enthalpic term may

compensate for the negative entropic term leading to an overall negative Gibbs free energy and spontaneous complexation.

The system will be selective (most negative ΔG and largest K) for the analyte species which causes the least amount of conformational rearrangement and 'strain' when a complex is formed as the least amount of entropy is lost. At the same time if the orientation and distance between the host and guest binding sites is ideal, suitable non-covalent bonds form between the host and guest giving the most negative enthalpic term and of course the most negative overall free energy. It is clear that the preorganisation of the host, cavity size complementarity and binding site orientation with the guest are critical for yielding a selective interaction.

*Host-Guest complexation with consideration for the solvent*

The introduction of solvent into the above system complicates matters somewhat. In all real life situations, solvent effects must be considered as they can have a large impact on selectivities observed and in the extreme can override favourable selectivities achieved by careful host design. When considering solvent effects, the equilibrium of complex formation is expressed as shown in Equation 1.6, clearly more complicated than the gas-phase or vacuum situation discussed above (equation 1.1):

$$\text{Host.Solvent1} + \text{Guest.Solvent2} \rightleftharpoons \text{Host.Guest} + \text{Solvent1} + \text{Solvent2} \qquad (1.6)$$

Solvent 1 and 2 may be the same solvent for example when the complexation process takes place in a single organic solvent. Solvent 1 and 2 may be different in a two phase system whereby complexation happens across an aqueous-organic divide for example.

Additional thermodynamic considerations are as follows. Before a host and guest can form complexation bonds, the bonds of each with the surrounding solvent must be broken. This is enthalpically unfavourable. However, as solvent molecules are released, they gain in disorder and so entropy is favourable. Ions in water for example tend to order solvent molecules with a reduction in entropy.

Summarising the energy changes of host-guest interactions with solvent considerations may be illustrated as in Figure 1.1.

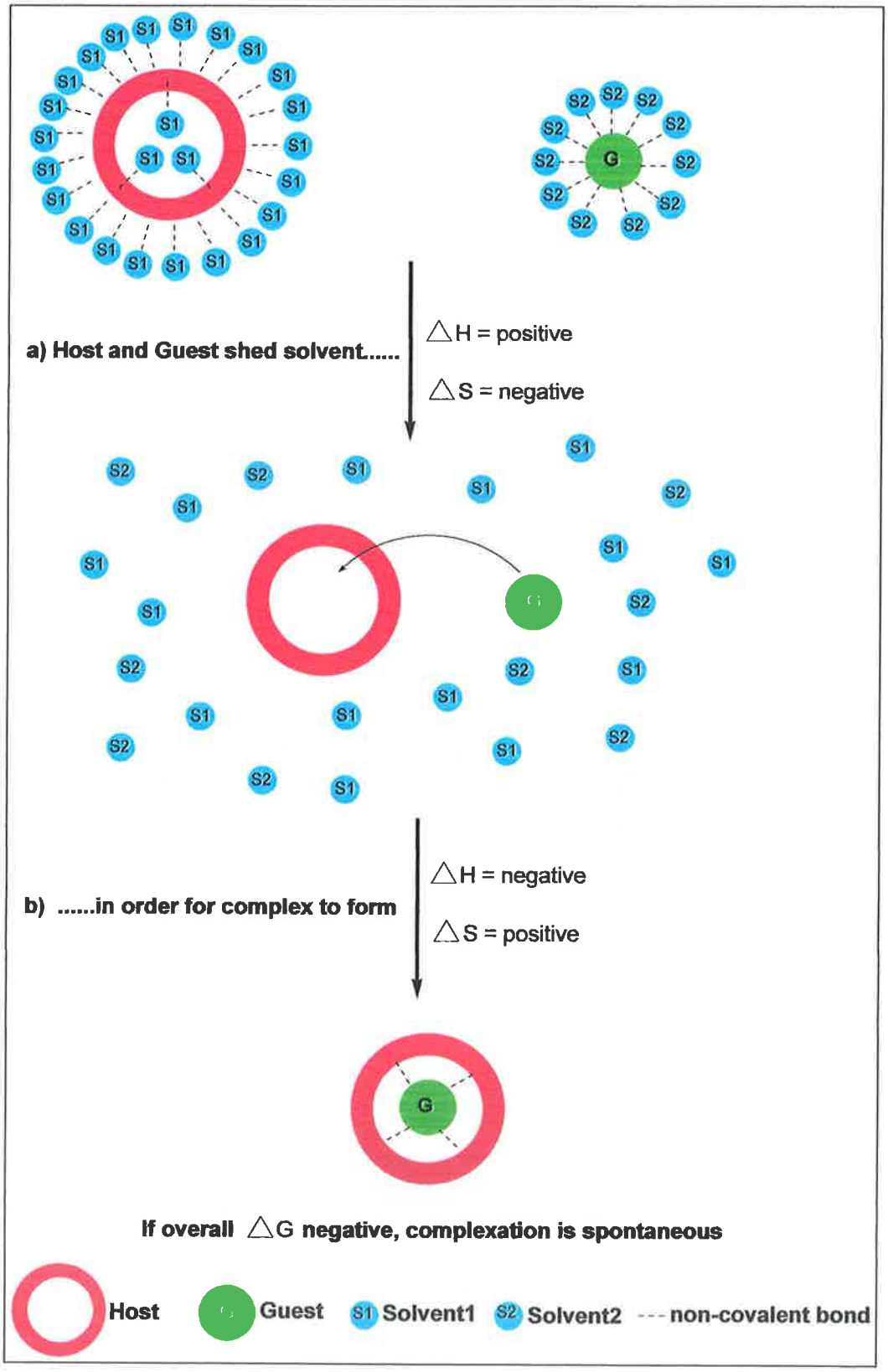


**Figure 1.1**. The main energy changes involved when complex formation takes place. This entails energy changes wrt a) solvents and b) host-guest complex formation. S1=S2 or S1≠S2. For negative Gibbs free energy ( $\Delta G = \Delta H - T\Delta S$ ), complexation is spontaneous.

If the net Gibbs free energy is negative for this process, spontaneous complexation can be expected and the host-guest equilibrium (Equation 1.6) is pushed to the right.

Where either host and/or guest are strongly solvated or the solvent interacts strongly with itself, the position of the complexation equilibrium in Equation 1.6 can be dramatically influenced. Two relevant scenarios to this thesis are considered. It must be remembered that these scenarios can exist in tandem. Solvents and a) electrostatic interactions and b) hydrogen bonding are considered.

a) For complexation via electrostatic interactions, the dielectric constant (Table 1.1) of the solvent must be considered. Solvents with high dielectric constants, and thereby very polar, interact with charged species (i.e. cations and anions) or partially charged species. This interaction is in direct *competition* with host-guest bonding and so can lower the overall free energy of complexation for some or all guests.

b) For complexation by hydrogen bonding, a solvent which acts as an electron pair acceptor or donor can also be in *competition* with complex formation as discussed above. The donor or acceptor number (Table 1.1) must be considered. A good donor solubilises cations better and an acceptor favours anions.

| Solvent | Dielectric Constant (ε) | Donor number | Acceptor number |
|---|---|---|---|
| **Water** | 80.1 | 33.0 | 54.8 |
| **DMSO** | 46.7 | 29.8 | 19.3 |
| **Acetonitrile** | 36.6 | 14.1 | 18.9 |
| **Methanol** | 33.0 | 19.0 | 41.5 |
| **Acetone** | 21.0 | 17.0 | 12.5 |
| **Hexane** | 1.9 | No donor atoms | 0.0 |

**Table 1.1**. The dielectric constants (ε) and donor/acceptor numbers of some common solvents[2].

Water is an extreme example of an excellent donor and acceptor solvent in addition to having a high dielectric constant. It is therefore clear that a technique, involving water as a solvent, that studies electrostatic or hydrogen bonding complex selectivities may reveal selectivity patterns that are largely, possibly exclusively, governed by solvent effects. This is called the Hofmeister series of response for anions ($SCN^- > NO_3^- > I^- > Br^- > Cl^- > F^- > SO_4^{2-}$) and cations ($Cs^+ > K^+ > Na^+ > Ca^{2+}$) in order of decreasing interaction with an apolar phase.

This effect can overshadow the host-guest complex formation process at times.

The ionic radii of the anions tested are shown in Table 1.2 and may be used to explain the selectivity order observed for a blank membrane based Ion Selective Electrode (ISE) as in chapter 2 for example, which contains no elements of preorganisation and an aqueous-organic divide that must be transgressed to observe complexation. This also sheds light on the origin of the Hofmeister series.

| Ion | Radius (pm) | $\Delta G_{DeHyd}$ (kJmol$^{-1}$)[a] |
|---|---|---|
| $I^-$ | 220 | +275 |
| $SCN^-$ | 213 | - |
| $ClO_3^-$ | 200 | +430 |
| $H_2PO_4^-$ | 200 | +465 |
| $HPO_4^{2-}$ | 200 | - |
| $Br^-$ | 196 | +315 |
| $NO_3^-$ | 189 | +300 |
| $Cl^-$ | 181 | +340 |
| $SO_4^{2-}$ | 230 | +1080 |
| $AcO^-$ | 162 | - |
| $F^-$ | 133 | +465 |
| $OH^-$ | 133 | - |

[a] $\Delta G_{DeHyd}$ = Dehydration energy

**Table 1.2.** Ionic radii and selected dehydration energies of anions tested shown in decreasing order of size[3] and corresponding increase in dehydration energy[2].

From Table 1.2 it can be seen that thiocyanate and iodide have the smallest charge to size ratio. The hydration sheath around these anions in water is therefore the smallest of all the anions listed and so is least costly in energy to shed. This effectively makes them the most liphophilic anions present, most likely to interact with lipophilic PVC ISE membranes. From table 1.2 this is apparent from the dehydration energies listed, which increase inversely with ionic radii.

For cations, the same correlation between ionic radii (or more specifically charge to surface area ratio) and dehydration energies applies as for anions, with the same consequence on the order of selectivity observed. From Table 1.3 it can be seen that caesium is the most liphophilic cation present, most likely to interact with lipophilic PVC ISE membranes, before any element of host preorganisation is even introduced to the sensing system.

| Ion | Radius (pm) | $\Delta G_{DeHyd}$ (kJmol$^{-1}$)[a] |
|---|---|---|
| $Cs^+$ | 170 | +250 |
| $NH_4^+$ | 148 | +285 |
| $K^+$ | 138 | +295 |
| $Na^+$ | 102 | +365 |
| $Ca^{2+}$ | 100 | +505 |
| $Mg^{2+}$ | 72 | - |
| $Li^+$ | 69 | +475 |

[a] $\Delta G_{DeHyd}$ = Dehydration energy

**Table 1.3.** Ionic radii of cations tested shown in decreasing order of size[3] and corresponding increase in dehydration energy[2].

## *1.3 The non-covalent bonds found in complexes*

The main types of non-covalent bonds found in complexes are given below:

- Electrostatic (ion-ion, ion-dipole and dipole-dipole)
- Hydrogen bonding
- Aromatic stacking interactions ($\pi$-$\pi$)
- Van der Waals forces
- Hydrophobic or solvatophobic effects

The two most frequently encountered complex types in this thesis are ion-dipole electrostatic interactions and hydrogen bonding. These are illustrated in Figure 1.2.


**Figure 1.2.** Examples of non-covalent bonds found in complexes. Hydrogen bond (left) and electrostatic ion-dipole bond (right).

For the current work, amide and urea functional groups form hydrogen bonds with anions. Electrostatic bonds are encountered when amide and urea carbonyls as well as nitriles interact with cations.

It must be borne in mind that non-covalent bonds are relatively weak compared to covalent bonds. Typical bond energies are 5-20kJmol$^{-1}$ and 200-800kJmol$^{-1}$ respectively. The magnitude of non-covalent bond energies (number of bonds and type) are directly relevant to the enthalpy term (negative $\Delta H$) in equation 1.6 and so contribute to an overall negative Gibbs free energy ($\Delta G$) of complex formation. Although far less energetic than covalent bonds, they have the key feature that they are more reversible, an important factor for a sensing system.

## 1.4 The common experimental techniques used for determining Selectivity

Binding constants of a host (and hence selectivities) can be determined in a number of standard ways. Sometimes selectivity is calculated directly without first calculating thermodynamic data (equations 1.1 and 1.2). The various methods are described in detail in numerous texts[2,4,5]. The main techniques found are outlined below, with particular emphasis on potentiometric ISE techniques as these were most commonly used in this thesis. The main criteria for making a selection amongst all commonly available techniques are discussed later in chapter 1.5.

*Nuclear Magnetic Resonance (NMR) methods.*

This is perhaps the most common technique used by organic chemists for evaluation of new host compounds. As NMR is a commonly used structural characterisation tool, it can be easily adapted to yield thermodynamic information on complexation events. If there are particular magnetic nuclei (particularly protons $^{1}H$) within a host cavity for

example, that are sensitive to a complexation event, the chemical shift change thereof can be monitored for varying ratios of H:G. One condition is that the H-G equilibria must be fast on an NMR timescale so that an *average* signal of the free and complexed species present is observed. Typically the host concentration is fixed and increasing amounts of guest are added into the deuterated NMR solvent. The changes in chemical shift values ($\Delta\delta$) of selected nuclei (typically proton nuclei) can be plotted as a function of the H:G ratio present. This method and variations thereof provide three main types of data. Firstly, the mode of complexation between a host and guest is revealed by examining *which* of the host's nuclei has undergone a chemical shift. This gives qualitative conformational data on how host and guest interact. Secondly, binding constants (hence selectivity) can be determined in this way for a sequence of analytes. Finally, the complex stoichiometry of H:G can be deduced. The NMR technique is still the single most commonly used technique to date for calixarene complex formation studies, used on their own or complementing another method.

*UV-Vis and fluorescence spectroscopy.*

When either the host or guest possess chromophores which show a change in emission or absorbance characteristics with varying H:G ratios, data can be obtained. Absorbance or emission intensities or ratios of multiple wavelength intensities are plotted against guest concentration for example, and by applying suitable equations, binding constants can be obtained. Furthermore, stoichiometric data can also be obtained with these techniques. Standard laboratory instrumentation is typically used. This method is being used increasingly for calixarene complexation studies where a chromophore transducer is incorporated into the supramolecular structure of the host.

This is as a direct result of the gain in popularity of optical sensors. The topic is introduced further in chapter 1.7 and expanded on in chapter 4.

*Calorimetric methods.*

Once again for this technique, a parameter is plotted as a function of added host or guest. A complexation reaction between a host and guest is conducted in a calorimeter. The heat change for the combination of a known concentration of host and guest in this controlled environment is related to the thermodynamic binding constant K[6-8]. Calorimetric methods are not commonly used for calixarene complexation studies[9-11].

*Extraction methods: Liquid-Liquid partitioning.*

This is one of the oldest techniques for determining complex formation constants between a host and guest. In general, this technique investigates the ability of a host to transport particular guests between hydrophobic and hydrophilic phases quantitatively. An example illustrating this technique is the work of Cram and co-workers, amongst the pioneers of supramolecular chemistry. Cram calculated complex formation constants of some crown ether compounds with group I metals[12]. This entailed an aqueous phase in contact with an organic phase under controlled standard conditions. The aqueous phase contained a metal picrate salt, whilst the organic phase contained the host. Driven by the affinity of the crown ethers for particular metals, the host could extract certain cations into the organic phase, each cation retaining its picrate counterion which has an intense yellow colour with an absorbance at around 380nm. By monitoring this absorbance in both layers, the *distribution* of cations between the two phases could be monitored. The extraction ability of each host could thereby be related to the thermodynamic binding constant. As usual, the ratios of these constants for a series of

cations yielded selectivity data (Equation 1.3). No specialised equipment is needed to use this technique. Liquid-Liquid partitioning is still used by a number of researchers investigating calixarene complexation[13-19]. The approach can use either thermodynamic or kinetic models.

*Potentiometric methods.*

Two broad approaches are discussed in the area of potentiometric methods:

a) Selectivity without thermodynamic data (equation 1.3).

b) Potentiometry for determining thermodynamic data (equation 1.2).

a) Selectivity without thermodynamic data.

This was the most commonly used method throughout the thesis for the determination of selectivity values[20]. The advantages of this method over the others are highlighted later.

An Ion Selective Electrode (ISE) potentiometric cell consists of a working electrode, a reference electrode and an aqueous solution containing ions of interest[21]. Within this cell there are several interfacial potentials such as between filling solutions and membranes and membranes and sample solution. Most of these potentials remain constant at all times except for the interface potential between the working electrode membrane surface and the sample solution. Due to ion exchange salts and/or ionophore hosts in the working electrode membrane there can be an uneven partitioning of analyte ions between the sample and the membrane surface. It is this partitioning and degree of partitioning that causes a change in potential to be observed for varying amounts of analyte ion in the sample. The potential of such a cell is expressed in terms of the Nernst equation (Equation 1.7):

$$E = CONSTANT + \frac{RT}{nF} \ln a_i \qquad \text{(Eqn 1.7)}$$

E is the observed potential. The 'constant' term is for all the potentials that remain unchanged at the various interfaces within the potentiometric cell. R is the gas constant, T is temperature, F is the Faraday constant and n is the charge of the analyte ion I (e.g. +1 for a monovalent cation). The analyte activity (concentration related) is $a_I$. For a potentiometric titration, if potential is plotted against log $a_I$, the theoretical slope of the linear portion of the plots will be 59.1mV and 29.6 mV for a monovalent and divalent ion respectively at a temperature of 298K. The sign of the slope is positive for cations and negative for anions. If such values (or close to) are observed, the response of the ISE is described as Nernstian. For solutions of equal activity but each containing a different ionic species, the cell potential is typically affected the most by the primary ion of interest (greatest potential change with activity). In practice, interferants will also contribute to observed potentials.

The extent of interference between primary ion I and interferant J is formally expressed as the selectivity coefficient, $K_{I,J}^{pot}$, or log function thereof. The Nicolskii equation forms the basis of calculating this coefficient (Equation 1.8).

$$E = \text{constant} + RT/nF \ln[a_I + K_{I,J}^{pot} \, a_J^{z_I/z_J}] \qquad \text{(Eqn 1.8)}$$

The charge of the primary ion and interferant are given by $z_I$ and $z_J$ respectively. There are several methods based on the Nicolskii equation to give selectivity coefficients for a sequence of ions[20,22]. The main methods are the Fixed Interference method (FIM), the

Separate solutions Method (SSM) and the Matched Potential Method (MPM). The SSM method is commonly used throughout this thesis. It is based on establishing potential values in separate aqueous solutions, each containing the same activity of a different ion. By taking the difference of pairs of potentials into account (primary ion I and each interferant, J, in turn) selectivity values are determined, according to Equation 1.9.

$$\text{Log } K_{IJ}^{pot} = \frac{z_I F(E_J - E_I)}{2.303RT} + \log\left(\frac{a_I}{a_J^{z_I/z_J}}\right) \qquad \text{(Eqn 1.9)}$$

$E_J$ and $E_I$ are the potential values for the interferant and primary ion respectively. The activities of the separate solutions are usually the same ($a_I$=$a_J$). These potentiometric methods for determining selectivities, unlike the other methods described, do not yield thermodynamic data. Binding constants for individual ions cannot be determined in this way, only ratios of such constants (Equation 1.3). The selectivity values obtained by this method are responses relative to a primary ion response and so represent a more qualitative approach. If thermodynamic data is required, modified potentiometric approaches can be used.

b) Potentiometry for determining thermodynamic data.

There are solvent polymeric membrane techniques, which are used to calculated stability constants, but having some similarities to classical potentiometry and were developed by the same research groups[23,24]. They utilise similar membranes to potentiometric ISEs, their response is based on Nernstian theory but signal transduction is optical. They rely on bulk phenomena, whereby an analyte ion distributes itself

within the bulk of a thin membrane (compared to potentiometric ISEs which operate by surface phenomena). These membranes typically contain a normal ionophore in addition to a $H^+$ sensitive chromoionophore, active in the visible portion of the spectrum (400-800nm). The degree of protonation or deprotonation of the chromoionophore dictates its absorbance characteristics and is related to the presence or absence of analyte ion within the membrane, allowing thermodynamic data to be deduced indirectly by spectrophotometric means.

The above optical methods were soon extended to the general ISE community, who had the equipment and knowledge to pursue potentiometric methods. A method using PVC type membranes using the so called segmented sandwich method has been described[25]. This crucially did not require the use of additional pH sensitive ionophores or chromoionophores (no sample buffering) and thereby simplified the process of attaining thermodynamic data for a given ionophore. First, potentials of a normal ISE containing the ionophore and ion exchange salt were measured in a known concentration of a single target analyte. The procedure was repeated using an identical electrode, however omitting the host ionophore from the membrane. Forming a sandwich of these two membranes and repeating the measurement yielded a change in potential, which was related mathematically to the complex formation constant between the ionophore and the analyte under investigation by Equation 1.10.

$$\beta_{IL_n} = \left( L_T - \frac{nR_T}{z_I} \right)^{-n} \exp\left( \frac{E_M z_I F}{RT} \right) \qquad \text{(Eqn 1.10)}$$

$\beta$ is the stability constant for ion I, L is the ionophore, n is the complex stoichiometry, $R_T$ is the concentration of the lipophilic ionic site additives, $L_T$ is the total concentration

of ionophore in the membrane segment and $E_M$ is the change in membrane potential between the individual membrane potentials (should be the same ±2mV) and the membrane sandwich.

The frequency of potentiometric methods for calixarene complexation studies appearing in the literature is perhaps second only to NMR methods with several reviews available on the subject[26-28].

## 1.5 Choosing a method to determine the Selectivity of a molecular host

When a new molecular receptor is synthesised, the proposed structure must first be verified. In addition to careful design, possibly molecular modelling and a fastidious synthesis, the analyte binding properties of the new host must be determined and verified by experimental means. The true selectivity of any host can be a surprising result quite different from the theory. This is due to the complex thermodynamic contributions, some already outlined, which govern selectivity. In choosing methods for determining selectivity, the first question is whether the selectivity data needed is purely for academic interest and perhaps further structural *tuning* OR whether the scientist is intent on going further and developing real life devices such as a functioning sensor, and makes this the primary goal of all research from the outset.

Most real life applications involve aqueous samples, such as in biological (e.g. the human body) or environmental applications (rivers, ocean, waste water pollution etc.).

The vast majority of techniques for screening synthetic hosts for selectivity utilise an organic phase to solubilise a host. This is particularly essential for highly organic neutral receptors including calixarenes. Any technique that has the potential to be extended for use in real life sensors or probes must typically involve an additional

aqueous component. For example liquid-liquid partitioning and Ion Selective membrane techniques explicitly contain aqueous components. Of these methods, only potentiometric ISEs can measure inorganic salts in water without further pre-treatment. Bulk optodes employing ion selective membranes are often pH sensitive meaning that samples must be carefully buffered prior to measurement[24]. The salts extracted from an aqueous layer by solvent extraction technique usually have artificially inserted chromophoric counterions such as picrates or chromates and therefore cannot be considered real life samples.

The choice of instrumentation, materials and skills required for each technique must be considered. The NMR, spectrophotometric, solvent extraction, ion selective bulk techniques for example are performed on standard and common laboratory instruments, which serve other diverse departmental functions such as structural characterisation and analytical procedures besides being used for thermodynamic analysis. There are usually numerous scientists well versed in their use and the relevant solvents are usually stock items. For ISEs, the construction of electrodes, preparation of membranes and conditioning routines can take several days. However, for development into commercial devices, ISEs can be readily made reproducible, mass produced, miniaturised and cheap and so lend themselves to commercialisation[21].

The range of response and associated Limit off Detection (LOD) is a factor to consider. NMR, solvent extraction and calorimetric techniques require mM or greater quantities of host and guest for characterisation. This is of little consequence academically, provided enough material is available. ISE and spectrophotometric techniques can detect analyte species to nM levels or lower[29-34]. In addition to requiring very small amounts of host and guest, these techniques can be used to measure environmentally relevant analytes for example, where legislative LOD specifications are often very low.

Regarding the nature of the sample, some techniques require pH buffering or the analyte ion contains an 'artificial' counterion such as when NMR techniques are used (Table 1.4). Such sample pre-treatment or perturbation can be prohibitive in terms of real life measurements using these techniques at a later stage.

Other considerations for choosing a selectivity technique include reversibility, sample recovery and toxicity (sample perturbation). NMR, spectroscopic, calorimetric, solvent extraction and ion selective bulk optode methods are techniques where the complexation of host and guest is not readily reversed. The host species is not easily uncomplexed and recovered. In the strict sense, a sensor used for continuous monitoring must show a reversible response[35]. Also, in the event of critically small sample availability this may be an important consideration. The complexation in ion selective membrane techniques is readily reversible, an essential characteristic for continuous and repeated sensing. The recovery of host from membrane cocktails is not practical however. However <10mg of host is usually required for full characterisation by these methods. The reversible nature of ion selective membrane techniques and the fact that the leaching of potentially toxic materials into the bulk of the sample phase is usually considered negligible is a particularly important consideration for human/biological applications.

Table 1.4 summarises the main considerations for choosing a technique for evaluation of host selectivity, outlining advantages and disadvantages and gives the author's opinion on whether they have potential to be developed into real life devices such as sensors and probes.

| Attribute | NMR | X-Ray Crystallography | UV-Vis and fluorescence spectroscopy | Liquid partitioning | Ion Selective Bulk optodes | Calorimetric titration | Potentiometric ISEs |
|---|---|---|---|---|---|---|---|
| **Materials and expertise** | Standard | Specialist | Standard | Standard | Specialist | Specialist | Specialist |
| **Necessary aqueous sample phase** | No | No | No | Yes | Yes | No | Yes |
| **Approx. LOD of analytes** | mM | Solid phase | ≤μM | mM | μM | mM | ≤μM |
| **Reversible** | No | Yes | No | No | Yes | No | Yes |
| **Stoichiometric data** | Yes | Yes | Yes | Yes | No | Yes | No |
| **Complexation mode detail[a]** | Yes | Yes | No | No | No | No | No |
| **'same day' analysis** | Yes | Yes | Yes | Yes | Yes | Yes | No |
| **Sample altering[b]** | Yes | No | Yes | Yes | Yes | Yes | No |
| **Sample pre-treatment[c]** | Yes | No | Yes | Yes | Yes | No | Yes |
| **Device potential[d]** | No | No | No | No | No | No | Yes |

[a]Method reveals some detail on the geometric arrangement of host with guest in for the complex
[b]Sample perturbation by significant leaching or mixing of materials into the sample
[c]Sample contains artificial counterions and /or requires pH buffering
[d]The development of real life/commercial devices requiring relatively little development

**Table 1.4**. Typical attributes of the various standard methods for determining thermodynamic and selectivity data of hosts for ionic guests.

A variety of calixarenes were tested for response with a series of cations and anions throughout this thesis. Potentiometric ISEs were the main tool used for determining selectivity information for each host. Chapter 4 also describes a very successful spectroscopic approach.

Some interesting selectivity patterns were observed, however relying on a sole technique for evaluating a host comes with a note of caution and wherever possible, the use of at least one additional complimentary technique is recommended. In the context of this thesis, these additional techniques were used to backup the findings of potentiometric studies. For example for anion host calixarene **4-3**, ISEs did not reveal a significant deviation from a Hofmeister or 'blank' order of response in the context of a series of anions as described in chapter 3.3.6. However, when an optical fluorescence based mode of transduction was used for the same host, unambiguous chloride selectivity was revealed. Crucially, the latter method was carried out in an organic solvent system and did not entail an aqueous phase or layer. In this way, the optical method was not subject to the solvent effects (chapter 1.2) to the same degree as aqueous-organic based ISE methods. This allowed the preorganised structure of the host to dictate selectivity and so 'useable' results were obtained. If only ISEs had been used to evaluate this host, it may have been disregarded and its development ceased due to the lack of a favourable response.

In conclusion, the use of more than one transduction mode is therefore recommended when investigating a host-guest complex system for the first time. It is suggested that one contain an aqueous component and the other does not. Success in one or both approaches can serve as the impetus to develop the system further according to required specifications.

## 1.6 Correlating ISE data to molecular structure

The earliest Ion Selective Electrodes (ISEs) were based on ion exchange salts as a means of providing ion partitioning between an organic phase and an aqueous phase[21]. The typical order of selectivity observed for such devices (and other analytical methods with an aqueous-organic divide) follows the Hofmeister order of response[36].

The best way to induce deviation from these orders of response is to additionally incorporate an ionophore into the ISE membranes.

To illustrate how ISEs can be used to evaluate a molecular receptor, the well known tetraester calix[4]arene was used as an example[28]. This neutral receptor provides a lower rim cavity with four ester carbonyls and four phenoxy oxygens. The cavity size, geometry and hard oxygen donors provide for good sodium selectivity amongst a series of group I and II metal cations via electrostatic ion-dipole interaction.

To demonstrate that the sodium selectivity was due to the calixarene structure and not some other intrinsic ISE characteristic, two ISE membrane types were prepared. One membrane contained PVC, plasticizer, an ion exchange salt and calix[4]arene ionophore. Another identical membrane was prepared, except that the calix[4]arene ionophore was omitted. This membrane was referred to as the blank. The two types of membrane were incorporated into otherwise identical ISE electrodes and tested in parallel, by noting the change in potential when the ISEs are immersed in log a = -2.0 aqueous solutions of potassium, sodium and lithium. Potassium and lithium are known to be the main interferants of the sodium ionophore[28]. Figure 1.3 graphically compares the response of the two ISEs.

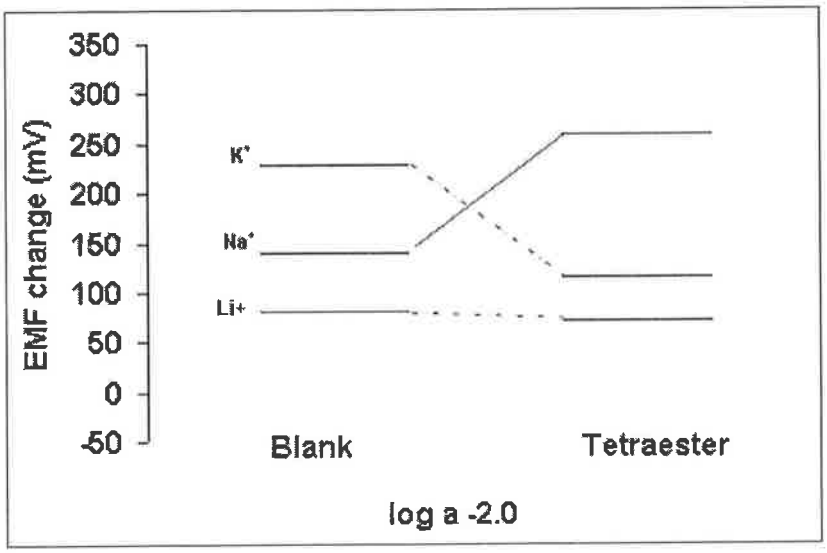


**Figure 1.3**. The potential changes of an ISE with (tetraester calix[4]arene) and without ionophore (Blank) exposed to a log a -2.0 aqueous separate solutions of the specified cation.

By comparing the tetraester response to the blank we ascertain valuable information *specifically* about the tetraester ionophore, as well as the overall response characteristics of the ISEs. It is clear that the sodium response is dramatically enhanced by the ionophore. There is a relative suppression of the potassium response and lithium remains un-changed compared to sodium. The ionophore cavity appears to be compatible with sodium. The larger potassium ion shows a greatly suppressed response probably by a size exclusion phenomenon. This was indeed verified by molecular models and other experimentation[37]. Lithium, being smaller than sodium, also fits within the calixarene cavity, but is too small to effectively form electrostatic bonds with all of the available cavity oxygens and so is not the preferred analyte. Furthermore lithium is the most hydrated of the cations, further reducing the net energetic favourability of a host-guest interaction.

Overall, the calix[4]arene has provided the energetic driving force, through host-guest complexation, to yield a strong deviation from Hofmeister selectivity *order*, whereby sodium replaces potassium as the primary ion.

In making a comparison with a blank membrane, we distinguish between the overall device properties and the 'active' ionophore. We can thereby directly correlate a readily obtained analytical result with the structural characteristics of a molecular receptor. This is useful to guide the organic chemist further in optimising receptor design.

*Potential change versus absolute potentials when comparing to a blank.*

To obtain the potential change values presented in Figure 1.3, the potentials of the electrodes are first noted in de-ionised water. The *change* in potential for the specified activities of analytes was then noted. Potential change values can be beneficial compared to the use of *absolute* potential values when two membranes with different compositions are compared as in Figure 1.3. This approach recognises composition differences as well as the different effects of preconditioning on the two membranes. Any differences between the two membranes can safely be attributed to ionophore effects alone, the purpose of the exercise.

Table 1.5 shows the selectivity values obtained by the Separate Solutions Method (SSM) for the tetraester, based on potential change values, recorded in triplicate. It is clear that the values obtained agree well with previously determined literature values, which use absolute potentials[38].

| Result | $Li^+$ | $K^+$ | $Na^+$ |
|---|---|---|---|
| **Experimental log $K^{pot}_{Na^+,J}$** | -3.38±0.01 | -2.6±-0.04 | 0 |
| **Literature[38] log $K^{pot}_{Na^+,J}$** | -3.4 | -2.7 | 0 |
| Note: I is the primary ion $Na^+$ and J is the interferant specified. The Separate Solutions Method (SSM) was used where $\log a_I = \log a_J = -2.0$. Reproducibility based on three ISEs. | | | |

**Table 1.5.** Selectivity Coefficients, log $K^{pot}_{Na^+,J}$ for sodium ionophore tetraester calix[4]arene and the two main interferants, calculated using the Separate Solutions Method (SSM).

*A note on the use of Nernstian equations*

It must be acknowledged that when an ionophore is tested for its selectivity pattern, not all ions respond in a Nernstian fashion. Of course this scenario was also observed in this thesis at times. However, Nernstian slopes for all ions tested is a prerequisite for accurately applying Nernstian based methods for calculating selectivity coefficients[22]. In particular some heavily discriminated interferants, in practice, may yield substantially sub-Nernstian responses. In such cases Nernstian based equations actually overestimate the interference of such ions and may be interpreted as 'worst case scenarios'. In these cases a selectivity coefficient, log $K^{pot}_{I,J}$, may for example be stated as <-3.0 instead of -3.0 by some researchers, to denote such a limiting value[20]. A much less commonly encountered scenario is where super-Nernstian slopes are obtained, usually due a strong primary ion response. Nernstian based selectivity values will underestimate the primary ion response, thereby again overestimating the response of interferants. This again leads to a 'worst case scenario' or limiting situation. It is perhaps reassuring that selectivity values obtained by classical Nernstian methods tend to be conservative and rarely exaggerate the performance of an ionophore[22].

Concerning the presentation of ISE selectivities, some literature recommendations for scenarios where non-Nernstian slopes are obtained include presenting the ISE titration curves themselves for the different ions tested and so comparisons can be made[39]. Figure 1.3, comparing responses of different ISEs to a series of ions, is a derivative of this approach as directly observed potential values are used for depicting membrane preferences. This serves as a good initial means to illustrate the selectivity of a new molecular receptor.

In all cases in this thesis, the approaches highlighted complement any formal selectivity coefficient data presented, as determined by the Separate Solutions Method (SSM).

## 1.7 Optical transduction and fluorescence introduced

The process of anion and cation recognition by calixarenes was most commonly monitored by $^{1}$H NMR titrations or Ion Selective Electrode (ISE) studies, as is apparent from the literature. NMR spectroscopy typically provides important fundamental information about ion binding selectivity, stoichiometry and which molecular sites are involved in bonding, which is critical in understanding the host-guest interplay. In ISEs, the selectivity information generally mirrors that of NMR, although differences can occur, as NMR experiments are usually carried out in one particular solvent, whereas ISEs involve partitioning between a sample (aqueous) phase and the sensor membrane (PVC-organic) phase. In this way, solvent effects have a greater impact on the final selectivity order observed.

ISEs are useful in practice as, unlike NMR spectroscopy, the technique is directly tangible with real life device applications. but typically only detect target species to the micro molar level[40]. Detection limits of ISEs have recently improved using well established host compounds, but invariably mean increased complexity for practical

devices[29-32]. $^{1}H$ NMR techniques suffer from poor sensitivity, requiring solution concentrations of about $10^{-2}$-$10^{-3}$M and can be subject to peak overlap and broadening upon complexation, detracting from the usefulness of the signal obtained[41].

The placing of molecular components, which absorb and/or emit electromagnetic radiation (chromophores) in the proximity of the guest recognition site to yield an optical sensing compound, is an interesting strategy for host design, opening the way for alternative means of determining selectivity of a host. Today, optical transduction is at the cutting edge of guest recognition tools. NMR spectroscopy often serves to complement and confirm binding mechanism discerned optically.

The binding of a guest causes an electronic, energy or conformational change, which is signaled to the analyst optically. More specifically, sensors involving fluorescence changes can draw on several advantages. This area has received much attention in the literature[33,35,42-48]. Such sensors can be simple in design with an excitation source and emission recorder as core features. They are mechanically relatively simple, with the advantages of not requiring reference elements and not requiring filling solutions as ISEs often do[35]. In analytical terms they can show very high sensitivity of detection often below micromolar levels down to a single molecule[33,34]. Response times are typically extremely fast and they can be on-off switchable with huge potential in sensors and IT technologies. Where visible emission occurs the analyst has direct communication with the molecule by the naked eye.

Chapter 4 expands on fluorescence techniques and optical transduction. Chapter 4 also details the application of a fluorescent ratiometric system for the development of an anion selective host. This host combines preorganised complexing functional groups with a pyrene monomer-excimer signaling mechanism.

## 1.8 Specific challenges of anion complexation

Anion recognition is a growing field of research and there are good introductory texts and reviews available on the subject[36,49-55]. This field of research has not yet mirrored the success achieved by cation sensing. There are several reasons why the design of anion receptors is challenging[56].

Cations are smaller than isoelectronic anions. Examples are shown in Table 1.6. The larger analytes require larger host cavities, which may represent a synthetic challenge if these larger cavities are to retain a rigid preorganised character, essential for generating selective responses.

| | | | |
|---|---|---|---|
| $Cs^+$ | 1.69 Å | $F^-$ | 1.36 Å |
| $K^+$ | 1.33 Å | $Cl^-$ | 1.81 Å |
| $Na^+$ | 0.95 Å | $I^-$ | 2.16 Å |

**Table 1.6**. The ionic radii of selected pairs of isoelectronic cation and anion pairs.

One of the smallest common anions, fluoride, has an ionic radius of 1.36 Å, similar to potassium (one of the larger common cations).

Anions also have a wide range of geometries such as the spherical halogens, linear, trigonal and tetrahedral. The most common anion geometries together with examples are shown graphically in Figure 1.4. Binding sites of both host and guest are considered divergent and convergent respectively and often highly directional in nature in the case of neutral hosts[1]. The deliberate placing of directional functional groups within a host can be an effective means of discriminating between anions of different geometries. The large variety of anion geometries may therefore be exploited to compensate for the lesser size variation of anions in general and their relatively large sizes compared to cations, in order to achieve selectivity by appropriate host preorganisation.

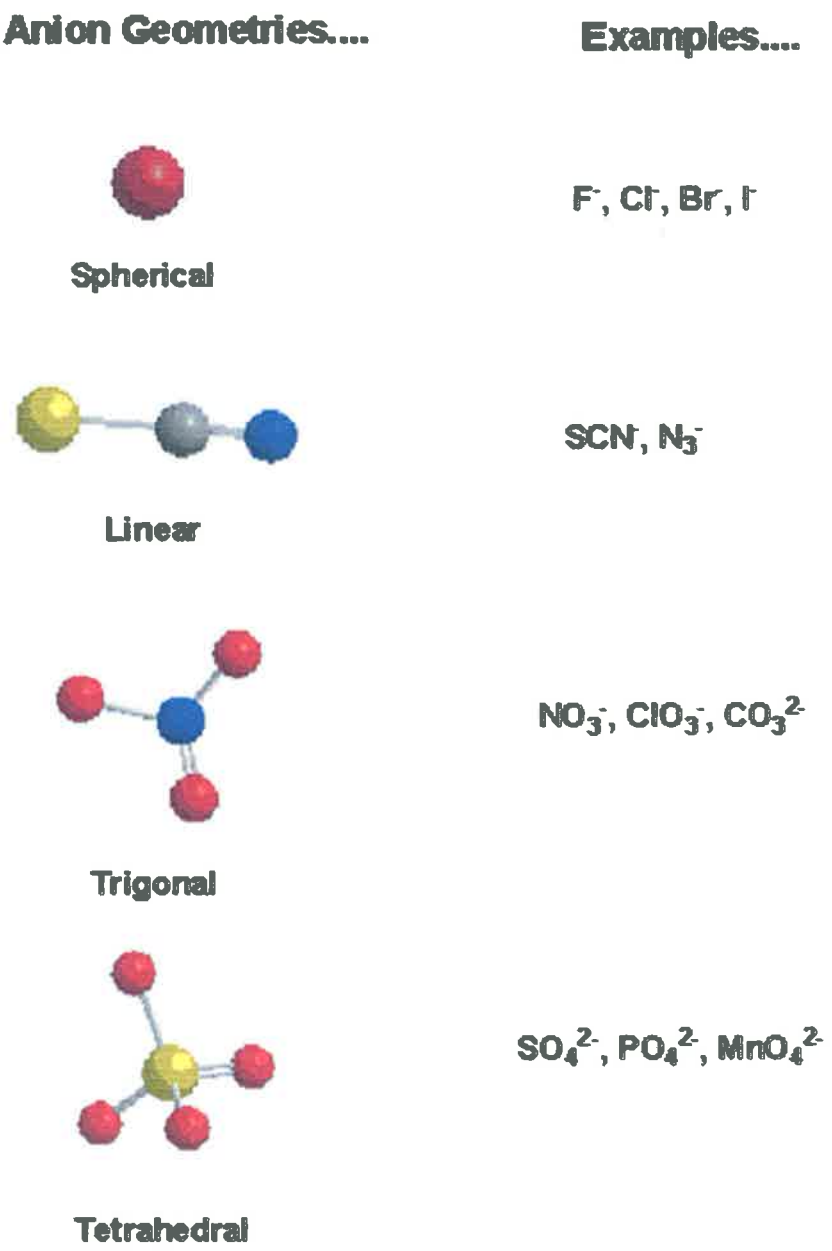


**Figure 1.4.** Common anion geometries encountered with examples, showing the structural varieties found.

Anions can lose their charge at low pH values due to protonation making recognition difficult.

Anions must compete with the surrounding solvent for the binding site that a host provides. Anions have higher energies of solvation compared to similarly sized cations and this is in competition with complex formation. For example $\Delta H_{hydration}$ ($F^-$) = -465kJmol$^{-1}$ and $\Delta H_{hydration}$ ($K^+$) = -295kJmol$^{-}$1.

Anions are typically saturated co-ordinatively (as they are negatively charged) and so typically form complexes via hydrogen bonding or van der Waal interactions. They usually cannot benefit from the stronger electrostatic ion-dipole bonds synonymous with cation complexation.

## 1.9 Anion complexation and (thio)urea functional groups

There are three broad functionality types for providing complexation points towards anions within the host[49]. These are electrostatic type interactions, metal or Lewis acid centred types and neutral H-bonding functional groups. The charged type, forming electrostatic interactions with anions, have perhaps been investigated the longest. Host structures are often macrocycles containing quarternary ammonium ions within the structure. The chief disadvantage in such cases is the general non-directional orientation of the host's charge. This generally does not lead to good selectivity characteristics. One approach to overcome this has been to incorporate charged quarternary ammonium groups into closed cage like structures as shown in Figure 1.5[57,58]. In this way, the selectivity is dictated by the physical constriction of the cage dimensions.

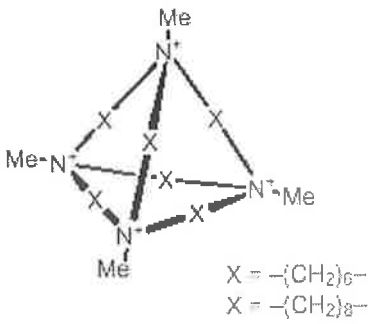


**Figure 1.5**. Cage type anion hosts with charged ammonium functional groups.

The smaller cage in Figure 1.5 displays selectivity for iodide whilst the larger cage is selective towards larger *p*-nitrophenolates.

The focus of this thesis however, is on the chemistry of several neutral anion hosts providing directional H-bonds.

Hydrogen bonding is a complex forming mechanism often chosen by nature. For example sulfate and phosphate proteins are vital receptors for active transport systems in cells and specific binding takes place invariably through hydrogen bonding[59,60]. Adding hydrogen bond donor groups to synthetic neutral organic hosts has also been a key tool in providing recognition for specific anion geometries[36,53]. The urea and thiourea functional groups provide such effective and *directional* H-bonds for anion recognition.

There are many examples of hosts that incorporate one or more urea group for anion binding, offering diverse binding geometries. Examples include open chain chelators or acyclic tweezers, tripodal and tetrapodal hosts. The structural design criteria for hosts in light of these geometries has been examined recently[53]. The field of supramolecular chemistry contains examples of larger cyclic structures containing cavities adorned with urea functionality such as cyclophanes[61,62] and calixarenes[63-74].

Early work on the development of urea based hosts recognized the wide variety of anion geometries available and exploited this to synthesise selective host systems. Hamilton[75,76] and Rebek[77] developed open chain chelators possessing two urea functional groups interacting well with certain dicarboxylates, which may be considered Y-shaped at both ends. Figure 1.6 shows an open chain chelator selectively complexing a molecule of glutaric acic which has a carboxyllate anion at each end. Both host and guest are hydrogen bond donors and acceptors forming a total of 4 interconnecting H-bonds. Despite relatively little preorganisation by way of steric constraint or cavity size

discrimination, good recognition of a specific anion due to a unique *geometric* compatibility was observed.

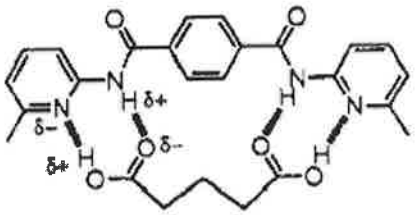

**Figure 1.6**. An open chain chelator selectively complexing a dicarboxyllic glutaric acid anion demonstrating the importance of good geometric compatibility between host and guest.

Calixarenes feature prominently in (thio)urea based anion hosts. Figure 1.7 shows selected urea hosts based on the calix[4]arene skeleton, illustrating the versatility of calixarenes as molecular platforms for supramolecular hosts. Figure 1.7 also includes a capsule complex, demonstrating the effect of intermolecular urea H-bonding between two urea calix[4]arenes[78]. The guest is trapped in a closed capsule held by steric enclosure, thereby *indirectly* complexed by the urea hydrogens, which serve to maintain the capsules 'seal'.

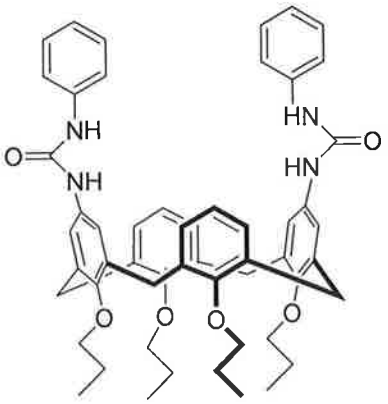

Upper rim substitution
(Stastny, 2002)

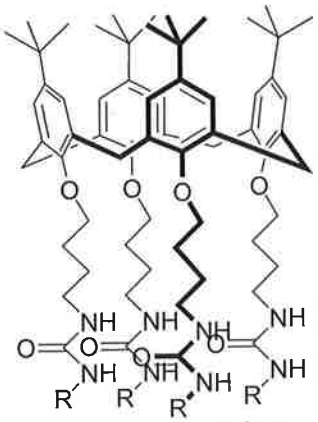

Lower rim substitution
(Scheerder, 1994)

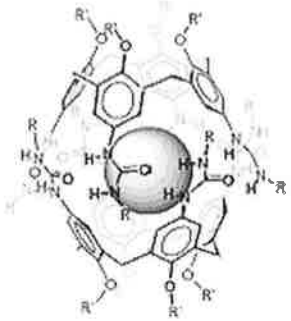

Guest inclusion in a capsule formed
by 2 H-bonding calixarene ureas (Rebek, 2000)

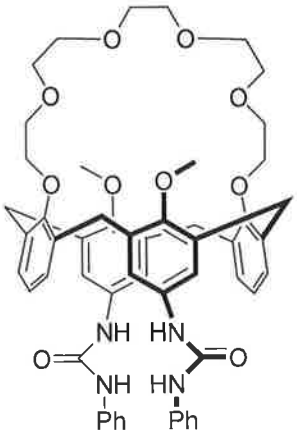

Simultaneous complexation of
cation (crown) and anion (urea)
(Tongraung, 2003)

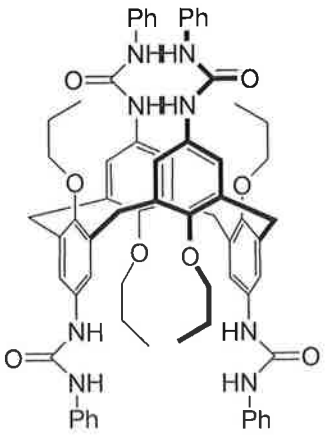

1,3-alternate twin cavity
anion host (Budka, 2001)

**Figure 1.7.** Selected urea calix[4]arenes appearing in the literature, studied for host-guest complexation.

For the various geometric variations that hosts may possess there is an acknowledged lack of true structural data revealing the orientation of urea hydrogens[53]. When designing a host for a specific anion it is hard to choose an acyclic platform or a complex supramolecular one. Selectivity patterns, in truth, often reveal themselves post synthesis by experimentation but there is a general logic underpinning the design. The incorporation of at least two coordination sites such as (thio)urea groups into the anion host design, is the only certain starting criterion for achieving selectivity by means of steric exclusion or advanced preorganisation.

For urea based hosts, a major specific factor when considering anion-host interaction is the competition from the solvation of anion and host initially present. Another competing factor is the phenomenon of inter and intramolecular H-bonding between urea groups. These effects have been studied for calixarenes[78-80]. These bonds can be in direct competition with the detection of anions. For example Reinhoudt reported a *tetra*-urea calix[4]arene showing lower association constants with chloride and poorer anion selectivity than an equivalent *di*-substituted calix[4]arene, despite the availability of 8 and 4 hydrogen bonds respectively[72]. What may initially be considered a hindrance or a competing factor to the functioning of an anion sensor can reward the chemist by discriminating against some anions, thus creating interesting selectivity patterns.

In chapters 3 and 4, urea functional groups are incorporated into calix[4]arene platforms and their selectivity pattern is determined by optical and electrochemical techniques.

## 1.10 An introduction to calixarene chemistry

The name calixarene stems from 'calix crater' a type of ancient Greek vase and by its very name conjures up images of selective containment[81].

Calixarenes are a class of supramolecular receptor, typically synthesised by phenol-formaldehyde condensation reaction, to give oligomers comprising a central macrocycle of varying repeat phenolic units linked by methylene groups at the ortho position. Since their description by Gutsche in the 1980s[81], many calixarene derivatives have been described, due to the ease of modification of the so called upper and lower rims of the calixarene's central annulus[26,27,82-85]. The calixarene family has thereby become synonymous with the forefront of complex chemistry.

There are numerous compounds based on the calixarene molecular platform which all have certain features in common, namely a central aromatic cavity or annulus, an upper rim and a lower rim, substituted as required. A general calix[4] arene structure is shown in Figure 1.8.

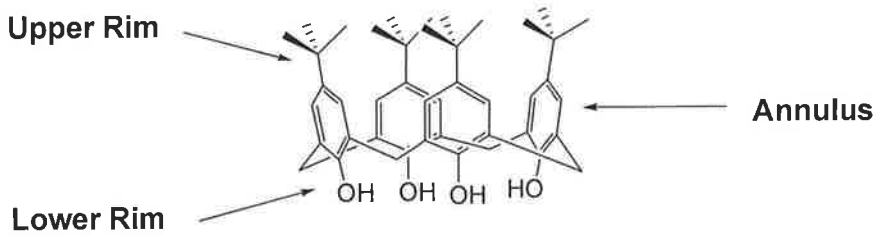


**Figure 1.8**. A typical calixarene (**1-1**) in a cup like cone conformation.

The number of phenolic repeat units may be higher than four, but by far the most commonly encountered calixarenes contain four repeat units. In addition calix[4]arene **1-1** contains upper rim *t*-butyl groups as a commonly encountered example. Much of the discussion in this thesis therefore focuses on structures based on **1-1** as a default. It must be emphasised that a multitude of calixarenes have been reported with varying upper and lower rim substituents or indeed the complete absence of substituents on either rim, having dramatic effects on properties such as conformational flexibility. In

summary, calixarenes make excellent platforms for the design of chemical sensor receptors for ions and neutral molecules. Several excellent publications are available describing the history, synthesis and characteristics of calixarenes[26,81,85-87].

Zinke was the first to obtain crystal calixarene products in the 1940s and by recrystallisation, pure enough material was available to propose a *cyclic* structure, with the general structure shown in figure 1.9[88].

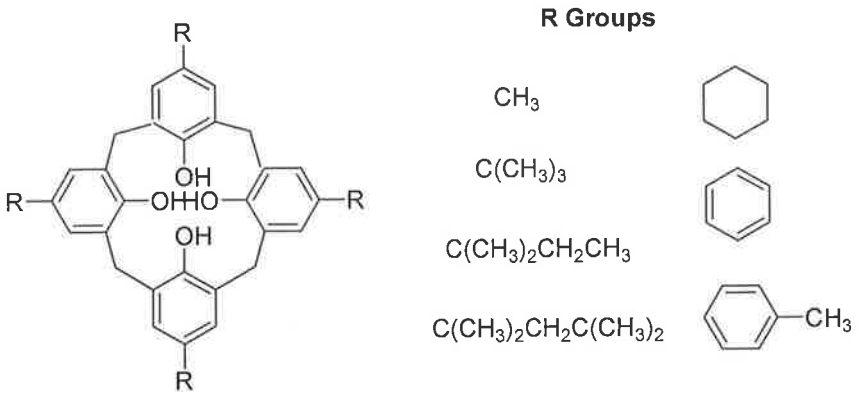


**Figure 1.9.** The structure of a calixarene as a *cyclic* structure as first proposed by Zinke.

This structure does not yet allude to the 3D cavity possibilities of calixarenes. The first calixarenes to be investigated for conformation were hydroxyl containing calixarenes in the solid state. X-ray crystallography was the best way to investigate possible conformations of such basic calixarenes as in solution, there is typically much conformational flexibility and an 'average' conformation only may be observed by NMR. Gutsche and co-workers have summarised these X-ray crystallography results where four distinct 'frozen' conformations of calix[4]arene are described. These are shown in Figure 1.10[89-91].

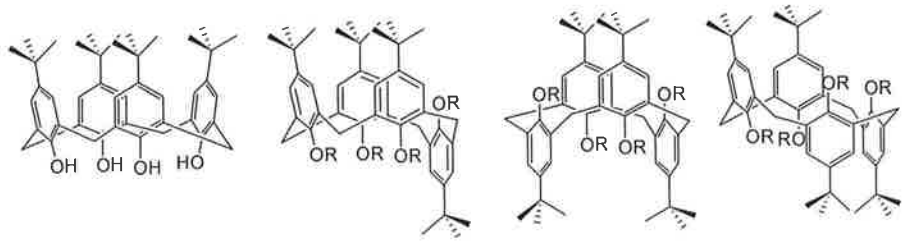


**Figure 1.10.** The 3D representations of the four conformers of calix[4]arenes.

Calixarenes with 5 repeat phenolic units also have four possible conformers with increasing numbers for 6 and more repeat units.

Before the emergence of calixarenes as a major contender of host-guest chemistry, Pedersen and Cram had investigated crown ethers and elegantly demonstrated the concept of inclusion of group I metals in the their cavities. Cram raised awareness of the concept of immobile baskets or 'cavitands' that contained rigid preorganised 'enforced cavities' large enough to engulf ions or molecules[92,93]. It was apparent that calixarenes had potential rigid cavities but the hydroxyl calixarenes of earlier studies had too much flexibility to fit such descriptions. To replicate the concepts and endeavours previously bestowed on crown ether chemistry, efforts were made to lock calixarenes in a cone or partial cone conformation. Researchers like the Parma group and McKervey and coworkers substituted ether and ester groups of appropriate dimensions to the lower rim hydroxyl groups to prevent the free rotation of hydroxyl groups through the calix[4]arene annulus[94,95]. These efforts were vindicated by x-ray analysis which indeed revealed cone and partial cone conformations with *rigid* preorganised cavities.

As X-ray crystallography is still far from a routine fast technique, an alternative technique of a universally applicable nature was needed to rapidly ascertain the

conformation of newly synthesised calixarene hosts. In tandem with conformational freezing strategies, $^1$H NMR techniques became available to assess conformations at room temperature. The groups of Ungaro and Gutsche assigned distinct $^1$H NMR splitting patterns to the calix[4]arene $CH_2$ (methylene) spacers of the annulus according to the conformation present[81]. These signals appear at a chemical shift of around 4.0ppm according to the splitting pattern detailed in Table 1.7.

| **Conformatiom** | **$^1$H NMR Pattern** |
|---|---|
| Cone | One pair of doublets |
| Partial Cone | A pair of doublets OR<br>A pair of doublets and a singlet |
| 1,2-alternate | A singlet and two doublets |
| 1,3-alternate | A singlet |

**Table 1.7.** The $^1$H NMR splitting patterns for the annulus $CH_2$ protons of specified calix[4]arene conformations.

Indeed for the calix[4]arenes synthesised in this thesis, the cone and a 1,3-alternate conformation were assigned using the same method. Figure 1.11 shows the structure of **5-5** (chapter 5) and its corresponding $^1$H NMR spectrum as an illustrative example. Some of the typical calix[4]arene signals encountered are indicated including signals for phenolic hydrogens, aromatic protons, methylene protons of the annulus (two doublets indicative of the cone conformation) and signals corresponding to the tertiary butyl protons of the upper rim.

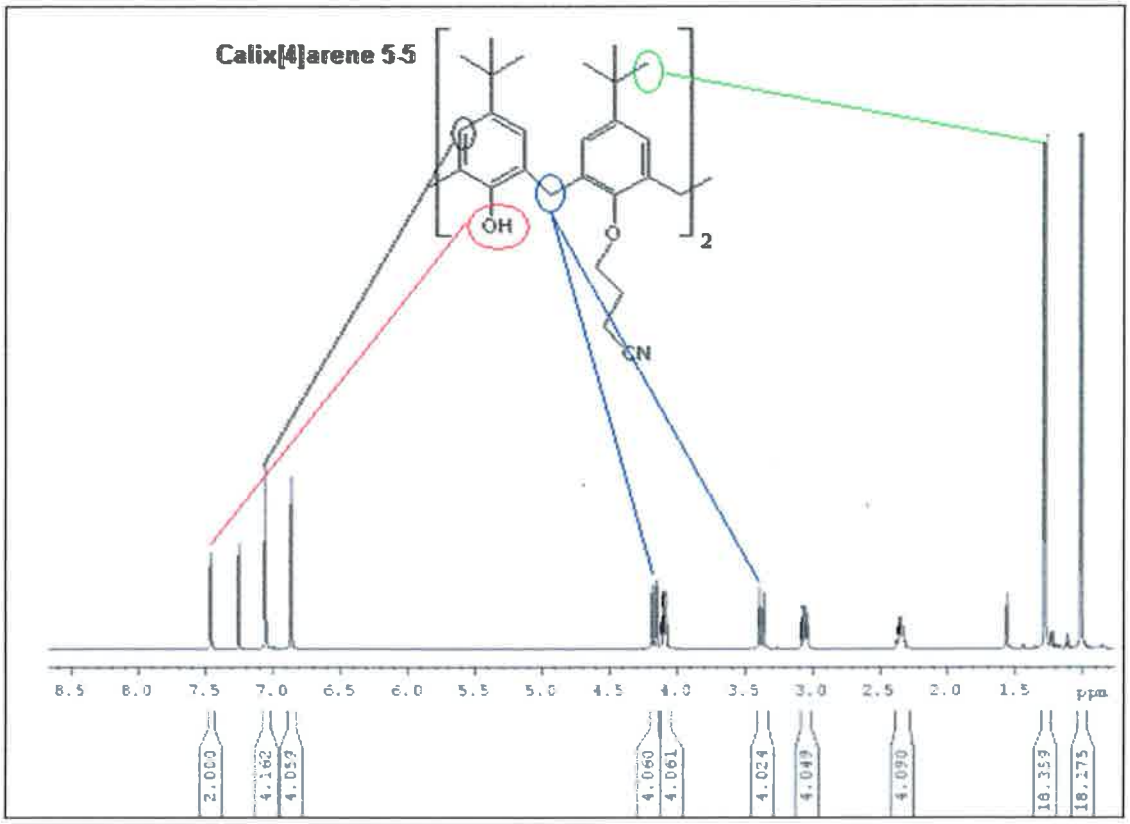


**Figure 1.11**. Characteristic $^{1}$H NMR signals of a typical calix[4]arene, **5-5** (chapter 5), including two doublets indicating the presence of the cone conformation.

From the 1980s onwards a plethora of cleverly substituted easily characterised calixarenes with rigid cavities for host-guest chemistry became available and synthetic efforts continue to this day.

From their discovery, a further 30 years of synthetic research was required to control the number of repeat units in the calixarene ring and workers like Kämmerer managed to synthesise 4/5/6/7 and 8 membered rings in a more controlled fashion instead of a complex mixture of these[96]. As well as the presence of multiple oligomers, workers like Cornforth detailed how several diastereoisomers of each calixarene can exist, with obvious implications for purification[97]. As purification and characterisation techniques evolved, the elegant 3D conformations of various calixarenes were elucidated.

Following the rigidification of *t*-butyl calix[4]arenes substitution with simple ethers and esters on the lower rim, the next goal was to create selective and useful complexation agents. In addition to preorganised rigid cavities and the 'best fit' or 'lock and key' principle which makes complexation thermodynamically favourable[1], suitably placed complexing *functional groups* within the calixarene cavity are also essential. Particular emphasis is placed on lower rim substitution, although upper rim chemistry is alluded to also. Only lower rim substitution was performed for compounds synthesised for this thesis. The most obvious starting point on the typical calix[4]arene starting material are the four lower rim hydroxyl groups. These can readily be deprotonated using a base followed by $S_N2$ substitution to append a large variety of moieties. Carbonate bases are used for the first two hydroxyl protons and disubstituted products are typically obtained. As the $pK_a$ of subsequent hydroxyl protons rises, hydride bases are often used to remove the remaining two protons to yield tetrasubstituted products.

In the case of calix[4]arenes the degree of substitution can vary from mono- to tetra-substituted. Shinkai and coworkers have altered reaction temperatures, solvents and choice of base in order to control and clearly define methods determining the final substitution[98]. Our own group has conducted studies into the synthetic conditions leading to partially and fully substituted ester calix[4]arenes at the lower rim by varying reaction parameters including solvent, temperature, base and stoichiometries[99]. Controlling substitution also controls guest complexation selectivities observed and so is vital knowledge generally, as shown by Diamond and Wall[100].

A wide variety of functional groups have been attached to calixarene scaffolds lending varied properties on the target macrocycles. Calixarenes substituted on the upper or lower rim of the annulus result in effective cavity based Host compounds for a wide variety of guests and there are excellent texts available bravely attempting to

comprehensively review these[27,28,83-85]. Neutral calixarenes are based on functional groups such as amines, amides, esters, phosphine oxides and ethers containing oxygen, nitrogen and sulphur donators. The majority of successful calix[4]arene hosts are selective towards inorganic cations. Alone focusing on the output of Diamond and coworkers over the years, serves as a broad illustration of the variety of selective hosts synthesized in the literature. Diamond and coworkers have synthesized calixarene based hosts for cations such as sodium[101], calcium[102], lead[103], europium[104] and lithium[105] as well as several enantioselective hosts for optically active neutral organic guests[106,107] as depicted in Figure 1.12. There are now robust and selective commercially available cation sensors based on some of this chemistry.

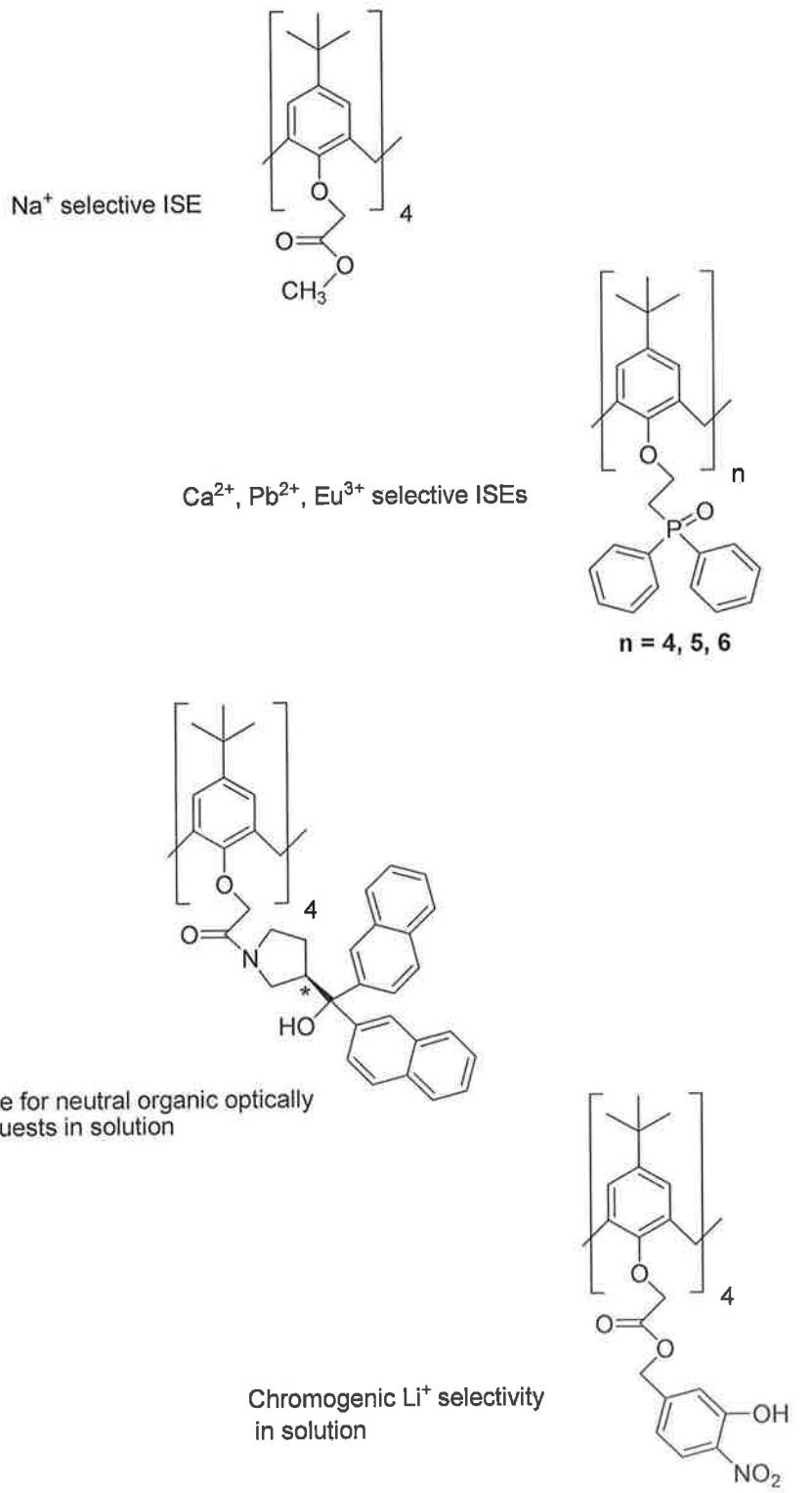


**Figure 1.12.** A selection of calix[4]arene hosts showing selectivity towards the specified species.

By and large, the same functionalized appendages can now be inserted on the lower and upper rim of calixarenes in a controlled manner. The main difference is that upper rim substituents provide an enlarged cavity for guests with greater dimensions compared to lower rim cavities. For example as anions are larger than isoelectronic cations, they require a larger host cavity. Such cavities are sometimes furnished by the substitution of urea functional groups onto the upper rim providing suitable cavities. The spacious arrangement of up to four appendages on the upper rim can lead to interesting phenomena such as intermolecular H-bonding and subsequent Host-Guest chemistry of resultant calixarene capsules[78]. As most starting material calixarenes typically contain upper rim *tert*-butyl groups (synthesized with best yields), these must first be removed prior to the addition of alternative appendages. This entails a reverse Friedel-Crafts reaction catalysed by $AlCl_3$ in toluene or phenol[108]. A general scheme for this is shown in Figure 1.13.

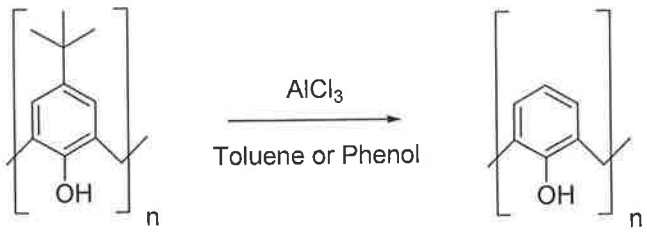


**Figure 1.13.** A general scheme for the removal of *p-tert*-butyl groups of calixarenes by reverse Friedel-Crafts reaction.

The remaining *para*-H can now be substituted by aromatic electrophilic substitution reactions[81]. However, fuctionalisation via para-Claisen rearrangement is perhaps a more interesting route. An interesting example of this is shown in Figure 1.14[109].

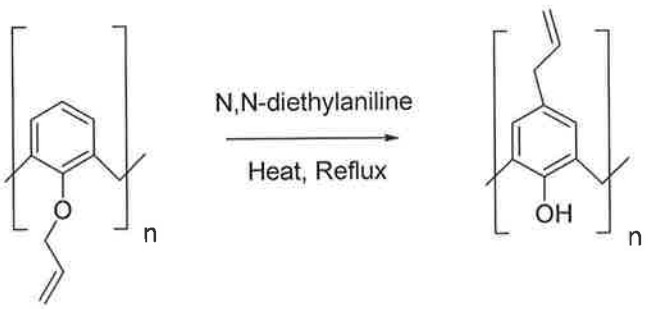


**Figure 1.14.** The functionalisation of calixarenes by *para*-Claisen rearrangement reaction.

The labile allyl groups can be polymerized into a chain or may serve as a handle, providing a *passive* covalent linker to a surface substrate (via the upper or lower rim), whilst the other substituent positions on the calixarene can contain the *active* functional groups engaged in complex formation and transduction chemistry. This type of approach is increasingly important in the context of modern sensor development. The strategy of host *immobilization* is important for real life sensors and in line with efforts to modifying proven *solution* phase chemistry for real life sensor devices. If only a single passive linker is required, perhaps to maintain the calixarenes overall flexibility or to prevent interference with the complexing mode, there are methods available leading to mono-allyl calixarenes as shown in Figure 1.15[110].

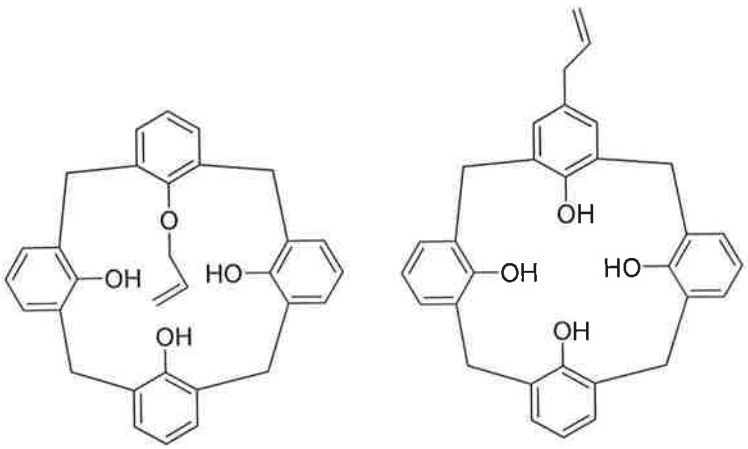


**Figure 1.15.** Mono-allyl calix[4]arene starting materials for further substitution.

Indeed Loctite attached metal chelating calixarenes to polymer supports via upper and lower rim attachment by a similar approach[111]. This is an example of the industrial relevance of calixarene chemistry. It is apparent that many of the calixarenes discussed in this thesis and in the literature could theoretically be subjected to this immobilization chemistry prior to attaching the complexing chemistry required.

## 1.11 *Investigating Calixarene complex formation*

The first attempts at investigating the complex formation ability of some simple calixarenes is credited to Izatt and coworkers and took place in the early 1980s[112,113]. Both the calix[4]arene hosts and the transduction methods used were relatively basic and of an academic nature. Since this research, the sophistication of calixarene structures has improved through unabated research effort, leading to selective practical devices available today. There are general reviews available on the broad topic of seminal calixarenes as sensing agents including electrochemical and optical transduction modes such as by Diamond and McKervey[27] and Böhmer[85]. The earliest work focussed on group I and II cation interactions and to this day it appears that most

calixarene hosts reported are cation selective although there are growing numbers of anion selective hosts. In addition there are several hosts for neutral organic guests. To illustrate the evolution of calixarene complex formation chemistry, some cation selective calixarenes are described. Izatt investigated the ability of a series of hydroxy calixarenes to transport cations between an organic and aqueous phase. Figure 1.16 shows the structures of hosts investigated.

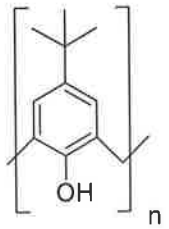


**n = 4, 5, 6, 7 and 8**

**Figure 1.16**. The structures of calixarenes investigated by Izatt for cation interaction.

Izatt and coworkers had experience with investigating crown ethers and cyclodextrins prior to calixarene investigations. The approach was always to investigate cyclic structures with central cavities of varying size by altering the number of repeat units, in a similar way to the calixarenes in Figure 1.16. These structures represented relatively simple cation hosts with no striking cation selectivity apparent. For transport to take place, strongly basic solutions of calixarene were required to deprotonate lower rim hydroxy groups thus providing an electrostatic interaction mechanism between $O^-$ and the cation. Group I cations interacted with the calixarenes in this way, unlike group II cations. Modest but seminal selectivity towards caesium was observed for the calix[6]arene in particular. In a control experiment, *p-tert*-phenol showed no transport ability. These studies were amongst the first evidence that a cyclic cavity effect was inducing selectivity towards certain guests through dimensionally specific preorganisation, similar to the case of crown ethers earlier.

Later studies also used multiphase liquid transport studies to test the complex formation ability of calixarenes. The calixarenes tested were derivatised in an increasingly sophisticated way. A series of lower rim substituted ether calixarenes revealed varied selectivities by McKervey and coworkers[114] including compounds with ester functionality similar to that shown in Figure 1.12. Similar compounds were investigated by Chang and Cho around the same time confirming these results[115]. Perhaps the most important discovery was the realisation that calix[4]arenes appear to manifest a kind of default selectivity for $Na^+$, due to a particularly good fit between host and guest. Besides the ester calixarenes, another major study was performed on amide derivatised calixarenes by Chang and coworkers[116]. These compounds were less effective at forming complexes with group I metal cations but were particularly good transport agents fro group II cations.

As the chemistry of the calixarenes became more sophisticated and ever better selectivities towards target analytes were achieved, the analytical tools for signalling guest recognition applied to these systems also changed. The quintessential cation selective ionophores, the crown ethers had been incorporated into PVC based ISE membranes revealing excellent analytical properties[117]. By applying such a transduction mode, the impressive host-guest chemistry of these compounds could be dramatically exploited to produce a real life analytical signal, where previously only multiphase liquid transfer experiments had yielded results. In this way molecular structures with proven solution based selectivity for group I alkali metals like potassium, were combined with a real life analytical technique that are potentiometric ISEs.

In the same way Diamond and coworkers investigated a series of known tetraester calixarenes for cation affinity using potentiometric ISEs[118]. This type of calix[4]arene

ester is amongst the first calixarenes with real preorganisation and the ability to selectively bind cations. They represent the academically most successful calixarene guest recognition agents employed to date also possessing considerable commercial merit[26]. The structure of these calix[4]arenes is shown in Figure 1.17.

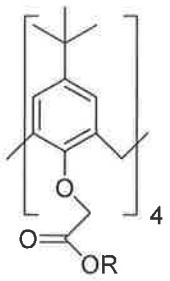


**Figure 1.17.** The general structure of tetraester calix[4]arenes as investigated by Diamond and co-workers[26]. R includes $CH_3$-, $CH_3CH_2$- and $CH_3OCH_2CH_2$-.

These neutral calix[4]arene hosts are symmetrically substituted lower rim tetraesters. The methyl and ethyl ester versions of this compound for example, showed excellent selectivity for sodium with 100-fold selectivity over the commonly prevalent sodium interferant potassium. The key features of this type of calix[4]arene are the nature of the upper and lower rims. On the lower rim there are eight oxygens which are available for forming ion-dipole electrostatic bonds with cations. Four phenoxy oxygens attached to the calixarene annulus and four carbonyl oxygens from the ester groups. The upper rim contains tertiary butyl groups which lock the calix[4]arene into a rigid cone configuration. This represents a host providing an ideal 'lock and key' fit cavity for the sodium ion as well as providing directional localized negative charge via the hard donor oxygens to coordinate effectively with sodium.

Extensive molecular modelling and X-ray crystallography confirm these experimental findings on a theoretical basis[114,119,120]. Figure 1.18 shows a tetraethyl ester *t*-butyl calix[4]arene coordinating a sodium ion, clearly demonstrating the involvement of eight oxygens in sodium coordination.

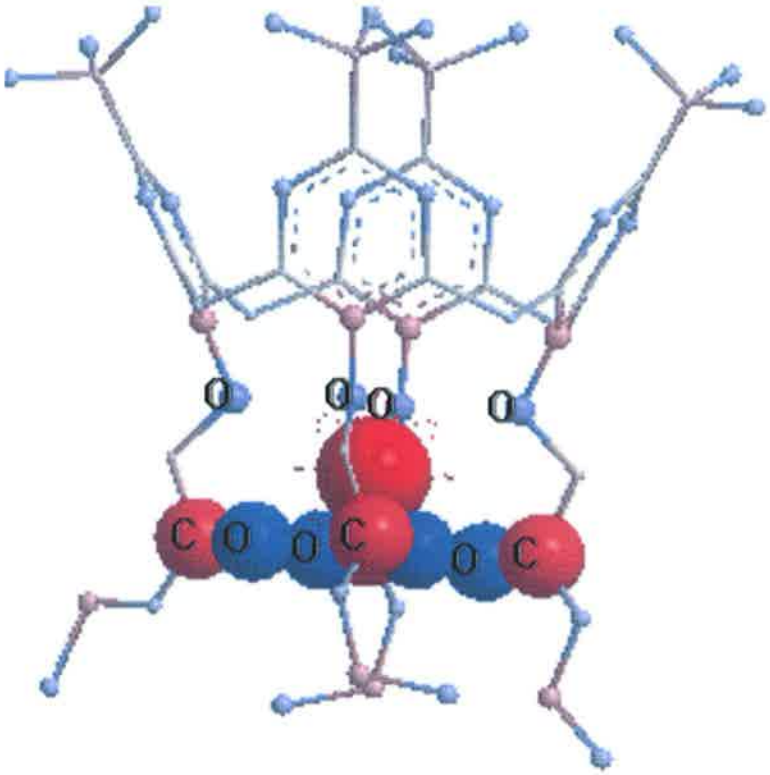

**Figure 1.18.** A tetraester calix[4]arene locked in the cone conformation, binds a sodium ion by a 'lock and key' interaction with eight lower rim oxygens. A similar model applies for tetraamide calix[4]arenes. Atoms are scaled by size according to Huckel partial charges. Red and blue are areas of positive and negative localised charge respectively.

The sodium selectivity of the tetraester may be considered a kind of default for calix[4]arenes in general due to the ideal fit in the lower rim cavities[28].

The calixarene hosts reported today have come some way from the early structures reported on by Izatt and coworkers. Hosts can operate in a charge neutral fashion with minimal pH interference and no sample pre-treatment. Cavities are rigid with appropriate dimensions and functional groups for selective analyte recognition. Concurrent with the structural changes, the analytical transduction modes employed have followed suit. Improved practical electrochemical and optical methods are now used[26]. Calixarenes are immobilised on and in the sensing surface. Fast reversible signals are obtained with desirable sensor parameters: Selectivity, range, LOD, lifetime

and reproducibility. Today's keywords include lab on a chip, miniaturisation, cost effectiveness, low power consumption, digital data handling and wireless networks. One example of these trends is the move from conventional ISEs to ion-selective field effect transistors (ISFETs) and coated wire electrodes (CWE) using calixarenes[121]. Internal filling solutions are eliminated and they can be miniaturised and mass produced according to semiconductor industry specifications. One note of caution for these alternatives to classical ISEs is that due to the lack of internal filling solutions, the interfacial interaction mechanism between membrane and wire or transistor is not as clearly understood as a filling solution-membrane contact. Indeed the analytical output of such devices is generally less stable than that of a classical ISE.

Both the fundamental chemistry *and* the device applications of calixarene chemistry are evolving from academic curiosities to miniaturised commercial devices.

Cation selective calixarene applications have reached a certain level of maturity, however contributions continue to be made like the Hg(II) and Ag(I) selective nitrile based calix[4]arenes described in chapter 5 . Perhaps the state of the art of calixarene chemistry today lies with anion or neutral guest selective hosts coupled with optical transduction techniques. To this end, a chloride selective calix[4]arene with ratiometric fluorescence transduction is described in chapter 4.

## 1.12 General experimental (for all chapters)

**Generation of molecular models.** All molecular models and were created using MM2 force field energy minimization. The energy was reduced to a minimum RMS gradient of 0.100. Debye-Hückel partial charge calculations were also performed with the same software. The software used was Chem3D Ultra 8.0 supplied by Cambridge Scientific Computing, Inc.

**The preparation of ISEs and titration procedures for Anion and Cation analysis.**

The following general procedure was followed for all potentiometric work unless stated otherwise. Potentiometric membranes were prepared using 250mg 2-Nitrophenyl octyl ether, 125mg PVC, 6.5mmol $kg^{-1}$ host ionophore and 2.7mmol $Kg^{-1}$ potassium tetrakis(4-chlorophenyl) borate (cation analysis) OR tridodecylmethylammonium chloride (anion analysis) dissolved in dry THF and evaporated slowly. A 'blank' membrane refers to the same membrane cocktail described above, however omitting the presence of an ionophore.

The electrochemical cell used consisted of a double junction reference electrode and a PVC membrane working electrode in the following arrangement:

Ag | AgCl | 3M KCl ‖ 0.1M LiOAc ‖ sample solution | PVC membrane | 0.01M NaCl | AgCl | Ag. Membranes were conditioned in 0.01M sodium chloride for 12 hours and deionised water for half an hour prior to ISE titrations. The sequence of ion titrations always went from the weakest responding to the strongest responding ion as observed using blank membranes and the primary ion last of all. This minimised preloading or contamination of the membranes with high affinity analytes. The potentiometric cell was interfaced to a PC using a National Instruments SCB-68 4-channel interface. All ISE measurements were performed in triplicate.

**A note on the use of ISEs:**

Generally in this thesis, ISE titrations are carried out in the activity ranges log a -6.0 - - 1,0, which is considered the classical linear response range of an ISE[21]. Many real life sensor applications require lower LODs, perhaps in the nanomolar range. The lowering of LODs for existing ionophores is a relatively recent endeavour with good theoretical and practical advancements in the field of ISEs achieved[122]. Typically, these methods require modifications of electrode filling solutions, conditioning solutions, perhaps

samples themselves, conditioning regimes and other factors. These endeavours are outside the scope of the current thesis, whose primary aim is to relate the structural characteristics of *novel* ionophores to ISE responses. In most cases these results give valuable information to the synthetic chemist on how to improve the ionophore structures. Once the ionophore molecular structures are *fully* optimised for selectivity in particular, the analytical chemist can set about optimising the sensors which incorporate these ionophores. This optimisation revolves around factors such as LODs, response range (sensitivity), sensor lifetime, reproducibility etc.

# 2. Chapter 2 Amide Calixarenes

## 2.1 ABSTRACT

The amide functional group is capable of forming complexes with both cations and anions. This is achieved via electrostatic ion-dipole carbonyl interactions and amide NH H-bonding respectively. Potentiometric ISEs in particular have been successfully used for the study of calix[4]arene amides and their interaction with cations. In recent times anion recognition research has been catching up with cation selective systems. There are inherent difficulties associated with the investigation of anion complexation in water in particular as discussed in chapter 1.2. The use of amide functional groups has been extended to the research of anion complexation. Such complexation and selectivities are often monitored by NMR or optical methods, but is rarely reported using potentiometric transduction methods.

Calix[4]arene amides **2-17, 2-18** and **2-19** were synthesised with varying degrees of substitution on the upper and lower rims. These ionophores were each incorporated into ISE membranes, configured in turn for cation or anion recognition, depending on the membrane ion-exchange salt. In this way the dual-use functionality of amides could be exploited, whilst minimising interference from analytes of the opposite charge sign to the target analyte.

Regarding cation analysis, no significant change in selectivity order was observed compared to an ISE with no ionophore (blank membrane following Hofmeister series of selectivity) for the 3 hosts. For **2-18** and **2-19** a modest improvement in response towards Na(I) and Ca(II) was observed. This is in agreement with the general size compatibility of these ions and the calix[4]arene lower rim cavity. When configured for anion recognition, **2-18** revealed bromide selectivity and a clear deviation from a

solvent dominated selectivity pattern (Hofmeister series). Molecular models suggest a peripheral mode of binding with bromide instead of a cavity inclusion mechanism. It is thought that the bulky naphthyl groups proximal to the amide functional groups provide some of the necessary preorganisation leading to the observed selectivity.

The presence of allyl groups provides a potential means of immobilising the host onto a sensor substrate as allyl groups can be converted into a covalent linker. This may be required for a practical sensor device application. An alternative strategy may be to polymerise the host into a chain via the present allyl groups, the resultant material serving as the sensor substrate.

## 2.2 INTRODUCTION

The Initial work on calix[4]arene amide ionophores in the literature involved structures with the general structure depicted in Figure 2.1[28].

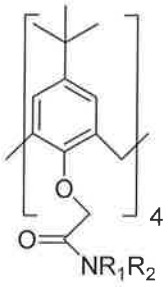


**Figure 2.1**. A general structure for tetraamide *t*-butyl calix[4]arenes. $R_1$ and $R_2$ are alkyl or aryl moieties.

They were typically symmetrically tetrasubstituted on the lower rim and provided four carbonyl oxygens (from amide functional groups) and four phenoxy oxygens (adjacent to calixarene annulus) for complexing cations. Their cavity dimensions and characteristics are quite similar to those of the calix[4]arene tetraester type hosts discussed in chapter 1. The mode of binding cations was therefore much the same as depicted by the molecular model complex of a tetraester seen in Figure 1.18. The

nature of substituents and preorganisation locked the entire structure into a cone conformation. It is no surprise therefore that, like with their tetraester analogues, sodium selectivity was indeed observed in many cases[28].

Most of the early studies revolved around potentiometric ISEs, investigating selectivity amongst a variety of cations. Over time, different amide substituents were fitted ($R_1$ and $R_2$ varied Figure 2.1) and the upper rim substitution was modified.

A comparison of amide and ester calix[4]arene ionophores and their similar attributes is therefore valuable, as most literature data for these classes of compounds was derived using potentiometry. Figure 2.2 shows the general structure of calix[4]arenes discussed and Table 2.1 gives details of the specific structures.

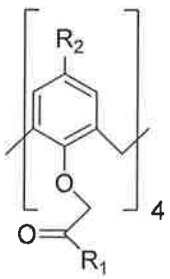


**Figure 2.2**. The general structure of calix[4]arene esters and amides discussed.

| Calix[4]arene | $R_1$ | $R_2$ |
|---|---|---|
| **2-1**[101] | $OCH_3$ | *t*-Butyl |
| **2-2**[101] | $OCH_2CH_3$ | *t*-Butyl |
| **2-3**[123] | $OCH_2Ph$ | *t*-Butyl |
| **2-4**[28] | $OC_{10}H_{21}$ | *t*-$C_4H_9$ |
| **2-5**[123] | $OCH(CH_3)_2$ | *t*-Butyl |
| **2-6**[124] | $OC(CH_3)_3$ | *t*-Butyl |
| **2-7**[124] | OPh | *t*-Butyl |
| **2-8**[123] | $OCH(CH_3)_2$ | H |
| **2-9**[123] | $OC(CH_3)_3$ | H |
| **2-10**[123] | $OCH_2Ph$ | H |
| **2-11**[100] | Diester version of 2-2 | |
| **2-12**[100] | Monoester version of 2-2 | |
| **2-13**[125] | $N(CH_3)_2$ | *t*-Butyl |
| **2-14**[124] | $N(CH_2CH_3)_2$ | *t*-Butyl |
| **2-15**[123] | $NHC_4H_9$ | *t*-Butyl |
| **2-16**[126,127] | $N(C_4H_9)_2$ | *t*-Butyl |

**Table 2.1**. Details of identity of R groups of the calix[4]arene ester and amide general structure in Figure 2.2.

Using potentiometric ISEs containing a particular ionophore to investigate host selectivity there are two main factors for modulating observed selectivity. One involves structural changes to the ionophore performed by the organic chemist, the other involves altering other parameters of the sensor. The latter approach may include varying the polarity of plasticizer used, changing filling solutions and conditioning regimes (chapter 5) or changing the ratio of ionophore to ion exchange salt within the membrane[122]. These measures do indeed alter the selectivities and other characteristics of ISEs, but to radically change the properties of a sensor usually requires structural modifications of the ionophore itself, the heart of any chemical sensor.

By keeping all sensor parameters constant but varying the ionophore, a link between an analytical signal and host structure change was established using potentiometric ISEs as discussed in later in this chapter (similar approach used in chapters 3 and 5). The

modifications and resultant properties are generally discussed relative to the parent *t*-butyl symmetrically tetrasubstituted calix[4]arenes. The discussion in this thesis confines itself to calix[4]arenes as the majority of calixarenes contain 4 repeat phenolic units including all calixarenes in this thesis. The topic is then extended to a number of calix[4]arene amides which have not previously been investigated.

Structural modifications are broken into 3 main categories: 1) The nature of ester or amide lower rim substituents. 2) The nature of upper rim substituents. 3) The number of lower rim substituents. Although the majority of these studies in the literature were carried out on calix[4]arene esters, it is well conceivable that a similar correlation between structural changes and observed selectivity patterns would apply to equivalent calix[4]arene amides.

### *2.2.1 The nature of ester or amide lower rim substituents*

Increasing the *length* of ester substituents gradually from from methyl to decyl (**2-1** – **2-4**) did not influence ISE behaviour greatly with similar sodium selectivity observed in all cases. However, changing the steric *bulkiness* of ester substituents (**2-5** – **2-7**), including *t*-butyl and aromatic substituents proximal to the ester carbonyls instead of simple linear alkyl groups, led to changes in the observed potentiometric selectivity coefficients. In addition, sensitivity is decreased, LOD is elevated and there is increased interference to sodium selectivity from potassium and caesium. The bulkiness of substituents is thought to force a larger cavity by steric means, which in turn reduces sodium selectivity, whilst enhancing the competitive effectiveness of larger cations ($K^+$ and $Cs^+$ for example).

### *2.2.2 The effect of removing upper rim t-butyl groups*

The effect of removing the *t*-butyl groups of a number of calix[4]arenes on the sensor characteristics has also been examined in comparison with the parent *t*-butyl calix[4]arene. Hosts **2-8 – 2-10** are compared to **2-3, 2-5** and **2-6**.

In general when upper rim substituents were replaced with hydrogen, poorer sensitivity and selectivity were observed as well as elevated LODs, with enhanced responses to the larger potassium and caesium in comparison to sodium. The absence of the upper rim *t*-butyl groups means that the bulky lower rim substituents can enlarge the cavity of the lower rim to relieve steric hindrance. Deviation from the rigid preorganised cone conformation is now possible. The analytical characteristics of such ionophores reflect this.

### *2.2.3 The number of lower rim appendages*

Lynch and co-workers compared the ISE characteristics of tetraester **2-2** with equivalent diester and monoester analogues **2-11** and **2-12** similar to the structures in Figure 2.3[100]. In each case, the response to sodium was compared with a blank ISE membrane (containing only exchange salt but no ionophore). It was found that only the tetraester showed convincing sodium selectivity. Due to the less preorganised open nature of the cavities of the diester and monoester, the diester shows reduced selectivity forming effective complexes with potassium and caesium as well as sodium, involving six oxygen donors in total. The monoester was found to show a very weak interaction with sodium (i.e. virtually identical to the blank). The monoester calixarene has very little preorganisation compared to the other calixarenes and the molecular model of the monoester-sodium complex shows the sodium well inside the calixarene annulus[100], confining interaction to the four phenoxy oxygens and limiting interaction with the remaining ester carbonyl oxygen. Perhaps as expected, the most preorganised

tetrasubstituted host showed the most favourable sodium selectivity. Figure 2.3 shows molecular models of tetra, di and mono substituted ethyl ester calix[4]arenes. Apart from experimental evidence, it can perhaps be intuitively foreseen that lower binding constants and less selectivity will ensue as substituents (complexation points) are removed and the cavities are opened up.

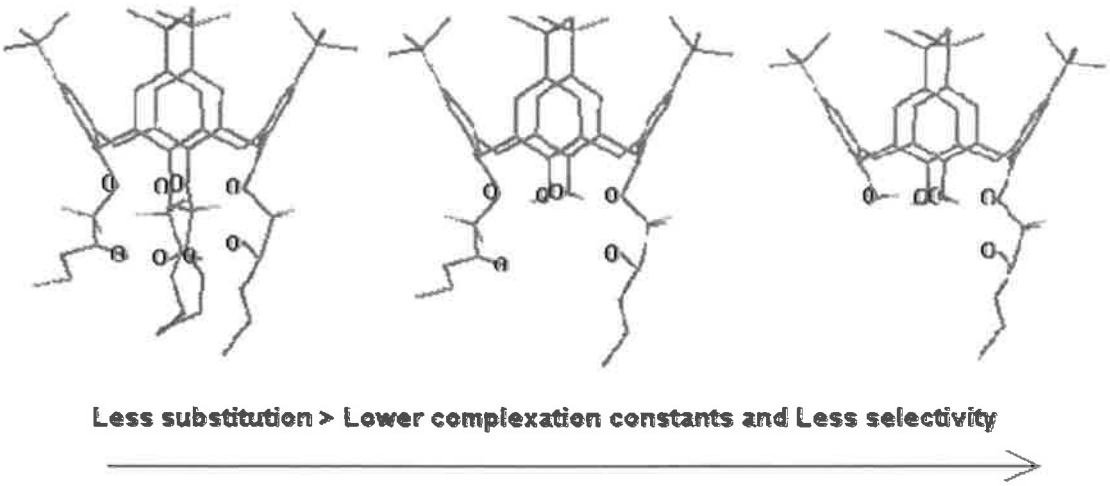


**Figure 2.3**. From left to right: tetra, di and mono substituted ethyl ester calix[4]arene. Less substitution results in weaker complexation and more general selectivity.

### *2.2.4 Calix[4]arene amides as cation hosts*

In general, for amide calix[4]arenes analogous to the esters described above, it is conceivable that changing the number and identity of upper and lower rim substituents would result in similarly modulated selectivities. However, some characteristics exclusive to amides and the impact on sensor applications of such ionophore hosts is discussed below.

In the absence of appropriate sodium selective preorganisation, an ionophore based on amide functional groups will prefer divalent cations over monovalent cations of similar size unlike an equivalent ester ionophore. This is because of the higher dipole moments of amide carbonyls in general, forming stronger electrostatic bonds with divalent cations. For example comparing the dipole moments of typical calix[4]arene ionophore

appendages for cation binding, ester $CH_3CO_2CH_2CH_3$ has a dipole moment of 1.78D compared to the amide $CH_3CONHCH_3$ which has a dipole moment of 3.73D according to models[116].

However with the appropriate preorganisation in place, good sodium selectivity and sensitivity can once again be observed, with the notable feature that there is increased interference from Ca(II), which has a similar ionic radius to sodium (ionic radii of 100 and 102pm respectively), and improved selectivity of Ca(II) over Mg(II)[128]. This was the case for **2-13 – 2-16** with the exception of **2-14** (Table 2.1). **2-14** illustrates an important feature of calixarene amide ionophores[123]. This cavity contains only tertiary amide groups. In effect this means that the uncomplexed ionophore can have its four carbonyl oxygens pointing inward. Minimal rearrangement is needed to accommodate a guest in this way, removing some of the impetus leading to selectivity. This coupled with the highly polar nature of amides (compared to esters) means that strong binding is observed for nearly all cations tested in picrate phase-transfer experiments, with a slight overall preference for calcium over sodium. The potentiometric trials involving **2-14**, mirrored this result in that no significant size discrimination was observed for a series of common inorganic cations, with the most notable interference attributable to alkali earth (divalent) metal cations probably arising from the highly polar nature of the amide functional groups. Conversely, with the non-tertiary calix[4]arene amides, where one or more hydrogens are attached to the amide nitrogen, there is a greater chance of achieving some selectivity but weaker overall complexation ability. This is due to the possibility of intramolecular H-bonding within the free calix[4]arene. Conceivably, intermolecular H-bonding and capsule formation may also be at play. This means that any potential ionic guest must compete with these H-bonds and subsequently additional significant rearrangement of the amide groups is required for all carbonyl oxygens to

point in a convergent manner into the complex cavity. These factors compete energetically with the binding of ionic guests, weakening the overall affinity for ions but crucially helping to induce useful selectivities. This competition appears analogous to the case of urea calix[4]arenes as discussed in chapter 1.9. In comparison to **2-14**, ionophore **2-15** shows sodium selectivity comparable to the best tetraester calix[4]arenes. In terms of sodium selective ionophores, ester calixarenes are preferred over the amide analogues, showing ideal intermediate binding constants, displaying the best sodium selectivity in sensors and displaying other excellent sensor characteristics in terms of ISE lifetime, sensitivity and LODs (literature references in Table 2.1).

### *2.2.5 The case of the calix[4]arene amides as anion hosts*

It is perhaps in the area of *anion* sensing that there is the most potential for investigating novel selectivities of calixarene amide ionophores. What is interesting about the amides is the presence of H-bonding potential from the NH in the alpha position to each amide carbonyl, in the case of non-tertiary amides. This in theory means that an ionophore with appropriate amide functionality can be configured for cation *or* anion analysis. The partial negative charge on the amide carbonyl provides a directional means of binding cations by an electrostatic ion-dipole interaction and the nearby NH protons with their partially positive charge can form H-bonds with anions. Figure 2.4 shows a molecular model of the simple amide acetamide, with emphasis on the partial charges of the molecule, whose atoms are sized and coloured according to charge type and magnitude to illustrate the above point.

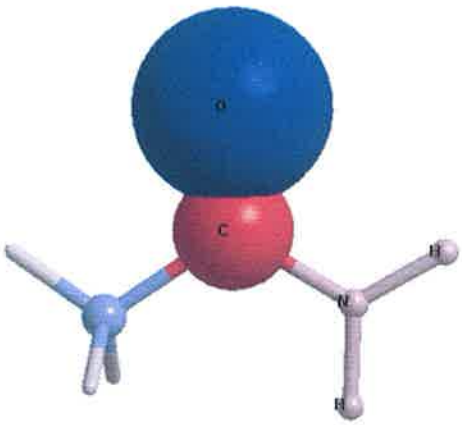

**Figure 2.4**. The energy minimised model of acetamide. Atoms are scaled in size and coloured according to the magnitude and type of Hückel partial charges. Amide oxygen is positive (blue) and amide hydrogens are negative (red).

Ester functional groups, lacking H-bonding ability, are confined exclusively to cation detection. It might be argued that a functional group with the ability to interact with both cations and anions may be subject to more scenarios of analyte interference in a sensor. One approach that effectively avoids this is when amide ionophores are used in ISEs. ISE membranes, in addition to the ionophore host typically contain an ion exchange salt[21]. The lipophilic ions exchange ions from the sample phase of the opposite charge, bringing them into the membrane phase, normally with selectivity that follows the Hofmeister series. Once in the membrane, the ligand (i.e. calixarene host) competes with the exchanger and ideally dominates the overall observed selectivity. At the same time the exchanger ions repel ions of the same charge and hence they dictate whether the membrane is overall cation *or* anion selective. This may be viewed as a means of pre-configuring an ISE for anion or cation analysis depending on the choice of lipophilic exchange salt. Amides may therefore be considered dual-use functional groups.

Urea or thiourea functional groups are the most popular H-bonding functional groups for the design of neutral anion selective ligands as each urea moiety provides two H-

bonds potentially. The nearby carbonyl groups mean these functional groups also have potential to complex both anions and cations. This is discussed further in chapter 3.

The application of amide functional groups for anion recognition is broadly divided into two categories of receptors. The first is neutral cyclic and acyclic organic receptors and the second is metal ion containing charged receptors. This area of research has recently been thoroughly reviewed[129]. The neutral amide host category of course contains examples based on calixarene platforms. They all generally have two or more amide groups on the upper or lower rim of a calix[4]arene platform, which results in preorganisation and a disposition towards showing some interesting anion selectivities. Examples of such calix[4]arenes include two or more amides providing H-bonds for Y-shaped carboxylate anions[130-136], $H_2PO_4$[137-139], fluoride[140-142] and chloride[137,143]. Figure 2.5 illustrates the diversity of such calix[4]arene amide ionophores tested for interaction with anions, as have recently appeared in the literature. This diversity is necessary to accommodate anions which have a larger variety of shapes and sizes compared to cations as discussed in chapter 1.8.

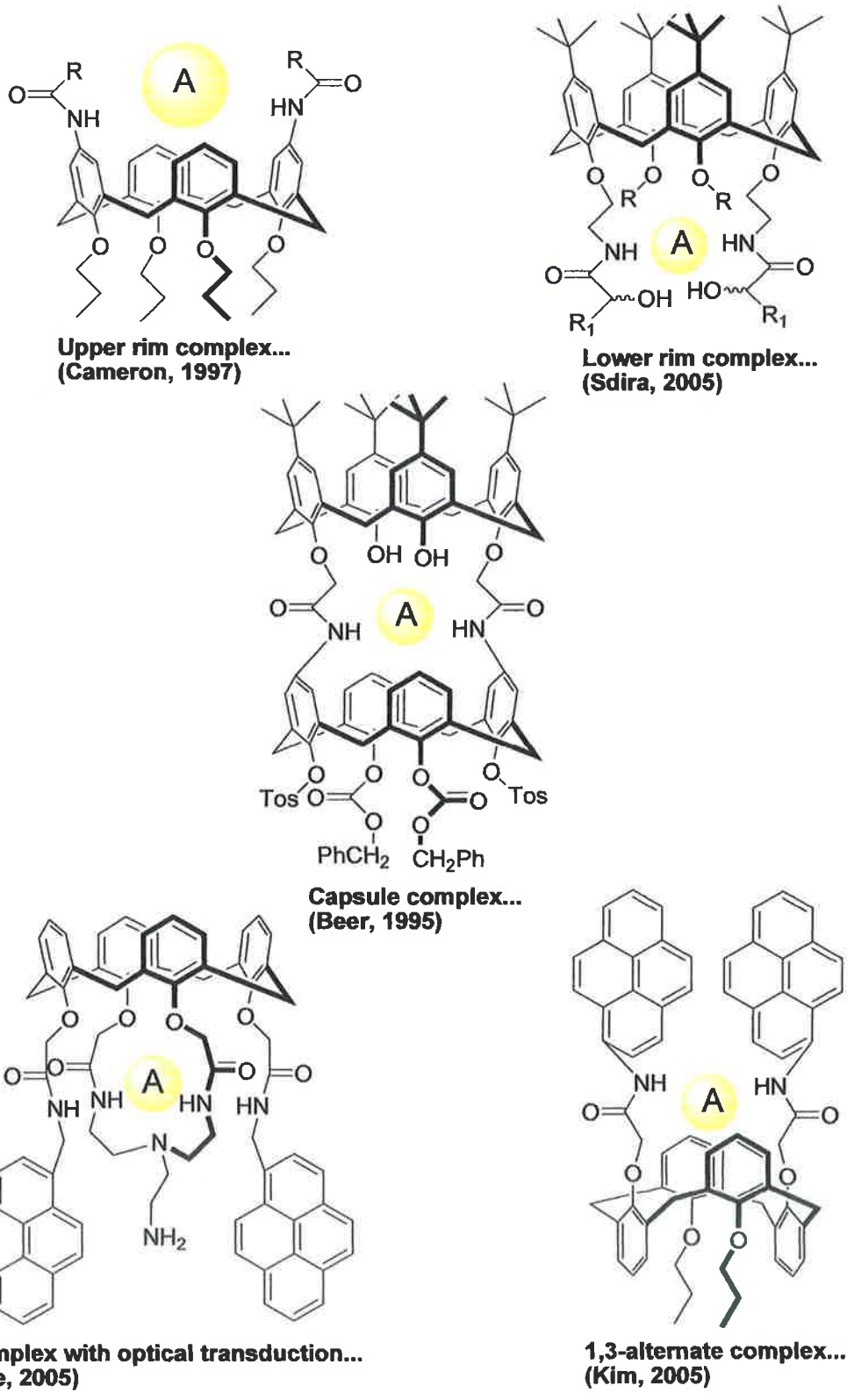


**Figure 2.5.** Selected examples of calix[4]arene amides in the literature used for anion (A) complexation.

As the amide protons are involved in hydrogen bonding anions, this provides a convenient means to monitor stoichiometries, binding constants and binding conformation by conducting $^{1}H$ NMR titrations and monitoring the chemical shift of relevant amide protons and so is the most popular tool for investigating such interactions. $^{1}H$ NMR screening of urea and thiourea interactions with anions is popular for similar reasons. The next most popular means of investigating anion binding of amide calixarenes is UV-Vis and fluorescence spectroscopy. This of course means there must be metal or organic chromophore moieties in proximity to the amide groups to signal the presence of an ionic guest to the analyst. Cyclic voltammetry has also been used. A minority of researchers rely solely on computer modelling to predict anion affinity in specific solvent environments.

There are very few examples in the literature where calixarene amide-anion interactions are monitored by potentiometric ISEs. Possibly the main reason for this discrepancy is the anticipated competition to anion binding from the aqueous H-bonding water environment, inherent in the use of potentiometric ISEs. These solvent effects are discussed in chapter 1.2.

## 2.3 RESULTS AND DISCUSSION

Calix[4]arene amides **2-17, 2-18** and **2-19** (Figure 2.6) were previously synthesised in our group[144].

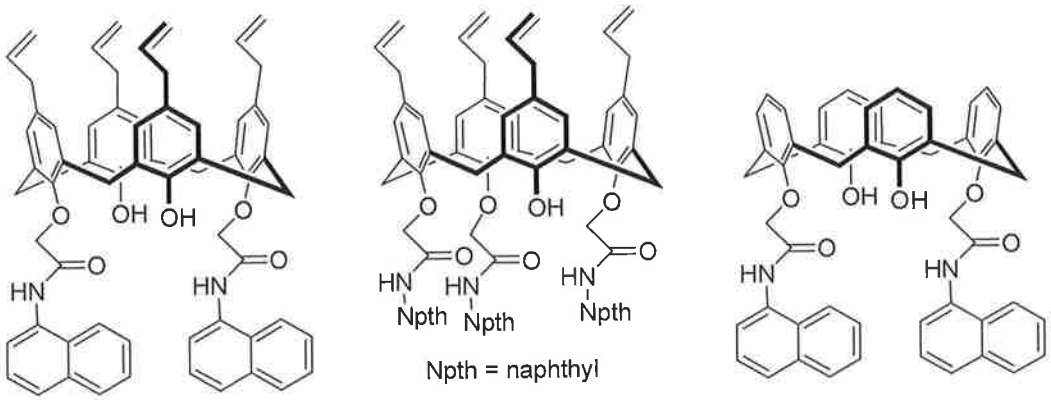


**2-17** **2-18** **2-19**

**Figure 2.6.** The structures of calix[4]arene amides **2-17, 2-18** and **2-19**.

These structures were incorporated into ISEs configured separately for either anion or cation detection. The selectivity pattern of these amide hosts was then established potentiometrically.

Structures were deliberately chosen, where there is likely deviation from the well-established 'default' sodium selectivity in order to find new potential uses for such compounds in cation or anion sensing applications. In light of this aim and the discussion in chapter 2.2, the structures presented have features including calix[4]arene amides with less than four lower rim appendages, bulky substituents proximal to amide functional groups, the absence of upper rim substituents and non-tertiary amides. Structures **2-17** and **2-18** contain upper rim *p*-allyl groups instead of the more commonly encountered *p-tert*-butyl substituents. Interestingly no more than three naphthyl amides could be attached to the lower rim, the addition of a fourth appendage presumably prevented by the increasing steric hindrance between naphthyls at the lower rim[144]. From the $^{1}$H NMR spectra of all these compounds, there is a pair of doublets

around 4ppm which correspond to the methylene protons of the calixarene's annulus spacers[144]. This is indicative of a cone conformation in all cases. It appears that the *p*-allyl groups together with the lower rim substituents are capable of preventing free rotation of the benzene groups through the central annulus, thus the structures **2-17** and **2-18** may be considered locked and preorganised into the cone conformation. The somewhat more bulky *p-tert*-butyl more commonly serves this function in calix[4]arene chemistry. Other potential functions of allyl calixarene substituents is that they provide the means of being polymerised into chains or they may act as a labile handle for covalently linking the host structure to polymer backbones and other surfaces. The immobilisation of host species can be an important step in the development of a practical sensor device. This is alluded to further in chapter 1.10.

### *2.3.1 ISEs of calix[4]arene amides 2-17, 2-18 and 2-19 for cation analysis*

ISE membranes were prepared with and without (blank) the specified ionophore according to the general experimental procedure in chapter 1.12. As an initial indication of the effectiveness of the ionophores, the response of blank and ionophore ISEs to log a -2.0 aqueous solutions of the specified cation were compared. Figure 2.7 shows deviations in response as a result of the presence of ionophore.

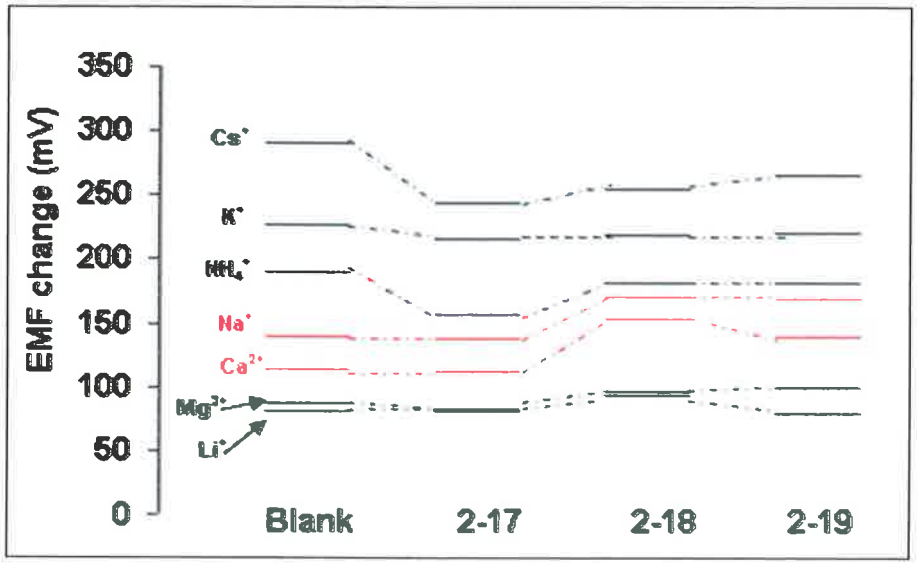


**Figure 2.7**. The comparison of potentiometric responses of a blank membrane with **2-17**, **2-18** and **2-19**. The potential change is for the specified cation at activity log a -2.0 compared to measurements in de-ionised water. The improved responses for **2-18** and **2-19** are highlighted in red. The ion exchange salt used was potassium tetrakis(4-chlorophenyl) borate.

The first observation from Figure 2.7 is that for all three compounds there is no change in the order of selectivity towards a series of common inorganic cations when comparing ionophore membranes to a blank. All ionophore membranes and the blank show $Cs^+$ selectivity in accordance with the Hofmeister series prediction (most lipophilic cation). $Cs^+$ selectivity is most likely driven by the ion-exchange component of the membranes and not the ionophore. The default sodium selectivity for calix[4]arene amides was not observed compared to some other calix[4]arene amides (Table 2.1). There is no dramatic improvement (increase) in potentiometric response towards cations for **2-17**. However, there is some improvement in potentiometric response for ionophores **2-18** and **2-19**. Some increased potential change is seen for these ionophores in the presence of Na(I) and Ca(II). Concurring with the theory, the high polarity of amides results in some expected interference from alkali earth metals and other divalent cations compared to equivalent ester ionophores[116].

Compared to tetraamide hosts there are only a maximum of two carbonyl oxygens available for cation binding for **2-17** and **2-19** (or 3 in the case of **2-18**), given correct orientation and cavity geometry. In analogy to the current observation, a reduction in sodium sensitivity and selectivity was noted going from tetraester to a monoester calix[4]arene as previously discussed[100]. Overall the responses are more akin to a monosubstituted calix[4]arene ionophore. In the case of monoesters, very little difference in response compared to a blank was observed.

As the amide groups are non-tertiary in nature for all three ionophores, there is the possibility of intramolecular H-bonding (C=O----HN) with which the cation guests must compete. Furthermore, in such cases, reorientation is necessary for all available carbonyl oxygens to point into the cavity for guest bonding. If this reorientation is not possible (e.g. for steric reasons) or energetically taxing, the response could effectively be that of a monoamide, a compound with little preorganisation to induce selectivity i.e. no significantly increased response towards any cations as in the case of **2-17**. Furthermore, the naphthyl groups in the immediate vicinity of the amide functional groups may sterically impede guest binding or perhaps reorientation of the host for optimal guest incorporation.

As stated above, an improved response towards sodium and calcium is observed for **2-18** and **2-19**. A cavity size selectivity effect could be at play here, as sodium and calcium have similar ionic radii (100 and 102pm respectively). **2-18** has an additional lower rim amide appendage compared to **2-17**, increasing the likelihood of electrostatic interaction with amide carbonyls. The removal of upper rim *p*-allyl groups as seen for **2-19**, means that the cavity can reorganise and open up somewhat to relieve steric strain present due to preorganisation or the bulky naphthyl groups for example. In this way some response is observed for sodium and calcium. Figure 2.8 shows a molecular

model as generated by Chem3D Ultra 8.0 of **2-18** encapsulating a sodium ion in the lower rim cavity. The presence of the cone conformation was initially verified by the presence of 2 doublets for the methylene calixarene annulus protons in the $^{1}H$ NMR spectrum of **2-17-2-19**[81,144] and this was used as a basis for models prior to energy minimisation.

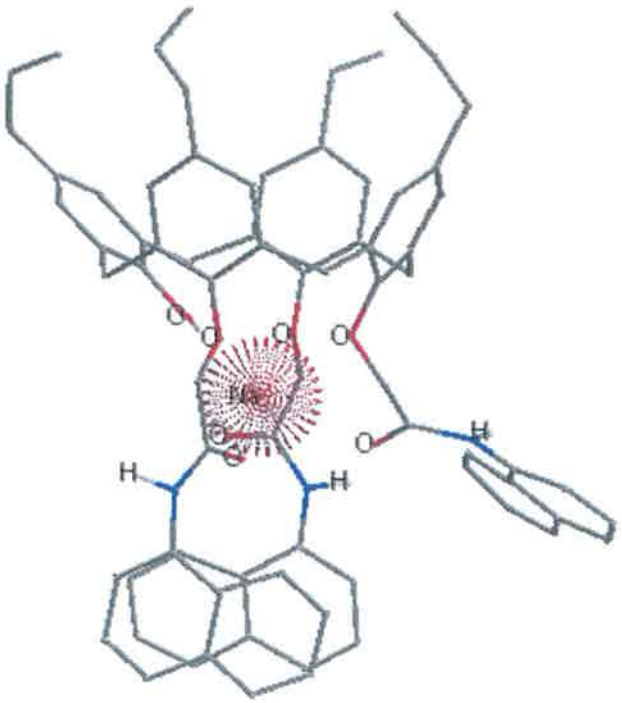


**Figure 2.8**. An energy minimised molecular model of **2-18** bonding a sodium ion.

The bulky nature of three naphthyl groups on the lower rim is quite apparent in Figure 2.8, probably preventing optimum orientation of the labelled lower rim ion-dipole bonding oxygens for sodium interaction. The relatively subtle response improvement compared to the blank for sodium (and calcium) seen in Figure 2.7 supports this claim. In comparison, **2-19** has no upper rim *p*-allyl groups and only two lower rim amides (Figure 2.9).

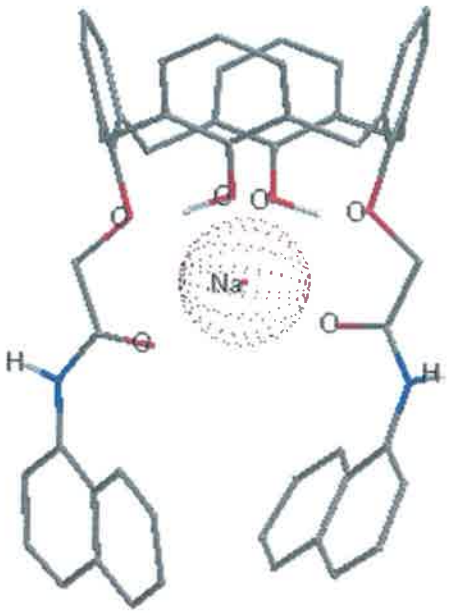


**Figure 2.9**. An energy minimised molecular model of **2-19** bonding a sodium ion.

Although there is one less carbonyl available for complex formation, the less preorganised and sterically strained nature of the compound's cavity appears to compensate for this inducing increased flexibility, possibly allowing a better orientation of functionality with the cationic guest. Supporting this claim is that similar affinity for sodium (and calcium) is observed as in the case of **2-18**. In the case of **2-17**, the presence of only two amide groups of a bulky nature, restrained in a cone conformation with the help of further upper rim substitution, appears to prevent any appreciable cation interaction and the response is approximately the same as that of the blank membrane ISE.

ISE titrations were carried out in the range log a -4.0 to log a -1.0 for the same series of cations. From this information, the performance of ISEs could be evaluated in terms of slope for linear portions of the curve and the determination of formal selectivity values by the Separate Solutions Method (SSM).

Tables 2.2 – 2.4 reveal the slope values obtained for **2-17, 2-18** and **2-19** ISE titration curves.

| Ion | Range (log a) | Slope (mV/decade) |
|---|---|---|
| $Cs^+$ | -4.0→-1.0 | +50.2 |
| $K^+$ | -4.0→-1.0 | +50.2 |
| $NH_4^+$ | -4.0→-1.0 | +48.9 |
| $Na^+$ | -4.0→-1.0 | +51.6 |
| $Li^+$ | -3.0→-1.0 | +48.0 |
| $Ca^{2+}$ | -4.0→-1.0 | +30.3 |
| $Mg^{2+}$ | -4.0→-1.0 | +27.7 |

**Table 2.2**. Slope values for ISE 2-17 for the indicated activity ranges.

| Ion | Range (log a) | Slope (mV/decade) |
|---|---|---|
| $Cs^+$ | -4.0→-1.0 | +50.0 |
| $K^+$ | -4.0→-1.0 | +52.5 |
| $NH_4^+$ | -4.0→-1.0 | +49.4 |
| $Na^+$ | -4.0→-1.0 | +59.6 |
| $Li^+$ | -3.0→-1.0 | +54.5 |
| $Ca^{2+}$ | -4.0→-1.0 | +42.2 |
| $Mg^{2+}$ | -4.0→-1.0 | +37.3 |

**Table 2.3**. Slope values for ISE **2-18** for the indicated activity ranges.

| Ion | Range (log a) | Slope (mV/decade) |
|---|---|---|
| $Cs^+$ | -4.0→-1.0 | +50.1 |
| $K^+$ | -4.0→-1.0 | +52.8 |
| $NH_4^+$ | -4.0→-1.0 | +49.6 |
| $Na^+$ | -4.0→-1.0 | +60.3 |
| $Li^+$ | -3.0→-1.0 | +53.0 |
| $Ca^{2+}$ | -4.0→-1.0 | +39.0 |
| $Mg^{2+}$ | -4.0→-1.0 | +35.6 |

**Table 2.4**. Slope values for ISE **2-19** for the indicated activity ranges.

Sub-Nernstian slope values were obtained for all cations in the case of **2-17**. Conversely, Nernstian or super-Nernstian slopes were observed only for sodium and the alkali earth metals for **2-18** and **2-19**. This is in agreement with the improved response seen for these cations compared to a blank membrane, as seen in Figure 2.7.

The selectivity values for **2-17, 2-18** and **2-19**, as obtained by the SSM (log $K^{pot}_{Na^+,J}$) are presented in Table 2.5, including an indication of reproducibility as obtained from replicate ISE titrations.

| Host | 2-17 | 2-18 | 2-19 |
|---|---|---|---|
| $Na^+$ | 0 | 0 | 0 |
| $Cs^+$ | 1.76±0.02 | 1.26±0.01 | 1.84±0.04 |
| $K^+$ | 1.12±0.04 | 1.07±0.04 | 0.97±0.01 |
| $NH_4^+$ | 0.50±0.04 | 0.04±0.01 | 0.40±0.01 |
| $Ca^{2+}$ | -1.52±0.04 | -1.20±0.05 | -1.10±0.02 |
| $Mg^{2+}$ | -2.03±0.02 | -2.06±0.01 | -1.78±0.02 |
| $Li^+$ | -1.01±0.05 | -1.03±0.02 | -0.93±0.02 |

**Note**: I is the primary ion $Na^+$ and J is the interferant specified.
The Separate Solutions Method (SSM) was used where log $a_I$=log$a_J$=-2.0. Reproducibility based on three ISEs.

**Table 2.5**. Selectivity Coefficients, log $K^{pot}_{Na^+,J}$, for **2-17, 2-18** and **2-19** calculated using the Separate Solutions Method (SSM).

From the selectivity values in Table 2.5, it is clear that all three calixarene amide ISEs show caesium selectivity, log K being the largest for caesium in each case. The blank membrane also shows a preference for caesium as was seen in Figure 2.7. Due to caesium having the smallest charge to area ratio of all cations tested (hence most lipophilic), it is by default the most likely cation to show interaction with the hydrophobic PVC ISE membranes.

By and large, the ionophores do not override the influence of the membrane ion-exchange salt, however **2-18** and **2-19** clearly resulted in ISEs showing an improved response towards sodium and calcium, which is interesting from a supramolecular point of view. In terms of sensor applications, ionophores yielding greater overall selectivity deviations from those caused by solvent effects are needed.

The next step was to configure ISE membranes in order to establish the selectivity order of the three calix[4]arene amides towards anions. In this way it was hoped that the ionophores could induce a selectivity order deviating more significantly from that of a blank membrane.

### *2.3.2 The ISE characteristics of calix[4]arene amides 2-17, 2-18 and 2-19 towards anions*

ISE membranes were prepared with and without (blank) the specified ionophore as before but configured for anion analysis by using the appropriate ion exchange salt for all ISE membranes. Membranes were prepared and used according to the standard experimental procedure in outlined chapter 1.12. As an initial indication of the effectiveness of the ionophores, the response of blank and ionophore ISEs to log a -3.0 aqueous solutions of the specified anion were compared as before.

Figure 2.10 shows the result of initial screening of ionophore membranes compared to a blank to establish possible selectivity.

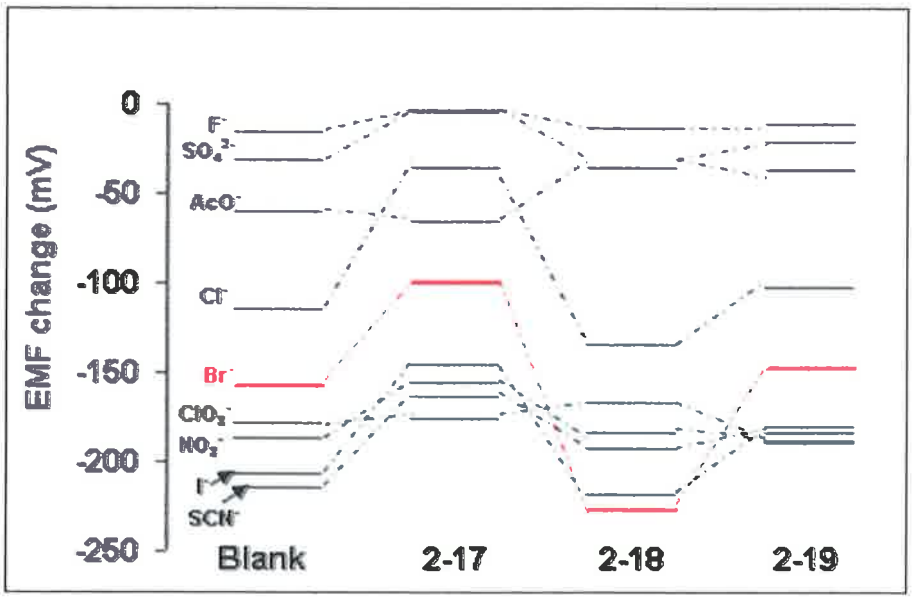


**Figure 2.10**. The comparison of potentiometric responses of a blank membrane with **2-17**, **2-18** and **2-19**. The potential change is for the specified anion at activity log a -3.0 compared to measurements in de-ionised water. The progression of potentials for bromide is highlighted in red. The ion exchange salt used was tridodecylmethylammonium chloride.

The most dramatic difference to the blank response (significantly greater potential change) is the bromide response observed for the ISEs of **2-18.** Compared to the blank response, the potential change for the ISE of **2-18** was about 70mV greater. Such a scenario was not observed for all other combinations of anion and ionophore.

The bromide selectivity observed is in contrast to the thiocyanate selectivity of the blank as seen in Figure 2.10. This represents a clear deviation from the blank (Hofmeister) order of selectivity.

For **2-17**, the response to most anions is suppressed by the ionophore but for chlorate it stays much the same compared to the blank resulting in overall chlorate selectivity. Similarly for **2-19**, anion responses are generally suppressed except for nitrate and chlorate responses which show an increased potential change. The ISE is left $ClO_3^-$ /$NO_3^-$ selective. For all three ionophores, unlike in the case of cations, a clear deviation from the response order and selectivity of the blank (Hofmeister order) is observed for

anions. It is therefore concluded that this time, the ionophore dictates responses to ions instead of the membrane ion-exchange salt.

ISE titrations were carried out in the range log a -6.0 to log a -1.0 for the entire series of anions. The reproducibility information from these curves in the form of error bars confirm that there is a clear improvement in response towards bromide observed for **2-18** as depicted in Figure 2.11.

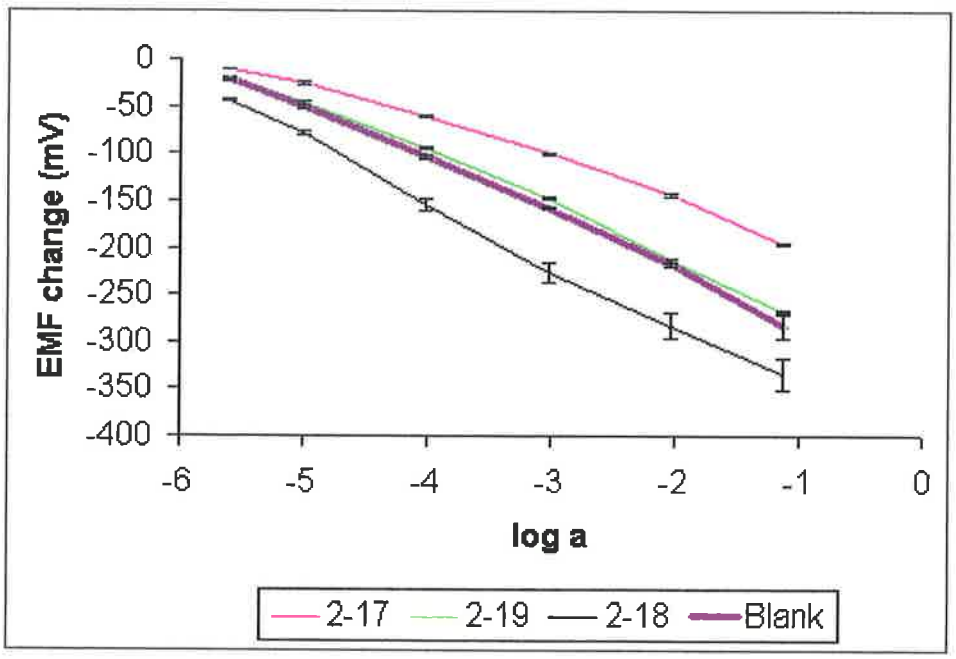


**Figure 2.11.** The comparison of bromide ISE titration curves of the blank with ionophore containing ISEs. Error bars give an indication of reproducibility (triplicate titrations).

In order to explain the bromide selectivity of **2-18** further, molecular modelling was used to elucidate a possible mode of interaction for the complex. Energy minimised models were generated according to the procedure given in chapter 1.12.

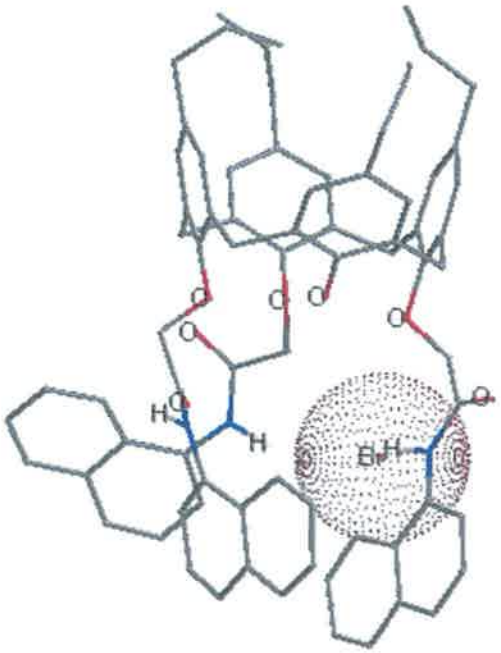

**Figure 2.12**. An energy minimised molecular model of a complex of **2-18** and a bromide anion.

Due to its size (196pm), the bromide ion is unlikely to sit within the cavity of **2-18** as it is almost twice as big as a sodium ion, more commonly complexed within the lower rim cavities of calix[4]arenes[28]. This is supported by the energy minimised model in Figure 2.12. Given that the upper rim *p*-allyl groups together with the three naphthyl groups on the lower rim must lend considerable rigid preorganisation and associated steric strain on the ionophore, the rearrangement to facilitate cavity inclusion of bromide is unlikely. A peripheral complex as depicted in Figure 2.12 is perhaps more likely. In such a scenario two amide NH protons from 1,2-substituted lower rim appendages in **2-18** may orientate to form a complex with bromide. As the other ionophores only contain two 1,3-substituted appendages, the same H-bonding possibilities are not available and so this mode of interaction cannot be observed. If in the absence of a cavity effect peripheral complexation dominates in the case of **2-18**, then the influence of the naphthyl groups immediately proximal to the amide functional groups (no spacer) may

be a significant means of providing some preorganisation or steric mechanism for discrimination between ions, explaining the bromide selectivity observed.

Table 2.6 shows the formal selectivity coefficients (log $K_{I,J}^{pot}$) calculated by the SSM method. Reproducibility characteristics of the ISEs are also given here.

| Host | 2-17 | 2-18 | 2-19 |
|---|---|---|---|
| $I^-$ | -0.41±0.12 | -0.02±0.22 | -0.07±0.12 |
| $SCN^-$ | -0.06±0.18 | -0.52±0.10 | -0.01±0.13 |
| $ClO_3^-$ | 0 | -1.01±0.04 | -0.02±0.05 |
| $Br^-$ | -1.25±0.02 | 0 | -0.68±0.01 |
| $NO_3^-$ | -0.32±0.02 | -0.73±0.02 | 0 |
| $Cl^-$ | -2.35±0.02 | -1.40±0.22 | -1.23±0.33 |
| $SO_4^{2-}$ | -4.55±0.01 | -4.64±0.13 | -4.26±0.11 |
| $AcO^-$ | -1.83±0.02 | -3.09±0.19 | -2.45±0.17 |
| $F^-$ | -2.88±0.01 | -3.58±0.05 | -2.97±0.06 |

**Note**: I is the primary ion (log K=0) and J is the interferant specified.
The Separate Solutions Method (SSM) was used where log $a_I$=log$a_J$=-3.0. Reproducibility based on three ISEs.

**Table 2.6**. Selectivity Coefficients, log $K_{I,J}^{pot}$, for **2-17**, **2-18** and **2-19** calculated using the Separate Solutions Method (SSM).

The selectivity values obtained further confirm the bromide selectivity observed for **2-18** but reminds us that there is some interference from iodide and other anions.

Tables 2.7 – 2.9 reveal the slope values and observed linear ranges for **2-17**, **2-18** and **2-19**.

| Ion | Range (log a) | Slope (mV/decade) |
|---|---|---|
| $F^-$ | -3.0→-1.0 | -8.9 |
| $AcO^-$ | -3.0→-1.0 | -45.4 |
| $SO_4^{2-}$ | | +ve slope |
| $Cl^-$ | -4.0 →-1.0 | -32.7 |
| $Br^-$ | -5.6→-1.0 | -41.2 |
| $I^-$ | -5.6→-1.0 | -52.2 |
| $ClO_3^-$ | -5.6→-1.0 | -57.1 |
| $NO_3^-$ | -5.6→-1.0 | -50.7 |
| $SCN^-$ | -5.6→-1.0 | -51.3 |

**Table 2.7.** Slope values for ISE **2-17** for the indicated activity ranges.

| Ion | Range (log a) | Slope (mV/decade) |
|---|---|---|
| $F^-$ | -4.0→-1.0 | -27.6 |
| $AcO^-$ | -3.0→-1.0 | -50.2 |
| $SO_4^{2-}$ | -4.0→-1.0 | -31.8 |
| $Cl^-$ | -5.0→-1.0 | -55.5 |
| $Br^-$ | -5.6→-1.0 | -66.1 |
| $I^-$ | -5.6→-1.0 | -57.7 |
| $ClO_3^-$ | -5.6→-1.0 | -54.8 |
| $NO_3^-$ | -5.6→-1.0 | -55.3 |
| $SCN^-$ | -5.0→-1.0 | -56.3 |

**Table 2.8.** Slope values for ISE **2-18** for the indicated activity ranges.

| Ion | Range (log a) | Slope (mV/decade) |
|---|---|---|
| $F^-$ | -4.0→-1.0 | -29.6 |
| $AcO^-$ | -4.0→-1.0 | -45.7 |
| $SO_4^{2-}$ | -4.0→-1.0 | -26.5 |
| $Cl^-$ | -5.6→-1.0 | -31.9 |
| $Br^-$ | -5.6→-1.0 | -55.8 |
| $I^-$ | -5.6→-1.0 | -58.0 |
| $ClO_3^-$ | -5.6→-1.0 | -60.6 |
| $NO_3^-$ | -5.6→-1.0 | -56.6 |
| $SCN^-$ | -5.6→-1.0 | -58.4 |

**Table 2.9**. Slope values for ISE **2-19** for the indicated activity ranges.

For heavily discriminated anions the linear response ranges are generally shorter, the LODs higher and some slopes are sub-Nernstian. Most results however showed good reproducibility and Nernstian slopes. Interestingly, **2-18** shows the only super-Nernstian response of 66.1mV/decade in Table 2.8, namely towards bromide over the linear range, indicative of a relatively strong interaction with the ISE membrane components. This is in agreement with previous data that shows that **2-18** is bromide selective.

Bromine gas, $Br_2$, and the more commonly encountered bromide ion $Br^-$ was amongst the last of the halogens discovered[145]. Bromide appears to have no essential biological role in the body. A 100mg dose of bromine can be fatal whereby only quantities above 30g bromide are considered life threatening. Historically bromides were used as tranquilisers but served as depressants if used in excess. Bromides are most commonly encountered as organobromides. Dibromomethane was used until recently with leaded petrol in order to prevent harmful lead deposits within engines by releasing lead bromide as part of the emission mixture. Other organobromides include pesticides, fire extinguishing materials and pharmaceutical intermediates. Many applications are being

ruled out due to the association of organohalogens with ozone depletion. Organobromides remain popular as synthetic intermediates as the bromide ion is a good leaving group in $S_N2$ nucleophilic displacement and bond forming reactions for example.

## 2.4 CONCLUSIONS

As was illustrated in the introduction, the use of potentiometric ISEs built on calixarene amides has been confined to cation sensing in the literature. From the results of testing of amides **2-17**, **2-18** and **2-19** a modest improvement of response towards sodium and calcium was observed for **2-18** and **2-19**, but no significant change in response order of a series of cations compared to a blank membrane was realised. The overall selectivity orders observed appear to be largely driven and dictated by cation lipophilicity and not the ionophore. Typically, a strong sodium/cation response is expected for ISEs based on calix[4]arene amides[28]. Probably due to the structural features of the amides tested, namely less than 4 lower rim substituents, bulky naphthyls proximal to amide functional groups and non *t*-butyl upper rim substituents, this 'default' response was not observed. Conversely, when configured for anion analysis, the ISEs built on **2-17**, **2-18** and **2-19** revealed bromide selectivity for **2-18** *and* a change in response order compared to a blank membrane. This result is particularly encouraging as it represents a definite deviation from a Hofmeister controlled response. The current study is amongst the first reported to use potentiometry to investigate calixarene amide responses towards anions. Further novelty is realised by testing each ionophore for both cation and anion responses, thereby increasing the possiblility of discovering a selectivity 'hit'.

Molecular models were used to relate observed analytical data with complex structures. $^1$H NMR data and molecular models predicted a cone conformation in all cases for the hosts. Molecular models suggested a cavity inclusion complex for **2-18** with

calcium(II) or sodium(I), suggesting a mode of binding akin to the well known tetraester sodium selective systems. This is a reasonable observation as both are based on the appropriately sized calix[4]arene backbone. Conversely, a peripheral binding mode between the cavity of **2-18** and the larger bromide may be preferred.

The strong interference from iodide in particular perhaps precludes the direct use of **2-18** in a real life bromide sensor where such an interferant is anticipated, but is encouraging to the synthetic chemist who can perform structural modifications to improve on the observed selectivity. Using **2-18** as a basis, several structural changes could be investigated. As anions are generally larger than isoelectronic cations, the use of the upper calixarene rim for attachment of amide groups would provide much enlarged cavities. Alternatively, longer spacers between the lower rim phenoxy oxygens and the amide groups (currently methyl spacers) may have a similar effect. Increasing the number of amide appendages to a maximum of four would allow for more possibilities of H-bonding with anions, but as a word of caution, may also increase the competition to complexation from inter and intramolecular H-bonding. Changing the bulky naphthyl groups proximal to the amide functional groups for other aliphatic and aromatic groups may also modify selectivities. Furthermore, spacers of varying length between the amide NH and such groups would moderate their steric influence and alter the ionophores complexation ability. In all cases a careful balance between overall analyte affinity and selectivity must be maintained.

# 3. Chapter 3 Urea Calixarenes

## 3.1 ABSTRACT

The synthesis of di-urea calix[4]arenes **3-1** and **3-2** is described. These hosts are incorporated into potentiometric ISEs in turn configured for cation and anion analysis. In all cases potentiometric results were compared to ionophore free blank membranes. No significantly improved response was observed towards cations and the selectivity order remained the same as for the blank. A strong general improvement in anion response was observed for the hosts, however a Hofmeister selectivity order was observed, similar to the blank membrane. Changing the membrane pre-exposure regime for **3-1** revealed that the magnitude of response towards certain anions could be modulated but the selectivity *order* remained broadly the same. A considerable margin of nitrate selectivity over chloride was observed for **3-1**, suggesting this ionophore may be of use in nitrate selective electrodes.

This chapter highlights the challenges of transferring functioning sensing regimes from non-aqueous to aqueous media.

## 3.2 INTRODUCTION

The general theme of anion recognition is introduced in chapter 1.8. In this context, chapter 1.9 goes on to explain that urea and thiourea functional groups are functional groups of choice for incorporation into various supramolecular platforms to yield anion selective hosts. These neutral hosts, including calixarenes, provide effective highly directional hydrogen bonds (2 per urea) for complex formation with anions. The urea or thiourea groups within the host's cavity is arranged to accommodate target anions according to their size and geometries.

Furthermore, in analogy to the amides described in chapter 2, urea functionality may also be viewed as a dual-functional group. In addition to the two NH hydrogen bonds available per urea for anion complexation by H-bonding, it is conceivable that the urea carbonyl group may engage in electrostatic ion-dipole interactions with cations by their localised negative charge, in a similar way to neutral amide or ester functional groups. It is the intention of this chapter to investigate this dual-use functionality. Depending on the choice of ion-exchange salt, a potentiometric ISE can be configured for either cation *or* anion response. This is the same approach as applied in chapter 2 for a series of amide calixarenes. Figure 3.1 shows a molecular model of the simple urea, propyl phenyl urea, with emphasis on the partial charges of the molecule, whose atoms are sized and coloured according to charge type and magnitude to illustrate the above point.

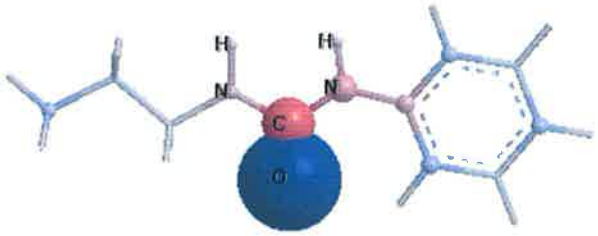


**Figure 3.1**. The energy minimised model of propyl phenyl urea. Atoms are scaled in size and coloured according to the magnitude and type of Hückel partial charges. Urea oxygen is positive (blue) and urea hydrogens are negative (red).

There are few literature examples of ISEs based on urea calixarenes showing selectivity for particular anions and none, to the best of our knowledge, investigating cation complexation. A di-phenyl (thio)urea calix[4]arene showing carbonate selectivity was recently described by Lee and coworkers[74]. There was considerable interference from $I^-$ and $ClO_4^-$ and the LOD was high at around $10^{-4}$M. Furthermore, buffered sample solutions were used. Adding to the list of adversities is the absence of any ion exchange salt additives added to the membrane cocktails. It has been demonstrated elsewhere that

ISEs cannot function well without these additives or impurities that fulfil the same role. Such ISEs were shown to manifest concentration independent behavior[122]. Other non-calixarene urea based potentiometric sensors for anions were reported. There are examples of chloride[146], sulfate[147] and hydrogen sulfite selective systems[148]. A rare example of a urea based system used for potentiometric cation detection (heavy metals) was reported by Garcia and coworkers[149].

Reports of generally modest success are typical in the field of potentiometric analysis of anions compared to the far more appealing results and selectivities obtained for cation selective systems. It is perhaps no surprise therefore, that in analogy to amide based anion hosts (chapter 2), the most frequently occurring methods for investigating urea-anion complexation revolve around non-aqueous methods based on NMR and UV/Vis, where competing solvent effects are less prominent.

The synthesis and characteristics of a number of such urea calix[4]arene hosts is described in this chapter. Diurea calix[4]arene hosts **3-1** and **3-2** were synthesised and their ability to complex both anions and cations was investigated by potentiometric methods. Based on the results of these experiments, ISE results for urea calix[4]arene **4-3** are discussed as a comparison. **4-3** has the benefit of a fluorescent optical mode of transduction in addition to potentiometric transduction. Having demonstrated definite chloride selectivity by optical transduction in non-aqueous media (chapter 4), an attempt is made to replicate this selectivity using potentiometry. From this work conclusions are drawn as to the choice of method(s) for investigating ion complexation in general and proposals for future work are made based on the current systems.

## 3.3 RESULTS AND DISCUSSION

### *3.3.1 Synthesis*

The synthesis of diurea calix[4]arenes **3-1** and **3-2** was performed according to Scheme 3.1.

**Scheme 3.1**. The synthesis of diurea calix[4]arenes **3-1** and **3-2**.

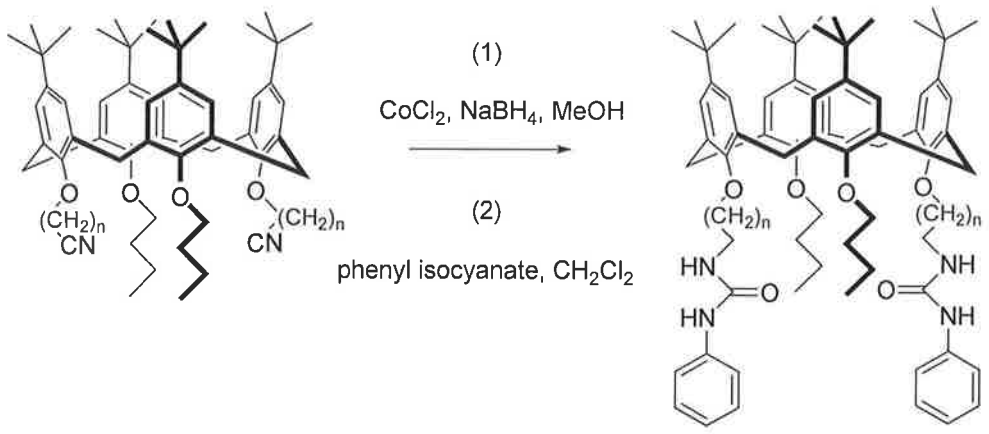


**3-1** n=3
**3-2** n=1

Step 1 took 48 hours and involved the initial reduction of the di-nitrile calix[4]arenes with $NaBH_4$ and $CoCl_2$ to di-amines, followed in step 2 by coupling with phenyl isocyanate over 12 hours to yield the target compounds. Both steps were conducted at room temperature under argon.

The synthesis of diurea calix[4]arenes **3-1** and **3-2** proceeded successfully. The final yields for these targets were 5.8% and 7.9% respectively. These rather low yields reflect some advanced degree of preorganisation, which through steric factors may suppress overall yields somewhat.

The synthesis was loosely based on a synthesis by Reinhoudt, who synthesised similar phenyl diurea calix[4]arenes and a symmetrically substituted tetra-phenylurea calix[4]arene with four butyl spacers between the urea functional groups and the calixarene phenoxy oxygens[150]. Reinhoudt obtained yields of 35% and 40% for the

diurea and tetraurea respectively. Attempts to synthesise **3-3**, a tetraurea calix[4]arene with pendant lower rim groups of varying length arranged as seen in Scheme 3.2 failed. The synthetic procedure followed that of **3-1** and **3-2** as closely as possible. Host **3-3** would have its urea functional groups arranged in a way that may provide ideal geometric complimentarity for tetrahedral anionic guests such as sulphate or phosphate. The dramatic differences in yield and reaction success discussed above attest to the major influence of apparently modest structural tuning of supramolecular structures.

**Scheme 3.2.** The attempted synthesis of **3-3**, an asymmetrically substituted tetra-urea calix[4]arene.

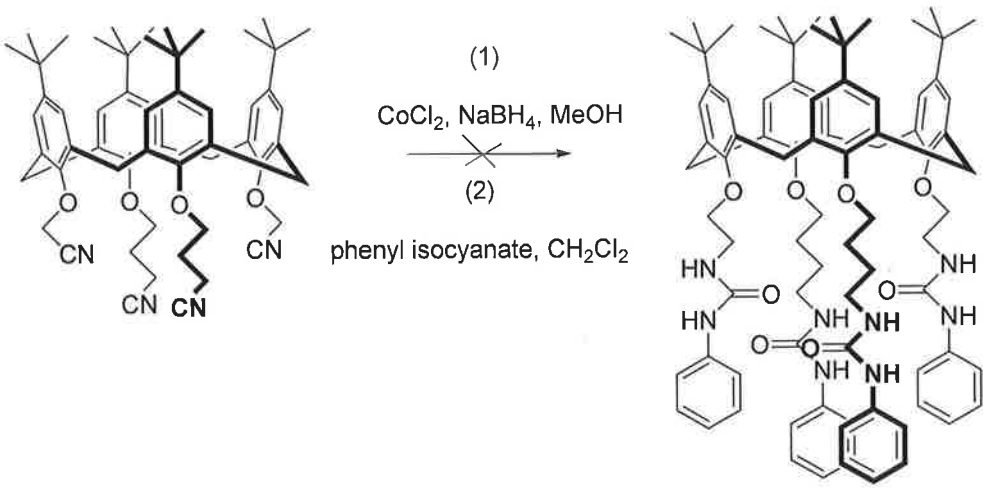


**3-3**

In addition to the influence on synthetic yields, it is clear that changes, however subtle, in preorganisation of elaborate supramolecular host structures can dramatically alter the analytical characteristics of these compounds. This also applies to the preorganisation of calix[4]arene type hosts where altering appendage length, number and symmetry can profoundly affect the selectivity manifested by the target compounds. Besides preorganisation and guest complementarity, factors like the degree of inter and intramolecular H-bonding of the uncomplexed urea host will be affected and of course the solvent effects pertaining to the compounds can all cumulatively generate diverse and surprising selectivity patterns.

### *3.3.2 Cation analysis with ISEs of di-urea calix[4]arenes 3-1 and 3-2*

ISE membranes were prepared with and without (blank) the specified ionophore. The response of blank and ionophore ISEs in log a -2.0 aqueous solutions of the specified cation were compared. Figure 3.2 shows any deviations in response as a result of the presence of ionophore.

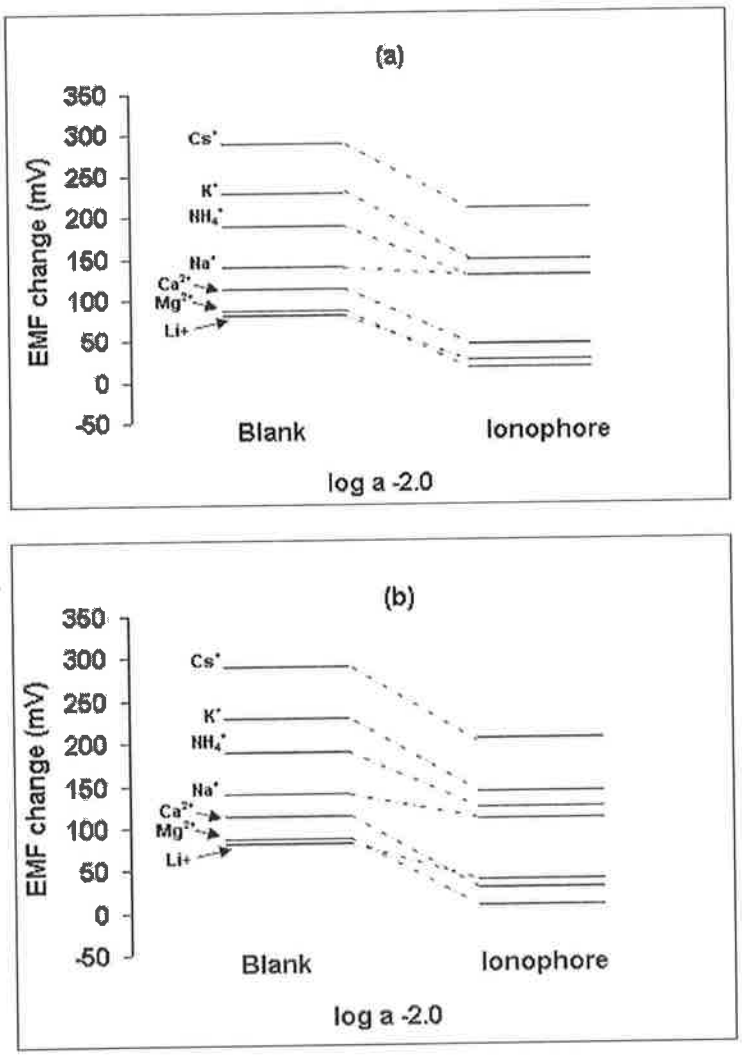


**Figure 3.2.** The comparison of potentiometric responses of a blank membrane with a) **3-1** b) **3-2**. The potential change is for the specified anion at activity log a -2.0 compared to the response in de-ionised water.

It can be seen that no general or specific increase in affinity towards cations is observed (increased potential change compared to a blank membrane). Furthermore there is no dramatic change in selectivity *order* compared to a blank membrane.

Table 3.1 reveals the formal selectivity coefficients (log $K^{pot}_{Na^+,J}$) calculated for **3-1** and **3-2** and confirms that ISE membrane interaction and selectivity order is dominated by cation size (Table 1.3) and associated solvent effects overriding any ionophore influence. This gives the Hofmeister response order.

| **Host** | **3-1** | **3-2** |
|---|---|---|
| $Na^+$ | 0 | 0 |
| $Cs^+$ | 1.34±0.29 | 1.63±0.06 |
| $K^+$ | 0.28±0.30 | 0.64±0.05 |
| $NH_4^+$ | -0.14±0.30 | 0.19±0.06 |
| $Ca^{2+}$ | -2.97±0.85 | -1.95±0.07 |
| $Mg^{2+}$ | -2.63±0.25 | -2.29±0.04 |
| $Li^+$ | -1.52±0.22 | -0.89±0.03 |

**Note**: I is the primary ion $Na^+$ and J is the interferant specified.
The Separate Solutions Method (SSM) was used where log $a_I$=log$a_J$=-2.0. Reproducibility based on three ISEs.

**Table 3.1**. Selectivity Coefficients, log $K^{pot}_{Na^+,J}$, for **3-1** and **3-2** calculated using the Separate Solutions Method (SSM).

The response slopes of the urea calixarene ISEs confirms a generally poor interaction with cations as sub-Nernstian responses are observed in all cases (Table 3.2 and 3.3).

| Ion | Range (log a) | Slope (mV/decade) |
|---|---|---|
| $Cs^+$ | -4.0→-1.0 | +49.2 |
| $K^+$ | -4.0→-1.0 | +47.6 |
| $NH_4^+$ | -4.0→-1.0 | +47.3 |
| $Na^+$ | -4.0→-1.0 | +44.8 |
| $Li^+$ | -3.0→-1.0 | +25.6 |
| $Ca^{2+}$ | -4.0→-1.0 | +17.1 |
| $Mg^{2+}$ | -4.0→-1.0 | +6.8 |

**Table 3.2**. Slope values for ISE **3-1** for the indicated activity ranges.

| Ion | Range (log a) | Slope (mV/decade) |
|---|---|---|
| $Cs^+$ | -4.0→-1.0 | +48.4 |
| $K^+$ | -4.0→-1.0 | +45.8 |
| $NH_4^+$ | -4.0→-1.0 | +44.8 |
| $Na^+$ | -4.0→-1.0 | +39.9 |
| $Li^+$ | -3.0→-1.0 | +27.6 |
| $Ca^{2+}$ | -4.0→-1.0 | +11.0 |
| $Mg^{2+}$ | -4.0→-1.0 | +3.2 |

**Table 3.3**. Slope values for ISE **3-2** for the indicated activity ranges.

### *3.3.3 Anion analysis with ISEs of di-urea calix[4]arenes 3-1 and 3-2*

ISE membranes were prepared for **3-1** and **3-2**, configured for anion analysis. As an initial indication of the effectiveness of the ionophores for anion analysis, the response of blank and ionophore ISEs in log a -3.0 aqueous solutions of the specified anion were compared. Figure 3.3 shows the results of this experiment.

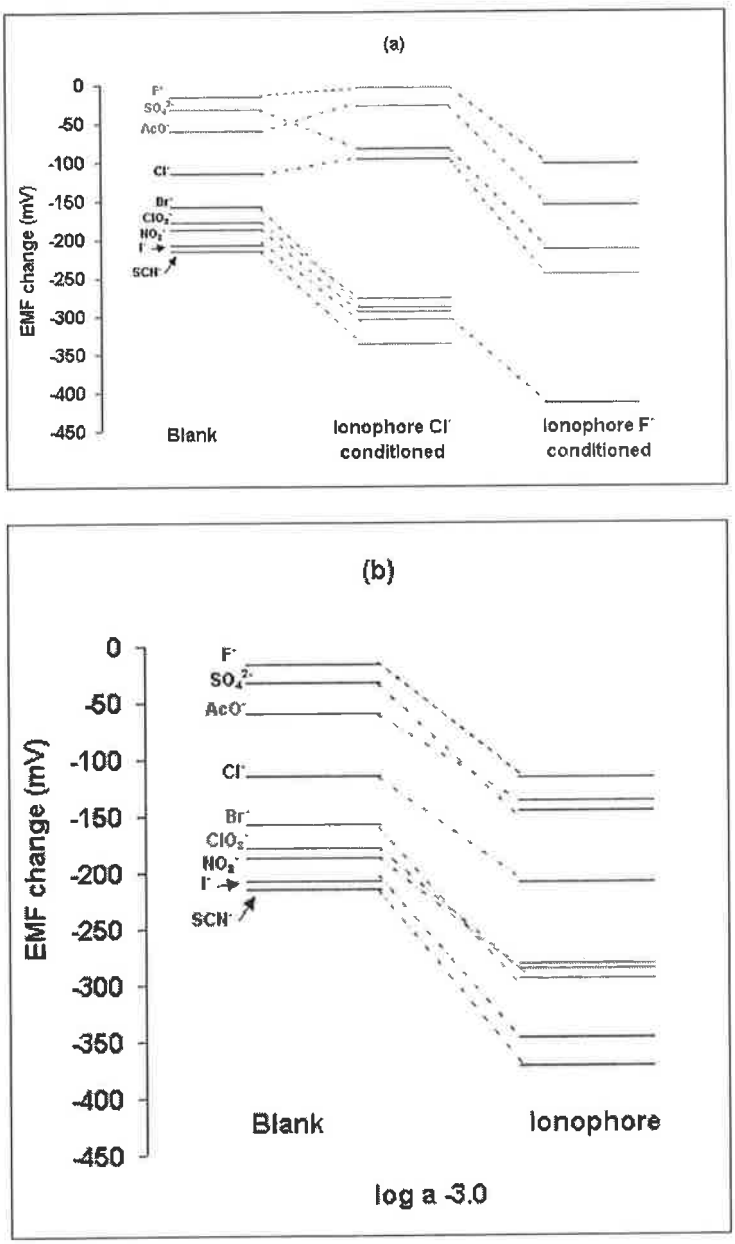


**Figure 3.3**. The comparison of potentiometric responses of a blank membrane with a) **3-1** b) **3-2**. The potential change is for the specified anion at activity log a -3.0 compared to a response in de-ionised water. Membranes were prepared and used according to the standard method (chapter 1.12) unless stated otherwise.

For both **3-1** and **3-2**, a strong enhancement of response is observed towards all anions in general, without a significant change in selectivity *order* with the exception of **3-1** showing an improved response towards $SO_4^{2-}$ and a deviation from the response order of the blank as seen in Figure 3.3a.

An exception to the generally enhanced anion responses is the case of **3-1**, where there is no improved response for chloride or smaller anions. It is interesting to note that the membranes were generally preconditioned in chloride solutions prior to ISE analysis, according to the standard ISE experimental procedure described in chapter 1.12. The choice of conditioning salt can have an effect on the responses of ISEs. Indeed, the use of a highly discriminated ion for conditioning the membranes can result in an enhanced response for the primary analyte and improved limits of detection, provided the membranes have not been in contact with any other ions previously[22]. This effect is not observed for a second or subsequent exposure to primary analyte ions. This strategy is sometimes used for optimising selectivities and LODs for ISEs. In the case where **3-1** is preconditioned with chloride a certain amount of preloading of the membrane with chloride ions occurs. Despite immersion in de-ionised water prior to ISE analysis, some of the chloride ions may have remained complexed to the ionophore within the membrane. This is indicative of strong affinity towards the anion by the ionophore, with the result of poor sensor reversibility.

The net effect of this is the observation that for **3-1** conditioned in chloride solutions, the response to chloride and the less lipophilic anions in the Hofmeister series (chapter 1.8) is generally reduced. These anions, due to their position within the Hofmeister series relative to chloride, cannot effectively displace chloride ions as they are less likely to interact with the ISE membrane. The exception appears to be sulfate, which is a doubly charged anion of high basicity, showing some improved response compared to a blank membrane from Figure 3.2a. Conversely, the more lipophilic members of the Hofmeister series succeed in *displacing* the chloride anions within the ISE membrane of **3-1**. This is clearly visible in Figure 3.2a, represented by a strong improvement in response compared to a blank membrane.

To further support this hypothesis, the ISE analysis using **3-1** is repeated using the least lipophilic anion present, fluoride, as the conditioning anion prior to analysis. For this experiment, 0.01M NaF is used as conditioning and filling solution of the working electrode. The ISE analysis is then repeated for selected anions and the results are also shown in Figure 3.3a. It is clear that the responses of all anions are enhanced in this way. In particular, the anions that previously showed no improved response compared to the blank, now show a strongly enhanced response. The reasoning behind this observation is that fluoride conditioning ions are easily displaced from the membrane phase by the more lipophilic members of the Hofmeister series.

The changing of conditioning salts (and other sensor parameters) may be used as a tool to modify the response of an ISE, but in this case the response and selectivity *order* was not changed greatly. Of course the most dramatic and permanent impact on selectivity comes from structural modifications of the ionophore itself.

Interestingly, the choice of conditioning salt did not affect **3-2** to the same extent as **3-1**. This is apparent in Figure 3.3b, where the response towards all anions is increased by more or less the same magnitude with the general chloride conditioning regime. This may indicate that the overall affinity for anions is greater for **3-1** than **3-2**, lower complexation constants being the best explanation for the better reversibility observed for **3-2**.

To further rationalise the stronger affinity (more *dependant* on conditioning salt) of **3-1** to anions than **3-2** (more *independent* of choice of conditioning salt), ISE data obtained is discussed in terms of the structural characteristics and differences between the two ionophores. Both **3-1** and **3-2** are locked into a cone conformation by upper rim *t*-butyl groups. This was initially revealed by the presence of the signature doublet pairs for the annulus methylene protons, indicative of a calix[4]arene cone conformation (see chapter

1.10 and chapter 3.5 experimental), from the $^{1}H$ NMR spectra of **3-1** and **3-2**[81]. The only difference between the two ionophores (Scheme 3.1) is the length of the spacers between the calixarene's lower rim and the urea substituents. **3-1** has a longer butylene spacer compared to the ethylene spacer of **3-2**. This confers greater flexibility on a larger lower rim cavity for **3-1**. With this greater freedom, there is reduced preorganisation and steric discrimination within the lower rim cavity. This allows the urea protons greater flexibility to orientate optimally with a greater variety of anion sizes and geometries. The net effect may be a more general, less selective response towards anions and the potential for larger complexation constants (worse reversibility). Figure 3.4 shows an energy minimised model of **3-1** incorporating a chloride anion. The large flexible lower rim cavity is apparent from the molecular model.

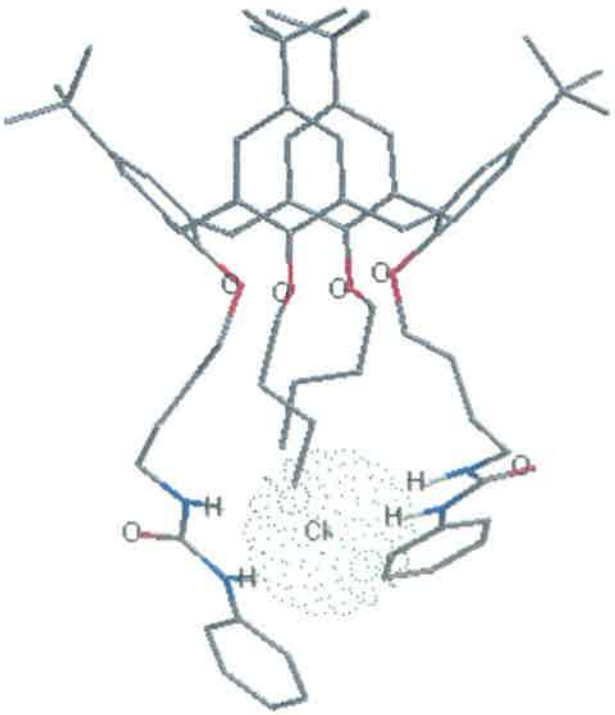


**Figure 3.4.** An energy minimised molecular model of a complex of **3-1** and a chloride anion.

The slopes of the linear response ranges for the ISEs of **3-1** and **3-2** are presented in Tables 3.4 and 3.5 for the titrations carried out.

| Ion | Range (log a) | Slope (mV/decade) | Range* (log a) | Slope* (mV/decade) |
|---|---|---|---|---|
| $F^-$ | -3.0→-1.0 | -36.4 | -4.0→-1.0 | -62.6 |
| $AcO^-$ | -3.0→-1.0 | -47.6 | -5.0→-1.0 | -52.8 |
| $SO_4^{2-}$ | -5.6→-1.0 | -27.7 | -5.6→-1.0 | -59.6 |
| $Cl^-$ | -5.0→-1.0 | -51.9 | -5.6→-1.0 | -71.9 |
| $Br^-$ | -5.6→-1.0 | -81.6 | | |
| $I^-$ | -5.0→-1.0 | -75.1 | -5.0→-1.0 | -82.2 |
| $ClO_3^-$ | -5.0→-1.0 | -66.1 | | |
| $NO_3^-$ | -5.6→-1.0 | -76.7 | | |
| $SCN^-$ | -5.0→-1.0 | -66.6 | | |
| *ISE membranes conditioned in $F^-$ prior to titrations. | | | | |

**Table 3.4**. Slope values for ISE **3-1** for the indicated activity ranges.

| Ion | Range (log a) | Slope (mV/decade) |
|---|---|---|
| $F^-$ | -5.6→-1.0 | -38.9 |
| $AcO^-$ | -5.0→-1.0 | -65.8 |
| $SO_4^{2-}$ | -5.0→-1.0 | -50.0 |
| $Cl^-$ | -5.6→-1.0 | -68.6 |
| $Br^-$ | -5.6→-1.0 | -79.4 |
| $I^-$ | -5.0→-1.0 | -75.0 |
| $ClO_3^-$ | -5.0→-1.0 | -74.3 |
| $NO_3^-$ | -5.6→-1.0 | -79.0 |
| $SCN^-$ | -5.0→-1.0 | -68.1 |

**Table 3.5**. Slope values for ISE **3-2** for the indicated activity ranges.

The slope values in Table 3.4 refer to those obtained using the standard chloride conditioning regime unless stated otherwise. Of note are the sub-Nernstian response slopes obtained for **3-1** to chloride, fluoride and acetate. These slopes are in agreement

with the generally poor responses observed for these anions, in that no improved response to a blank membrane (Figure 3.3a) was noted (no apparent ionophore influence). However, when conditioning is performed with fluoride, thus avoiding the chloride *preloading* of membranes and the resultant suppressed sensitivity, responses generally started at lower concentrations and dramatically increased slopes were observed (Table 3.4). This coincided with a marked improvement in responses compared to a blank membrane as seen in Figure 3.3a.

All the slope values obtained are super-Nernstian for **3-2**, further supporting the theory of a generally strong anion affinity with little selectivity and independence from choice of conditioning salt.

Table 3.6 shows the formal selectivity coefficients (log $K_{I,J}^{pot}$) for **3-1** and **3-2** as calculated by the SSM.

| **Host** | **3-1** | **3-2** |
|---|---|---|
| $I^-$ | 3.56±0.04 | 2.44±0.16 |
| $SCN^-$ | 4.11±0.05 | 2.77±0.05 |
| $ClO_3^-$ | 3.07±0.04 | 1.25±0.06 |
| $Br^-$ | 3.3±0.05 | 1.58±0.23 |
| $NO_3^-$ | 3.41±0.06 | 1.44±0.19 |
| $Cl^-$ | 0 | 0 |
| $SO_4^{2-}$ | -1.72±0.02 | -2.44±0.18 |
| $AcO^-$ | -1.15±0.01 | -1.20±0.05 |
| $F^-$ | -1.56±0.01 | -1.53±0.08 |

**Note:** I is the primary ion $Cl^-$ and J is the interferant specified.
The Separate Solutions Method (SSM) was used where log $a_I$=log$a_J$=-3.0. Reproducibility based on three ISEs.

**Table 3.6.** Selectivity Coefficients, log $K_{I,J}^{pot}$, for **3-1** and **3-2** calculated using the Separate Solutions Method (SSM).

Table 3.6 confirms that selectivity *order* more or less follows the Hofmeister order of response for both ionophores.

### *3.3.4 ISE characteristics of 3-1 and 3-2 and proposed further strategy*

In general, ionophores **3-1** and **3-2** bind all anions strongly, manifested by potential changes of increased magnitude when compared to the blank. These potential changes are such that the response order of anions and hence selectivity is more or less the same as a blank membrane. This response order is related to the Hofmeister series and anion basicity.

It is clear that in future work, the anion affinity must be maintained or even reduced whilst increasing the preorganisation of ionophores and hence improving their ability to discriminate more between anions by steric means.

One aspect of the results for future consideration is the use of **3-1** applied in nitrate selective electrodes. Existing commercial nitrate ISEs are largely based on ion-exchange salts only, which, like the calix[4]arene based ISEs in this chapter, show selectivity based on the Hofmeister series. Strictly speaking these ISEs are not nitrate selective but rely on the margin of selectivity of nitrate over chloride, the most prominent interferant of nitrate in freshwater samples. These sensors are used in the context that anions higher (of greater or similar lipophilicity as nitrate) in the Hofmeister series like bromide, iodide and thiocyanate, due to their absence or negligible presence in typical freshwater samples, are not considered major interferants for nitrate anaylis. The margin of selectivity between nitrate and chloride for **3-1** (Figure 3.3a) appears favourable compared to some commercially available nitrate ISEs[151,152]. This will be investigated in future research.

### *3.3.5 Improving selectivity: Tetra-urea calix[4]arene 4-3 with additional optical transduction*

In light of the results obtained for calix[4]arene ureas **3-1** and **3-2,** two strategies were pursued, using these ionophores as a basis for comparison, to achieve selective anion sensing.

Ionophore **4-3** (Figure 3.5) embodies these strategies.

1. *Structural changes of the calixarene urea ionophores.*
2. *Using additional, alternative modes of transduction.*

The synthesis of the 1,3-alternate structure of tetra-urea calix[4]arene **4-3** is described in chapter 4.

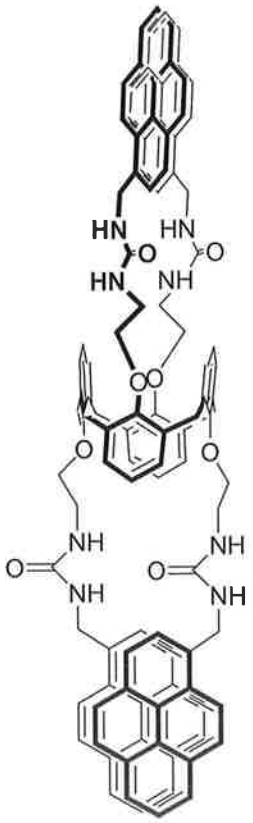


**4-3**

**Figure 3.5.** The 1,3-alternate conformation of tetra-urea calix[4]arene **4-3.**

*1. Structural changes of the calixarene urea ionophores.*

Host **4-3** contains two separate cavities for anion detection within a 1,3-alternate structure. The intention from the synthesis of **4-3** was not to achieve a tetrasubstituted calixarene in the cone conformation, hence the de-*tert*-butylated clixa[4]arene starting material was chosen. The reason for this is that the anion binding ability of a cavity with only two urea groups has proven sufficient. The universally strong anion affinities of **3-1** and **3-2**, super-Nernstian slopes and extensive response ranges demonstrated this. Conversely, the presence of four instead of two urea groups within the same calix[4]arene cavity have been shown to lead to a decrease in selectivity and complexation constants as shown by Reinhoudt[150]. This was thought to be due to increased competition to anion binding from inter and intramolecular H-bonding of the ureas. In this light, **4-3** represents an ionophore with two distinct cavities, each containing two urea functional groups.

The alkyl spacer between the calixarene phenoxy oxygens and the urea functional groups was shortened to an ethylene compared to the butylene spacer of **3-1**. It was hoped that the choice of the shorter spacer would decrease the cavity dimensions whilst increasing steric preorganisation thus leading to better selectivity patterns compared to **3-1**, which had a large flexible cavity thought to be responsible for the somewhat general anion affinity observed.

The nature of substituents proximal to a calixarenes complexing functionality was studied extensively in the literature, and was shown to have a strong bearing on ion affinities and selectivities as was discussed in chapter 2.2, particularly in terms of bulkiness and steric influence. For calixarene amides **2-18** and **2-19**, the naphthyl groups positioned directly next to amide functional groups may have contributed to the generally subtle ion binding observed by providing a steric barrier to unimpaired ion

association. Although the pyrene moieties of **4-3** are considerably larger than naphthyls, their steric influence on the complex formation ability of the nearby urea groups is thought to be relieved somewhat by the presence of an additional methylene spacer. It was hoped that some selectivity could be introduced in this way whilst avoiding a complete suppression in response to guest ions.

2. *An alternative mode of transduction.*

The pyrene moieties also have the role of conferring an optical mode of transduction on ionophore. **4-3**.

In chapter 4 the selectivity and binding affinity of **4-3** towards a series of anions is investigated. To this end, the ratiometric fluorescence properties of **4-3** and a non-aqueous titration medium were used. This represented a radical alternative to an aqueous based electrochemical transduction approach. In this way, the unambiguous virtually exclusive chloride selectivity of **4-3** was established.

**4-3** was incorporated into an ISE to see if the chloride selectivity observed optically could be replicated electrochemically. This attempt is discussed below.

### *3.3.6 Anion analysis with an ISE of tetra-urea calix[4]arenes 4-3*

For casting the ISE membranes an alternative anion exchange salt was used. The alkyl ammonium iodide salt was use instead of the standard chloride salt. As **4-3** was found to be chloride selective by optical transduction, the interference of chloride from within the membrane cocktail was thus avoided. The possible interference from iodide was considered unlikely from fluorescence investigations where no change in optical signal was caused by iodide (chapter 4). A $^{1}$H NMR study also reached the same conclusion that iodide, unlike chloride, did not appear to cause a change in chemical shift of the urea protons on exposure to a large excess of iodide ions (chapter 4.3.3). For

conditioning ISE membranes and for internal filling solutions of working ISEs, a 0.01M solution of NaI was used instead of the usual 0.01M NaCl.

The ISEs of **4-3** were initially compared to a blank membrane response, when exposed separately to a series on anions at log a -3.0. Figure 3.6 shows the results of this study.

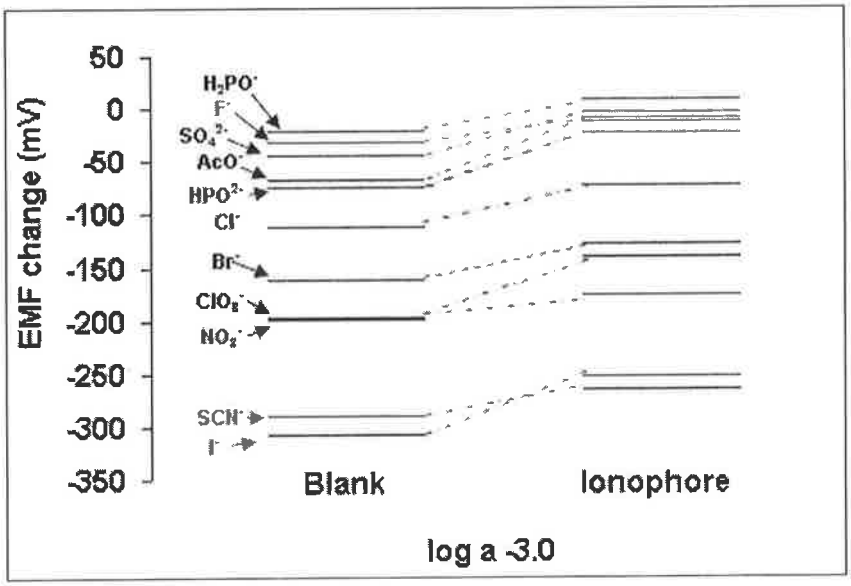


**Figure 3.6.** The comparison of potentiometric responses of a blank membrane compared with an ISE additionally including **4-3**. The potential change is for the specified anions at activity log a -3.0 compared to the response in de-ionised water.

Surprisingly, no improvement signified by increased potential change, is observed for **4-3** for any anion, including chloride. Table 3.7 shows the formal selectivity coefficients ($\log K_{I,J}^{pot}$) as calculated by the SSM for **4-3**.

| Host | 4-3 |
|---|---|
| $I^-$ | -0.21±0.01 |
| $SCN^-$ | 0 |
| $ClO_3^-$ | -1.49±0.02 |
| $Br^-$ | -2.31±0.01 |
| $NO_3^-$ | -2.09±0.01 |
| $Cl^-$ | -3.24±0.01 |
| $SO_4^{2-}$ | -5.92±0.01 |
| $AcO^-$ | -4.25±0.01 |
| $F^-$ | -4.34±0.00 |
| $H_2PO_4^-$ | -4.64±0.01 |
| $HPO_4^{2-}$ | -5.59±0.02 |
| (H) $Cl^-$ | -3.48±0.02 |
| $OH^-$ | -2.40±0.07 |

**Note**: I is the primary ion $SCN^-$ and J is the interferant specified.
The Separate Solutions Method (SSM) was used where log $a_I$=log$a_J$=-3.0. Reproducibility based on three ISEs.

**Table 3.7**. Selectivity Coefficients, log $K_{I,J}^{pot}$, for **4-3** calculated using the Separate Solutions Method (SSM).

The selectivity order follows the Hofmeister order of response. As an anecdote, titrations with NaOH and HCl revealed little interference pointing to a negligible pH sensitivity of the ISE.

This result clearly illustrates the difficulty with aqueous based ion detection methods. The chloride selectivity observed optically for **4-3** in chapter 4 could not readily be replicated by ISE analysis. It must be noted that the association constant calculated for **4-3** using fluorescence methods was of the order $10^4 M^{-1}$ which is quite low but typical for anion analysis. 150 equivalents of $Cl^-$ were required before there was no more optical signal change.

The *general* improved anion response compared to a blank observed for **3-1** and **3-2** was not seen for **4-3**. This may be due to factors that compete with the anion binding of **4-3** as previously suggested by the low chloride complexation constant observed. The chloride selectivity was most likely overshadowed by strong solvent effects associated with aqueous-membrane techniques such as potentiometry, whereby a Hofmeister order of selectivity is observed.

It is clear that a practical sensor based on **4-3** must rely on a compromise between the practical requirements of a sensor and the inherent consequences of aqueous based sensing and associated solvent effects. An optical transduction mode appears more useful for **4-3**. This is so because the analytical signal is solely dictated by an ionophoric phenomenon (the conformational stacking/unstacking of pyrenes, discussed in detail in chapter 4).

Although the magnitude of the *optical* chloride selectivity observed for **4-3** may be influenced by solvent effects and anion basicity, the fundamental presence or absence of the analytical signal is largely independent of these influences. This circumnavigates any mode of analyte-sensor interaction not causing changes in optical properties of the ionophore, which would simply not be detected.

Conversely, in potentiometry, the sensor's analytical signal cannot be assigned unambiguously to only an ionophoric phenomenon. The potentiometric signal is in fact generated by a broader range of sensor components which cumulatively determine the analyte distribution equilibrium between the aqueous sample and the ISE membrane surface[21]. Besides the ionophore, the ion exchange salt and membrane plasticizer polarity for example have a large bearing on the observed signal.

For an optical mode of transduction there is of course the possibility of guest complex formation which does not perturb the optical signal generated by the sensor host. For

example if one postulated a peripheral mode of guest binding by **4-3**, this may not result in the necessary un-stacking of the pyrene moieties present and so the complexation event would not be detected by the analyst.

Ultimately, the exact mechanism generating the analytical signal is inconsequent to the functioning chemical sensor, where the *net* observed analytical signal is paramount.

## 3.4 CONCLUSIONS

Using potentiometric ISEs, di-urea calix[4]arenes **3-1** and **3-2** did not reveal an improved response towards cations compared to a blank ISE membrane. Conversely, a strong affinity towards anions was observed, without significant deviation from a Hofmeister (blank) series of response. These results confirmed that urea functional groups are more suitable for anion complexation by H-bonding and show weaker electrostatic cation complexing ability via the urea carbonyl lone pairs than esters or amides for example. The magnitude but not the order of responses could be modulated somewhat by choice of ISE conditioning and filling solution as shown in the case of **3-1**. Due to a good margin of nitrate selectivity over chloride achieved by **3-1**, this ionophore may have some potential in a nitrate selective ISE.

Tetra-urea calix[4]arene **4-3**, which had revealed unambiguous chloride selectivity in non-aqueous media, albeit with a low binding constant of $10^4 M^{-1}$ in chapter 4, did not reveal an improved response towards any anions including chloride using ISEs. This revealed the potent effect of host structural tuning on sensor properties, when compared to **3-1** and **3-2**. Notably however, the results also demonstrated the general difficulty of replicating non-aqueous anion complexation phenomena in aqueous media. For all aqueous based ISE measurements, the response orders mirrored those of a blank

membrane, indicative of selectivity dominated by solvent effects and the Hofmeister series.

It is clear that the choice of transduction mode for analyte detection of an ionophore can introduce an inherent selectivity bias, particularly where aqueous sample phases are involved. Conversely, aqueous based methods may have more potential for real life applications, such as in water based environmental and clinical sensing.

In conclusion then, the use of more than one transduction mode is strongly recommended when developing new analyte recognition systems. This multifaceted approach gives vital information to the developer of sensors regarding molecular structural changes that may improve host selectivity *in addition* to highlighting the challenges of translating such useful phenomenon at the molecular level into practically useful sensing device.

Future development work on ionophores like **4-3**, could involve immobilisation into a lipophilic membrane by mixing or covalent attachment onto a sensor substrate. In this way the repeated and reversible analysis of *water* based samples could be carried out. A key feature for such a device could be the use of spectrofluorimetry as an alternative to electrochemical transduction, to reveal more specific, ionophore driven complexation events. For example the use of LED technology could be applied as a source and detector of electromagnetic radiation, as recently developed in our group, offers many practical advantages in this regard[153-155].

## 3.5 EXPERIMENTAL

The general procedure for assembling ISEs and using these for data acquisition is outlined in chapter 1.12. A deviation from these methods is the preparation of ISE membranes incorporating **4-3**, where the alkyl ammonium iodide exchange salt was use

instead of the chloride salt. ISEs of **4-3** were conditioned and filled with 0.01M NaI instead of NaCl.

**5,11,17,23-Tetra-*p-tert*-butyl-25,27-bis[[(N'-phenylureido)butyl]oxy]-26,28-dibutoxycalix[4]arene (3-1).** $CoCl_2.6H_2O$ (0.64g, 2.7mmol) was heated at 200°C for 20 minutes to produce blue dehydrated $CoCl_2$. This was stirred under argon in 7ml MeOH for 15 minutes. Calix[4]arene **5-4** (0.3g, 0.34mmol) was added to the suspension. 5 x 0.1g batches of $NaBH_4$ (0.5g, 13.4mmol) were added on an hourly basis and the mixture stirred at room temperature for 24 hours. $NaBH_4$ (0.5g, 13.4mmol) was added batchwise again and the mixture left for a further 24 hours. 20ml of $CH_2Cl_2$ were added and 3M HCl until the suspended black solid was largely dissolved. 25% $NH_3$ was added until the solution turned basic. The solution was extracted with $CH_2Cl_2$ (3 x 20ml). The combined organic layers were washed with 20ml water and 20ml brine and dried with $Na_2SO_4$. Upon evaporation of the solvent, 0.1g of an oily solid remained. This was placed into 2ml chloroform and phenyl isocyanate added (60µl, 0.55mmol). The resulting clear brown solution was left stirring under argon for 12 hours. Into the clear green solution, 3ml water was added to give a brown emulsion. The organic layer was extracted with chloroform (3 x 10ml), washed with water (10ml) and brine (10ml) followed by dring with $Na_2SO_4$. 0.1g of a brown oil remained. LC-MS analysis of the product revealed this crude to consist of 37.6% **3-1**. 22.7mg of a white solid were recovered by SP-HPLC, representing an LC recovery yield of 60.4% and an overall yield of 5.8% **3-1**. The SP-HPLC purification and isolation method used is described in detail in chapter 6. mp: 245-247 °C. IR (KBr): 3338, 1645cm$^{-1}$. 1H NMR (400MHz, $CDCl_3$): δ 7.61 (m, 2 H, Ar*H*), 7.15 (d, 4 *H*, Ar*H*), 7.09 (s, 4 *H*, Ar*H*), 6.09 (m, 4 H, Ar*H*), 6.42 (m, 4 H, Ar*H*), 5.72 (s, 2 H, ArN*H*CO), 5.65 (t, 2 H, CON*H*$CH_2$), 4.33 and 3.10 (ABq, 8 H, Ar$CH_2$Ar, J=12.4), 3.94

(t, 4 H, $CH_3(CH_2)_2CH_2OAr$), 3.80 (t, 4 H, $NH(CH_2)_3CH_2OAr$), 3.64 (m, 4 H, $NHCH_2$), 3.39 (m, 4 H, $NHCH_2CH_2$), 1.99 (m, 4 H, NH(CH2)$_2$CH2), 1.81 (m, 4 H, $CH_3CH_2CH_2$), 1.45 (m, 4 H, $CH_3CH_2$), 1.29 (s, 18 H, *t*-butyl), 0.90 (t, 6 H, $CH_3CH_2$), 0.82 (s, 18 H, *t*-butyl). $^{13}C$ NMR (50MHz, $CDCl_3$): 151.2, 142.3, 132.5, 127.2, 117.3, 106.3, 105.1, 97.1, 64.1, 32.1, 29.8, 23.1, 22.4, 18.6, 16.2 ppm. ESI MS +m/e 1163.8 ([M + $Na^+$], calcd 1163.8). HPLC purity: 98.1%.

**5,11,17,23-Tetra-*p-tert*-butyl-25,27-bis[[(N'-phenylureido)ethyl]oxy]-26,28-dibutoxycalix[4]arene (3-2).** Calix[4]arene **5-6** (0.40g, 0.48mmol) underwent $NaBH_4$ reduction using an identical procedure as for the synthesis of **3-1**. In this way, 0.27g of a brown oily solid was obtained. This was placed into 8ml of chloroform and phenyl isocyanate (175µl, 1.6mmol) was added. The solution was left stirring under argon for 12 hours and the work up proceeded as in the synthesis of **3-1**. 0.18g of a brown oil remained. LC-MS analysis of the product revealed this crude to consist of 29.0% **3-2**. 41.2mg of a white solid were recovered by SP-HPLC, representing an LC recovery yield of 78.9% and an overall yield of 7.9% **3-2**. The SP-HPLC purification and isolation method used is described in detail in chapter 6. mp: 258-260 °C. IR (KBr): 3343, 1648$cm^{-1}$. 1H NMR (400MHz, $CDCl_3$): δ 7.45 (m, 2 H, Ar*H*), 7.31 (d, 4 *H*, Ar*H*), 7.08 (s, 4 *H*, Ar*H*), 6.92 (m, 4 H, Ar*H*), 6.39 (m, 4 H, Ar*H*), 5.60 (s, 2 H, ArN*H*CO), 5.05 (t, 2 H, CON*H*$CH_2$), 4.32 and 3.11 (ABq, 8 H, Ar$CH_2$Ar, J=12.4), 3.92 (m, 4 H, $NHCH_2$), 3.71 (t, 4 H, $NHCH_2CH_2OAr$), 3.62 (t, 4 H, $CH_3(CH_2)_2CH_2OAr$), 2.41 (m, 4 H, $CH_3CH_2CH_2$), 1.32 (s, 18 H, *t*-butyl), 1.22 (m, 4 H, $CH_3CH_2$), 0.88 (t, 6 H, $CH_3CH_2$), 0.74 (s, 18 H, *t*-butyl). $^{13}C$ NMR (50MHz, $CDCl_3$): 135.9, 132.1, 129.4, 124.9, 68.5, 34.2, 32.3, 30.0, 28.2, 24.2, 22.6, 16.7, 14.4 ppm. ESI MS +m/e 1107.9 ([M + $Na^+$], calcd 1107.7). HPLC purity: 97.6%.

# 4. Chapter 4 Optical Sensing: A Chloride Selective Calix[4]arene

## 4.1 ABSTRACT

A neutral 2-site chloride selective compound has been developed (**4-3**), based on a 1,3-alternate tetra-substituted calix[4]arene providing a preorganised supramolecular scaffold. The resultant supramolecular cavity is amongst the first to combine urea functional groups bridged with single methylene spacers to pyrene moieties. It combines a naturally and synthetically proven H-bonding system with the elegant ratiometric fluorescent signalling properties of an intramolecular pyrene excimer system, triggered by conformational changes upon anion coordination. The excimer emission of **4-3** is quenched, with a simultaneous rise in the monomer emission solely by the chloride anion amongst a wide variety of anions tested. **4-3** has an association constant of $2.4\times10^{4}M^{-1}$ with chloride. The suitability and advantages of ratiometric optical sensor compounds like **4-3** for use in practical sensor devices is discussed. **4-3** has an LOD of $8\times10^{-6}M$ with chloride in acetonitrile-chloroform (95:5 v/v). A dynamic fluorescence study revealed a response time of <3 seconds. A recently developed and simple HPLC based purification method complimented conventional organic work up methods to yield pure product.

## 4.2 INTRODUCTION

The combination of molecular platforms with (thio)urea functionality crowned with fluorescent signal transduction provides the basis for powerful optical sensors for anions and has received much interest amongst researchers recently[42,156-163].

General desirable properties for organic fluorophores are rigid, planar systems with ample multibond conjugation. Fluorescent moieties available to the scientist, in addition to conjugated aliphatic entities (e.g. alkene based) include aromatics such as optionally substituted benzenes (e.g. nitrobenzene), anthracenes, naphthalenes and pyrenes.

Within organic supramolecular chemistry and guest recognition systems derived therefrom, there are four main approaches for generating fluorescence emissions that will be briefly introduced here with illustrative examples[33]. There are many reviews and books on the subject, and the state of the art has recently been reviewed[47].

*Photoinduced Electron Transfer (PET)*

Photoinduced Electron Transfer systems (PET) are the most widely encountered to date. In the case of supramolecular hosts these systems contain a fluorophore linked by a spacer to a cavity or other guest recognition site. The fluorescence signal is influenced by the presence or absence of a guest, which in turn influences the movement of electrons to and from the fluorophore from a nearby redox site, depending on redox potentials. The azacrown compound in Figure 4.1 illustrates this principle[164]. The crown unit serves as a means of selectively complexing $K^+$ ions via the formation of electrostatic bonds with the nitrogen and oxygen lone pairs. The recognition site is linked to an anthracene fluorophore by a methylene spacer. With all the required components in place there is an absence of fluorescence for the uncomplexed host. This is because of a PET of the lone pairs within the crown moiety to the fluorophore, thus quenching fluorescence. In the complexed state the lone pairs are occupied by the electropositive potassium ion and so cannot undergo PET to quench the fluorescence as

they no longer have a suitable redox potential. In this case the fluorescence is turned on.

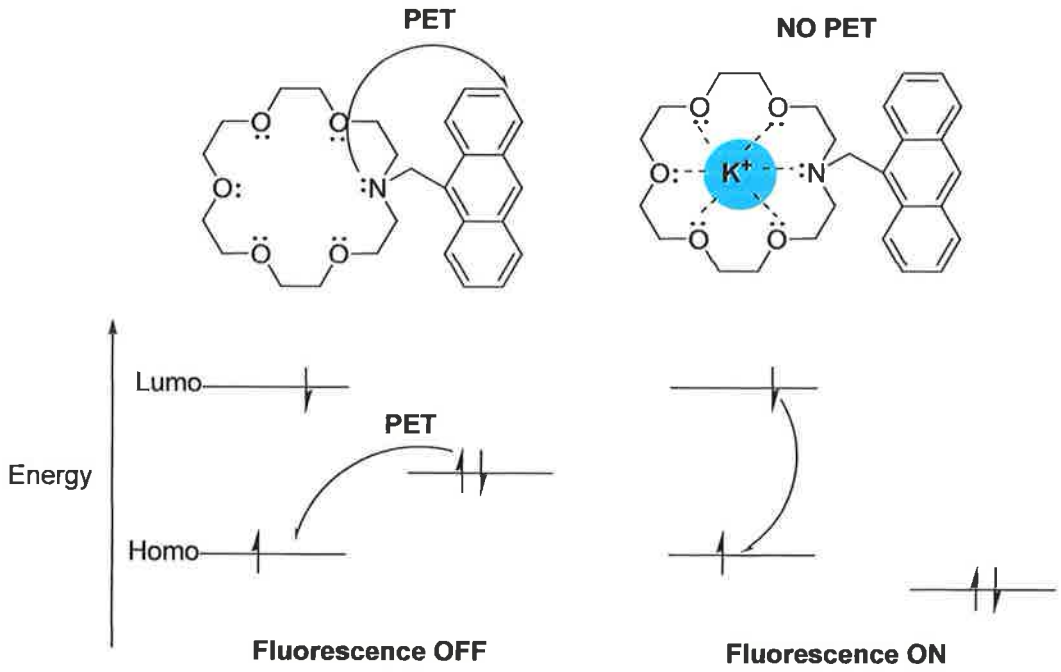


**Figure 4.1**. The complexation of potassium by an azacrown and the resultant switching ON of fluorescence by Photo Electron Transfer (PET). This is illustrated in terms of structures and associated frontier orbital energy diagrams.

There are several variations on this theme, for example reverse PET, whereby electrons are transferred from a fluorophore to an electropositive centre. This also turns off fluorescence. In all cases an On/Off fluorescence scenario correlates usefully to the prescence or absence of an appropriate target guest.

*Electronic Energy Transfer (EET)*

Electronic Energy Transfer (EET) systems, which contain at least two non-identical photoactive units, are also used to obtain systems that exhibit chemically mediated fluorescence. The signaling mechanism is largely based on the relative orientation and distance between the photoactive units. Being non-identical, each unit has an excited

state energy of different magnitude. The higher energy excited state transfers energy to the lower excited state. If the photoreactive units are particularly close, orbitals can overlap, at somewhat greater distances (about 0.5nm and greater) there is dipole overlap. The degree of proximity between the units dictates the overlap of the donor emission and the acceptor absorption spectra. The EET quantum efficiency is thereby directly influenced. At the same time each excited state produces its own unique emission and thereby a ratiometric emission signal can be obtained. The key advantages of ratiometric systems are there intrinsically self-calibrating nature. EET is exploited analytically in host-guest chemistry by guests who selectively control the relative distance and orientation between photoactive units, thereby generating a useful signal. An elegant example of EET was given by Valeur and co-workers who detected $Pb^{2+}$ using a coumarin based bichromophore[165].

The structure in Figure 4.2 wraps around a $Pb^{2+}$ ion bringing donor and acceptor close together to facilitate EET. The structure is an open chain crown, forming a cyclic-like structure by electrostatic interaction of oxygen and nitrogen lone pairs with the $Pb^{2+}$.

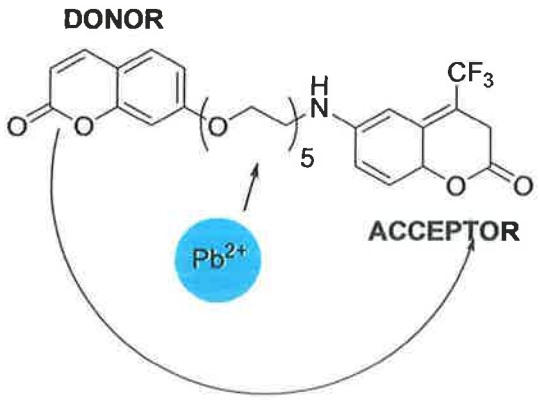


**Figure 4.2.** The complexation of lead ($Pb^{2+}$) results in cyclisation of the depicted coumarin bichromophore, facilitating increased proximity between donor and acceptor moieties which enable Electron Energy Transfer (EET).

The $Pb^{2+}$ binding event results in a plethora of optical signal changes. In addition to the ratiometric emission signal change, there are wavelength and intensity changes in both the absorption and emission spectra. The resultant output may be viewed as complex optical signatures, but conversely allow considerable scope for analytical signal interpretation.

*Internal Charge Transfer (ICT)*

Another type of signal is generated by an organic Internal Charge Transfer (ICT) mechanism. Such hosts ressemble PET systems somewhat, but without a distinct spacer between the remaining two host components, a lumo/fluorophore and the recognition site. An intimate overlap of relevant orbitals is possible in this case. Such structures contain an electron rich donor part and a suitably positioned acceptor part. These are linked for example by suitable conjugation. A considerable excited state dipole is generated upon excitation as electrons redistribute within the system. The presence of a suitable guest (or solvent related species such as protons) interacts with this dipole and the charge transfer process. The result can be a shift in both absorption and emission spectra wavelengths, providing a variety of means to probe host-guest interaction. There is a contrast with the character of a PET signal therefore. The signal for ICT systems is intensity ratiometric based due to guest induced wavelength shifts. The PET signal is more single wavelength, largely emission intensity based and displays extremes of signal chracter: ON or OFF. It is perhaps more robust and simple in construction and modus operandi. Figure 4.3 shows a simple phenoxazinone chromo/fluorophore host to illustrate a functioning guest recognition system based on ICT[166]. It is worth noting that this structure slightly ressembles the azacrown in Figure

4.1, perhaps the most noteworthy exception being the absence of a methylene spacer between the guest recognition site and the lumo/fluorophore.

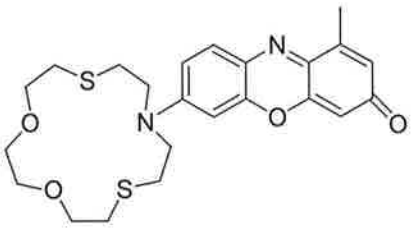


**Figure 4.3**. A phenoxazinone chromo/fluorophore host with crown receptor moiety signalling guest complexation by Internal Charge Transfer (ICT).

The chromo/fluorophore in Figure 4.3 contains the prerequisite donor group, which is the amino group within the crown moiety. The carbonyl group serves as acceptor completing the donor-acceptor couple required for ICT. Both the crown moiety and the carbonyl group have additional functions in that both can conceivably bind electropositive species such as cations or protons via electrostatic interactions.

When the phenoxazinone is subjected to a series of cations including protons the absorption spectrum shows a red shift, except for exposure to $Hg^{2+}$. This is thought to be due to carbonyl coordination whereby the acceptor character of the system is enhanced through an increased positive character. This favours enhanced charge transfer from the amino donor moiety, lowering the energy gap between frontier orbitals and raising the absorbed wavelength. Conversely, when subjected to $Hg^{2+}$, complexation is thought to occur within the crown moiety and not via the carbonyl, restraining the amino donor electrons and so reducing the system's conjugation, manifested by a blue shift of relevant absorption bands. The emission spectra reveal further truths about the system[167]. If the acceptor part of a host complexes a heavy metal like $Hg^{2+}$ there would be a tightening of the bond with the carbonyl oxygen upon excitation, in the case of the above example. This would lead to fluorescence quenching

by energy or electron transfer. On the other hand, if the donor part of an ICT type host complexes a cation, the excited state of the complex would lead to cation ejection and so no major difference in the emission spectra between the free and complexed forms would be observed. The phenoxazinone in Figure 4.3 continues to emit in the $Hg^{2+}$-complexed state, suggestive of excited-state decoordination from the *donor* part of the fluorophore. This serves as a useful analytical signal in addition to providing evidence regarding the mode of host-guest interaction. The $Hg^{2+}$ was clearly shown to complex in the crown moiety of the phenoxazinone and not the carbonyl group, unlike all the other cationic analytes tested.

*Monomer-Excimer systems*

The final type of fluorescence signal discussed is based on Monomer-Excimer systems, also the main focus of this thesis chapter. Monomer-Excimer systems are similar to EET systems in that the signal is generated by two or more fluorophore units typically linked in an intramolecular fashion, the signal characteristics being directly related to the distance and orientation between two appropriate fluorophores and the overlap of appropriate orbitals. For an excimer emission to be obtained these fluorophores are identical. The presence or absence of an appropriate guest results in a conformational stacking or un-stacking of the fluorophore moieties and so dictates the signal observed by the analyst. Anthracene and pyrene are typical examples. However, the main subject of this chapter is a monomer-excimer type signaling based on pyrene moieties.

The main distinguishing feature of monomer-excimer systems analytically, is that the signal comprises at least two distinct emission wavelengths. The analytical signal is therefore ratiometric as opposed to single wavelength intensity based. The principal

advantage of a dual wavelength or ratiometric system is that it is self-calibrating to a certain extent.

For now it will suffice to say that the organic chemist generally employs one of two strategies to harness the potential of monomer-excimer systems. Consider a supramolecular host system for example, with two intramolecularly linked pyrene moieties. If appropriate guest complexing functional groups are placed within the supramolecular scaffold, the presence of a guest can dictate the relative orientation and distance between the two pyrene moieties. The guest either levers the moieties apart or it may bring them together. Either strategy will lead to a clear change in emission signal signifying the presence of that guest. Figure 4.4 illustrates a general mechanism for one of the strategies whereby guest complexing levers apart the previously stacked pyrene moieties and a typical change in the emission spectrum to be anticipated is revealed. In this case the excimer emission, always at the higher wavelength, is reduced, with a concurrent rise in monomer emission. The ratio of these intensities comprises the analytical signal.

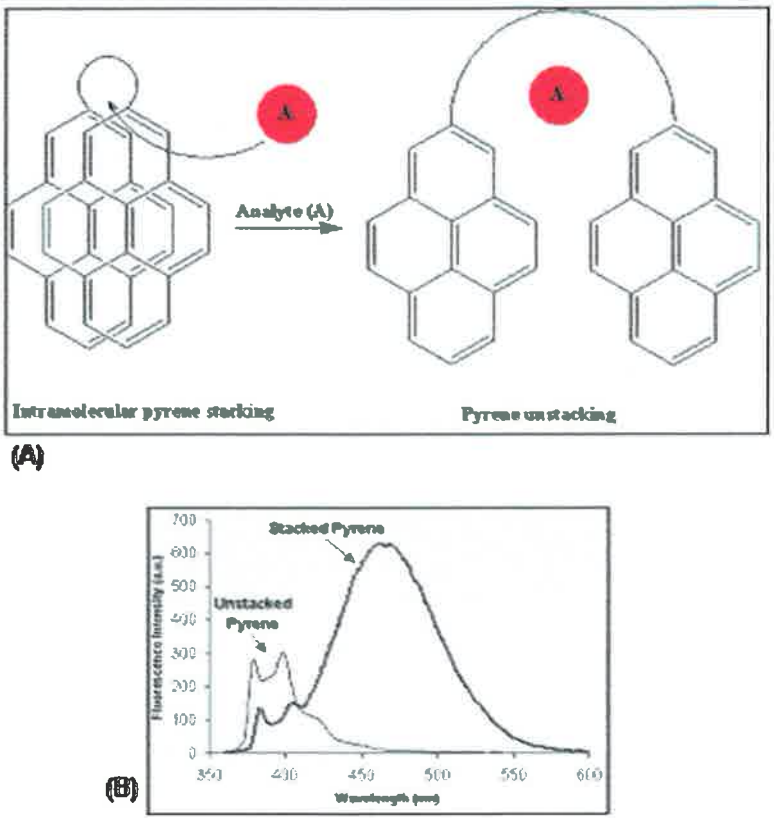


**Figure 4.4**. (A) An uncomplexed host complexes guest analyte A in its preorganised cavity levering apart the previously stacked pyrene moieties. (B) The excimer emission, always at the higher wavelength, is reduced with a concurrent rise in the monomer emission[†]. The two emission bands form the basis of a ratiometric signal.

In chapter 4.2.1, the chemistry of pyrene and the exploitation of monomer-excimer ratiometric fluorescence signaling will be elucidated in more detail.

*Some practical considerations when chosing an emission mode*

For the designer of sensor systems, some obvious advantages and disadvantages of the various approaches to fluorescent signal generation must be considered. For a start, the nature of the real life sample matrix or solvent where the sensor is to be applied must be considered. If the target analyte is a metal cation for example and the sample solvent is known to show great variations in pH, one must be aware that PET and ICT

[†] The illustrative emission spectra are of host **4-3** discussed in chapter 4.3.3.

are particularly pH sensitive mechanisms. Both involve the movement of electrons along clearly defined redox pathways. The perturbation of this movement, caused by the analyte, is intrinsic to the analytical signal. Protons and pH, like other cations, may be considered as a potential interferant and being the smallest of cations are uncanny at occupying the complexing sites of many carefully designed preorganised recognition systems. Science can take advantage of this, whereby the proton becomes the target analyte and so a pH sensor is born. There are numerous ICT based pH sensors for example[168].

For EET and monomer-excimer systems, the analytical signal is largely based on a relative physical orientation and distance between two or more fluorophores. The guest recognition function or cavity within the host is comparatively discreet from this process and so solvent pH and polarity are not *as* important. Of course solvent characteristics can rarely be completely ignored, for example solvent viscosity can control the dynamics of approach or distancing of the fluorophores in a monomer-excimer system affecting the sensor signal[169]. Solvent polarity can also affect bifluorophoric systems. For example two pyrene units, being apolar and hydrophobic, will aggregate more-so in polar solvents as this is energetically more favourable. This increased proximity will change (but not eliminate) the ratiometric emission signal (This was also the case for host **4-3** as discussed in chapter 4.3.5). The change is not as dramatic as in PET systems for example where a signal ON or OFF situation prevails.

EET, ICT and monomer-excimer systems all yield more than one signal wavelength, meaning a ratio of emission or absorbance wavelength intensities comprises the analytical signal. The PET system typically relies on the intensity of a single emission wavelength. The former three mechanisms are therefore somewhat self-calibrating, whereas PET sytems are not. This can be rationalized for a sensor operating in a

riverine situation. A change in water turbidity (and hence the transmission of electromagnetic radiation through the sample) cannot easily be distinguished from a change in analyte concentration for single wavelength systems, but in the same scenario, wavelength intensity *ratios* need not be affected. The practical advantages of ratiometric systems are elaborated on in chapter 4.3.5.

In light of the above discussion, Photoinduced Electron Transfer (PET) systems do not seem very practically appealing. It is however the sheer versatility and simplicity of PET systems that has led to the PET mechanism being relied on in the majority of fluorescence based recognition systems to date. The elaborate structural re-orientations required for monomer-excimer and EET systems are irrelevant. Via a spacer, one of many fluorophores with an appropriate redox potential can be attached covalently to many preorganised guest recognition systems. Synthetically, this can often be straightforward and thereby a fluorescent recognition sytem is born out of well characterized and reliable preorganised systems with relative ease. The selective affinity of crown ether towards potassium has been well known for many decades in a non-chromophoric capacity. By attaching an anthracene fluorophore to an azacrown recognition moiety via a methylene spacer (Figure 4.1), a powerful and selective recognition event was harnessed and brought into the realm of optical sensing[164].

The practical reality of sensor design is that it is a long road from conceptual design to a functioning sensor device. The synthetic effort required to achieve good analyte selectivity alone is easily underestimated. To overcome some of the problems discussed above, two or more fluorescent signal generating mechanisms may be combined. This can have the advantage of a broader variety of output signals (ratiometric and intensity based etc.) and can facilitate versatile multi-analyte recognition. A hybrid approach is perhaps a new trend in chemistry or science as a whole, where we see increasing

overlap of previously compartmentalized disciplines and approaches. The fluorogenic calix[4]arene in Figure 4.5 is a recent example of this approach employing both PET *and* monomer-excimer emission signal principles[140].

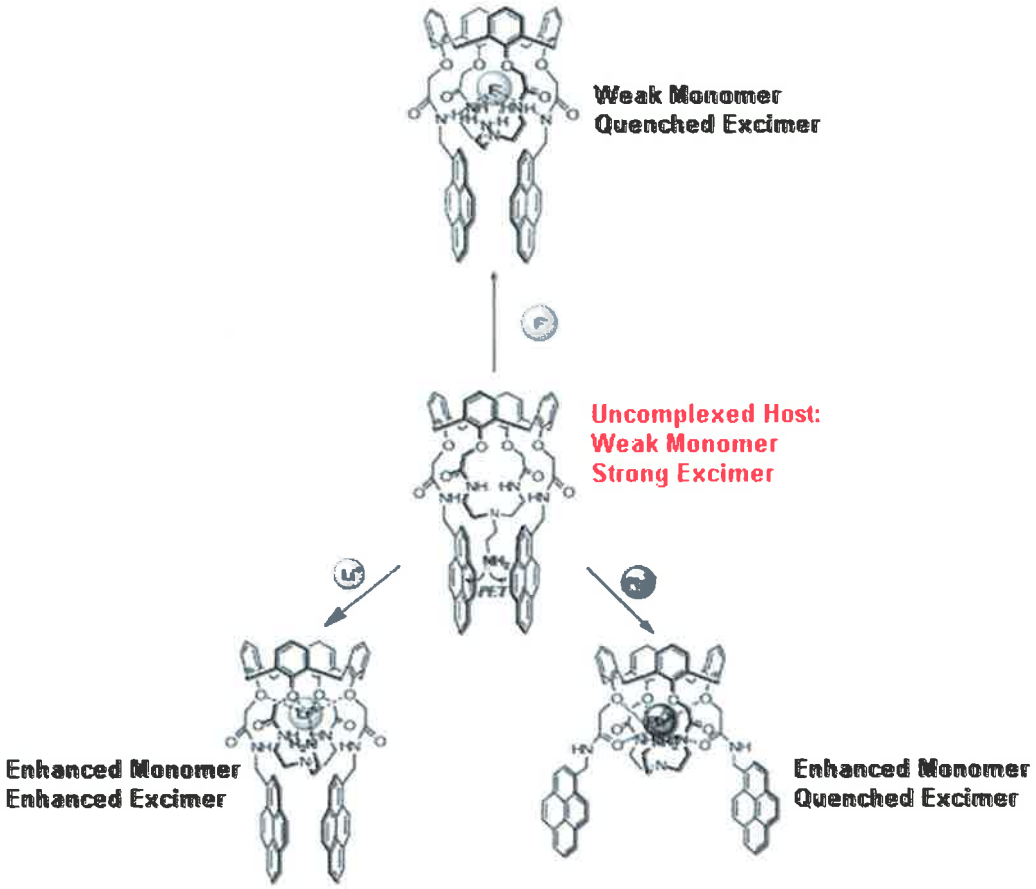


**Figure 4.5**. A fluorogenic calix[4]arene with an analytical signal based on PET *and* monomer-excimer mechanisms.

The free calix[4]arene shows a weak monomer emission due to PET from the amine lone pair and a strong excimer signal as two pyrenes are stacked appropriately. The redox potential is not appropriate for the amine lone pair to quench the excimer emission. Adding $Li^+$ disables the PET and so the monomer emission is enhanced. The excimer emission is enhanced as the pyrenes remain stacked. Adding $Pb^{2+}$ to the free host also disables PET by arresting the movement of the amine lone pair. A conformational rearrangement results in pyrene separation and a concurrent quenching

of the excimer emission. Anions interact with the amides and amine by hydrogen bonding. The free host selectively complexes $F^-$. The redox potential of the $F^-$ present is appropriate to subdue both monomer and excimer emissions by PET. Three distinct analytes, including oppositely charged ones, could be detected and distinguished with one host system. If one considers the hypothetical scenario where one pyrene is removed from this calix[4]arene (and thereby the availability of any excimer emission), only a PET mechanism would remain to optically detect the presence *and* identity of the guest. $Li^+$ and $Pb^{2+}$ could still be detected as monomer emissions would be enhanced but they could not be distinguished as easily as any conformational change of the host would not be relayed to the analyst. Furthermore, the host would most likely be poorly sensitive to anions as only a weak monomer emission would be observed in the free and complexed form. Clearly, the maximum analytical potential of the fluorogenic calix[4]arene in Figure 4.5 could only be realised by employing more than one mechanism for generating a fluorescent signal.

### *4.2.1 Pyrene chemistry and ratiometric fluorescence signalling*

Pyrenes are a particularly elegant basis for monomer-excimer ratiometric based optical sensors, with the ratio of two emission wavelengths typically used to generate the analytical signal[170,171]. Further discussion will focus on such systems to illustrate monomer-excimer chemistry in general. Förster discovered the useful features of the pyrene emission spectrum in 1954[170]. When excited around 340nm, the fluorescence spectrum of pyrene systems can contain two distinct emission regions, due to monomer and excimer (excited dimer) emissions. There are two sharp monomer emissions typically around 375nm and 400nm ($\lambda_{max}$). When two pyrene moieties overlap in an *intramolecular* fashion, there is a resultant $\pi$-$\pi$ orbital interaction which leads to a broad

characteristic excimer emission, typically at 480nm ($\lambda_{max}$). This phenomenon is possible because an excited state monomer (like a single pyrene) has a sufficiently long lifetime to interact with a ground state pyrene partner (shorter lifetime) to form an excimer. This explains the observed red-shift relative to the monomer emission and the broad nature of the emission. Furthermore there is a lack of vibrational features in the excimer signal.

The excimer and monomers exist in a state of dynamic equilibrium. The equilibrium position of the system is controlled by excitation energy (electromagnetic radiation) and local concentration of fluorophores. Rigid preorganised supramolecular structures are an ideal means to providing this close, preferably reversible intramolecular proximity or local concentration. The photophysics of excimer formation was studied in detail by authors like Birks[171].

Excimer emission may occur due to *intermolecular* association of fluorophores, but this is relatively rare and requires a certain forcing together of fluorophores to emulate the high *local* concentrations obtained in intramolecular systems. Besides using un-practically high concentrations to force intermolecular pyrene association, a similar effect can for example be achieved via the pseudo-intramolecular interlocking of complimentary DNA strands derivatised with pyrenes[172]. The remainder of this discussion will focus on intramolecular pyrene interactions.

A useful way to control intramolecular pyrene 'stacking' and 'unstacking' is by placing guest coordinating functionality in the proximity of an intramolecular pyrene system to yield a preorganised host. The addition of a guest may selectively 'stack' or 'unstack' such a system due to a steric levering apart of two pyrenes or the reverse. This is the basis for an excellent analyte sensing mechanism.

To date the pyrene excimer-monomer system has been exploited mainly for cation sensing[82,173-183] but there is an increasing focus on anion sensing[141,184-186]. Some recently published pyrene derivatives for cation and anion recognition are shown in Figure 4.6.

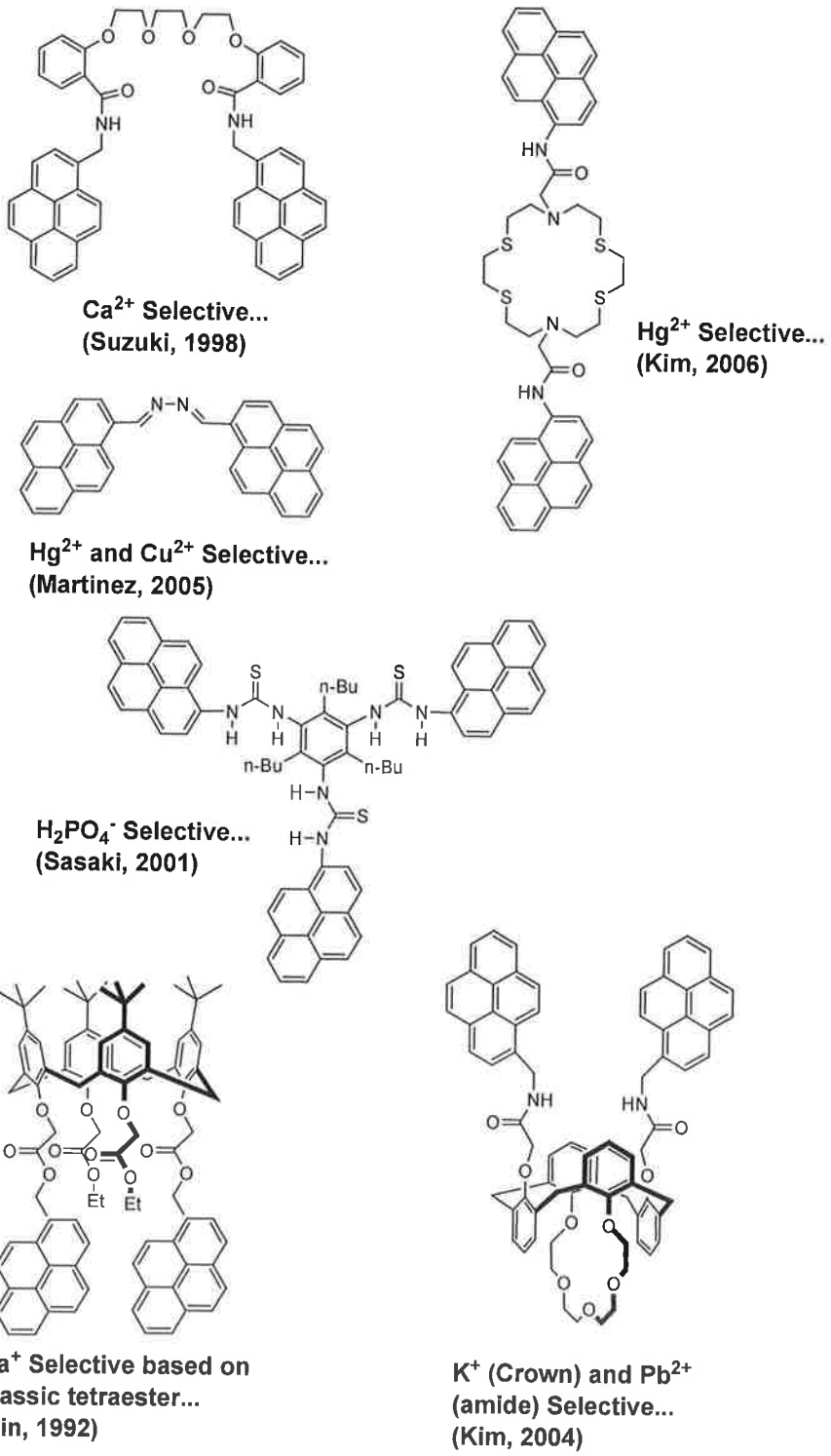


**Figure 4.6**. Examples of fluorescent ion recognition systems, which all include a pyrene excimer emission component. Some calix[4]arene examples are also included.

The host structure labeled '$Ca^{2+}$ selective' in Figure 4.6 for example shows no excimer emission in the uncomplexed state. The inclusion of $Ca^{2+}$ by complexing with oxygen lone pairs and NH hydrogen bonds gives rise to an excimer emission. The $Ca^{2+}$ complexing event induces a conformational bringing together of the fluorophore units[183]. Conversely, the tetraester calixarene with two pyrene moieties labeled '$Na^{+}$ selelective' in Figure 4.6 reveals a strong excimer emission in the uncomplexed form. $Na^{+}$ positions itself between the pyrenes resulting in their spatial separation and a quenching of the excimer signal with a concurrent rise in the monomer emission[175].

### *4.2.2 Building the host: Previous combinations of pyrenes with (thio)urea functional groups*

To the best of our knowledge there are few examples where pyrene and (thio)urea systems have been proximally combined in anion receptors[187,188] and none based on a calixarene platform.

Sasaki and coworkers synthesized a tripodal anion host (Figure 4.7) with pyrenes directly adjacent to 3 thiourea groups[187].

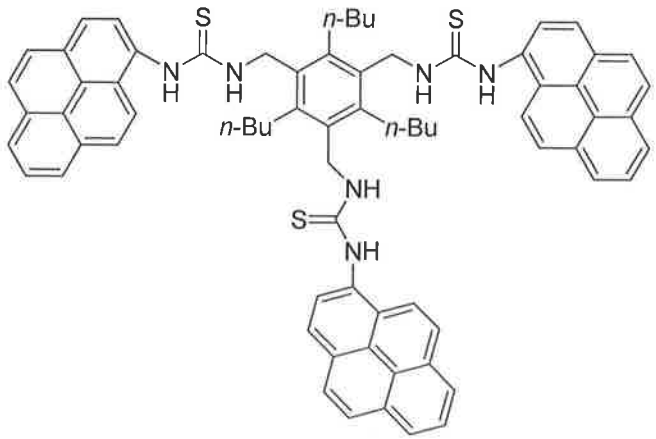


**Figure 4.7.** A fluorescent tripodal host for anions with urea functionality and pyrene moieties.

This structure revealed a fluorescent monomer-excimer emission that could be exploited for anion recognition. Modest $H_2PO_4^-$ selectivity with interference from $CH_3COO^-$ and $Cl^-$ was observed. Furthermore, only modest deviation from a typical Hofmeister selectivity, following anion basicity order was observed.

Werner describes a tripodal nucleotide anion host, shown in Figure 4.8, which has relatively long propyl spacers between pyrene moieties and ureas[188]. These long spacers meant that complexation did not yield an analytically useful changing monomer-excimer signal as there was inefficient communication between guest binding sites and the pyrene signaling moieties, presumably due to a lack of suitable preorganisation and excessive flexibility of the pyrene pendant groups.

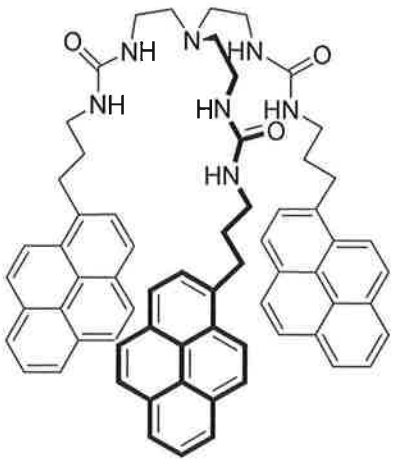


**Figure 4.8**. A tripodal nucleotide anion host based on urea and pyrene moieties.

This chapter describes the combination of more than one pyrene moiety within the same calix[4]arene scaffold, also containing anion complexing urea functional groups, linked to pyrene moieties via a methylene spacer, leading to host **4-3**. This is envisaged as the basis for a ratiometric fluorescent anion sensor. When two pyrene moieties stack in an intramolecular fashion and an excitation wavelength of about 340nm is applied, an excimer emission appears at about 450nm and there is a smaller monomer emission at

around 400nm in the uncomplexed state. When this host binds an appropriate anionic guest, conformational changes occur as described above, whereby the pyrenes are *unstacked.* Subsequently, the excimer emission is reduced whilst the monomer emission increases, thereby signalling the presence of the guest to the analyst.

## 4.3 RESULTS AND DISCUSSION

### *4.3.1 Synthesis*

Typically the synthesis of a urea based host compound is advanced to a stage where there are one or more amine appendages present. The final stage is the addition of an appropriate isocyanate and under mild conditions (e.g. room temperature, 3 hours) the (thio)urea forms in good yield. The large number of isocyanates commercially available, mild reaction conditions and useful target properties contribute to the popularity of (thio)urea based hosts for anion detection.

A typical synthesis of **4-3** would normally have been performed starting from a tetranitrile calix[4]arene precursor via reduction to tetraamine and subsequent reaction with an appropriate isocyanate in the final step. Scheme 4.1 summarises such a reaction path.

**Scheme 4.1**. The theoretical synthesis of **4-3** via an appropriate isocyanate.

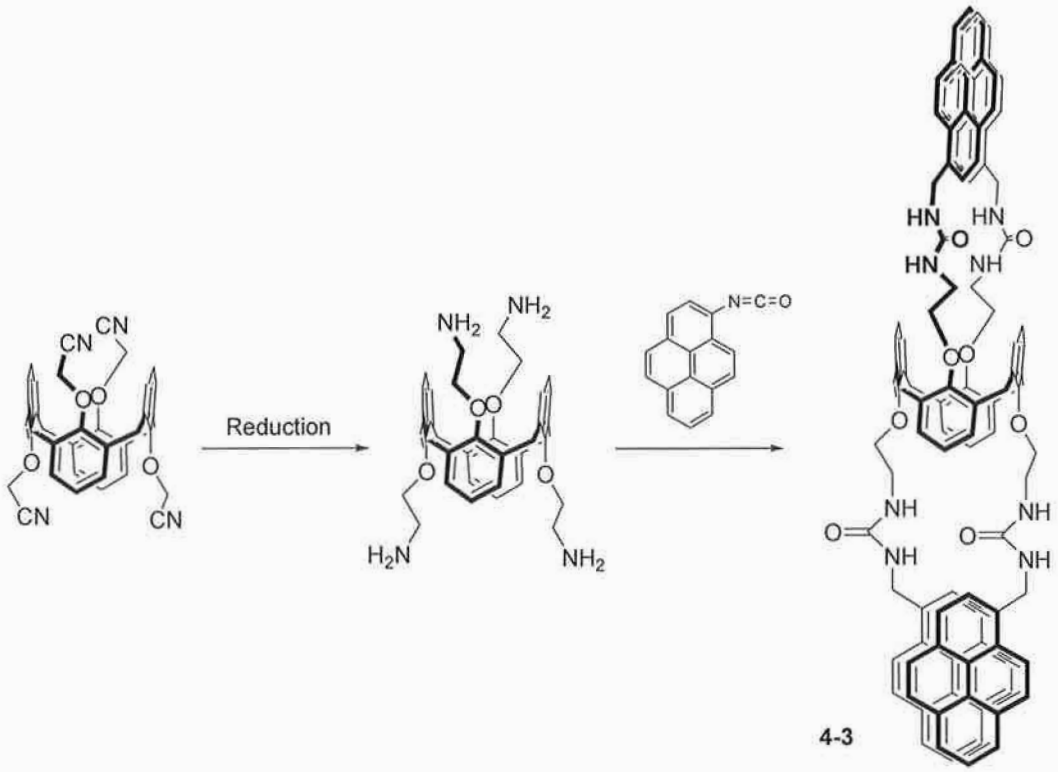


As the necessary isocyanate was not readily available, the synthetic route to **4-3** depicted in Scheme 4.2 was chosen instead.

**Scheme 4.2.** The synthesis of precursors **4-1** and **4-2** and calix[4]arene **4-3**.

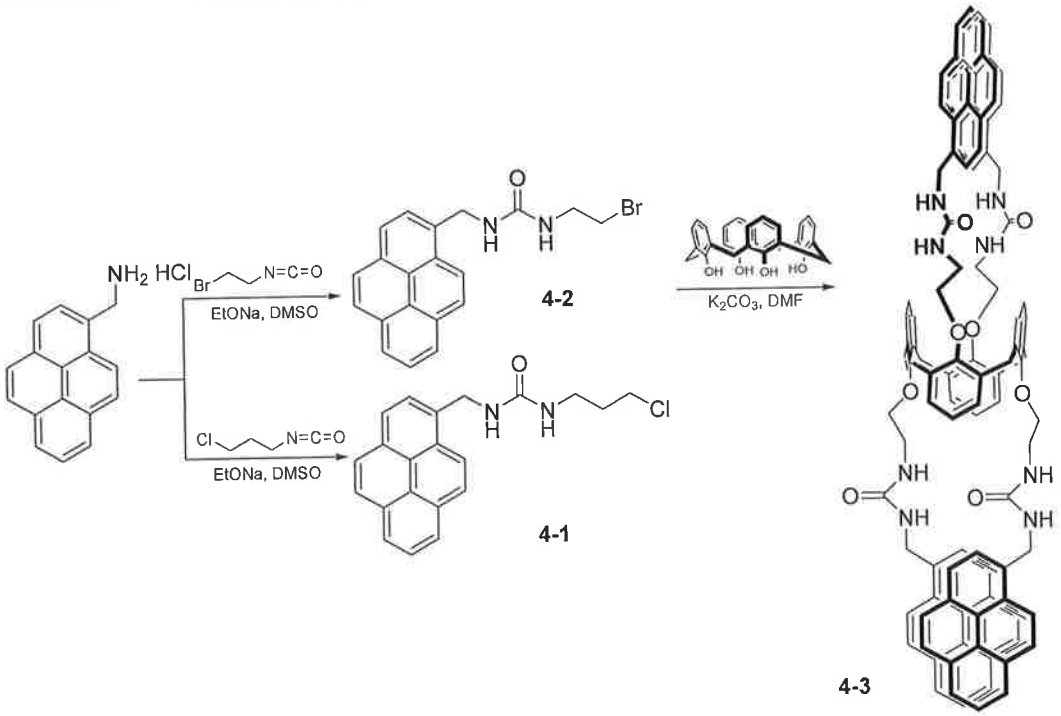


Full experimental conditions can be found in chapter 4.5. The pyrenyl urea appendages **4-1** and **4-2** were synthesized in a one pot synthesis by the reaction of deprotonated 1-pyrenemethylamine hydrochloride with 3-chloropropyl and 2-bromoethyl isocyanates respectively. The obvious advantage is that precursors **4-1** and **4-2** represent new 2 in 1 fluorophore-ionophore packages which in future can be attached to other molecular scaffolds or precursors, besides calixarenes, yielding useful host compounds, possibly in a single reaction step. The reduction in the number of synthetic steps is an attractive prospect for the future synthesis of highly preorganised structures based on **4-1** and **4-2** where inherently low yields may be coupled with difficult purification regimes. Interestingly, **4-1** did not react with calix[4]arene under the same conditions as the reaction of **4-2**. Presumably as bromide is a better leaving group in substitution reactions, **4-2** is expected to be the more labile reagent. **4-2** was reacted with calix[4]arene by base induced $S_N2$ substitution reaction to yield **4-3** in a further step.

An initial qualitative screening of the crude mixture from this reaction by TLC, revealed a blue/green spot when the plate was irradiated with long wavelength ($\lambda$ >300nm) UV light. This spot was not present in the TLC of **4-2**. Furthermore, the appearance of an excimer emission at 452nm ($\lambda_{max}$) was also seen in the crude mixture of **4-3** only, by fluorescence screening. This was the first evidence that a compound with intramolecular pyrene interaction was present. Following initial workup of the reaction mix, a crude mixture containing 37% **4-3** (of total peak areas) was present as shown by HPLC analysis (Figure 6.12). Workup products from the reaction mixtures obtained from the synthesis of **4-1**, **4-2** and **4-3** showed very poor solubility in most common low polarity solvents, marginally better solubility in MeOH and ACN and good solubility in DMSO or DMF. The preference for highly polar solvents is probably dictated by the polar urea groups and salts present. This affected the ease of purification of **4-2** and **4-3** in particular as chromatographic methods had to be used to achieve purities in excess of 95%. For **4-3**, an efficient semi-preparative HPLC method proved essential. This instrumental approach, previously developed in our group for supramolecule isolation, is of particular benefit when dealing with complex mixtures and low yielding reactions[189]. The method used was a fast, efficient means of purifying mg quantities of a product using a scaled up analytical HPLC method based on widely available analytical instrumentation. Chapter 6.3.4 deals with this HPLC method in detail and the purification of **4-3** in particular. HPLC analysis of the product obtained by this purification approach gave a single peak, revealing an overall product purity of 98% (Figure 6.13).

From the $^1$H NMR spectrum of **4-3**, there is a single peak for the methylene groups of the calix[4]arene annulus. This is indicative of a 1,3 alternate structure[81] as depicted in Scheme 4.2. The attachment of 4 sterically bulky appendages like **4-2** to a calix[4]arene

platform may result in a deviation from the more common cone conformation to a less hindered 1,3-alternate configuration. This deviation from the cone conformation is particularly feasible as the calix[4]arene benzene groups are free to rotate through the central aromatic cavity, given the absence of the commonly present upper rim tertiary butyl groups.

The two urea protons of start material **4-2** appeared deshielded from 6.3 and 6.8 ppm into the aromatic region for **4-3**. This signals a large change in the chemical environment of the urea protons in **4-3**. This de-shielding of urea protons may be due to proximal pyrene moieties and increased inter or intramolecular H-bonding of the urea groups of **4-3**.

### *4.3.2 Stability testing*

A $^1$H NMR temperature degradation study of **4-1**, **4-2** and **4-3** revealed that degradation generally occurred at temperatures of 80°C and above. Increased number of peaks and increased integration numbers for aromatic protons suggested cleavage of the bulky pyrene moiety (Figure 4.9).

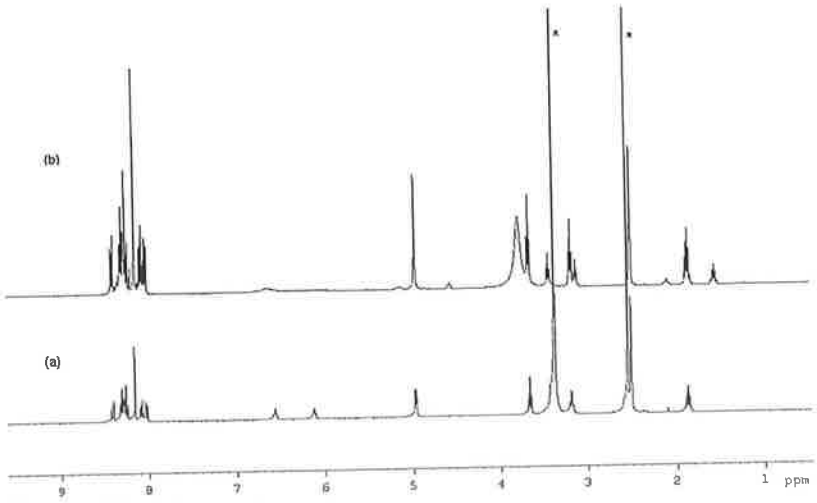


**Figure 4.9**. A $^1$H NMR degradation study in DMSO reveals degradation of **4-1** (similar for **4-2** and **4-3**) occurs at temperatures of 80°C and above. (a) $^1$H NMR spectrum of **4-1** at 25°C before heat treatment. (b) $^1$H NMR spectrum of the DMSO-**4-1** solution at 25°C after being heated at 80°C for 12 hours.

The consequences of these findings were that a maximum temperature of only 70°C for the subsequent synthesis of **4-3** could be used. This coupled with the solubility and purification issues discussed above may have contributed to the somewhat low final yield of 2%.

For the characterization of purified **4-3**, several attempts were made to obtain DI-MS data. Both ESI and Maldi MS techniques were applied using non-acidified and acidified matrices in a variety of solvents including acetonitrile and water. No satisfactory mass spectrum was obtained for **4-3** due to difficulties in ionising **4-3** and limitations in general stability. Some useful clues as to the degradation mechanism of **4-3** were obtained however. Interestingly, most attempts at obtaining a single peak corresponding to **4-3** using ESI-MS resulted in spectra with numerous fluctuating peaks of a large variety of masses generally lower than the target mass for **4-3** of +m/e 1624.67. Figure 4.10 shows a typical ESI-MS obtained.

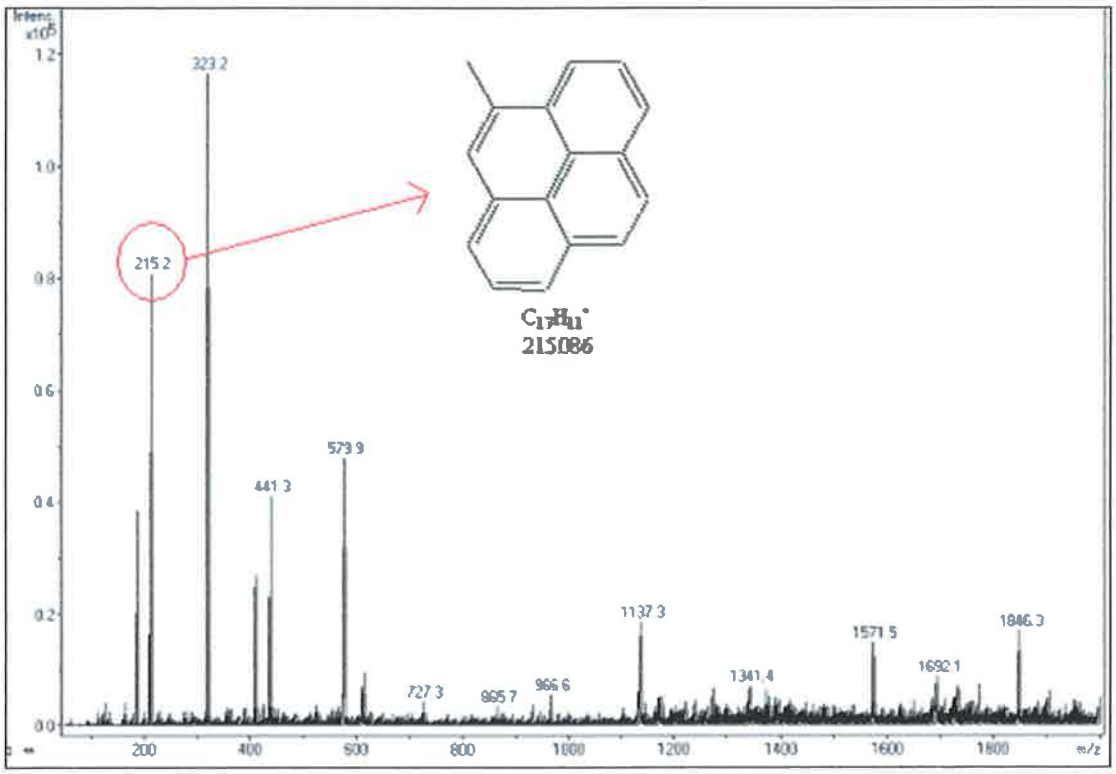


**Figure 4.10**. A typical ESI-MS obtained for **4-3** showing a large diversity of peaks. The peak of mass 215.2 corresponding to a pyrenyl moiety remained constant as other masses fluctuated.

The fragment corresponding to 215.2 (pyrenyl) was the only peak prominently visible and constant for **4-1**, **4-2** and **4-3** whilst a multitude of fluctuating other masses also appeared in the case of **4-3**, perhaps indicating the ease with which this bulky moiety is cleaved from the parent structure. From the MS evidence above, it may be deduced that the cleavage of pyrenyl units may be the first step in this degradation. This would also explain the increased integration of aromatic protons following temperature induced degradation of **4-3** (Figure 4.9) as additional aromatic species are formed.

### *4.3.3 Analytical Characterisation*

The excitation spectra of tetraphenol calix[4]arene, **4-2** and **4-3** are shown in Figure 4.11.

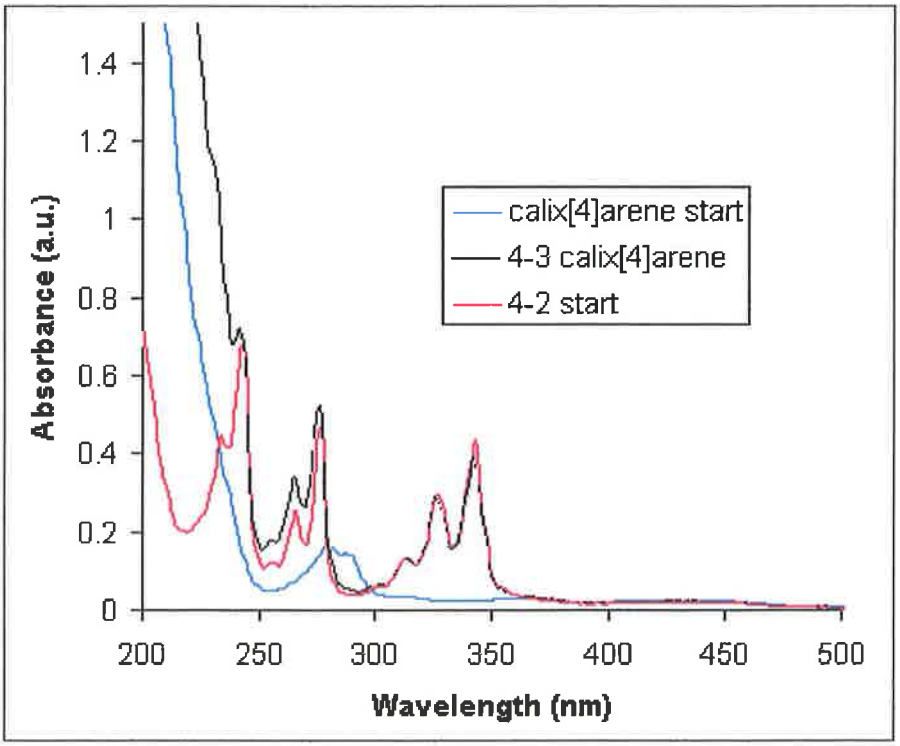


**Figure 4.11**. The UV/Visible absorption spectra of tetraphenol calix[4]arene, **4-2** and **4-3** in 100% acetonitrile.

Figure 4.11 reveals a $\lambda_{max}$ of 340nm as an ideal excitation wavelength for **4-2** and **4-3**. It is the ideal excitation wavelength for the pyrene moieties, as there are no significant absorbance features above 350nm, the region where fluorescence emission is anticipated. Furthermore, the calix[4]arene sub-structure does not compete for excitation photons at 340nm.

The tetraphenol calix[4]arene absorbance shows a large shoulder below 250nm (> 0.8 a.u.). **4-3** also shows such a shoulder. **4-3** therefore reveals a hybrid absorption spectrum, revealing both features from pyrene moieties and the tetraphenol calix[4]arene starting material. This serves as further proof of the structure of **4-3**.

Figure 4.12 shows the emission spectrum of **4-2** and **4-3** in acetonitrile-chloroform (95:5 v/v) when excited at 340nm. **4-2** reveals two monomer emission peaks at 376nm and 398nm ($\lambda_{max}$). There are no significant emission features >430nm, indicating the

absence of excimer formation. **4-3** shows the monomer emissions as well as a much larger broad emission band at 452nm ($\lambda_{max}$), characteristic of an intramolecular pyrene excimer emission.

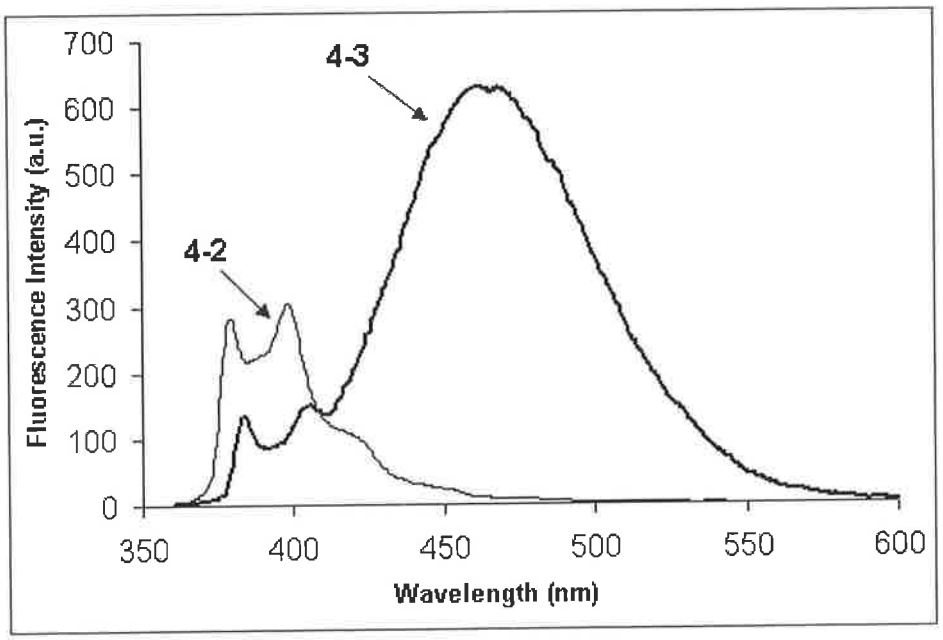


**Figure 4.12.** Emission spectra of **4-2** and **4-3** ($1\times10^{-6}$M) in acetonitrile-chloroform (95:5 v/v) showing monomer maxima at 376nm and 398nm. Only **4-3** shows an additional broad band at 452nm due to excimer formation. The excitation wavelength was 340nm.

In contrast to the fluorescence spectra of **4-1**, **4-2** and all other fractions collected during the purification of **4-3** by semi-preparative HPLC, only the pure fraction of **4-3** exhibited the characteristically broad pyrene excimer emission.

For **4-3**, the ratio of excimer (452nm) to monomer (398nm) emission remained unchanged at 4.4 in the concentration range $1\times10^{-7}$ to $1\times10^{-5}$M (Figure 4.13). This further confirmed the presence of pyrene units interacting by an intramolecular mechanism, not an intermolecular one. Emission detector saturation occurs above log $10^{-5}$M **4-3** and a lack of instrument sensitivity below $10^{-7}$M lead to decreasing ratios and a plateau below $10^{-9}$M **4-3**.

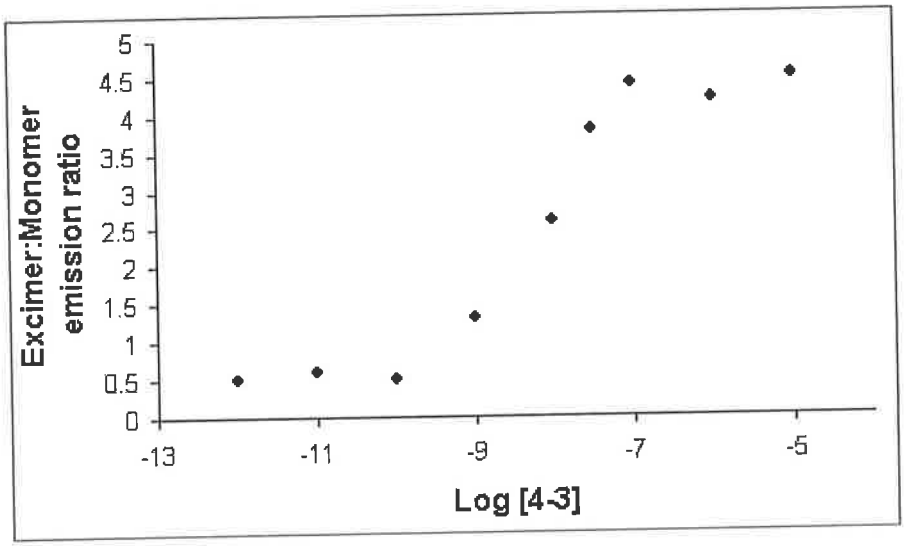


**Figure 4.13.** The ratio of excimer (452nm) to monomer (398nm) emission with changing concentration of **4-3** in acetonitrile-chloroform (95:5 v/v).

The ditopic chromoionophore **4-3** is built on a calix[4]arene platform, lending preorganisation to the overall host. Four urea groups providing eight possible H-bonds for anion binding are in close proximity to pyrene moieties, whose orientation relative to each other is thought to change upon guest inclusion. Such a binding event can in principle be monitored by ratiometric changes in the emission spectrum (excimer:monomer ratio) of **4-3**.

The changes in the emission spectrum of **4-3** were examined when screened with eleven common anions. These spanned a comprehensive range of sizes and shapes. 100 equivalents of the tertiary butyl ammonium salt of each anion was added to $1\times10^{-6}$M solutions of **4-3** in acetonitrile-chloroform (95:5 v/v). The change in excimer and monomer emission was monitored and the results tabulated in Table 4.1.

**Table 4.1**. Fluorescence changes ($I-I_0$) for **4-3** upon addition of 100 equivalents of specified anion[a].

| | Fluorescence change ($I-I_0$) | | | | | | | | | | | |
|---|---|---|---|---|---|---|---|---|---|---|---|---|
| $\lambda_{em}$ | $Cl^-$ | $F^-$ | $Br^-$ | $I^-$ | $NO_3^-$ | $ClO_4^-$ | $AcO^-$ | $SCN^-$ | $CN^-$ | $HSO_4^-$ | $H_2PO_4^-$ | $H_2O$[b] |
| **398** | +270 | -7 | 0 | -6 | -6 | -1 | +2 | -8 | +2 | 0 | +6 | -36 |
| **452** | -591 | +2 | +5 | -1 | -4 | +6 | -4 | 0 | -8 | -5 | -3 | +36 |

[a]Conditions: **4-3**, $1.6\times10^{-6}$M in acetonitrile-chloroform (95:5 v/v), excitation at 340nm. $I_o$: fluorescence emission intensity of free **4-3**. I: fluorescence emission intensity of **4-3** with 100 equivalents of specified anion in the form of tertiary butyl ammonium salts. [b]1000 equivalents added.

Remarkably, only chloride caused a dramatic change in the emission spectrum of **4-3**. There is a sharp decline in excimer emission with a corresponding increase in monomer emission. These observations suggest that the chloride anion selectively coordinates with the urea protons in the cavity of **4-3** so as to 'unstack' or lever apart the π-π stacked pyrenes. The process is represented by the molecular models in Scheme 4.3.

**Scheme 4.3**. Energy minimised molecular models showing the binding of chloride ions by **4-3**. Quenching of Excimer emission (452nm) caused by a perturbation of the pyrene π-π interaction by the conformational 'unstacking' of pyrene moieties.

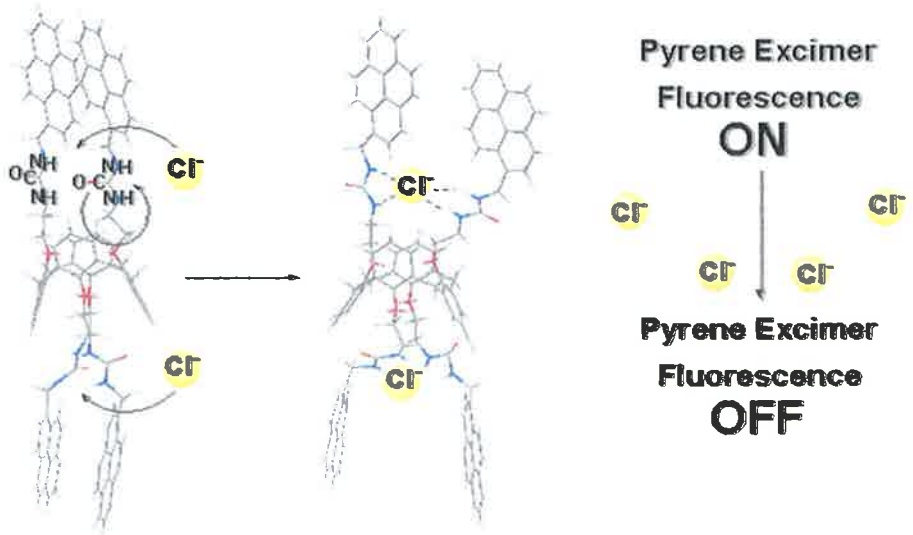

The 'unstacking' of the pyrene moieties is justified by the strong reduction of the excimer emission and concurrent rise in monomer emission upon complexation of chloride as seen in Table 4.1. A Photoinduced Electron Transfer (PET) effect from the negative $Cl^-$ to the pyrene moieties is unlikely, as this would have resulted in a reduced excimer *and* monomer emission (compare with $F^-$ selective calix[4]arene in Figure 4.5). An unambiguous monomer-excimer mechanism appears to be at play.

The excimer emission of 452nm ($\lambda_{max}$) signifies a considerable blue shift compared to other intramolecular pyrene excimer systems, which typically show a $\lambda_{max}$ of 480nm[170]. The comparison of the pyrene excimer emission of sandwich-like systems (full overlap) with partially overlapping systems is normally explained in this way[190,191]. Sandwich-like systems are described as dynamic excimers, in that pyrene moieties are *free* to fully overlap. Partially overlapping pyrenes are described as static because some force is inducing a partial overlap. In the case of free **4-3**, there is a strong likelihood of H-bonding between urea groups in addition to steric factors, thereby offering a plausible explanation for the observed partially overlapped static excimer.

To further support the mode of binding proposed, selected tetrabutylammonium anions were added in excess to **4-3** in deuterated acetone and examined by $^1H$ NMR spectroscopy (Figure 4.14).

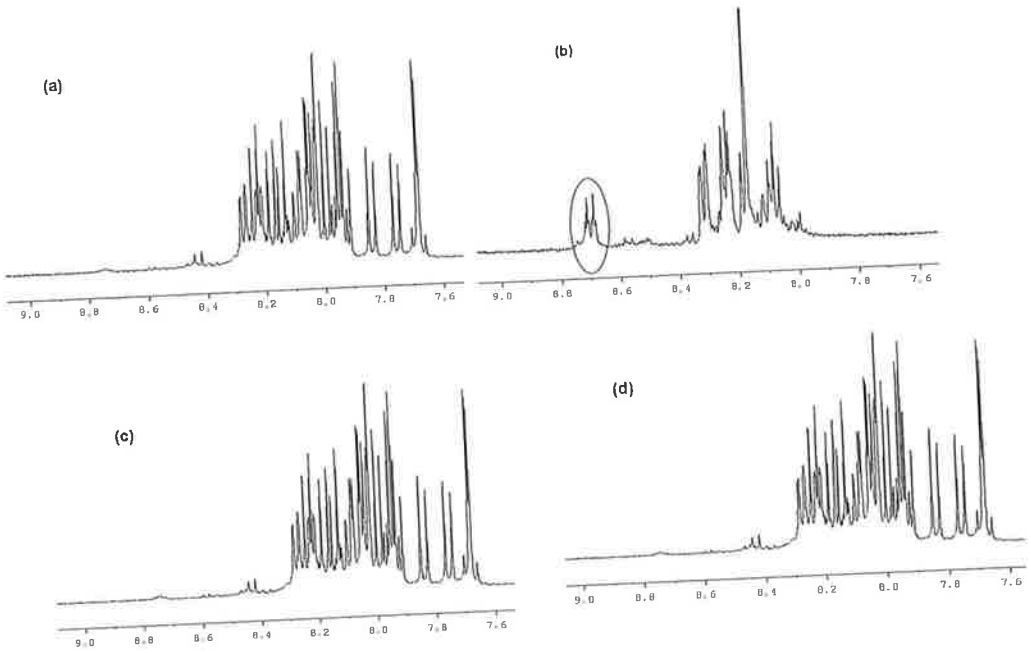


**Figure 4.14**. The $^1$H NMR in d-acetone of **4-3** with 300 Equivalents of *t*-butyl ammonium anion salt (a) Free (b) chloride (c) fluoride (d) bromide.

Only the chloride salt caused a downfield shift of urea protons, indicative of an H-bonding interaction. Upon addition of 300 equivalents of $Cl^-$, the two triplet signals for the urea protons appear shifted downfield, clear of the main aromatic region at 8.69ppm and 8.71ppm. This shows clearly that chloride ions form an inclusion complex within the cavities of **4-3** involving urea protons. No such discernible change was observed for the smaller fluoride and the larger bromide anions, confirming chloride selectivity.

Furthermore, the aromatic protons of **4-3** appear considerably deconvoluted by the addition of $Cl^-$, suggesting a more symmetrical complex structure compared to the free Host. The resultant separation of previously π-stacked pyrene moieties may reduce the effects of the π-electron clouds from the planes of the two pyrene moieties. These results mirror the findings of the fluorescence study, where a response appeared exclusive to $Cl^-$. It appears that a specific cavity effect controls the anion binding characteristics of **4-3**. A 'lock and key' or 'best fit' model appears to yield an

energetically favorable host-guest interaction in this case. This is in contrast to a scenario where an anion host offers little preorganisation, where selectivity is typically dictated by anion basicity[49].

When 0-500 equivalents of chloride are added to **4-3**, the change in emission can be followed and is shown in Figure 4.15.

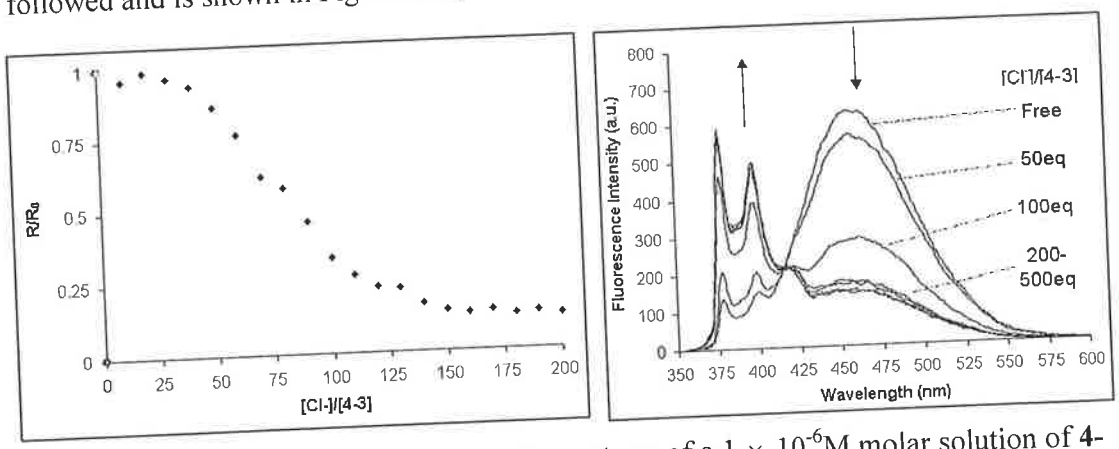


**Figure 4.15**. Changes of the fluorescence spectrum of a $1 \times 10^{-6}$M molar solution of **4-3** in acetonitrile-chloroform (95:5 v/v) upon addition of the specified number of equivalents of chloride ([$Cl^-$]/[**4-3**]). $R_0$: Ratio of excimer ($\lambda_{em}$=452nm) to monomer ($\lambda_{em}$=398nm) of free **4-3**. R: Ratio of excimer to monomer with varying [$Cl^-$]. The excitation wavelength was 340nm.

This experiment yielded further valuable information. At 412nm there is an isoemissive point which indicates that only one type of complexing mechanism (equivalent in both cavities of **4-3**) is at play perturbing the excimer emission of **4-3**[185].

From the change in excimer to monomer ratios observed with chloride added, an association constant of $2.4 \times 10^4 M^{-1}$ was obtained‡. The association constants of crown and cryptand alkali metal hosts are typically about $10^6 M^{-1}$ and $10^{10} M^{-1}$ respectively[1]. It appears that selective anion hosts seldom reach association constants of this magnitude and are in fact lower by several orders of magnitude.

‡ The association constant was calculated by non-linear regression analysis and the fitting of experimental data with a standard fluorescence equation by minimizing the sum of square residuals. The standard Microsoft Excel add-in SOLVER was used.

The reasons for this include the competitive factors inherent in anion sensing. These typically revolve around solvation effects (choice of solvent) and factors such as competitive H-bonding (chapter 1). Additional factors competing with anion coordination specific to **4-3** may include the cost in energy to separate the overlapping pyrene π-π bonding systems. Furthermore, as each equivalent di-urea cavity of **4-3** binds a chloride anion, the resultant repulsion between these two ions of same charge within **4-3** may further lower the overall association constant. However, viewed positively, the net effect of the factors responsible for low association constants may also be driving factors for good selectivity. In the case of **4-3**, these factors may contribute significantly to the observed selectivity for chloride over other anions.

Other strategies for modifying association constants and selectivity have involved varying the acidity of urea protons. For example Lang replaced a porphyrin with a nitrophenyl group proximal to the ureas of a calix[4]arene. The increased electron withdrawing ability of the nitrophenyl group resulted in increased urea proton acidity and an increase in association constant with chloride by 1 order of magnitude[63]. Thiourea groups are more acidic than urea groups and have been shown to lead to higher anion association constants for otherwise identical hosts[75]. Conversely, a decrease in association constants may also occur by increasing the acidity of urea protons for the simple reason that increased affinity for anions may result in a simultaneous rise in competition from urea-urea and urea-solvent H-bonding [72].

The selectivity of **4-3** towards chloride can also be explained classically by a 'best fit' or 'lock and key' model. In addition, the unique cavity preorganisation of **4-3** with its directional H-bonds provided by the ureas may provide for selective chloride recognition. It is most likely several cumulative factors that contribute to what is ultimately the most important parameter of a sensor design: Selectivity.

### *4.3.4 Stoichiometry*

The subjest of complex stoichiometry between chloride and **4-3** warrants further discussion. $^1$H NMR titrations or spectroscopic titrations between a host and guest normally reveal the point of signal saturation (no further change) for a given stoichiometry of Host:Guest. By generating simple Job plots, the stoichiometry of the host-guest complex can be unambiguously assigned and are typically 1:1 or 2:1. In the case of **4-3,** the fluorescence emission intensities only stopped changing after adding about 150 equivalents of chloride to 1 equivalent of **4-3** (Figure 4.15). Clearly, a realistic complex stoichiometry cannot be deduced from such a host:guest ratio. Regarding the $^1$H NMR spectrum of **4-3**, the relevant urea protons appear to be obscured by the complex aromatic region of the spectrum, only emerging downfield of this region when a large excess of chloride ions are added. This precludes the use of this technique to closely follow the urea proton chemical shift with changing ratios of host:guest, particularly for ratios relevant for revealing stoichiometric information of the complex formed.

A 1:2 host:guest ratio for **4-3** is proposed, based on experimental observations and on the findings of other workers on calixarene urea systems as discussed below. As both cavities in the symmetrical 1,3-alternate system of **4-3** are exactly equivalent, an event occurring in one cavity is as likely to occur in the second cavity. A total quenching of the excimer emission for **4-3** was observed when chloride ions were added, and can only be seen if *both* cavities undergo anion induced conformational unstacking of the pyrene moieties. The distance between the two complexed chloride ions in the molecular model of Scheme 4.3 was calculated to be about 14Å. This distance is too large to rule out complexation of two ions by repulsion of like charges[67].

The possibility of observing a negative allosteric effect as seen by Budka and coworkers is very unlikely[67]. Budka investigated the stoichiometry of a tetrasubstituted

1,3-alternate urea calix[4]arene with two equivalent cavities towards anions (Figure 4.16). By means of $^1$H NMR titrations, Budka observed a 1:1 stoichiometry and concluded that the complexation of an anion in one cavity prevented a second anion being complexed in the second cavity of the same molecule. The binding of the first anion was thought to cause a closing of a two propoxy tweezer *para* to the urea appendages. This effectively appeared to block any complexation in the second cavity. This negative allosteric effect is shown graphically in Figure 4.16.

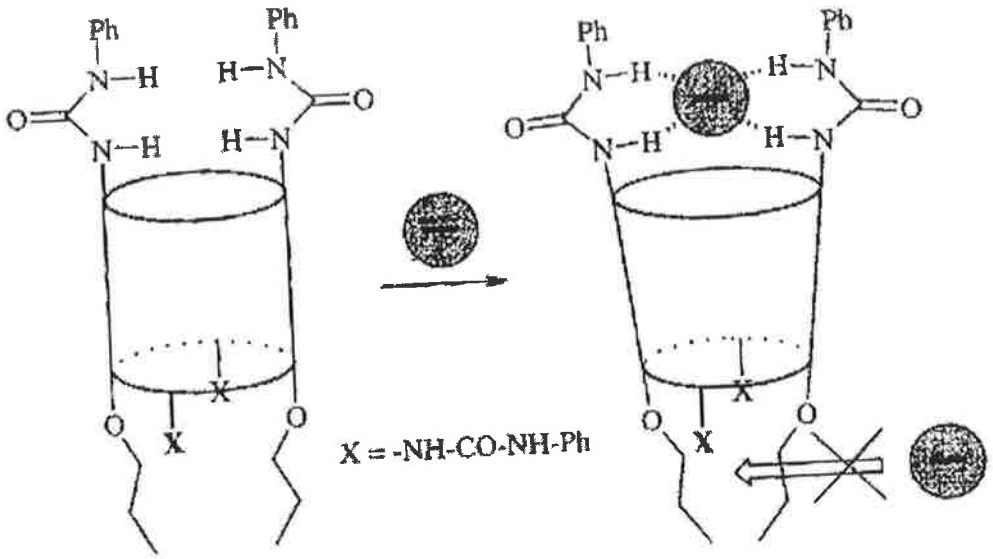


**Figure 4.16**. The complexation of one anion in a Host with two complexation sites blocks complexation of a second anion due to a propoxy tweezer: A negative allosteric effect.

A similar effect is clearly *not* at play for **4-3** which has no substituents *para* to the urea appendages.

The formation of dimers or capsules comprising more than one calixarene has been shown to occur due to intermolecular H-bonding of urea protons. Such an effect can effectively block ion complexation[80]. This effect applies specifically when ureas are present at the broader upper rim of a calixarene, not at the lower rim, as is the case for

**4-3**. Furthermore, in the unlikely event of such capsules interfering with anion complexation of **4-3**, both equivalent cavities would be affected equally thus complexaton is either blocked or allowed in *both* cavities. In any case, significant inter *and* intra-molecular H-bonding between ureas in **4-3** is quite unlikely due to to the sterically bulky nature of the pyrene moieties proximally attached to each urea. With these arguments we conclude that a Host:Guest stoichiometry of 1:2 is the most likely scenario for **4-3**.

### *4.3.5 Practical sensor design principles in the context of 4-3*

A developer of practical fluorescent probes or sensors can choose from three broad fluorescence signal types[192]. Intensity based probes rely on the change of intensity of single wavelengths. The biggest disadvantage here is that for accurate sensing, the exact sensor host concentration must be known. Typically factors like host degradation or leaching into the sample result in ever changing host concentration. Other factors like sample turbidity, intensity of incident light, scattering, inner-filter effects and photo bleaching strongly affect the signal reliability. These disadvantages are largely absent for the other two categories, life-time based and wavelength-ratiometric fluorescent sensing methods. **4-3** belongs to the latter class, whereby a changing ratio of two fluorescence intensities comprises the analytical signal. Such devices in contrast to single wavelength intensity based ones are self-calibrating to an extent, in that wavelength ratios are not affected by the above problems to the same degree.

It is apparent from the literature that there are quite a number of fully characterized fluorescent sensor compounds available with elegant spectroscopic properties. The operating wavelengths of many of these compounds, including **4-3** (excitation 340nm), fall within the UV region of the spectrum. A major challenge for developing fluorescent sensor devices from these compounds is the availability of optically

compatible sensor materials[35,193-195]. Many currently available materials can contribute to interferences and auto fluorescence of a sensor, particularly in the UV region (<400nm). The search is on then to continue to lower the UV transparency cut-off point of components. Central to any fluorescent optical sensor is the need for an excitation source and an emission detector. Laser diodes and Light Emitting Diodes (LEDs) lead the field when it comes to developing miniaturized, cheap and effective sensor devices[196]. As material scientists work to increase the UV-transparency of device components, organic chemists strive to raise the 'useful' wavelengths of a sensor compound towards the visible region. In future it is hoped that these efforts will converge. Both monomer and excimer emission intensities of **4-3** at a concentration of $1 \times 10^{-6}$M were found to be about 75% and 10% at excitation wavelengths of 350nm and 360nm respectively, compared to an excitation wavelength of 340nm. Despite the decrease in emission intensities, analytically useful signals were still obtained. Indeed, there are LEDs available commercially at the time of writing that operate at predefined wavelengths from the visible down into the UV range as low as 247nm[§].

A system where a bulk 1:1 Host to Guest concentration results in a plateau of the measured signal upon further addition of guest may be described as a switch. Conversely, **4-3** displayed a *range* of response of about $5 \times 10^{-5}$M to $1.5 \times 10^{-4}$M chloride (50-150 equivalents of chloride added to $1 \times 10^{-6}$M of **4-3**) as seen in Figure 4.15. The larger the response range of a sensor, the easier it is to tune a device to yield both qualitative and quantitative data on a guest and the more it lends itself to continuous sensing[35].

Chloride (usually from sodium chloride) is essential for human health with typical levels at 0.1M in blood serum. In soil typical levels are 100ppm[145], whereas the typical

[§] Sensor Electronic Technology, Inc., USA, www.s-et.com

chloride levels in the oceans are about 0.5M[197]. For such applications a particularly low LOD for chloride is not required. For the many other analytes however, ever lower LODs are essential, several orders of magnitude below the above examples.

The upper and lower LODs and linear response ranges of systems like **4-3** can be tuned to a certain degree. At the minimum instrument sensitivity settings signal saturation was observed above $10^{-5}$M **4-3**. Analytically useful excimer/monomer bands are still observed down to concentrations of $1 \times 10^{-8}$M **4-3** (Figure 4.17), using the maximum sensitivity threshold of the instrumentation.

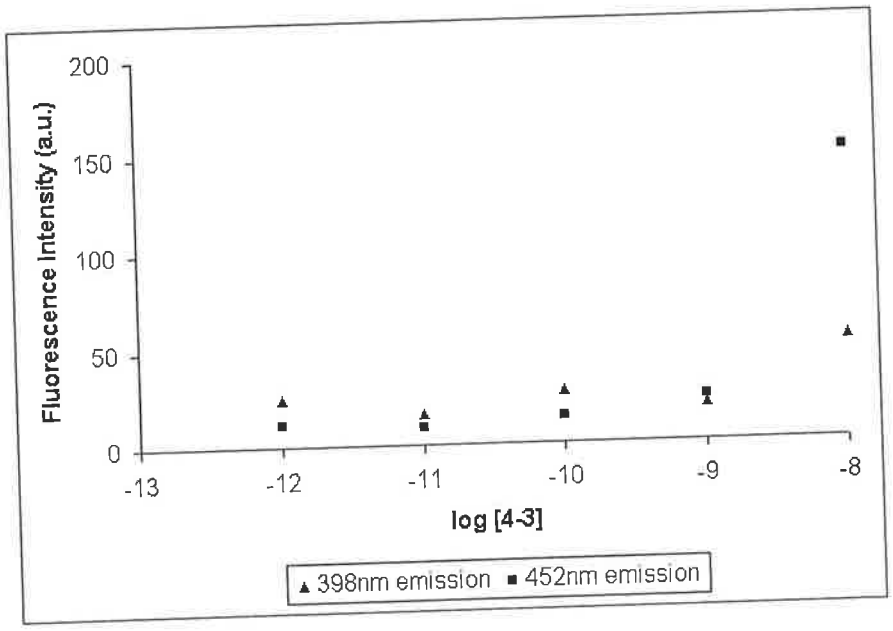


**Figure 4.17.** The monomer (398nm) and excimer (452nm) emission intensities of varying concentrations of **4-3** in acetonitrile-chloroform (95:5 v/v). $1 \times 10^{-8}$M **4-3** was the lowest analytically useable concentration for sensing chloride, using the available instrumentation. Excitation and emission slits were set at a maximum possible 15nm.

Based on this concentration an LOD of $8 \times 10^{-6}$M chloride was observed. This amounts to a chloride concentration that is only 6-fold lower than the LOD for a starting concentration of $1 \times 10^{-6}$M **4-3**. Due to a lack of instrument sensitivity at these concentrations, a reduced excimer:monomer ratio of around 3.0 (Ratio was 4.4 bewteen

$10^{-5}$M and $10^{-7}$M **4-3**) was observed for **4-3**, leaving less scope for signal change on complexation. Furthermore at concentrations of $1 \times 10^{-8}$M **4-3**, the monomer-excimer signals are likely to be more prone to baseline interference and errors. Indeed 800 equivalents of chloride were needed to get a reproducible signal change at the lower concentration of **4-3**.

Where upper or lower LOD changes are required for ratiometric fluorescence sensors incorporating hosts like **4-3**, it is perhaps also useful to carefully adjust other sensor parameters. Such a strategy may involve starting with a constant concentration of **4-3** in the range $1\times10^{-7}$ to $1\times10^{-5}$M, where an optimal high excimer:monomer ratio of 4.4 was observed. By carefully tuning the sensor sample pathlength, characteristics of source and detector (LEDs, photodiodes etc.) or excitation/emission bandwidths for example, the sensitivity towards the analyte could be modulated. If the host is incorporated into a liquid polymer membrane, the polarity of this environment via choice of polymer or plasticizer for example can also have a profound effect on analyte sensitivity.

In a dynamic analyte environment, response time is important. A dynamic experiment involving **4-3** was carried out. A sample of $1\times10^{6}$M **4-3** was spiked with 100 equivalents of chloride and the response measured over time. No mechanical stirring was provided. Once again a strong chloride response was observed, with a stable final emission signal after about 3 seconds as seen in Figure 4.18.

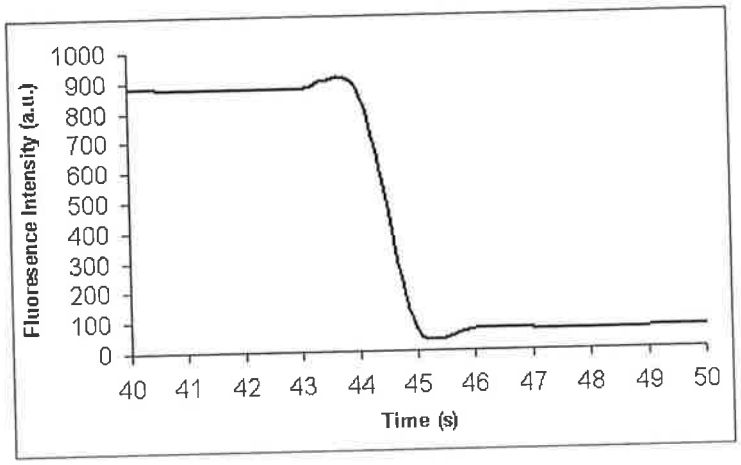


**Figure 4.18**. The dynamic response of a $1 \times 10^{6}$M solution of **4-3** when spiked with 100 equivalents of chloride. Excitation 350nm and bandwidth 5nm. Fluorescence was monitored at 452nm. With no mechanical stirring, a stable signal was obtained in about 3 seconds.

Most useful sensors must be able to operate in an aqueous environment. This is immediately clear when considering environmental and medical applications. When 1000 equivalents of water were added to **4-3** as seen in Table 4.1, there was no reduction in the excimer emission and so it is not in direct competition with chloride complexation. On the contrary, the excimer:monomer ratio increased to 4.8. Water may enhance the pyrene $\pi$-$\pi$ interactions possibly due to an increase in aggregation of organic moieties in an environment of increasing polarity.

When considering incorporating a host compound into a chemical sensor, this typically involves either the mixing of the compound into a hydrophobic polymeric membrane cocktail (e.g. PVC membrane of an Ion Selective Electrode) or covalent attachment to a polymer backbone or other substrate. The latter approach has the main advantage that it can prevent leaching of the compound into the sample matrix during analysis. Neutral calixarenes based hosts are ideal for both strategies. As calixarenes present numerous substitution opportunities at the upper and lower rim, calixarenes can for example be co-polymerised into polymer backbones with the aid of passive linkers.

In tandem, active complexing substituents can operate independently. One sample strategy is to convert the upper rim to *p-allyl* groups prior to functionalising the lower rim[109,198,199]. Labile *p-allyl* groups are then co-polymerised onto a polymer and thereby securely 'fastened' to the sensor substrate. This is also described in chapter 1.10.

In time, it is envisaged that with the current pace of progress, ratiometric receptors like **4-3** and similar systems in the literature may soon see applications in real life devices.

## 4.4 CONCLUSIONS

The synthesis of pyrene ureas **4-1**, **4-2** and **4-3** was successfully carried out. The precursor compounds **4-1** and **4-2** have great potential to be applied to other (supra)molecular platforms to produce libraries of anion selective hosts. They may be considered 2 in 1 systems in that they provide urea functional groups and pyrene moieties for signalling anion recognition via excimer-monomer emission ratios in systems with at least two pyrene moieties orientated correctly.

**4-3** is a ratiometric fluorescent calix[4]arene showing near exclusive chloride selectivity amongst a large variety of common inorganic anions and does not show interference in the presence of a large excess of water. Besides the excellent potential for the synthesis of derivatives and subsequent characterisation of hosts similar to **4-3**, such hosts may lend themselves to incorporation into practical sensor devices in future.

**4-3** performed favourably in terms of selectivity, LOD and fast response time. Ratiometric fluorescent hosts like **4-3** are self-calibrating compared to single wavelength intensity based sensors. With these advantages in mind, suggested future work could entail the mixing or covalent immobilisation onto a sensor surface of **4-3**. The useful wavelength operating range of **4-3** is 340-460nm approximately. As the excitation wavelength is about 340nm, in the Ultra Violet region, UV transparent sensor

components may be needed. LED technology already operates in this range and may be applicable as source and detector in such a sensor.

## 4.5 EXPERIMENTAL

**1-(3-chloropropyl)-3-(pyren-1-yl methyl)urea (4-1).** Under argon, 1-pyrenemethylamine hydrochloride (3.00g, 11.20mmol) and sodium ethoxide (0.84g, 12.32mmol) was stirred in 200ml dry DMSO for 1 hour at room temperature. 3-Chloropropyl isocyanate (1.26ml, 12.32mmol) was added to the vessel and stirring continued for a further 12 hours at room temperature. A dense white solid was obtained by filtering the mixture. The solution was cooled on ice and 200ml water at 0°C was added slowly yielding a white ppt. After filtering, the filtrate was washed 3 times with 20ml aliquots of 0 °C de-ionised water and 3 times with 10ml aliquots of MeOH at 0 °C. Upon drying, 3.01g (77%) of **4-1** was obtained as a white solid. mp: 195-200 °C. IR (KBr): 3320, 1619, 655 $cm^{-1}$. 1H NMR (400MHz, $CD_3C0CD_3$): 8.00-8.50 (m, 9 H, Ar*H*), 6.56 (t, 1 H, $ArCH_2N\mathit{H}$, J = 5.6), 6.12 (t, 1 H, $CH_2CH_2N\mathit{H}CO$, J = 5.6), 4.96 (d, 2 H, $ArC\mathit{H}_2NH$, $J$ = 5.6), 3.65 (t, 2 *H*, $CH_2C\mathit{H}_2Cl$, $J$ = 6.4), 3.18 (m, 2 H, $NHC\mathit{H}_2CH_2$, $J$ = 6.4), 1.85 (m, 2 H, $CH_2C\mathit{H}_2CH_2$, J = 6.4). $^{13}C$ NMR (50MHz, $CD_3C0CD_3$): 158.4, 134.7, 131.2, 130.7, 130.3, 128.3, 127.8, 127.2, 126.6, 125.5, 125.1, 124.4, 124.3, 123.6, 43.4, 41.5, 40.7, 37.2, 33.3 ppm. ESI MS +m/e 373.2 ([M + $Na^+$], calcd 373.1). Anal. Calcd for $C_{21}H_{19}ClN_2O$: C, 71.89; H, 5.46; N, 7.98. Found: C, 71.94; H, 5.14; N, 7.77. HPLC purity: 96.0%.

**1-(2-bromoethyl)-3-(pyren-1-yl methyl)urea (4-2).** Under argon, 1-pyrenemethylamine hydrochloride (10.00g, 37.35mmol) and sodium ethoxide (2.80g, 41.10mmol) were stirred in 700ml dry DMSO for 1 hour at room temperature. 2-

Bromoethyl isocyanate (3.71ml, 41.10mmol) was added to the vessel and stirring continued for a further 12 hours at room temperature. The solution was cooled on ice and 700ml water at 0°C was added slowly yielding a white ppt. After filtering, the filtrate was washed 3 times with 50ml aliquots of 0 °C de-ionised water and 3 times with 20ml aliquots of MeOH at 0 °C. Chromatography on silica gel with EtOAc-hexane (1/3) as eluent gave 3.29g (23%) of **4-2** as a white solid. mp: 155-160 °C. IR (KBr): 3322, 1622, 626cm$^{-1}$. 1H NMR (400MHz, $CD_3C0CD_3$): 8.00-8.50 (m, 9 H, Ar*H*), 6.84 (t, 1 H, $ArCH_2N\mathit{H}$, J = 5.6), 6.35 (t, 1 H, $CH_2CH_2N\mathit{H}CO$, J = 5.6), 5.00 (d, 2 H, $ArC\mathit{H}_2NH$, $J$ = 6.0), 3.66 (t, 2 *H*, $CH_2C\mathit{H}_2Br$, $J$ = 6.2), 3.43 (m, 2 H, $NHC\mathit{H}_2CH_2$, $J$ = 6.2). $^{13}$C NMR (50MHz, $CD_3C0CD_3$): 157.9, 134.1, 130.9, 130.2, 129.8, 127.7, 127.3, 126.9, 126.2, 125.1, 124.5, 123.9, 123.0, 44.5, 41.2, 41.0 ppm. ESI MS +m/e 383.1 ([M + $H^+$], calcd 383.1). HPLC purity: 95.4%.

**25,26,27,28-tetrakis[[*N*-(1-pyrenylmethylureido)ethyl]oxy]calix[4]arene (4-3).** Under argon, calix[4]arene (1.00g, 1.54mmol) and $K_2CO_3$ (0.85g, 6.16mmol) were heated in 100ml DMF for 3 hours at 70 °C. **4-2** (2.36g, 6.16mmol) was added and the reaction progress monitored by HPLC. No further reaction occurred after 2 days. The solution was cooled on ice and 100 ml de-ionised water at 0 °C was added to yield a beige ppt. The product was extracted from the solid with 3 10ml aliquots of chloroform. The combined chloroform aliquots were washed with 3 10ml aliquots of de-ionised water. The resultant chloroform layers were combined, dried with $Na_2SO_4$ and reduced to 2ml by evaporation. This solution was shown to contain 37% **4-3** by HPLC. Purification by semi-preparative HPLC gave 0.04g (2.03%) **4-3** as a white solid. The SP-HPLC purification and isolation method used is described in detail in chapter 6. mp: 190-191 °C. IR (KBr): 3320, 1690cm$^{-1}$. 1H NMR (400MHz,

$CD_3C0CD_3$): δ 8.30-7.91 (m, 36 H, Ar*H*, pyrene), 8.30-7.91 (t, 4 *H*, urea), 8.30-7.91 (t, 4 *H*, urea), 7.84 (d, 4 H, Ar*H*), 7.55 (d, 4 H, Ar*H*), 7.68 (m, 4 H, Ar*H*)), 5.11 (d, 8 H, $ArCH_2NHCO$, $J = 5.6$), 5.02 (s, 8 H, $ArCH_2Ar$), 4.54 (t, 8 H, $NHCH_2CH_2$, $J = 6.8$), 4.07 (t, 8 H, $NHCH_2CH_2O$, $J = 6.8$). $^{13}C$ NMR (50MHz, $CD_3C0CD_3$): 153.8, 152.2, 135.8, 133.9, 132.6, 132.07, 131.4, 129.9, 128.9, 128.7, 128.4, 128.0, 127.3, 126.5, 126.2, 126.0, 125.8, 124.5, 124.2, 66.1, 49.3, 44.7, 42.8 ppm. Anal. Calcd for $C_{108}H_{88}N_8O_8$: C, 79.78; H, 5.46; N, 6.89. Found: C, 80.10; H, 5.11; N, 6.86. HPLC purity: 97.8%.

**Method for analytical and semi-preparative HPLC.** HPLC was carried out using a HP1050 instrument with UV detection. Mobile phase used was HPLC grade methanol in isocratic mode. Chloroform served as the sample solvent. Detection wavelengths were 210nm and 340nm. For analytical HPLC, a Synergy 150.0 × 2.0mm, 4μm Fusion-RP column was used. Flowrate was 0.2ml/min. Injection volume was 10μl. For semi-preparative HPLC, a Synergy 250.0 × 10.0mm, 10μm Fusion-RP column was used. Flowrate was 5.0ml/min. Injections volume was 100μl filtered sample. Fraction collection was carried out manually or with a Gilson 204 fraction collector in automation mode.

For LC-MS and direct injection MS work, a Bruker/Hewlard-Packard Esquire system, using a positive ESI source and the software's default 'smart' settings. For direct injection MS work the solvent used was MS grade acetonitrile with a 0.25% formic acid content.

**General details for absorption and fluorescence studies.** UV/Vis absorption spectra were recorded using a Perkin Elmer model Lambda 900 UV-Vis spectrophotometer. Fluorescence spectra were recorded with a Perkin Elmer luminescence spectrometer model LS50B. In all cases, 1cm quartz cuvettes were used. $1 \times 10^5$M stock solutions of

**4-1**, **4-2** and **4-3** were prepared in acetonitrile-chloroform (95:5 v/v). For ratiometric complexation studies, 0.01M stock solutions of the tetrabutylammonium salt of each anion were prepared in acetonitrile-chloroform (95:5 v/v). For all fluorescence work, an excitation wavelength of 340nm was chosen with excitation and emission slits at 3nm unless stated otherwise. For fluorescence titrations and dynamic response time measurements, $1\times10^{6}$M solutions of **4-3** were used, adding the appropriate volume of the 0.01M chloride stock solution. From the change in excimer (452nm) to monomer (398nm) ration with chloride added, the association constant was calculated by non-linear regression analysis and the fitting of experimental data with a standard fluorescence equation by minimizing the sum of square residuals. The standard Microsoft Excel add-in SOLVER was used. The LOD of chloride for **4-3** was calculated by observing the decrease in excimer and increase in monomer emissions of decreasing concentrations of **4-3**, upon addition of chloride. The LOD was considered the lowest concentration of chloride that caused a change in both the monomer and excimer intensities, greater than three times the standard deviation of the baseline noise intensities of free **4-3**. Excitation and emission slits were 15nm for LOD work, the maximum permissible by the instrument used.

**Procedure for binding site investigation by $^{1}$H NMR.** A 1.6mM solution of **4-3** in deuterated acetone was prepared. To 1ml of this solution, 300 equivalents of tetrabutylammonium anion were added and the main chemical shifts noted.

**Temperature degradation study of 4-1, 4-2 and 4-3 by $^{1}$H NMR.** A 1.6mM solution of each compound in the relevant NMR solvent was placed in a temperature control oven in anhydrous conditions and left for 12 hours at incremental temperatures between 30°C and 100°C. Following a return to room temperature, the spectra were examined for changes.

# 5. Chapter 5 Nitrile Calix[4]arenes for Soft Metal Analysis

## 5.1 ABSTRACT

The current work is amongst the first to examine the potential usefulness of the nitrile functional group in potentiometric analytical sensors for soft metals. Nitrile functionality has hereby been incorporated into a calix[4]arene skeleton to give a series of new cation selective hosts. The analytical sensing behaviour of these hosts was examined by Ion Selective Electrode (ISE) based potentiometry. In all cases a preference for soft metals was observed, explained primarily in terms of soft-soft compatibility between calix[4]arene nitrile hosts and metal guests in combination with a classical 'lock and key' best fit mechanism. Hosts **5-1, 5-4** and **5-6** showed very strong responses towards Hg(II) ions, with Ag(I) being the main interferant. The introduction of electron delocalising aromaticity proximal to the nitrile functionality was thought to reduce the availability of negative charge for cation coordination, apparently affecting the Hg(II) cation in particular. An acute fall in Hg(II) response coupled with the emergence of Ag(I) as the primary ion was observed for **5-7** and **5-8**. This chapter again demonstrates how the structural change of an ionophore was correlated with a change in analytical sensing signal.

## 5.2 INTRODUCTION

### *5.2.1 Nitriles as soft donor groups and their incorporation into complex forming hosts*

Typical soft donor atoms are sulphur and nitrogen, made soft by their relatively polarizable nature. Hard electron donor groups will interact with hard analyte acceptors and conversely, soft electron donor groups will show a preference for complexing soft analyte acceptors, according to a well established rationale[200].

Relatively little reference is made in the literature to the cation coordinating ability of nitriles in analytical sensors. The nitrile functional group resembles an alkyne, except that a hydrogen is replaced with a tightly held sp-hybridised lone pair on the nitrile nitrogen. Figure 5.1 shows the most common interaction mode of nitriles with metals.

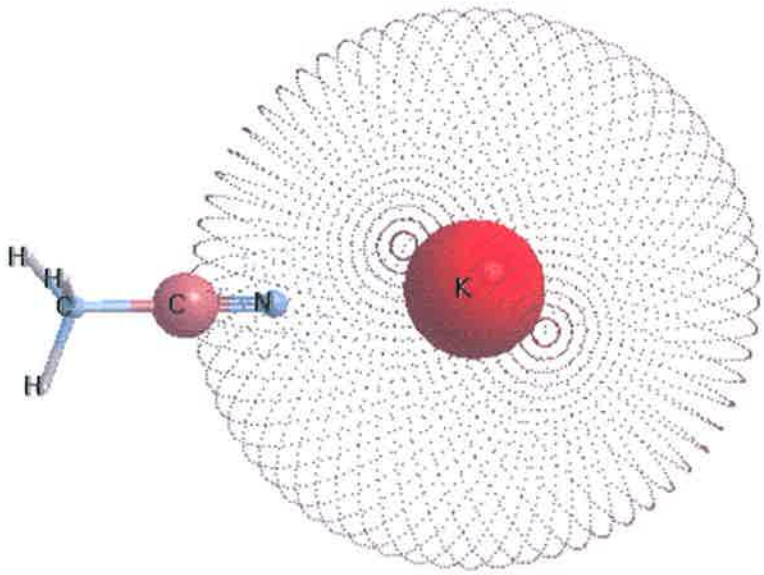


**Figure 5.1.** Nitriles as σ-donors for metal coordination with a nitrogen lone pair (complex with $K^+$ shown). The model's atoms are sized according to Debye-Hückel partial charges. Red and blue colour intensity signifies the magnitude of positive and negative charge respectively.

The weak σ-donor ability of the nitrile nitrogen lone pair is involved in coordinating cations[201]. In addition the highly polarizable π-systems of the nitrile groups induce a

preference for soft metal guests. The complex model in Figure 5.1 has atoms sized and coloured according to Debye-Hückel partial charges. This reveals the strong coulombic positive charge of the metal ion and the more subtle negative dipole charge on the nitrile nitrogen. The interaction depicted is classed as an electrostatic ion-dipole interaction. The basicity of a typical nitrile such as acetonitrile is $pK_b \sim 24$ ($pK_a \sim -1$). This makes the nitrile group very weakly basic, also explaining its general inertness and stability. Acetonitrile for example, a common solvent, is considered stable and widely used in the laboratory. One common reaction of nitriles is hydrolysis to a carboxylic acid[202]. A strong acid is required for this transformation due to the weak basicity of the nitrile lone pair. Organonitriles have been reviewed as versatile and convenient starting materials for organic chemists[203]. Their stability coupled with versatility mean they offer much potential for the designer of complex supramolecular host compounds.

Some authors suggested that the ability to reversibly and continuously monitor a target analyte are apt requirements in the definition of a "sensor"[35]. Where an irreversible process takes place like in a medical test strip for pregnancy or cardiac infarction, the term "probe" is more appropriate. For further examples such as industrial scrubbers or other multiphase extraction systems, *reversible* guest binding is not a core issue and so such applications cannot be labelled as "sensors".

### *5.1.1 Combining nitrile functionality with calixarene scaffolds: From probing to sensing soft cations.*

The general discussion in chapter 1.8 highlights the fact that most of the applications of calixarenes to date have been for hard cation sensing, namely group I and group II cations in the periodic table. Similar but somewhat less celebrated success was achieved when soft donor groups are used. Selectivity has been observed for softer cations (e.g. transition metals, lanthanides and heavy metals)[204-206].

In previous cases where nitrile groups have been incorporated into a molecular backbone such as a calixarene or a bis-calixarene, these compounds have been used (in monomeric form or attached to a polymer backbone), to perform multiphase extraction experiments of metals[14-16,207,208]. Hg(II) in particular was found to be extracted well in most cases. The best Hg(II) selectivity was observed for the alkyl nitrile substituents[209]. Aryl nitrile substituents enabled a delocalisation of nitrile electrons over the proximal π-electron cloud leading to less pronounced selectivity.

**Monomers:**

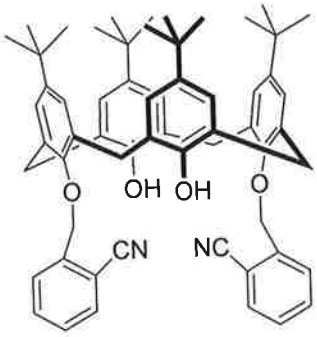


(Gungor, 2005)

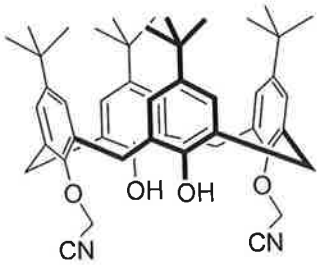


(Alpoguz, 2003)

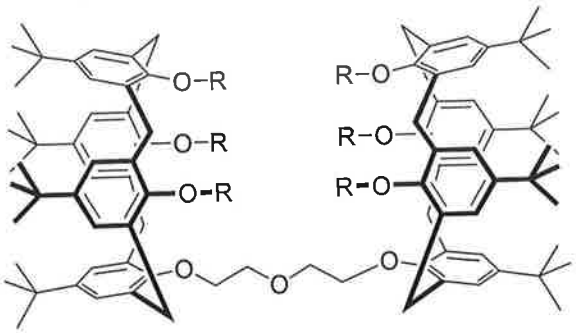


R = CN

(Alpoguz, 2002)

**Polymer linked:**

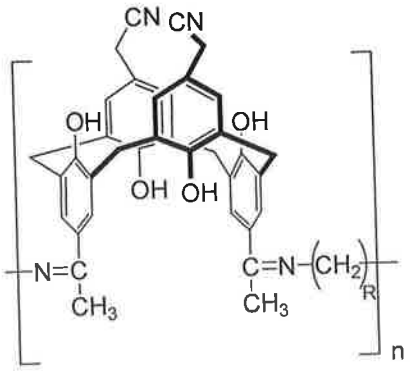


(Memon, 2002)

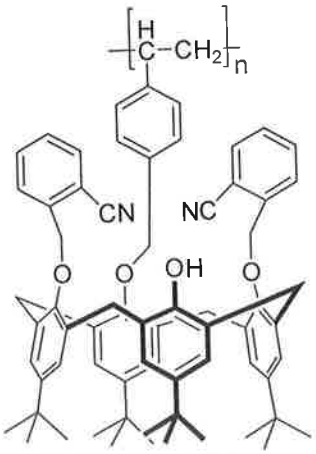


(Gungor, 2005)

**Figure 5.2.** A sample of the nitrile calix[4]arenes in the literature used for Hg(II) recognition by liquid-liquid extraction.

Figure 5.2 reveals a selection of the Hg(II) selective nitrile calix[4]arenas appearing in the literature. The study of these compounds revolves almost exclusively around liquid-liquid transport experiments.

The synthesis of the asymmetric (two types of lower rim appendage of varying length) tetranitrile calix[4]arene **5-1** was previously described[189] and is detailed in chapter 6. Wall attempted the synthesis of an equivalent asymmetric tetraester based on the well known **5-2**. This reaction proved very difficult, and resulted in a tetracarboxylic acid instead of the anticipated ester product[210]. In contrast, the relative inertness of the nitrile functional group may be the reason for much greater yields of the equivalent nitrile compound **5-1**.

LC-MS monitoring of the reaction mixture revealed that **5-1** was stabilised by ammonium ions, probably originating from the synthetic workup. This was interesting, as sodium or potassium stabilised molecular ions are far more common in the mass spectrometry of calixarenes[100]. Initial potentiometric screening of **5-1** confirmed the absence of sodium selectivity. This prompted the screening of **5-1** and related alkyl nitrile calix[4]arenes **5-4** and **5-6** by potentiometry for response towards a comprehensive range of hard and soft cations. A pattern of marked selectivity for Hg(II) and Ag(I) was thus revealed. The structural variants of these hosts, **5-7** and **5-8** showed how this selectivity could be tuned. The importance of sensing with reversibility is intrinsic for potentiometric analysis.

### *5.1.2 Hg(II) sensing using hosts without nitrile functionality*

Electrochemical Hg(II) sensors (showing *reversible* analyte recognition) developed recently include an ISE of a calix[4]crown based on imine[211], an ISE of a mercapto based system with it's soft nitrogen and sulphur donors[212] and a more classical thia-crown ether based ISE[213] amongst others[214,215]. Several charged compounds used in

electrodes for Hg(II) detection have also been reported[216-218]. There are numerous optical Hg(II) sensor compounds, which are largely solution characterised[35,219-229]. No Hg(II) or Ag(I) reversible *sensing*, based on nitrile functional groups, has been reported in the literature to date to the best of out knowledge.

A broad selection of Hg(II) selective hosts in the literature is shown in Figure 5.3.

**Potentiometric Sensors:**

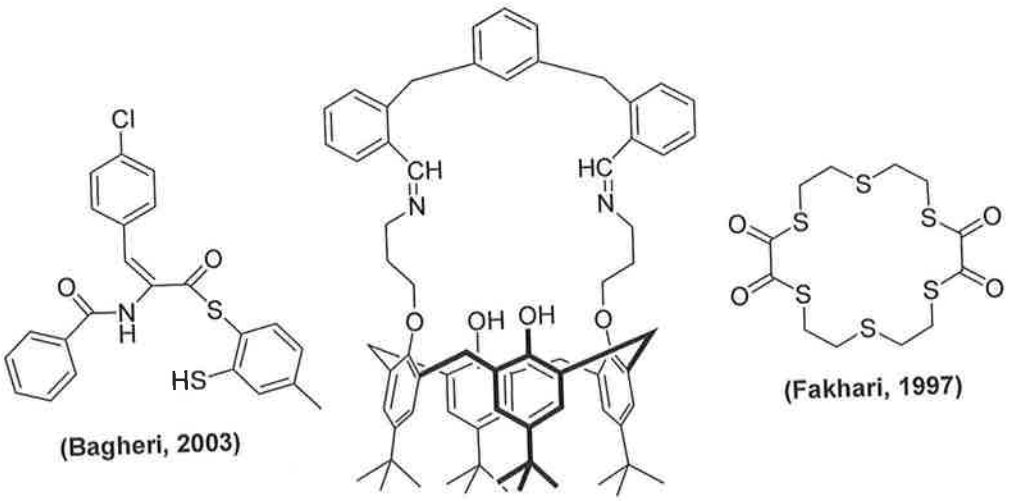

(Bagheri, 2003)

(Mahajan, 2004)

(Fakhari, 1997)

**Optical Sensors:**

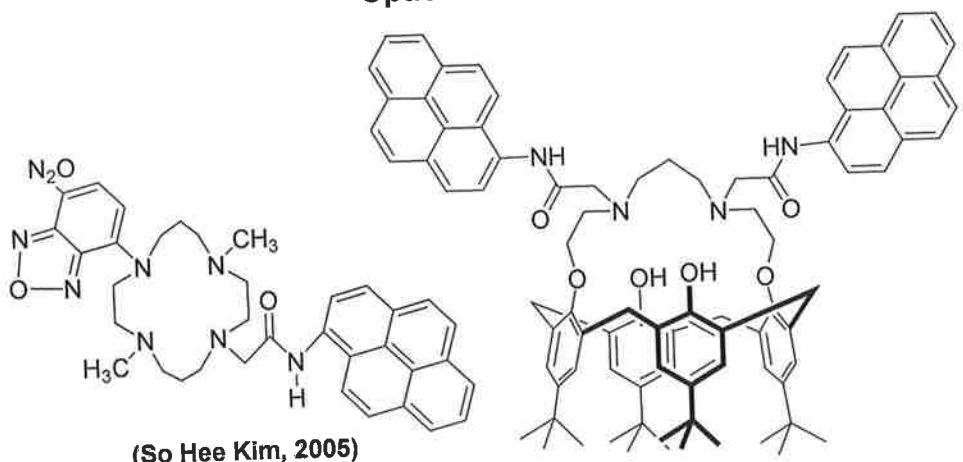

(So Hee Kim, 2005)

(Ju Hee Kim, 2004)

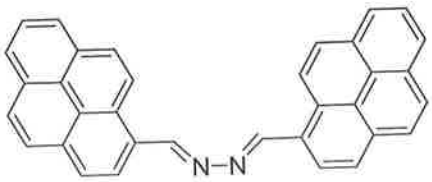

(Martinez, 2005)

**Figure 5.3.** Hg(II) selective hosts without nitrile functionality used for reversible sensing.

The early work on Hg(II) coordination involved solvent extraction experiments using macrocyclic polythiaether ligands[230-233]. These studies revealed Ag(I) as the main co-extractant (equivalent to interferant in sensor terms). Furthermore, recent developers of Hg(II) sensitive compounds often implicate Ag(I) as a major co-analyte[35,211,234-236]. Some of the recent publications on mercury extraction and to a lesser extent sensor reports omit testing for a Ag(I) response. From a supramolecular point of view in addition to a practical point of view, Ag(I) interference studies cannot be omitted.

### *5.1.3 An introduction to mercury(II) and silver(I)*

Hg(II) has no biological role in the body and is a toxic contaminant in waste waters around the world with severe associated health and environmental risks[145]. Mercury can affect the central nervous system and cause fetal deformities. In history it was used in elemental form for a variety of purposes such as treating skin conditions, a household antiseptic, treating syphilis and even as a beauty aid. Needless to say undesirable side affects were common. Today, sources of mercury are from industrial uses of mercury including electrolysis of sodium chloride and electrical devices. Dentistry uses mercury for fillings. Agricultural applications include the treatment of seed corn against fungus although this practice is being phased out.

Ag(I) has no biological role in the body. It is particularly toxic to lower organisms[145]. The high levels of hydrochloric acid in the stomach precipitate most Ag(I) thereby rendering it relatively harmless to humans, although irritations and death can occur in some cases. Historically uses of silver were manifold from curing warts, preventing blindness to anti-smoking tablets. Today, the main sources of silver are from photography, electrical goods, cutlery and jewellery. Dentistry also employs silver. The most promising future application is to kill antibiotic-resistant strains of infection.

Despite being less toxic to humans than Hg(II), Ag(I) is an industrially important ion and must be of interest to the designer of soft metal sensors[236-241].

The Hg(II) ion prefers to form linear 2 coordination complexes whereas Ag(I) is able to adopt a wide variety of complex geometries and hence is found in numerous forms[242]. In the context of the current work, Ag(I) was previously shown capable of forming linear complexes with nitrile calixarenes by crystallography[243]. Ag(I) salts dissociate much more readily than say the very stable Hg(II) chloride in water and were found to coordinate to ligands much more readily in this dissociated form[244]. Ions rich in d-electrons, forming complexes with low coordination numbers are particularly common to the right of the d-block in the periodic table[242]. The best known linear 2 coordination complexes formed at ordinary laboratory conditions are from ions of group 11 and 12, the homes of silver and mercury respectively. These factors may explain why the soft ions Ag(I) and Hg(II) are often encountered as co-analytes.

Relatively little reference is made in the literature to the cation coordinating ability of the soft nitrile functional group in analytical sensors. The use of nitrile functionality in calixarene (or other scaffolds) based Ion Selective Electrodes (ISEs) has not been reported to date to the best of our knowledge.

The aims of the current work were, using potentiometry to (1) investigate the mode of binding towards metals of a series of nitrile calixarenes and compare selectivity patterns (2) change ISE membrane parameters like polarity and host structure and correlate these changes to an analytical signal (3) discuss viability of calix[4]arene nitriles for use in chemical *sensors* for soft metals by focussing particularly on reversible and selective analyte detection and (4) to allude to future work and structural tuning strategies for synthesising improved supramolecular hosts with nitrile functionality.

## 5.3 RESULTS AND DISCUSSION

### 5.3.1 *Synthesis*

The synthesis of **5-4** and **5-6** were carried out according to Scheme 5.1 and Scheme 5.2 respectively. **5-1**, **5-2**, **5-7** and **5-8** were synthesised elsewhere as detailed in the experimental section (structures in Figure 5.4).

**Scheme 5.1**. The synthesis of **5-4**.

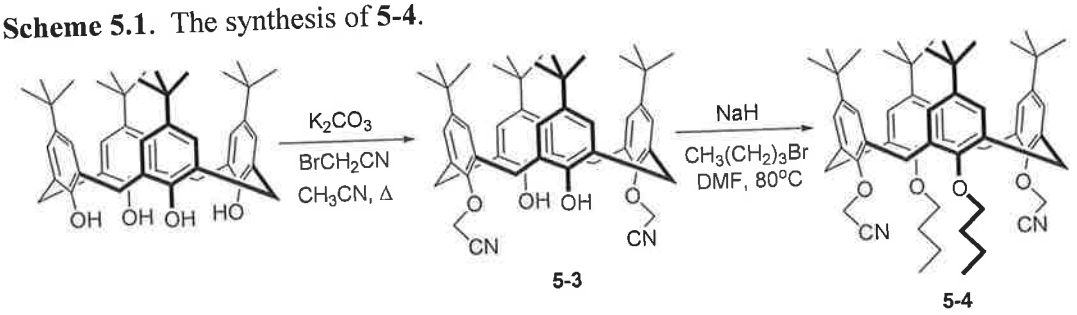


**Scheme 5.2**. The synthesis of **5-6**.

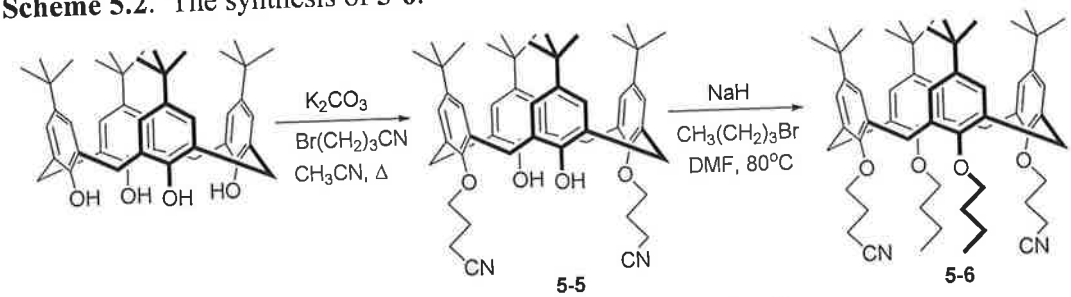


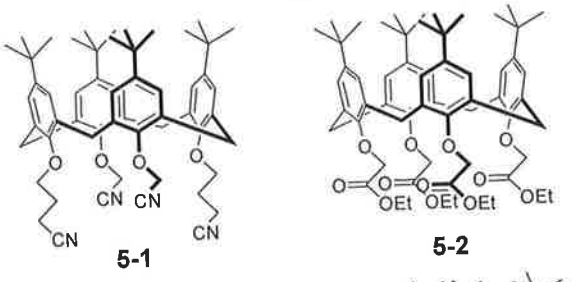


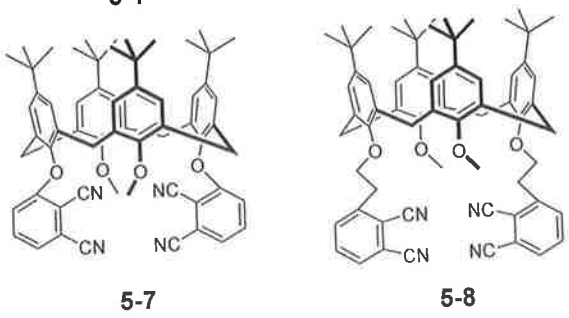


**Figure 5.4**. Structures of calixarenes **5-1**, **5-2**, **5-7** and **5-8**.

Neutral hosts **5-4** and **5-6** are asymmetrically tetrasubstituted on the lower rim, each containing four alkyl groups. In each case, two of the alkyl chains terminate with nitrile groups. The two possible cation binding sites within each of these compounds are the four hard phenoxy oxygens just below the calixarene's annulus and the two soft nitrile groups, either of which may interact with cations. Host **5-4** contains the two possible binding sites in close proximity, thus allowing possible cooperative binding between the two sites. Host **5-6** contains the two sites at a greater distance from each other and so in contrast a cation guest is more likely to interact with one *or* the other. The other host calixarenes discussed in the current report are shown in Figure 5.4.

### *5.3.2 The potentiometry of ISEs containing 5-1, 5-4 and 5-6*

Figure 5.5 highlights some of the ISE potentials observed when **5-1** was screened separately with a selection of cations in aqueous solution of specific activity, log a = -2.3. These responses were compared to the response of a blank membrane, where no ionophore is present.

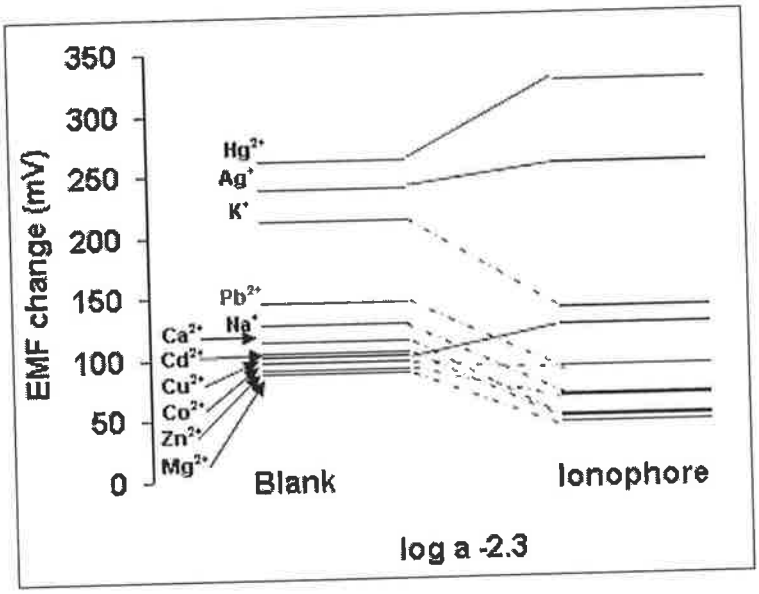


**Figure 5.5**. The comparison of potentiometric responses of a blank membrane with **5-1**. The potential change is for the specified cation at activity log a = -2.3 compared to de-ionised water**.

It can be seen that **5-1** shows a strongly enhanced response towards Hg(II), Ag(I) and to a lesser extent Cu(II). Conversely, all other cations reveal a reduced response compared to the blank (Hofmeister series) membrane. The most dramatically enhanced response is observed for Hg(II). The selectivities of ISEs are expressed formally by selectivity coefficients, $K_{IJ}^{pot}$, based on the Nernst equation[20,22]. Using the Separate Solutions Method (SSM), the selectivities were calculated for **5-1**, **5-4** and **5-6**. Table 5.1 shows selectivity coefficients for a comprehensive range of cations tested.

** The typical concentration of divalent cations, equivalent to log a = -2.3, is $10^{-3}$M.

| Host | 5-1 | 5-6 | 5-4 | 5-1 |
|---|---|---|---|---|
| Plasticizer | NPOE | NPOE | NPOE | DOS |
| $Hg^{2+}$ | 0 | 0 | 0 | 0 |
| $Ag^{+}$ | -0.19±0.07 | 0.95±0.14 | -0.25±0.12 | 2.25±0.10 |
| $Pb^{2+}$ | -7.86±0.07 | -7.20±0.00 | -7.03±0.14 | -3.02±0.02 |
| $Cu^{2+}$ | -7.00±0.09 | -7.73±0.02 | -6.56±0.19 | -1.62±0.03 |
| $Co^{2+}$ | -8.21±0.10 | -7.74±0.14 | -8.03±0.07 | n/a |
| $Cd^{2+}$ | -9.41±0.07 | -8.64±0.02 | -8.84±0.12 | -5.04±0.03 |
| $Zn^{2+}$ | -8.82±0.07 | -8.88±0.02 | -9.32±0.12 | -4.75±0.02 |
| $H^{+}$ | -5.52±0.14 | -5.02±0.02 | -5.00±0.33 | 0.72±0.02 |
| $Mg^{2+}$ | -9.32±0.05 | n/a | n/a | n/a |
| $Ca^{2+}$ | -8.82±0.05 | n/a | n/a | n/a |
| $Li^{+}$ | -7.48±0.05 | n/a | n/a | n/a |
| $K^{+}$ | -3.91±0.07 | -2.49±0.02 | -3.45±0.24 | 0.72±0.02 |
| $Na^{+}$ | -6.23±0.08 | -4.94±0.00 | -5.31±0.19 | -0.25±0.02 |

**Note**: I is the primary ion $Hg^{2+}$ and J is the interferant specified. The Separate Solutions Method (SSM) was used where log $a_I$=log$a_J$=-2.3. Reproducibility based on three ISEs. n/a = Data not available.

**Table 5.1**. Selectivity Coefficients, log $K^{pot}_{Hg^{2+},J}$, for **5-1**, **5-4** and **5-6**, calculated using the Separate Solutions Method (SSM).

The very strong selectivity towards silver (I) and mercury (II) is immediately apparent from Figure 5.5 and confirmed in Table 5.1. It is thought that that perhaps the nitrile functionality of the current host series dictates the response rather than the phenoxy oxygen atoms, which is consistent with the predicted conformation from theoretical models (Figure 5.6).

The theoretical molecular models in Figure 5.6 shows the well-established the classic calixarene cone conformation adopted by **5-2**, which facilitates the selective binding of sodium ions by tetraester **5-2**, involving phenoxy and ester carbonyl, oxygens by a well established complexing mechanism (chapter 1.11). Conversely, the energy minimised structure of the Hg(II) complex of **5-1** (and related calixarene nitriles) suggests that

binding occurs by association with nitrile functional groups as seen in Figure 5.6. This example of **5-1** coordinating a cation shows a more peripheral cavity binding at a greater distance from the annulus, not significantly involving the calixarene phenoxy oxygen atoms. Apart from molecular model, the complexing mode of **5-1** is supported by the assertions that Hg(II) ions are too big to occupy the calix[4]arene vaity as sodium does in the case of **5-2**. Furthermore, Hg(II) is likely to prefer a soft-soft ion-dipole interaction with the nitrile nitrogens.

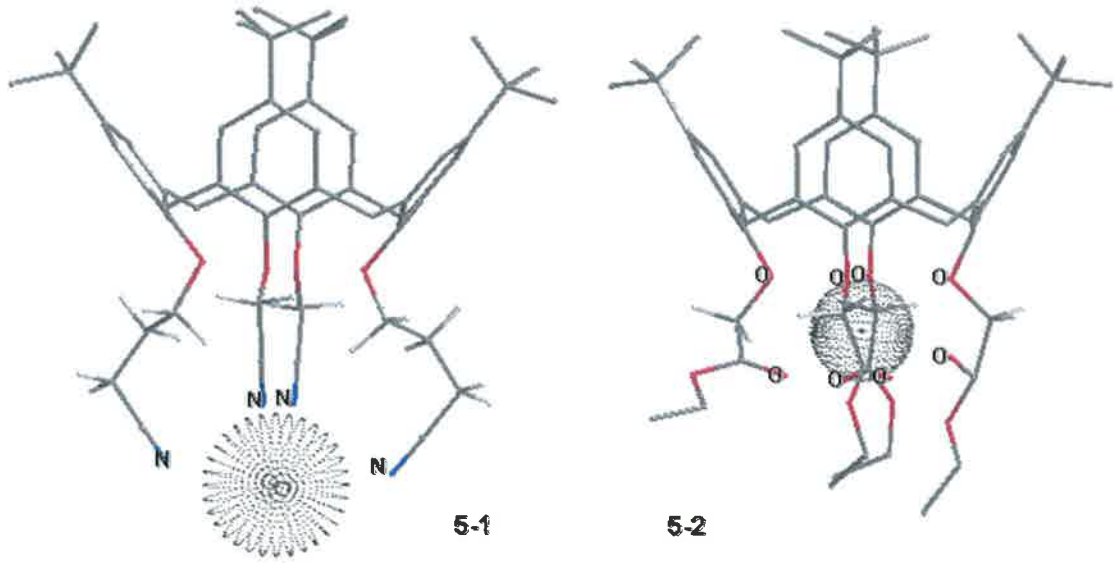


**Figure 5.6**. Molecular models showing the general modes of complexation of **5-1** with Hg(II) and **5-2** with Na(I).

The cone conformation of calix[4]arene **5-1** was initially confirmed by its $^{1}$H NMR spectrum[189]. A pair of doublets at 4.33 and 3.28ppm, correspond to the protons of the methylene groups linking the central benzenes (Figure 6.1). This suggests a cone conformation according to a method of determining calix[4]arene conformation described by Gutsche[81]. Furthermore the upper rim *p-tert*-butyl groups and lower rim substituents of **5-1** are likely to prevent significant deviation from the cone conformation by blocking free rotation of benzenes through the central cavity. The

cone conformation was prevalent for all other calix[4]arenes discussed in this chapter also and was confirmed using NMR data.

### *5.3.3 Modifying ISE response by changing membrane polarity*

The selectivity of an ISE can be modified by a number of strategies[20]. For example ISE membrane polarity can influence selectivity. Selectivity for divalent cations is generally enhanced in more polar membrane phases[245]. The polarity of the ISE membrane of **5-1** was changed by changing the plasticizer from NPOE (dielectric constant $\varepsilon_r$ = 23.9) to DOS ($\varepsilon_r$ = 3.9). This spans the majority of the polarity range of common ISE plasticizers.

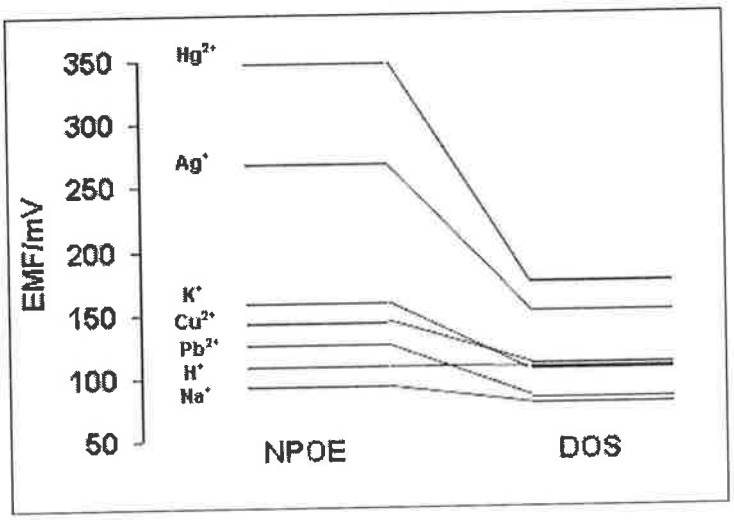


**Figure 5.7.** Potentials of an ISE based on **5-1** screened with a selection of cations, each at log a = -2.3. Membranes based on high polarity NPOE and low polarity DOS compared.

From Figure 5.7 it can be seen that the resultant ISE potentials observed were lower and more closely merged for DOS membranes in general accompanied by somewhat more reduced selectivity as seen in Table 5.1. The interference from group I metals like sodium and potassium is much greater for DOS membranes with log $K_{IJ}^{pot}$ values increasing by approximately six and five orders of magnitude respectively compared to

NPOE based membranes. Similarly, proton interference was a greater factor with DOS membranes indicative of greater pH sensitivity. These observations are due to a much smaller margin of response between Ag(I)/Hg(II) and other cations when DOS plasticizer was used instead of NPOE (Figure 5.7). In light of these observations, it was decided to use only NPOE for all further ISE work on Hg(II)/Ag(I) selective systems based on further receptors.

### *5.3.4 Reversibility of a potentiometric sensor and Donnan failure*

Table 5.2 reveals the ISE titration slopes obtained for Ag(I) and Hg(II) of the ISEs tested.

| Host | Ion | Plasticizer | Range (log a) | Slope (mV/decade) | Donnan Failure (log a) |
|---|---|---|---|---|---|
| **5-1** | $Hg^{2+}$ | NPOE | -4.0→-1.0 | +49.7 | -1.6 |
| **5-1** | $Hg^{2+}$ | DOS | -4.0→-1.0 | +29.0 | -1.6 |
| **5-4** | $Hg^{2+}$ | NPOE | -4.0→-1.0 | +46.1 | -1.6 |
| **5-6** | $Hg^{2+}$ | NPOE | -4.0→-1.0 | +37.0 | -1.6 |
| **5-1** | $Ag^{+}$ | NPOE | -4.0→-1.0 | +56.9 | NO |
| **5-1** | $Ag^{+}$ | DOS | -4.0→-1.0 | +54.8 | NO |
| **5-4** | $Ag^{+}$ | NPOE | -4.0→-1.0 | +55.2 | NO |
| **5-6** | $Ag^{+}$ | NPOE | -4.0→-1.0 | +53.4 | NO |

Note: NO=Not Observed. Theoretical Nernstian slopes are 59.6 and 29.3mV/decade for mono and divalent ions respectively.

**Table 5.2.** Characteristics of ISEs based on **5-1**, **5-4** and **5-6** for the indicated activities.

This ISE data was used to shed light on the complex formation process specifically. All slopes obtained for Hg(II) were super-Nernstian, except for the DOS membrane. Concurring with the slope values for mercury(II) is the abrupt Donnan failure (Figure 5.8) of the titration curves at higher concentrations of Hg(II) (log a ~ -2.0) .

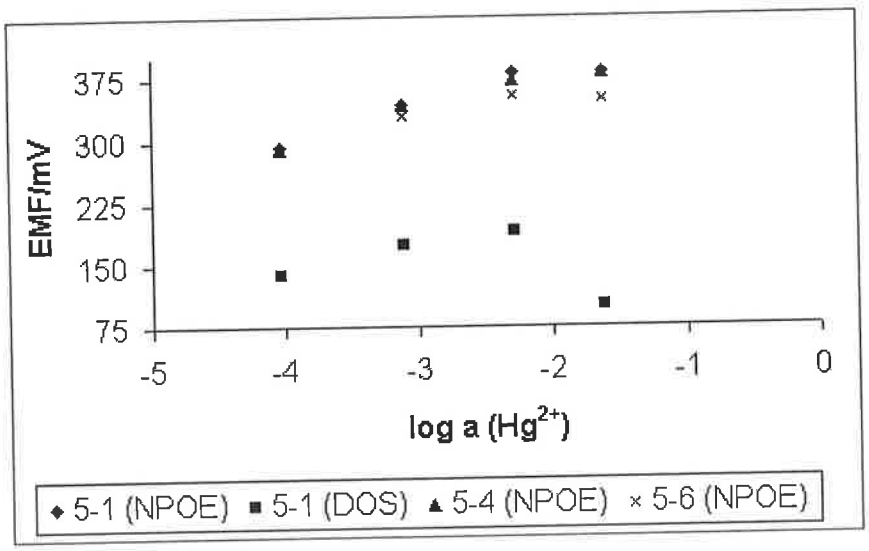


**Figure 5.8.** ISE titrations of **5-1**, **5-4** and **5-6** showing Donnan failure occurring at higher cation concentrations.

Donnan failure is caused by the co-extraction of counter ions of measured ions and can be symptomatic of very high affinities of an ISE towards the measured ion.

The complex formation process is known to be a major perpetrator causing Donnan failure with high analyte affinity or complex stabilities (i.e. binding constants) lowering the upper concentration limit at which the phenomenon takes place[246]. When developing a potentiometric sensor from a host compound, Donnan failure and its causes, as observed, would certainly impair the process of optimising the lower limit of detection (LOD) below the frequently observed classical LOD in the μM region. In addition, such a sensor would show poor reversibility[22,29,122].

Donnan failure and/or super-Nernstian slopes were observed for **5-1, 5-4** and **5-6** in response to Hg(II) in all cases at log a ~ -2.0, regardless of membrane polarity. The phenomenon was further probed in the case of **5-1**. Figure 5.9a shows the dynamic response when an ISE containing **5-1** was placed from water into a $10^{-2}$M solution of $Hg^{2+}$ and placed directly back into water. Even after 1.5 hours, the sensor had not recovered its starting potential. Analogously, an ISE of **5-1** conditioned and filled with

0.01M $HgCl_2$ instead of 0.01M NaCl showed very little sensitivity towards Hg(II) over a large concentration range (Figure 5.9b). It was concluded that after a first exposure of the membranes to Hg(II), subsequent ISE titrations would show a suppressed Hg(II) response. This is due to the pre-loading of membranes with Hg(II) and slow reversibility. Therefore, in order to show *unbiased* selectivity coefficients, a non-primary salt, NaCl, was generally used for ISE filling and conditioning for the current work[22].

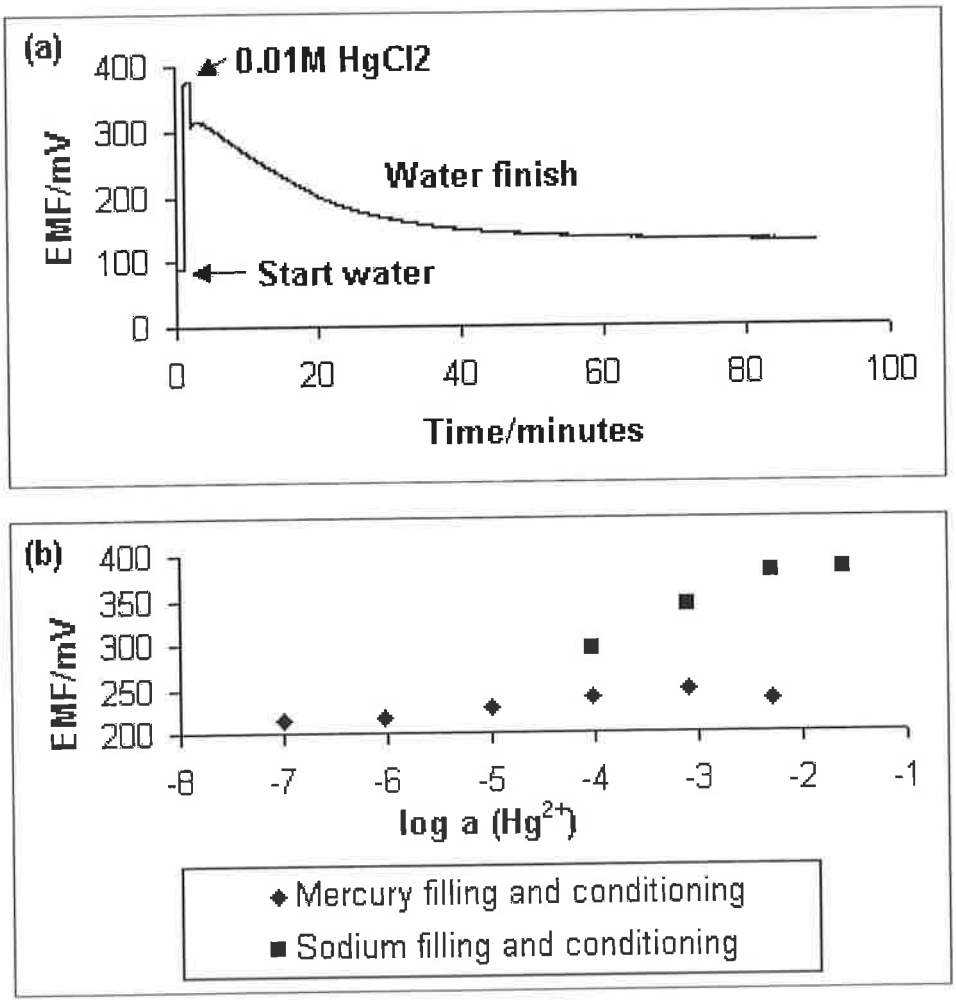


**Figure 5.9**. (a) The dynamic recovery of an ISE of **5-1** after exposure to 0.01M $HgCl_2$: Partial recovery after 1.5 hours. (b) The reduced sensitivity of an ISE of **5-1** with $HgCl_2$ filling and pre-conditioning .

### *5.3.5 Modifying ISE response by changing ionophore structure*

Another strategy to change the ISE sensor characteristics was to structurally modify the ionophore/host itself to modulate the interaction with guests. For example to lower the Hg(II) affinity or improve Ag(I) selectivity, strategies had to be applied to weaken the affinity of nitrile calix[4]arenes towards mercury (II) ions.

Hosts **5-4** and **5-6** contain only two instead of the previous four possible coordinating nitrile groups. It was thought that this would generally reduce complex stability. Furthermore, **5-4** has a smaller and more rigid lower rim cavity than **5-6**, which has longer alkyl nitrile appendages yielding a larger more flexible cavity.

The availability of somewhat more confined preorganised cavities in **5-1** and **5-4**, with nitriles closer to the calix[4]arene annulus, may have resulted in the near identical selectivities towards Hg(II) observed (Table 5.1), with marginal selectivity over Ag (I) for both hosts. Conversely, **5-6** showed a modest selectivity for Ag(I) over Hg(II). The larger silver ion may favour the greater flexibility of the two nitrile groups in the cavity of **5-6**. Table 5.3 compares the ionic radii of some selected cations[247].

| Ion | Radius (pm) | Coordination |
|---|---|---|
| $K^+$ | 138 | VI |
| $Na^+$ | 102 | VI |
| $Hg^{2+}$ | 102/69 | VI/II |
| $Ag^+$ | 115/67 | VI/II |

**Table 5.3**. Ionic radii of selected cations.

Unlike with Hg(II), **5-1**, **5-4** and **5-6** yielded Nernstian or near Nernstian slopes for Ag(I) and Donnan failure was not observed in the activity ranges of titrations carried out.

By and large, Hg(II) selectivity values over other cations are quite similar for **5-1**, **5-4** and **5-6** (Table 5.1). Lowering the number of nitriles from four to two did not yield a

noticeably weaker Hg(II) interaction. As Hg(II) ions are known to preferably form two coordinate linear complexes[248], the tetrahedral arrangement of nitrile functionality offered by **5-1** may not necessarily lead to stronger complex formation compared to di-nitriles **5-4** and **5-6**.

In order to maintain the selectivity of Ag(I)/Hg(II) over the other cations but to discriminate more between them, hosts **5-7** and **5-8** were synthesised. These structures introduce aromatic moieties proximal to the nitrile functionality (Figure 5.4), and, in addition, each lower rim benzene ring contains two nitrile groups, the idea being that one nitrile of each benzene ring would serve as guest coordinator whilst the other nitrile group and benzene ring would serve as electron withdrawing and delocalising agents respectively. It was hoped that the net effect would be to weaken the affinity for cations of these hosts by reducing the availability of negative charge. It was thought that this would suppress the excessive Hg(II) affinity previously observed and possibly induce discrimination between Ag(I) and Hg(II). With the large margin of selectivity of Hg(II)/Ag(I) previously enjoyed over the other cations for **5-1**, **5-4** and **5-6**, a modest loss in overall selectivity could be sustained.

Figure 5.10 compares the response of ISEs containing **5-7** and **5-8** to a blank membrane providing an overview of ISE performance.

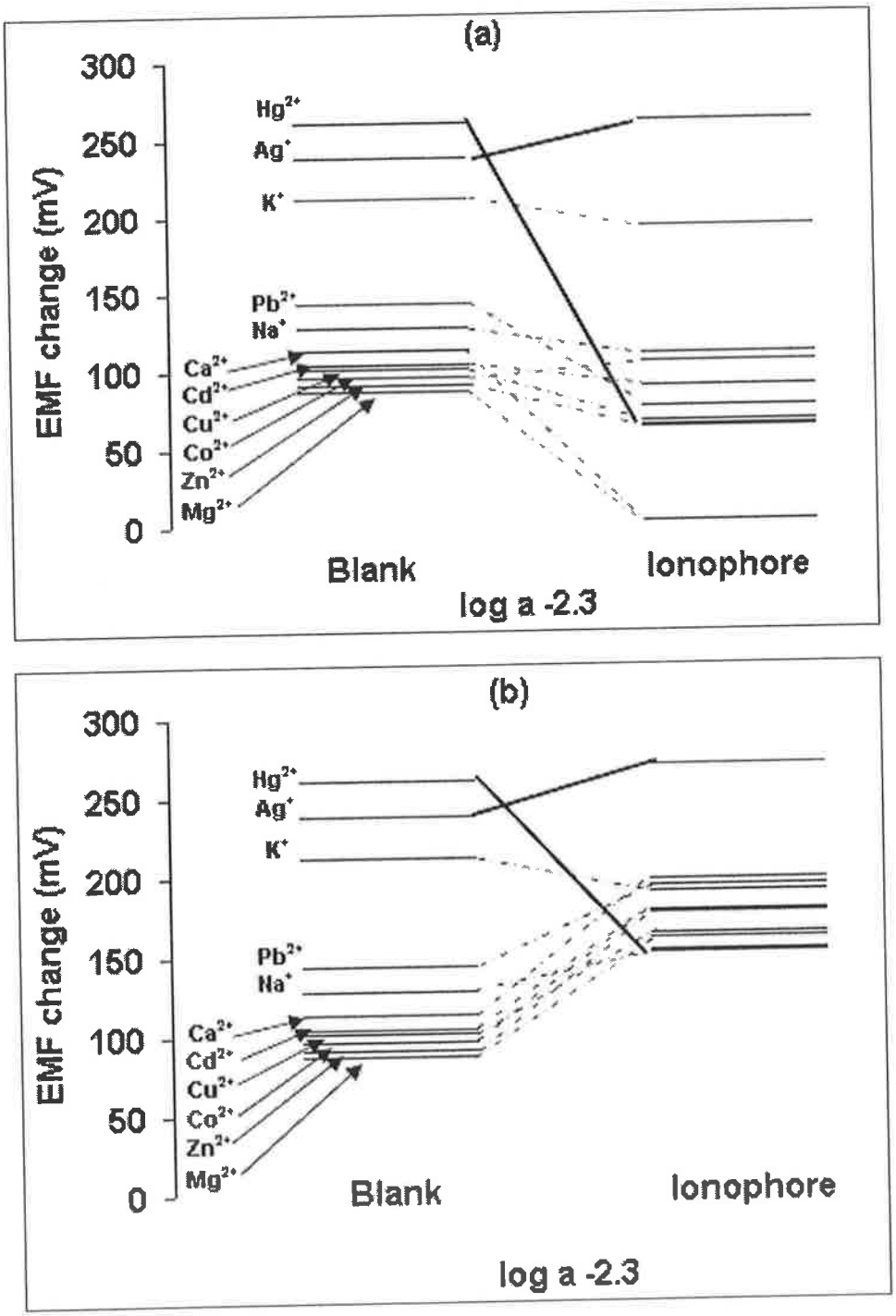


**Figure 5.10**. The comparison of potentiometric responses of a blank membrane with a) **5-7** b) **5-8**. The potential change is for the specified anion at activity log a -2.3.

Table 5.4 shows the selectivity values obtained for **5-7** and **5-8**, from ISEs prepared in an identical fashion to the other receptors described.

| Host | 5-7 | 5-8 |
|---|---|---|
| **Plasticizer** | NPOE | NPOE |
| $Hg^{2+}$ | -5.09±0.05 | -3.26±0.02 |
| $Ag^{+}$ | 0 | 0 |
| $Pb^{2+}$ | -4.50±0.02 | -2.25±0.12 |
| $Cu^{2+}$ | -4.90±0.02 | -3.07±0.14 |
| $Co^{2+}$ | -4.57±0.03 | -2.80±0.11 |
| $Cd^{2+}$ | -4.96±0.04 | -2.63±0.04 |
| $Zn^{2+}$ | -5.09±0.04 | -2.80±0.06 |
| $H^{+}$ | -3.86±0.05 | -2.29±0.06 |
| $Mg^{2+}$ | -6.66±0.10 | -3.07±0.07 |
| $Ca^{2+}$ | -6.11±0.10 | -2.49±0.02 |
| $Li^{+}$ | -4.00±0.01 | -2.46±0.05 |
| $K^{+}$ | -1.78±0.03 | -1.26±0.03 |
| $Na^{+}$ | -3.38±0.03 | -2.09±0.01 |

**Note**: I is the primary ion $Ag^{+}$ and J is the interferant specified.
The Separate Solutions Method (SSM) was used where log $a_I$=log$a_J$=-2.3.
Reproducibility based on three ISEs.

**Table 5.4**. Selectivity Coefficients, log $K^{pot}_{Ag^+J}$, for **5-7** and **5-8**, calculated using the Separate Solutions Method (SSM).

What is immediately apparent from these results was the suppression of Hg(II) sensitivity but maintenance of the Ag(I) response for both ionophores.

Interestingly, selectivities are more uniform in the case of **5-8** and the margin of selectivity of Ag(I) over the other cations is greater for **5-7** (e.g. log $K^{pot}_{Ag^+Hg^{2+}}$ of -5.1 and -3.3 for **5-7** and **5-8** respectively). Perhaps this is due to the larger more flexible cavity of **5-8** discriminating less between cations than the more rigid preorganised cavity of **5-7**. The ISE characteristics of **5-7** and **5-8** (Table 5.5) confirmed that they are poor hosts

for Hg(II) as response slopes went from previously observed super-Nernstian to sub-Nernstian (Typically >+40mV/decade for **5-1, 5-4** and **5-6** compared to <+15mV/decade for **5-7** and **5-8**). Furthermore, Donnan failure is absent in the activity ranges examined. Slopes closer to Nernstian values were observed for Ag(I) in all cases.

| Host | Ion | Range (log a) | Slope (mV/decade) | Donnan Failure (log a) |
|---|---|---|---|---|
| **5-7** | $Hg^{2+}$ | -4.0→-1.0 | +14.8 | NO |
| **5-8** | $Hg^{2+}$ | -4.0→-1.0 | +14.0 | NO |
| **5-7** | $Ag^{+}$ | -4.0→-1.0 | +58.3 | NO |
| **5-8** | $Ag^{+}$ | -4.0→-1.0 | +53.1 | NO |
| Note: NO=Not Observed. Plasticizer used: NPOE. | | | | |

**Table 5.5**. Characteristics of ISEs of **5-7** and **5-8** at the indicated activities.

To illustrate and compare the binding modes of the two structural classes of nitrile calix[4]arenes presented (with and without aromatic moieties proximal to nitrile functional groups), molecular models of Ag(I) complexes with **5-4** and **5-8** are shown in Figure 5.11 and 5.12 respectively as examples.

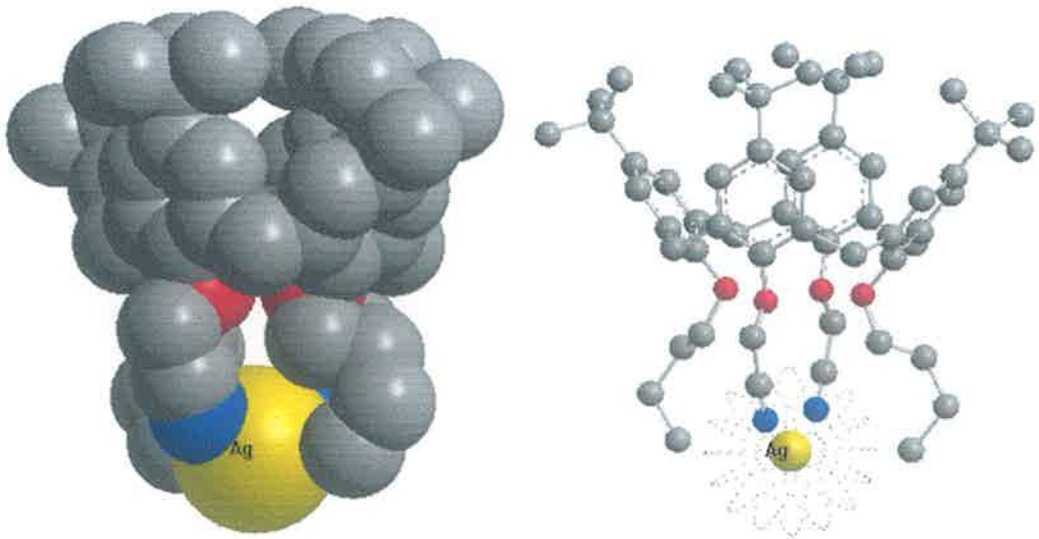

**Figure 5.11**. The energy minimised Ag(I) complex of **5-4** shown in both space filling (left) and normal (right) formats.

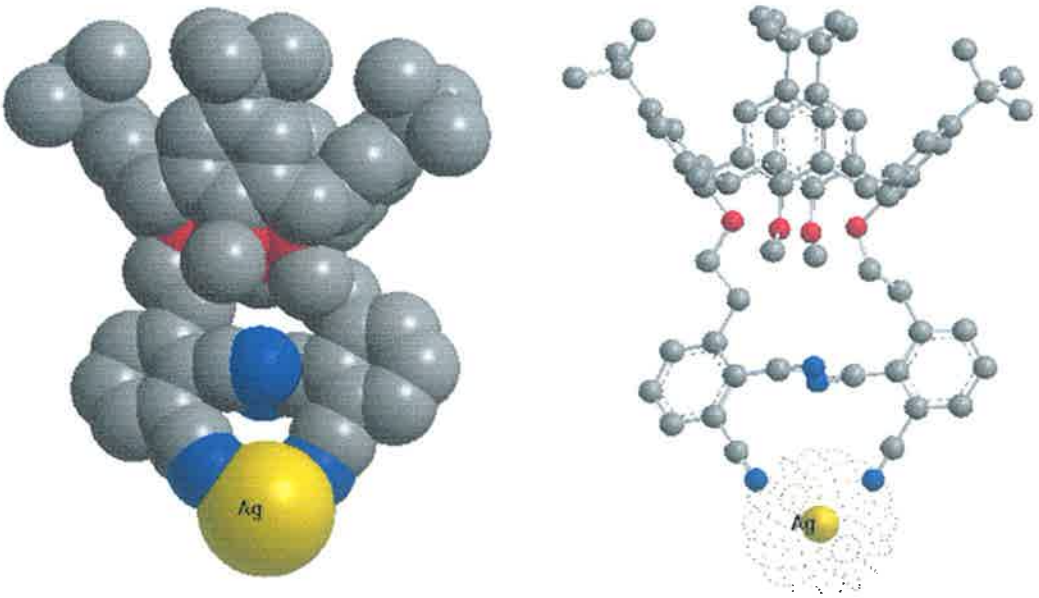

**Figure 5.12**. The energy minimised Ag(I) complex of **5-8** shown in both space filling (left) and normal (right) formats.

It is proposed that the influence of the delocalising ability of aromatic moieties proximal to nitrile functional groups dictates the selectivity patterns observed, more so than a size-exclusion phenomenon. This can be rationalised further from the models, where it can be seen that complexation of the large Ag(I) ion for example occurs at a distance from the calix[4]arene annulus for the nitrile calix[4]arenes, in what appear as quite flexible cavities lacking the rigid pre-organisation of the cavity in tetraester **5-2** for example. Physical encapsulation of the smaller sodium guest appears more complete in the case of **5-2** (Figure 5.13), as can be seen when comparing the space filling molecular models of **5-4**, **5-8** and **5-2**.

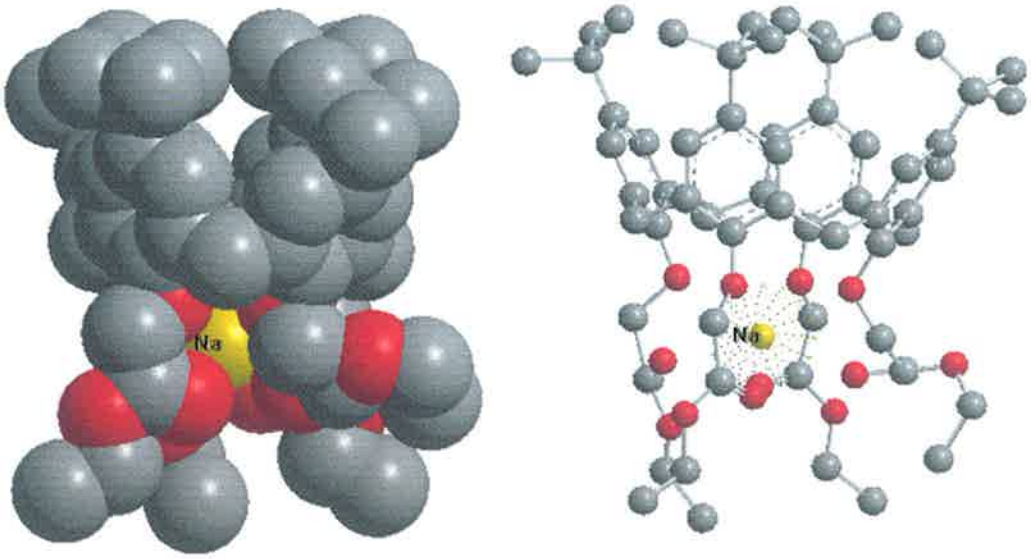


**Figure 5.13**. The energy minimised Na(I) complex of **5-2** shown in both space filling (left) and normal (right) formats.

## *5.4 CONCLUSIONS*

The current work describes calix[4]arene host systems based on nitrile functional groups, which display excellent Hg(II)/Ag(I) selectivity over other cations. In the course of the work described, an 'overtuning' of host structure led to the near suppression of a formerly overly-strong Hg(II) response, leaving Ag(I) as the primary analyte. In all cases changes in potentiometric ISE data could be correlated to the structural differences between hosts examined. ISEs were found to be an excellent tool for assessing selectivities of host systems, as they conveniently served to evaluate the work of the organic chemist whilst representing an analytical technique known to be readily implementable in real life practical sensors.

It was found that structural modifications of the host ionophore had a more dramatic effect on selectivity patterns observed than changing other ISE membrane components like membrane plasticizer (affecting polarity). The positioning of electron withdrawing groups and delocalising aromaticity proximal to the coordinating nitriles (**5-7** and **5-8**) led to a dramatic suppression of the Hg(II) response observed before and a

corresponding Ag(I) selectivity emerged. On the other hand, changing the number of nitrile groups available for binding and changing cavity dimensions (**5-1**, **5-4** and **5-6**) did not appear to dramatically change the high affinity for Hg(II). It is thought that Hg(II) forms a two coordinate complex with two nitrile groups per calixarene host, perhaps in a tweezer like fashion. This is in agreement with the theory suggesting Hg(II) ions ideally form linear two coordinate complexes.

The structural fine tuning of present hosts is ongoing. In future, efforts could focus on modifying the chemistry proximal to the nitrile groups in a way that could yield a practical and reversible Hg(II) sensor, by controlling the localisation of negative charge available for cation coordination. A further strategy could be to adorn other molecular scaffolds, apart from calixarenes, with presently under-exploited cation coordinating nitrile groups for the purpose of soft metal sensor development.

## 5.5 EXPERIMENTAL

The synthesis of hosts **5-1**, **5-3**[189] (chapter 6), **5-2**[26], **5-7** and **5-8**[249] were described elsewhere. NaH used was a 60% dispersion in mineral oil. All reactions were carried out under argon. The name *p-tert*-Butylcalix[4]arene was used instead of the IUPAC name for convenience: 5,11,17,23-tetra-*p-tert*-butyl-25,26,27,28-tetrahydroxycalix[4]arene.

HPLC was carried out using a HP1100 with UV detection. For LC-MS and direct injection MS work, a Bruker/Hewlard-Packard Esquire system, using a positive ESI source and the software's default 'smart' settings were used. Mobile phase used was isocratic LC grade Acetonitrile with 0.25% formic acid content. This also served as the sample solvent. A Synergy 150.0 x 2.0mm, 4μm Fusion-RP column was used. Flowrate was 0.2ml/min. Detection wavelength was 210nm. Injections were 5μl of 0.5mg/ml sample.

The general procedure for preparing ISEs and obtaining potentiometric data outlined in chapter 1.12 was followed.

Energy minimised molecular models were generated using Chem3D pro v.8.0 software, using the MM2 forcefield method.

**5,11,17,23-Tetra-*p-tert*-butyl-25,27-bis[(cyanomethyl)-oxy]-26-28-bis[(butyl)-oxy]calix[4]arene (5-4)**. Calixarene **5-3** (2.0g, 2.76mmol) and NaH (0.22g, 5.52mmol) was stirred 1 h at room temperature in anhydrous DMF (100ml). 4-Bromobutane (0.82g, 5.52mmol) was added batch wise and the mixture was stirred at 75 °C for 24 h and a further aliquot of NaH and 4-bromobutane added as above. The reaction was monitored by HPLC-MS. After a further 24 h, the DMF was evaporated and the residue taken up in $CH_2Cl_2$ (200ml), washed with 1N HCl (100ml), $H_2O$ (50ml), brine (50ml) and saturated $NH_4Cl$ (50ml) and dried with $Mg_2SO_4$. After filtration the $CH_2Cl_2$ was removed to yield an oily solid. Upon washing with 20ml MeOH at 0°C, 0.84g of a white solid was obtained: yield 37%; mp 165-170 °C; IR (KBr) 2174cm$^{-1}$ (CN); $^1$H NMR δ 7.16 (s, 4H), 6.42 (s, 4 H), 5.01 (s, 4H), 4.39 and 3.24 (ABq, 4H, J = 13.0), 3.78 (t, 4H), 1.97 (m, 4H, J = 7.2), 1.49 (m, 4H, J = 7.6), 1.35 (s, 18H), 1.00 (t, 6H, J = 7.2), 0.79 (s, 18H); $^{13}$C NMR δ 152.6 (s), 151.9 (s), 147.6 (s), 144.7 (s), 135.8 (s), 131.4 (s), 126.1 (s), 124.6 (s), 117.2 (s), 76.1 (s), 57.8 (s), 34.8 (s), 33.6 (s), 32.5 (s), 31.6 (s), 31.0 (s), 22.7 (s); 19.5 (s), ESI mass spectrum +m/e 861.4 ([M + Na$^+$], calcd 861.5); HPLC purity: 95.6%. Anal. Calcd for $C_{56}H_{74}N_2O_4$: C, 78.46; H, 8.94; N, 3.27. Found: C, 78.42; H, 9.18; N, 2.90.

**5,11,17,23-Tetra-*p-tert*-butyl-25,27-bis[(cyanopropyl)-oxy]-26-28-dihydroxycalix[4]arene (5-5)**. *p-tert*-Butylcalix[4]arene (5.0g, 7.72mmol), $K_2CO_3$ (1.28g, 9.26mmol) and bromobutyronitrile (2.41g, 16.20mmol) was heated in $CH_3CN$ (80ml) at 80 °C for 5 days. The reaction was monitored by LC-MS. The solvent was

evaporated and the residue taken up in $CH_2Cl_2$ (300ml), washed with 1N HCl (100ml), $H_2O$ (50ml) and brine (50ml) and dried with $Mg_2SO_4$. $CH_2Cl_2$ was evaporated and the residue was recrystallised from $CHCl_3$/MeOH yielding 3.7g of a white solid: yield 61%; mp 295-300 °C; IR (KBr) 2250 $cm^{-1}$ (CN), 3406 $cm^{-1}$ (OH) ; $^1H$ NMR δ 7.46 (s, 2H), 7.05 (s, 4 H), 6.86 (s, 4H), 4.16 and 3.37 (ABq, 4H, J = 13.0), 4.09 (t, 4H, J = 5.6), 3.05 (t, 4H, J = 7.2), 2.34 (m, 4H, J = 5.6), 1.27 (s, 18H), 1.00 (s, 18H); $^{13}C$ NMR δ 150.3 (s), 148.8 (s), 147.6 (s), 142.1 (s), 132.6 (s), 127.5 (s), 125.8 (s), 125.3 (s), 119.5 (s), 73.3 (s), 34.0 (d), 31.8 (d), 31.0 (s), 26.6 (s), 14.2 (s); ESI mass spectrum +m/e 805.5 ([M + $Na^+$], calcd 805.5); HPLC purity: 97.3%. Anal. Calcd for $C_{52}H_{66}N_2O_4$: C, 79.76; H, 8.50; N, 3.58. Found: C, 79.64; H, 8.44; N, 3.54.

**5,11,17,23-Tetra-*p-tert*-butyl-25,27-bis[(cyanopropyl)-oxy]-26-28-bis[(butyl)-oxy]calix[4]arene (5-6).** Calixarene **5-5** (4.0g, 5.12mmol) and NaH (0.41g, 10.21mmol) was stirred 1 h at room temperature in anhydrous DMF (100ml). 4-Bromobutane (1.52g, 10.21mmol) was added batch wise and the mixture was stirred at 75 °C for 24 h and a further aliquot of NaH and 4-bromobutane added as above. The reaction was monitored by HPLC-MS. After a further 24 h the DMF was evaporated and the residue taken up in $CH_2Cl_2$ (200ml), washed with 1N HCl (100ml), $H_2O$ (50ml), brine (50ml) and saturated $NH_4Cl$ (50ml) and dried with $Mg_2SO_4$. After filtration the $CH_2Cl_2$ was removed to yield an oily solid. Upon washing with 40ml MeOH at 0°C, 3.89g of a white solid was obtained: yield 85%; mp 190-195 °C; IR (KBr) 2244$cm^{-1}$ (CN); $^1H$ NMR δ 7.06 (s, 4H), 6.52 (s, 4 H), 4.30 and 3.17 (ABq, 4H, J = 12.8), 4.06 (t, 4H, J = 7.2), 3.74 (t, 4H, J = 7.2), 2.64 (t, 4H, J = 7.6), 2.41 (m, 4H, J = 7.6), 1.86 (m, 4H, J = 7.6), 1.49 (m, 4H, J = 7.6), 1.28 (s, 18H), 1.02 (t, 6H, J = 7.6), 0.88 (s, 18H); $^{13}C$ NMR δ 153.4 (s), 152.3 (s), 145.5 (s), 144.3 (s), 135.1 (s), 132.1 (s), 125.6 (s), 124.7 (s), 119.9 (s), 75.7 (s), 72.7 (s), 34.1 (s), 33.7 (s), 31.7 (s), 31.2 (s), 30.9 (s), 25.9 (s);

ESI mass spectrum +m/e 917.4 ([M + $Na^+$], calcd 917.5); HPLC purity: 97.5%. Anal. Calcd for $C_{60}H_{82}N_2O_4$: C, 80.49; H, 9.23; N, 3.13. Found: C, 80.50; H, 9.41; N, 3.01.

# 6. Chapter 6 Developing an Efficient Instrumental Procedure for Isolating Pure Supramolecular Hosts

## 6.1 ABSTRACT

A simple analytical LC-MS (Liquid Chromatography-Mass Spectrometry) method and associated instrumentation has been adapted for use by the organic chemist to yield mg quantities of target compound from a reaction mixture.

The isolation of pure **5-1** is described in detail to illustrate the approach used to develop a HPLC based purification regime. Following the success of this method, appropriate modifications were applied to isolate pure **3-1**, **3-2** and **4-3**. These are also described in this chapter. Chapter 6 focuses in particular on the purification aspects of synthesis. The classical organic components of synthesis aswell as the analytical properties of the hosts isolated, as relevant to the development of sensors, is described in other chapters.

Calix[4]arene **5-1** was identified as representing 51% of total peak area of a reaction mixture containing no less than 10 components, using LC-MS. This peak corresponded to a mass of 878.8, equivalent to a complex of **5-1** and an ammonium cation. Molecular models further rationalise this observation by showing that the asymmetric binding cavity of **5-1** is suitable for binding tetrahedral guests like the ammonium ion.

By scaling up the LC method, using analytical instrumentation, 55mg of 98% pure **5-1** were isolated with a recovery yield of 90% in 1 hr.

The methods described represent a powerful and easily adapted tool for monitoring challenging synthesis, which combines identification, efficient separation and partial characterisation for reaction mixture components using readily available

instrumentation and methods. The methods are intended to easily compliment the synthetic toolbox of any supramolecular chemist and are applicable beyond calixarene chemistry.

## 6.2 INTRODUCTION

### *6.2.1 The initial synthesis and first evidence of analytical potential of 5-1*

The synthesis of **5-1** was carried out according to reaction Scheme 6.1.

**Scheme 6.1.** The synthesis of **5-1**.

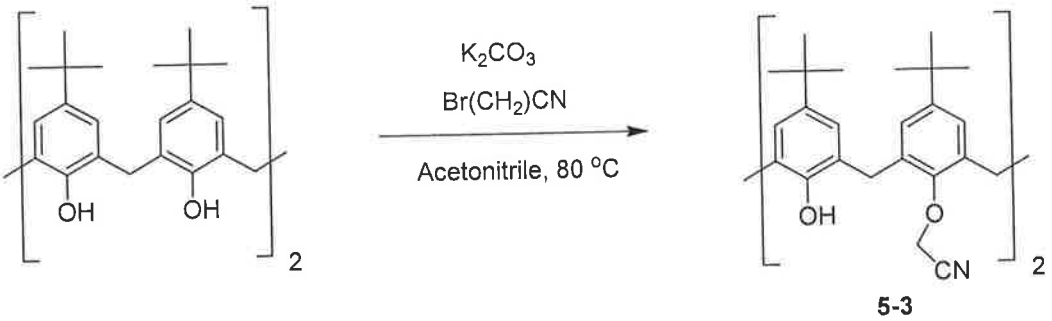


**5-3**

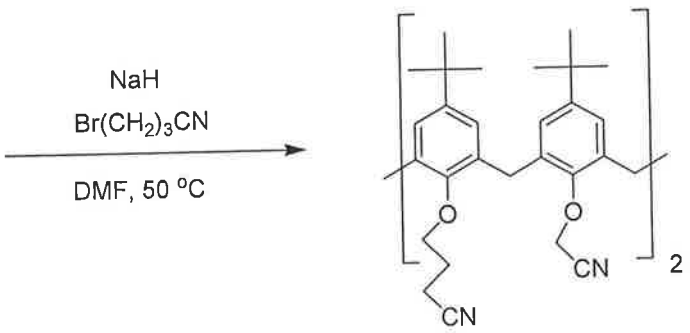


**5-1**

Structure **5-1** was envisaged as a precursor of a host for non-spherical shaped cations and anions. This is due to the differing lengths in the alternate pendant groups represented in the spatial arrangement of functionality on the lower rim. Initial evidence for this calix[4]arene cone conformation was gleaned from two doublets observed at 4.33 and 3.28ppm for the methylene protons in the calixarene's annulus, as seen in the proton NMR of **5-1** (Figure 6.1).

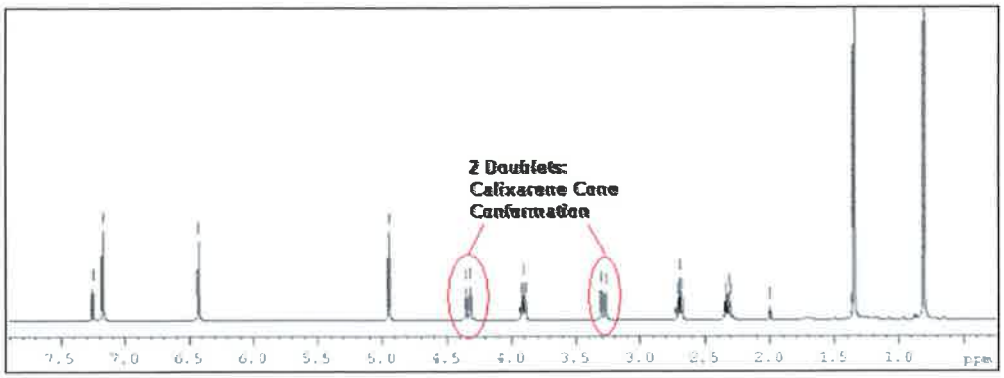


**Figure 6.1**. The $^{1}H$ NMR of **5-1** showing the peaks corresponding to the methylene protons of the central annulus, indicative of a calix[4]arene cone conformation.

One low energy conformation is that shown in Figure 6.2 as obtained by energy minimised molecular models. The procedure of generating models follows the general guidelines given in chapter 1.12. A calix[4]arene cone conformation is favourable for generating rigid preorganised structures as discussed in chapter 1.8.

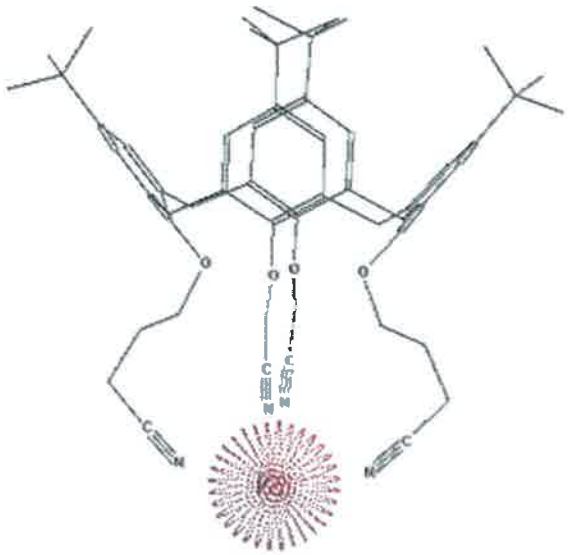

**Figure 6.2**. An energy minimised molecular model of **5-1** complexed with a potassium ion.

The mixture from the synthesis of **5-1** was analysed by LC-MS. The peak labelled **5-1** in Figure 6.3 corresponds to a molecular ion +m/e 878.8 ([M + $NH_4^+$], calcd 878.6) with an area of 51% relative to total peak area. Ammonium ions, presumably originating from the synthetic workup, appeared to stabilise **5-1**.

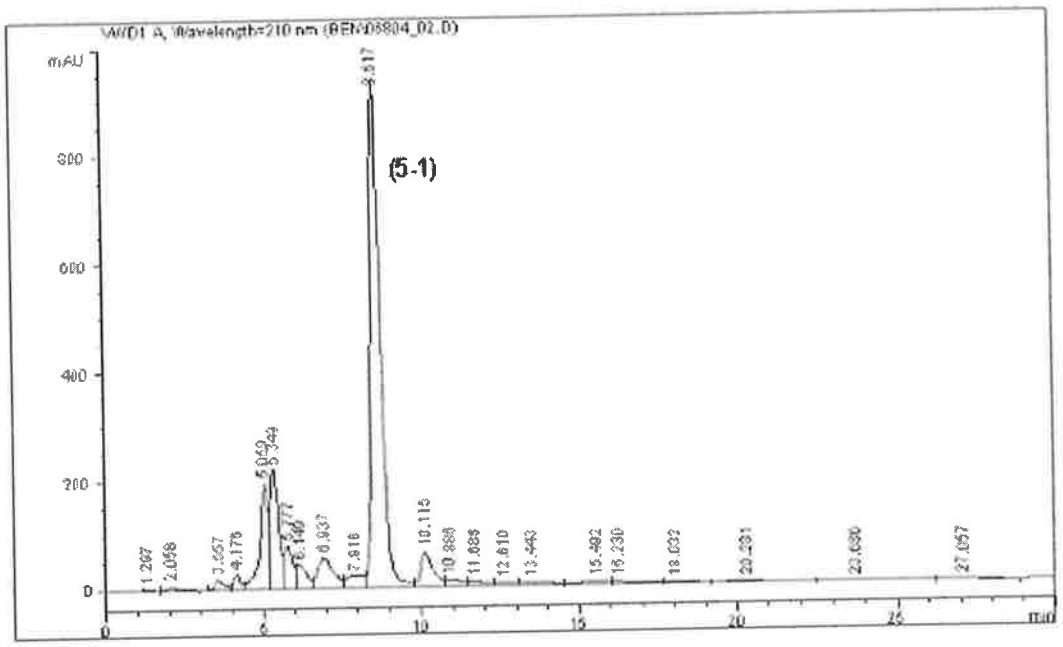


**Figure 6.3**. LC chromatogram of reaction mixture; **5-1** identified by MS. Detection is at 210nm.

These and further observations justified the expenditure of effort to isolate quantities of pure **5-1**.

The observation that **5-1** may be predisposed towards binding tetrahedrally shaped cations, like ammonium, could be due to the spatial arrangement of its binding sites. Indeed, following purification, preliminary potentiometric screening of **5-1** further confirmed significant responses towards a number of cations. Table 6.1 depicts the potential change of an ISE containing **5-1** when in contact with a $10^{-1}$M aqueous solution of the indicated cation compared to equivalent measurements in deionised water. This demonstrates that complex formation is indeed occurring with a particular order of selectivity, which favours ammonium and potassium over the 'default' sodium selectivity observed for calix[4]arene tetraesters and ketones[28,26,210].

| Cation | Potential change (mV) |
|---|---|
| $K^+$ | +216.0 |
| $NH_4^+$ | +206.9 |
| $Na^+$ | +154.0 |
| $Ca^{2+}$ | +79.4 |
| $Li^+$ | +71.4 |
| $Mg^{2+}$ | +62.4 |

**Table 6.1**. Potential changes of an ISE containing **5-1** immersed in $10^{-1}$M aqueous solutions of the indicated cation chloride, compared to the equivalent potential in deionised water.

Figure 6.2 reveals that **5-1** has rather lengthy lower rim appendages and so a larger more flexible cavity is plausible. This enables larger cations such as potassium and ammonium to be complexed compared to say a tetraester calix[4]arene which disposes of a smaller more rigid cavity closer to the annulus and so is more suitable complexing smaller sodium cations. A comparative model of this can be seen in Figure 5.6.

A glimpse at the identity, percent purity *and* analytical character of **5-1** was obtained using LC-MS *prior* to any attempts at purification and isolation. Purification is arguably by far the most arduous and time consuming component of many a complex synthesis[100]. Any advance reassurance that embarking on lengthy purification is worthwhile must be welcomed by the chemist. The application of analytical tools by the synthetic chemist is extolled, another example of the increasingly interdisciplinary nature of chemistry and science.

### *6.2.2 More intricate target hosts demand more powerful characterisation and isolation techniques*

Chapter 1.10 outlines the well known properties of tetraester calix[4]arenes with the general structure shown in Figure 1.17 and a specific examples shown in Figure 6.4. These hosts display excellent sodium selectivity for a number of transduction approaches, most notably potentiometric transduction. Above all, this was shown to be

due to suitable preorganisation of the host and a particularly good fit between sodium and the host cavity.

Wall and co-workers initiated research to synthesise derivatives of these 'parent' *symmetric* tetraesters to create new ester calix[4]arene hosts with partially substituted lower rims and subsequent *asymmetric* tetraesters, with appendages of varying length[99,100,210]. The aim of this research was to induce selectivities deviating from sodium selectivity. In particular the asymmetric hosts were to have cavities of suitable dimensions, rigidity and suitably orientated electrostatic bond forming carbonyls to form complexes with *tetrahedral* cationic guests. A selection of these structures is depicted in Figure 6.4[100].

**'Parent' symmetrical tetraester:**

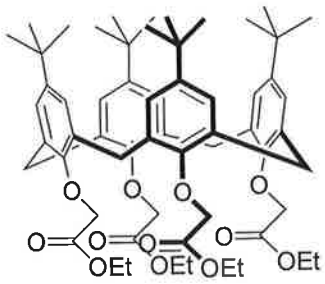

**Partially substituted ethyl ester calix[4]arenes:**

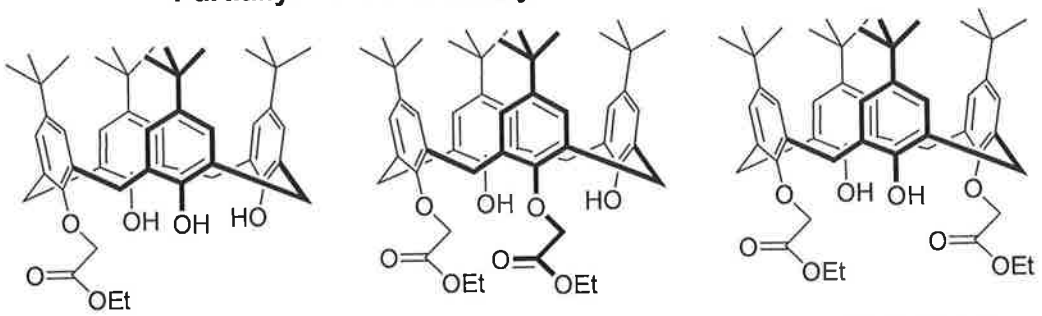

**Monosubstituted** **1,2-disubstituted** **1,3-disubstituted**

**6-2**

**Asymmetric tetraester calix[4]arene:**

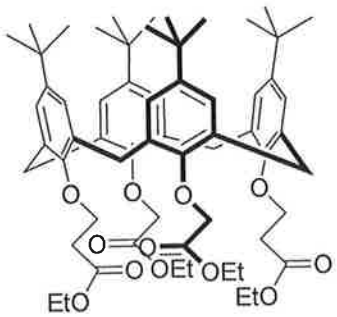

**6-3**

**Figure 6.4.** Structure of ester calix[4]arene derivatives.

The 1,3-disubstituted calix[4]arene **6-2** is clearly a precursor to the asymmetric tetraester **6-3** also depicted in Figure 6.4. The crude mixture from the synthesis of **6-2** was analysed by DI-MS revealing a good yield of the desired product[99]. UV-HPLC also told a similar story. However, when extending the examination using LC-UV-MS and LC-DAD, a much more complex picture emerged. The additional presence in

considerable quantity of 1,2-substituted product and mono-substituted products were confirmed. This information enabled the optimisation of reaction conditions to maximise the yield of the desired 1,3-tetra-ester calix[4]arene. It is quite clear that using only the traditional organic workup tools of TLC, conventional column chromatography and recrystallisation, neither the separation efficiency nor the detailed characterisation of closely related product species could have been achieved.

Wall described the arduous synthesis of the asymmetric tetraester calix[4]arene **6-3** shown in Figure 6.4[210]. Despite the apparently subtle structural changes compared to the symmetric 'parent' calix[4]arene (**6-2**), the target host, although *identified* in a complex mixture by the techniques outlined above[100], was never *isolated* in quantity. The work described in this chapter aims to extend this approach by applying a scaled up analytical scale LC method to isolate practical quantities of a target host compound from a synthetic mixture (for further characterisation, use in sensors etc.). This can be described as semi-preparative HPLC purification.

The synthesis of **5-1**, depicted in Scheme 6.1, did not proceed as readily as an equivalent *symmetric* tetra-nitrile described in the literature[150]. This tetra-nitrile described by Scheerder and co-workers contains four identical propyl nitrile appendages on the lower rim. The unusually complex reaction mixture of **5-1** obtained, in comparison, is perhaps analogous to the attempted synthesis of **6-3**.

Reasons for the dramatic difference in ease of synthesis between apparently very similar tetra-substituted calix[4]arene structures may include (a) the high degree of substitution, (b) increasing difficulty to deprotonate successive phenol hydrogens, (c) the sterically hindered nature of target compounds and (d) the different chemical environment of the hosts functional groups.

The complex crude mixture obtained for **5-1** prompted the use of more advanced work up tools.

### *6.2.3 Tools to compliment conventional organic work-up techniques*

Techniques such as TLC, paper, flash and open-column chromatography, all LC techniques, have been used for many years as conventional separation tools by the organic chemist[250]. These methods are cheap, easy to implement and little training is required. However, in some cases, for example when a product is required routinely (industry) or if a separation is particularly tedious (research), then the use of preparative HPLC becomes an advantage.

All LC techniques have a common theoretical basis. HPLC is a common analytical technique which generally has much better separating efficiency then open column or flash chromatography[251]. This improved efficiency can prove critical when dealing with a low yield of product in a complex mixture. Woodward, who completed the total synthesis of Vitamin $B_{12}$ claimed that HPLC was of 'crucial importance' for his work and predicted that HPLC would be 'indispensable' for future organic chemists[252]. This view showed great foresight at the time.

The development of HPLC came about due to a desire to save time and money. Compared to more conventional LC methods, HPLC offers convenience, accuracy, speed and the ability to perform difficult separations, not possible by other methods[253]. Classical column chromatography typically involves a glass column packed with stationary phase (e.g. normal phase silica gel) and relies on a gravity fed mobile phase (atmospheric pressure usually). The stationary phase is discarded after each use and so represents a time and material loss. Reproducibility may suffer as columns are hand packed each time a separation is performed. On the other hand, HPLC columns are usually factory packed and can be used repeatedly. Mobile phase is pumped in a

controlled manner at pressures of many atmospheres (atm) if required (hundreds of atm). The result is better reproducibility, controlled flow rates and above all better efficiency, accuracy and precision. In terms of basic theory, this can be rationalised simply, but not exclusively, in terms of the theoretical plates number, N, of a separation column's stationary phase as shown in Equation 6.1.

$$N = \frac{16(t_R)^2}{t_w} \qquad \text{(Eqn 6.1)}$$

Theoretical plate count = N, retention time = $t_R$ and band or mixture component width = $t_W$.

N may be considered as the effective area of a stationary phase with which the components of a given mixture can interact in a useful manner to induce varying retention. HPLC can combine smaller particle size and denser packing due to the high-pressure mobile phase available, with the result of much greater interaction with a sample mixture. From this it can be deduced that for higher values of N, the components of a mixture to be separated can be spread over a longer total elution time ($t_R$), each band or component occupying a narrower time window or band width ($t_W$) within this total run time. This is clearly not possible to the same degree with gravity fed hand packed conventional column chromatography. Although there are numerous factors dictating the separation power of an LC system, N is a convenient means to rationalise overall separation efficiency.

For analytical applications the advantages of HPLC separation have been exploited extensively, but particularly in organic research circles, HPLC in preparative mode is a relatively rarely encountered technique.

The use of HPLC for *preparative* purposes, where components from a mixture are collected in quantity (mg to kg) instead of going to waste, has largely been the preserve of industry since dedicated instrumentation can be expensive to acquire and run and as

such, preparative HPLC has been perceived as a specialist technique by most organic research chemists. Early researchers, such as Pirkle and Anderson in 1974, identified the power of HPLC for resolving mixtures in a *preparative* fashion[254]. Analytical HPLC was becoming widespread at the time, however the variety of stationary phases and instrumentation available for preparative applications were few and expensive. These early authors designed and constructed their own preparative systems using silica gel or alumina. The application of reverse phase stationary phases soon followed[255]. By and large, commercial systems were specialist, slow and expensive. Today, the technology has improved and systems are available with wide applicability and user-friendly software. However, price has risen in tandem with sophistication and preparative HPLC continues to be perceived as specialist and inaccessible by most organic research chemists.

Several useful analytical HPLC methods have been developed for calixarene analysis[256]. McMahon and co-workers have attempted to consolidate and review available literature references for analytical scale HPLC as applied to calixarenes in recent times[99].

To date, conventional organic LC techniques have been sufficient to separate and recover calixarene compounds (and other classes of supramolecular compounds). Dedicated preparative instrumentation and materials have been used for calix[4]arenes without MS in the past[257]. This instrumentation was specialist and one could not revert to an analytical mode for routine analysis.

While scaling up of an existing analytical method for use in preparative HPLC must be done with care, it is conceivable that good separation can be achieved in a relatively straightforward manner.

It is my view that the ease of extending the use of *analytical* scale HPLC for semi-preparative (mg or g quantities) product characterisation, isolation and collection has

not been sufficiently highlighted in the literature. The key advantage being that any chemistry department will have access to *analytical* HPLC instrumentation and the expertise to operate it. When scaling up an analytical method, lengthy optimisation to achieve attractive chromatograms is not necessary. The parameters of purity and recovery yield of final product are the important parameters where preparative HPLC is concerned.

Along with HPLC, MS is a very valuable tool for the organic chemist and is becoming more prevalent in research for checking identity and purity of products. Together, HPLC and MS are a powerful combination. By running an HPLC-MS chromatogram of a crude reaction mixture, the presence of the target and any related products or impurities can be quantitatively identified at the reaction vessel stage. The decision whether to proceed with a potentially lengthy reaction work-up is made easier. Conventionally, TLC of the same mixture reveals only the number of products in the mixture, but their identification can only follow when full reaction work-up is complete.

The borrowing of analytical methods by the organic chemist can mean the difference between an abandoned synthesis and isolating useful quantities of a desired product. To go some way to rectifying this, aspects of the current chapter have been published[189].

After more then 100 years, calixarene chemistry is at an advanced stage of its life cycle, where many future structural improvements will demand the routine use of ever more sophisticated separation and characterisation techniques. Only by using HPLC and MS can fast throughput of characterised targets be envisaged.

In this report, we highlight the importance of using advanced analytical characterisation (LC-MS) of reaction products coupled with semi-preparative methods for scaling up the associated separation process in order to obtain reasonable quantities of more elusive

derivatives such as the asymmetric calix[4]arene **5-1**. The process is also described for calix[4]arene hosts **3-1**, **3-2** and **4-3**.

## 6.3 RESULTS AND DISCUSSION

### *6.3.1 The illustration of principle: Isolation of 5-1*

The chromatogram in Figure 6.3 revealed the complex nature of the reaction mixture obtained for the synthesis of **5-1**. Numerous peaks or bands are present with considerable co-elution. **5-1** and some other components in the mix could be identified by LC-MS. Starting materials are seen at about 5 minutes, including **5-3**. Between 5 and 8.6 minutes (peak of **5-1**) are various breakdown fragments of **5-1**. Interestingly, molecular ions of **5-1**+$K^+$ were seen in this region too. An unidentified component of greater mass than **5-1** was seen at about 10.1 minutes. The reverse phase character of the column stationary phase ensures that components larger (and less polar) than **5-1** emerged after 8.6 minutes. By-products and un-reacted or partially reacted starting materials were therefore largely confined to retention times below 8.6 minutes.

With a rather complex reaction mixture containing **5-1** present, it was decided that the analytical HPLC method would be scaled up to isolate **5-1** as efficiently as possible, instead of resorting to conventional column chromatography for separation. If normal phase chromatography was used instead, the compound of interest would elute early and would be less likely to be resolved from related compounds. This scenario applies to the use of open column chromatography where silica gel is often used as a stationary phase.

Using a simple scale up factor as a guideline, supplied by most column manufacturers, HPLC parameters were altered for semi-preparative work, critically retaining the same

*analytical* instrumenation. Column width went from 2.0mm to 10.0mm with a larger particle size of the same stationary phase. The stationary phase used for this work, Synergy Fusion-RP, has both reverse and normal phase characteristics meaning that a mixture with a broad range of polarities can be effectively separated in the one chromatogram, thus saving time and consumables.

Flow rate was increased from 0.2ml/min to 5ml/min. These flow rates correspond to a flow rate of 1ml/min on a more typical 4.6mm diameter column. The injector, pump, detector cell and tubing manifolds of most analytical HPLC hardware are capable of running at these conditions. Indeed, even with a flow rate of 5ml/min, the back pressure never rose above 33bar, well within the instrument's maximum limit.

The 100µl standard analytical injection loop fitted was retained as it is more beneficial to increase injected sample concentration than volume for efficient separation[258]. Sample concentration was increased for preparative work from 0.5mg/ml to 300mg/ml. Being aware that the UV detector cell was designed for analytical concentrations, it was decided to change the wavelength used for preparative work to one showing less sensitivity towards the sample, thus avoiding detector saturation. **5-1** absorbs about 6 times less UV radiation at 280nm than at 210nm. The analytical wavelength of 210nm was therefore changed to the less sensitive 280nm for preparative work. For sample collection, a Gilson 204 fraction collector was used. Injections were performed and the relevant peaks collected using an automation facility on the fraction collector, requiring minimal supervision. It was also possible to manually collect fractions without the use of a fraction collector. In a short space of time with only small modifications, the analytical instrumentation was ready for semi-preparative work.

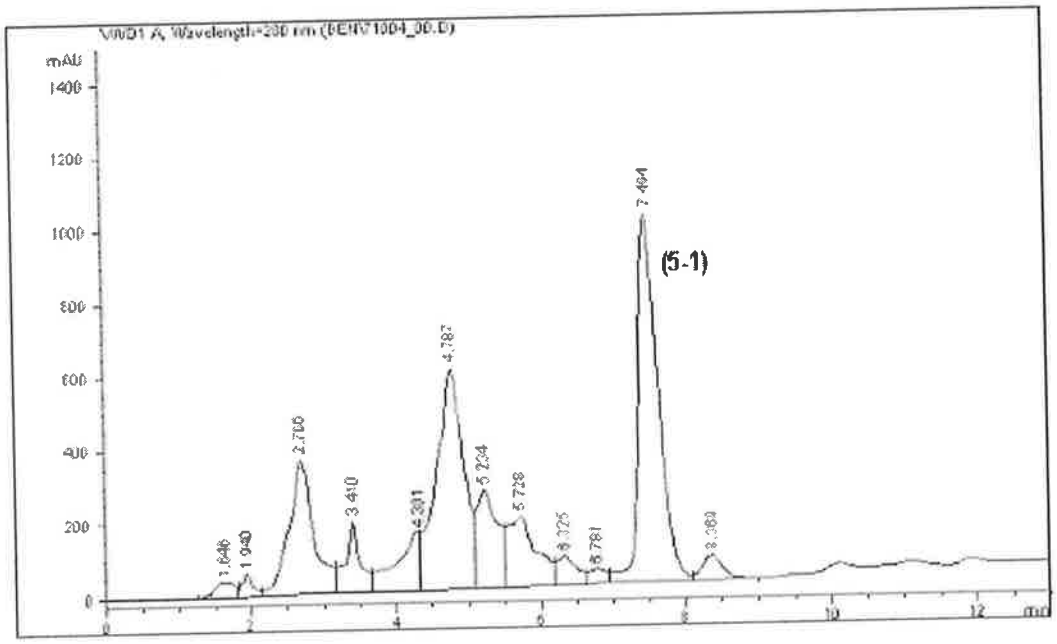


**Figure 6.5.** A semi-preparative scale HPLC chromatogram obtained for a mixture containing **5-1** (labelled). Detection is at 280nm.

Figure 6.5 shows a typical semi-preparative chromatogram from the original synthesis mixture of **5-1**. As expected, all retention times are faster than in the equivalent analytical chromatogram in Figure 6.3 and resolution is generally lower, due to the higher sample concentrations and volumes injected[259]. Ultimately, the recovery yield and percentage purity of the target are the important parameters. In one hour, unattended, 55mg of 97.6% pure **5-1** was isolated from 120mg of a mixture of no less than ten components as seen in the analytical scale chromatogram in Figure 6.6. This represents a recovery percentage of about 90%. These Figures assume a similar absorption coefficient of all species present in the mixture. This is reasonable as target **5-1** and **5-3** are structurally similar and based on the same calix[4]arene back-bone.

Theoretically, conventional column chromatography could not have matched this separation in terms of separation efficiency or time on its own[251]. In addition, practical considerations include the fact that conventional chromatography is more prone to operator error, with increased possibility of product loss.

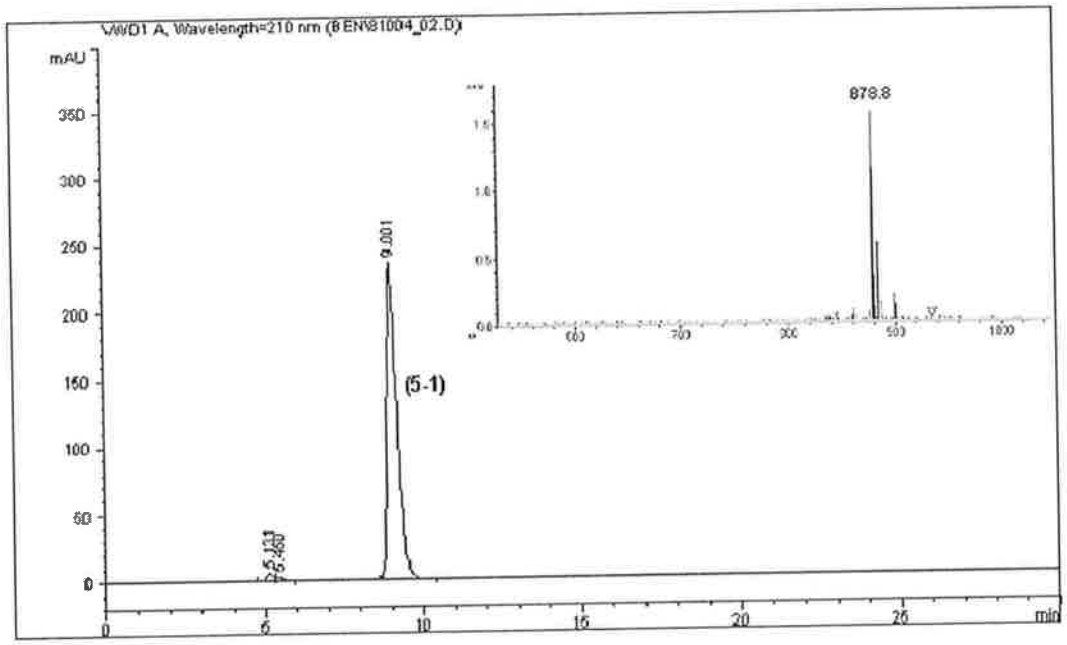


**Figure 6.6**. LC-MS chromatogram showing 97.6% pure **5-1** following semi-preparative HPLC separation. Detection is at 210nm. Inset shows MS identification of **5-1**.

### *6.3.2 The isolation of 3-1*

The synthetic conditions and further discussion on the analytical applications of di-urea calix[4]arene **3-1** are found in chapter 3.

An initial screening of the crude mixture from the synthesis of **3-1** by LC-MS indeed revealed the presence of **3-1** at 6.9 minutes as seen in Figure 6.7. **3-1** represents 37.6% of total peak area excluding the solvent peak at around 3 minutes.

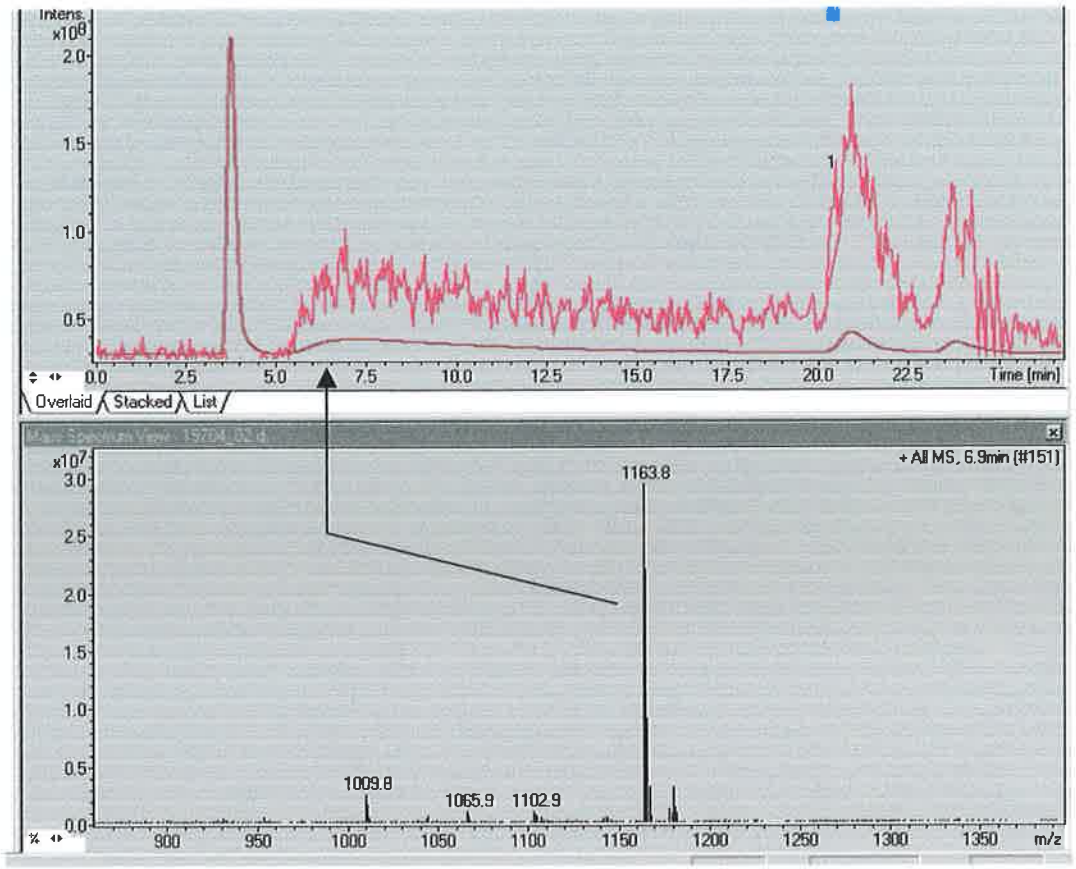


**Figure 6.7.** The LC-MS chromatogram of the crude reaction mixture from the synthesis of **3-1**. The UV trace of 210nm (lower) superimposed on the Total Ion Chromatogram (upper) reveals the presence of **3-1** at 6.9 minutes in a broad peak. Also shown is the corresponding mass spectrum confirming the identity of **3-1**.

From previous LC chromatography of calixarenes, a good starting point for a solvent system was ≥95% ACN[100]. To this water can be added for more polar systems and stronger organic solvents like THF can be added to produce more apolar mobile phases. For the semi-preparative isolation of **3-1** using a scaled up analytical method, the solvent system was examined first. It is clear from Figure 6.7 that peaks are quite broad and over 20 minutes is required to elute all products. To elute all peaks quicker and to improve peak shape (peak efficiency) the isocratic solvent strength (organic component) was increased. This entailed increasing the proportion of THF in a THF/ACN mixture. The formic acid was omitted as it only served as an ionisation aid for MS analysis. For further work, the LC solvent also served as the sample solvent. The instrument

wavelength was increased from 210nm to 220nm as the UV cut-off for THF is 212nm. Figure 6.8 shows some spectra from preliminary work with the peak corresponding to **3-1** marked in each case. The chromatograms of the crude mixture have varying proportions of THF as indicated.

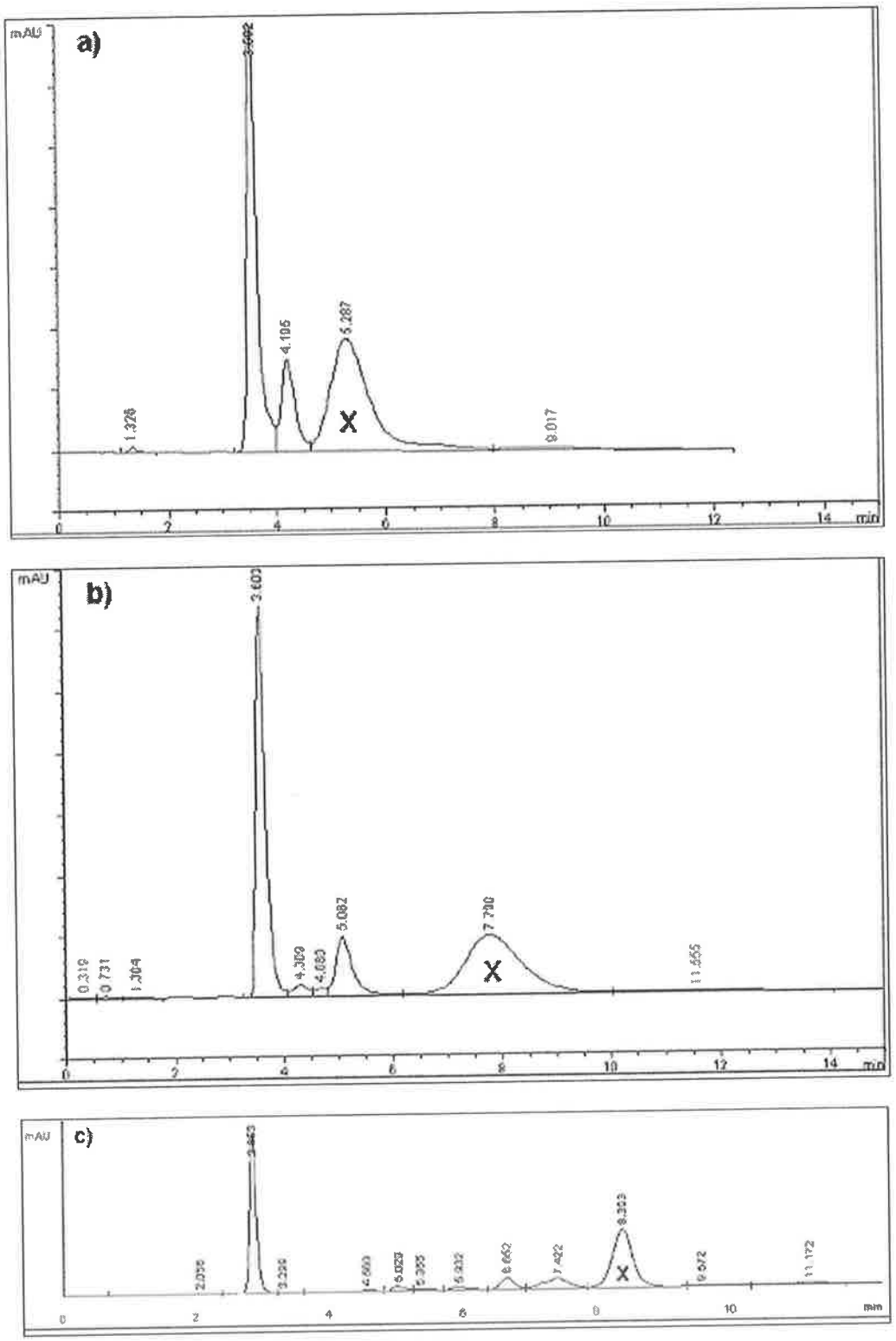


**Figure 6.8**. The HPLC spectra of crude **3-1** with decreasing proportion of THF in the mobile phase ACN:THF v/v : a) 60:40 b) 70:30 c) 80:20. The peaks of **3-1** are marked **X**. Detection wavelength is 220nm.

The resolution from neighbouring peaks is clearly improved with decreasing THF content, however the overall runtime was thereby increased. The chromatogram in Figure 6.8b appears to be the best compromise between good resolution of the desired peak whilst minimising the total run-time. The chromatogram in Figure 6.8a shows relatively poor resolution for the peak of **3-1**.

The transfer of the solvent systems (ACN:THF v/v : 70:30 and 80:20) to semi-preparative mode is illustrated in Figure 6.9. This entailed, as before, switching to the larger column, increased flow rate to 5ml/minute, increased sample loading and a less sensitive wavelength of 280nm to prevent signal overloading of the detector UV cell (see experimental section for more detail). The main difference to be anticipated is poorer resolution when comparing equivalent analytical and SP chromatograms. This is mainly due to the much greater column loadings used for SP runs, which is known to reduce separation efficiency.

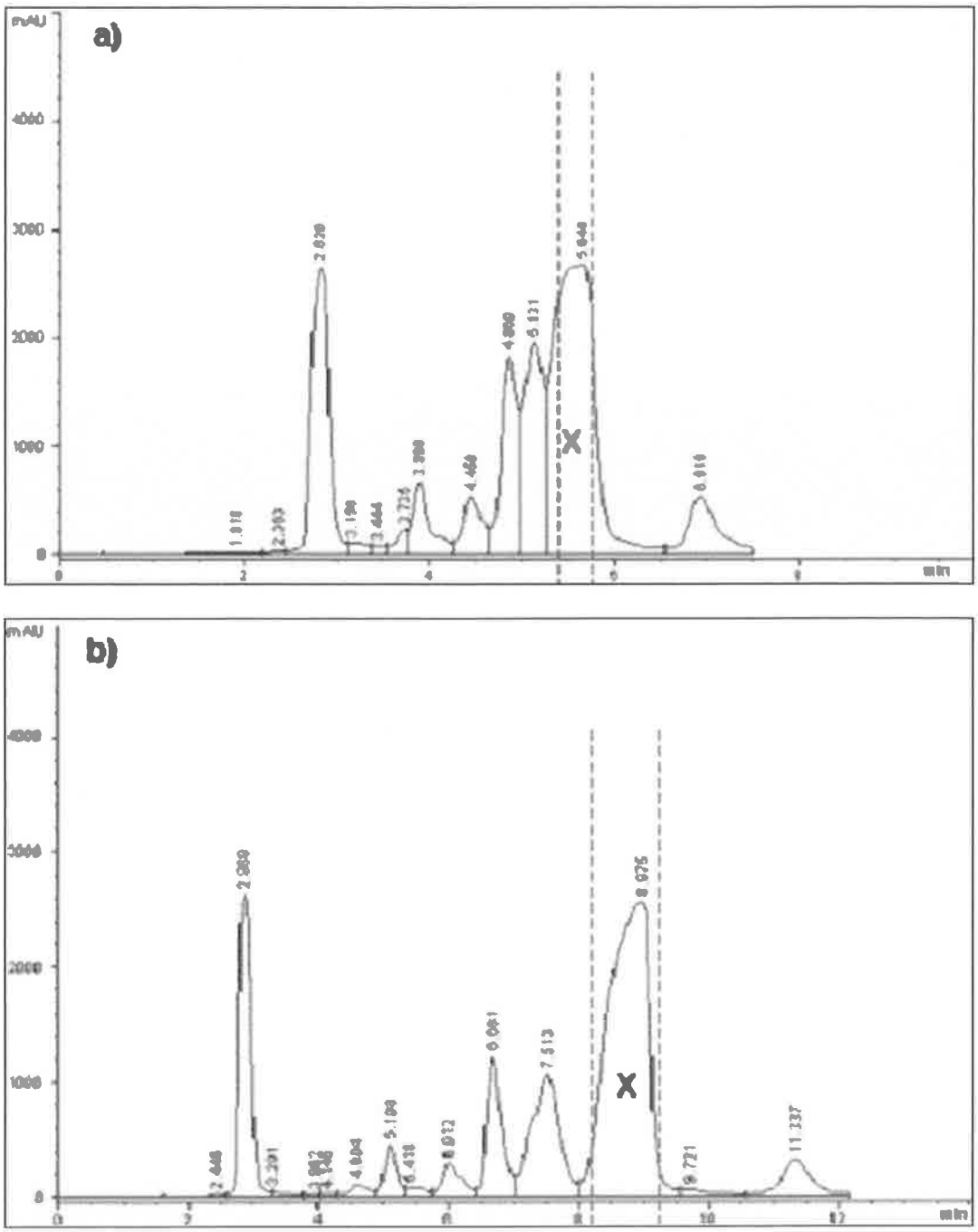


**Figure 6.9**. The separation of **3-1** in semi-preparative mode with mobile phase ACN:THF v/v : a) 70:30 b) 80:20. The peak of **3-1** is marked **X**. Detection wavelength is 280nm. Broken red lines denote sample collection window.

It can be seen visually from Figure 6.9a that using mobile phase systems with 70:30 v/v ACH:THF (and by inference more THF) results in considerable overlap of the **3-1** peak with neighbouring peaks. This poor resolution could diminish the final purity of

collected **3-1** and diminish yield as the time collection window (indicated by the broken red lines in Figure 6.9) would have to be narrowed to isolate only pure product. With a solvent system of 80:20 v/v ACH:THF there is good resolution from neighbouring peaks as can be confirmed visually in Figure 6.9b, whilst minimising the time to elute all peaks. Decreasing the proportion of THF below 20% by volume, may result in even better resolution for **3-1** but the overall run time would be increased, meaning more time spent obtaining sufficient quantities of pure product, the consumption of more solvent and more instrument wear and tare already operating near upper limits of flow rate (5ml/minute). An SP system with a solvent system of 80:20 v/v ACH:THF was therefore chosen for the purification of **3-1**.

Using a coloured dye and stop watch, the time delay between the HPLC detector and the product SP collector outlet was exactly determined previous to purification, for the flow rate used (5ml/minute). In this way the start and end of the window of collection of each product peak could be specified with sufficient accuracy according to the relevant chromatogram (Figure 6.9b).

Manual or automatic collection modes were available with the collector used. Generally, the manual collection mode was used as factors such as laboratory temperature fluctuations could occur, which caused slight variations in retention times over the course of the day and so the potential of introducing impurities if the system was left unattended. Using the above described method, 22.7mg of purified **3-1** product was obtained in about 4 hours.

Textbook like peak shapes normally mandatory for analytical purposes are not required as the sole purpose of SP purification was to tune the chromatographic efficiency to obtain reasonably pure product (>95% purity) using the least amount of solvent and in a reasonably quick time.

Figure 6.10 shows the final pure product **3-1** as examined by the analytical scale HPLC method. 98.1% purity was achieved and an LC recovery yield of 60.4%. The identity of **3-1** was reconfirmed with DI-MS.

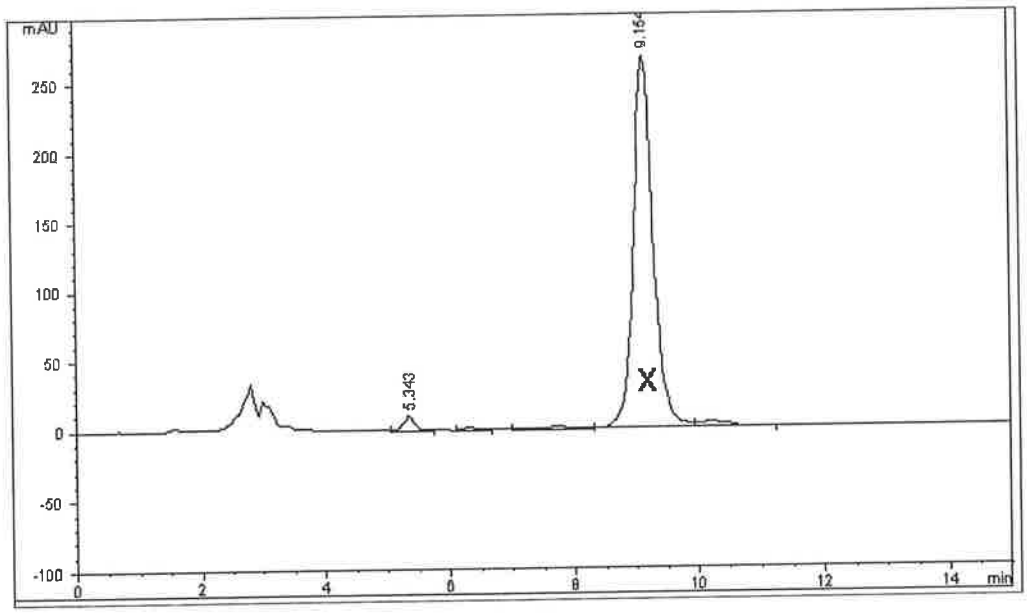


**Figure 6.10**. The analytical HPLC chromatogram of **3-1**, marked **X**, following SP isolation. 98.1% purity was achieved.

### *6.3.3 The isolation of 3-2*

The synthetic conditions and further discussion on the analytical applications of di-urea calix[4]arene **3-2** are found in chapter 3.

It must be noted that each chemical mixture is unique and varying the proportions of components or chemical and physical properties of the components in a mixture will affect each retention time. For this reason some development work must be carried out before isolating products from different synthesis by SP-HPLC. This need not require complicated or extensive effort.

As **3-2** is structurally similar to **3-1**, and the conditions of synthesis are near identical, it is reasonable to expect broadly similar components to be present in the crude synthetic

mixture. Analogously, the SP-HPLC isolation conditions can also be expected to be similar.

An initial screening of the crude mixture from the synthesis of **3-2** by LC-MS revealed the presence of **3-2** to be 29.0% of total peak are as seen in Figure 6.11.

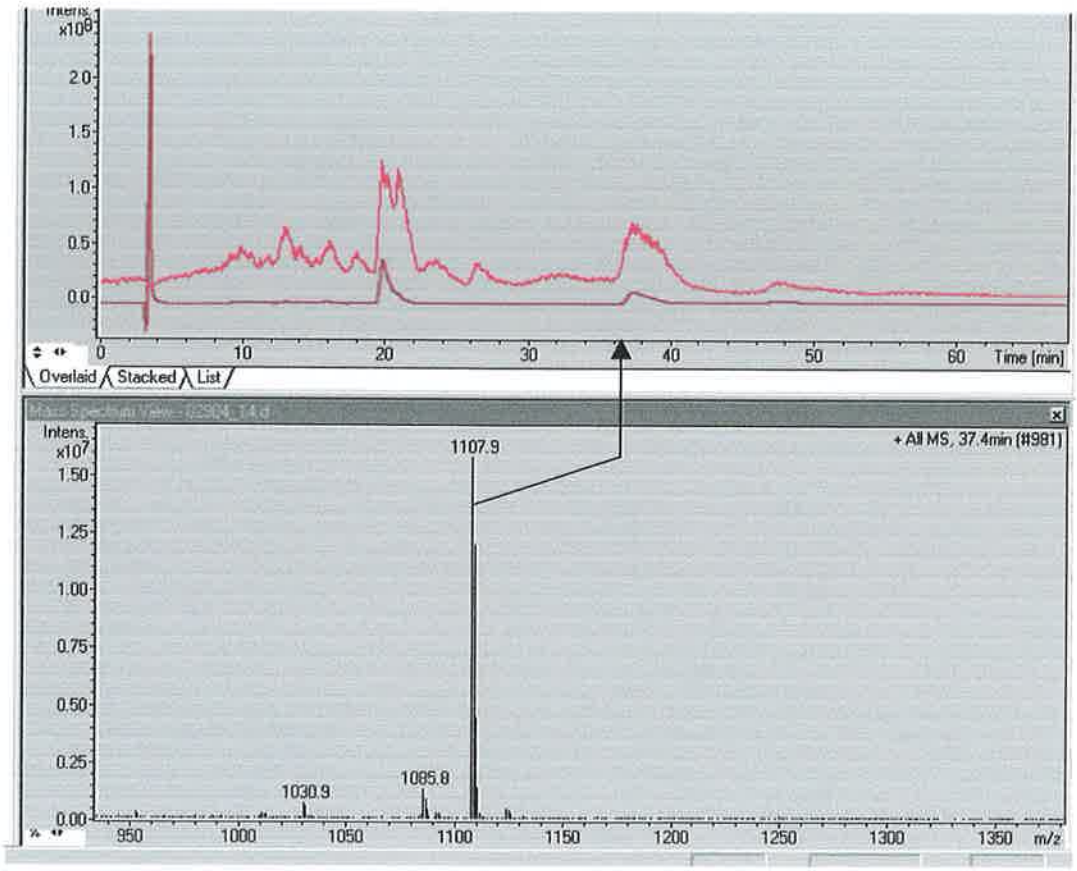


**Figure 6.11.** The LC-MS chromatogram of the crude reaction mixture from the synthesis of **3-2**. The UV trace of 210nm (lower) superimposed on the Total Ion Chromatogram (upper) reveals the presence of **3-2** at about 37.4 minutes in a broad peak. Also shown is the corresponding mass spectrum confirming the identity of **3-2**.

The retention time for the peak corresponding to **3-2** is 37.4 minutes which is 30 minutes more than the structurally similar **3-1** (Figure 6.7). Given this structural similarity, this rather dramatic retention time difference observed was not expected. A central theme in this thesis has been the possibility of dramatic change in complexing properties of structurally similar host compounds. This can of course encompass interaction with a HPLC stationary phase, also a reversible non-covalent interaction. In

this case however, we feel the large retention time range observed was due to the analytical HPLC column reaching the end of its life. The broad tailing HPLC peaks also attest to non-optimal compound retention. Further optimisation of the method was carried out using the system configured for SP use.

The optimum solvent system was found in a similar manner to **3-1**. Figure 6.12 shows a SP chromatogram of **3-2** using 90:10 v/v ACN:THF as mobile phase.

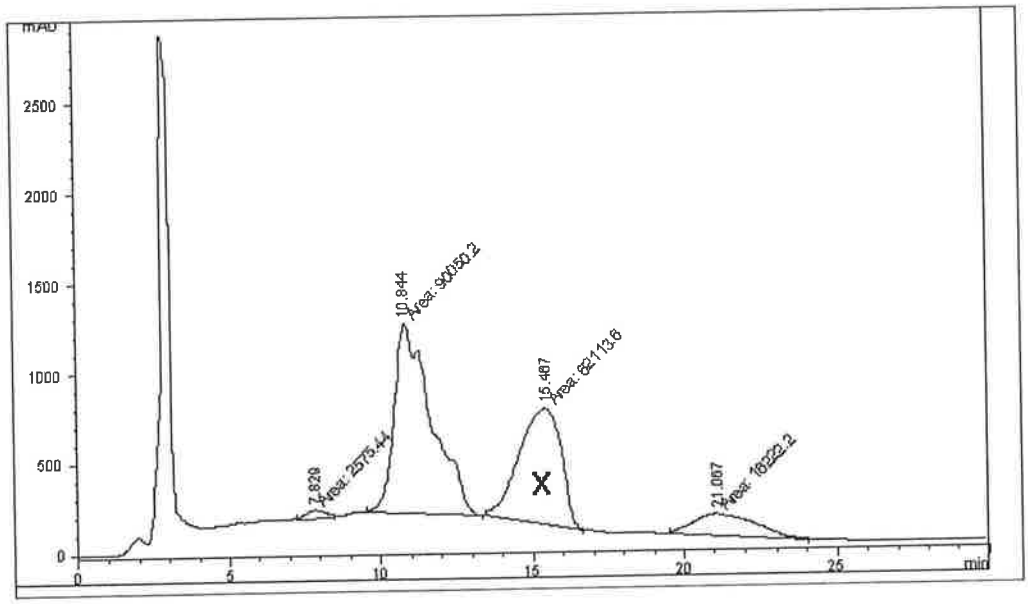


**Figure 6.12**. The separation of **3-2** in SP mode with mobile phase ACN:THF v/v 90:10. The peak of **3-2** is marked **X**. Detection wavelength was 280nm.

Using the above described method, 41.2mg of purified L14 product was obtained in about 4 hours. The final pure product **3-2** was examined by the analytical scale HPLC method. 97.6% purity was achieved and an LC recovery yield of 78.9%. The identity of **3-2** was reconfirmed with DI-MS.

The recovery yield of 78.9% is better than that for **3-1** (60.4%) perhaps because the nature of the crude mixture (less impurities) and the solvent system chosen allowed better resolution between **3-2** and neighbouring peaks (comparing Figure 6.9b and

Figure 6.12). Because of this a longer SP product collection window could be allowed for **3-2**, resulting in a slightly greater percentage recovery of product compared to **3-1**.

### *6.3.4 The isolation of pyrene urea calix[4]arene 4-3*

The synthetic conditions and further discussion on the analytical applications of urea-pyrene calix[4]arene **4-3** are found in chapter 4.

It was immediately apparent from the synthesis of **4-3** that the reaction products showed very poor solubility in most common organic solvents except in DMSO and DMF, where good solubility was observed. These solvents are very polar in nature and generally give unfavourable results in chromatography, particularly in normal phase stationary phases (associated commonly with conventional column chromatography) where streaking and poor band resolution is observed due to the excessive affinity of mobile phase for the stationary phase. Furthermore the post-purification complete removal of solvent from product would be difficult due to the non-volatile nature of DMF and DMSO (boiling points of 153°C and 189°C respectively). Additionally, as was revealed in chapter 4, **4-3** is unstable at temperatures of 80°C, a further obstacle to using DMF and DMSO. 100% methanol was chosen as the general HPLC mobile phase as this was the most polar solvent available besides DMF and DMSO with an acceptable volatility and practical boiling point of 65°C. Good chromatography was possible with this solvent. An absorption wavelength of 340nm was chosen based on the maxima from the UV-absorbance chromatogram of pyrene (chapter 4.2.1). These modifications of the standard HPLC conditions were applied for both the analytical and SP-HPLC of **4-3**.

For routine analytical analysis of the product mixture of **4-3** by HPLC, solubility was not critical, as typical concentrations of 1mg/ml were known to be sufficient. For SP-HPLC higher concentrations of about 300mg/ml are desirable for practical reasons

saving time and materials. The synthesis of **4-3** involved a chloroform extraction step to isolate **4-3** from the DMF mobile phase. Large volumes of chloroform (approximately 1g of crude material in 30ml) were reduced carefully to about 2ml of a relatively concentrated solution of **4-3** for use in SP isolation. Further solvent removal quickly led to unwanted precipitation. This approach appeared to be more effective than re-dissolving an isolated crude solid in solvent.

Even with the use of SP-HPLC an overall yield of only 2% **4-3** was achieved attesting to a difficult synthesis. It is clear that the use of less efficient conventional column chromatography would inevitably have resulted in an even lower yield, perhaps making the entire synthesis unfeasible.

The use of ESI-MS did not prove successful with **4-3** as with the other hosts described in chapter 6, and **4-3** could not definitively be identified in the crude reaction mixture (see chapter 4.3.2). As the stationary phase used was largely reverse phase in character, it was reasonable to assume that the last chromatographic peak to emerge would be the largest most substituted organic product (least polar and longest retained) corresponding to the tetra-substituted **4-3**. Earlier peaks would most likely correspond to partially substituted calix[4]arenes and other impurities. Furthermore as the detection wavelength used was 340nm, all peaks observed presumably contained one or more pyrene moieties and were therefore all potentially the desired product or a related compound. The starting tetraphenol calix[4]arene did not absorb UV light above 300nm (Figure 4.11). In the absence of MS evidence of identity, it was decided to proceed with the purification based on this rationale.

The SP-HPLC purification was carried out collecting the peak labelled **4-3** in Figure 6.13.

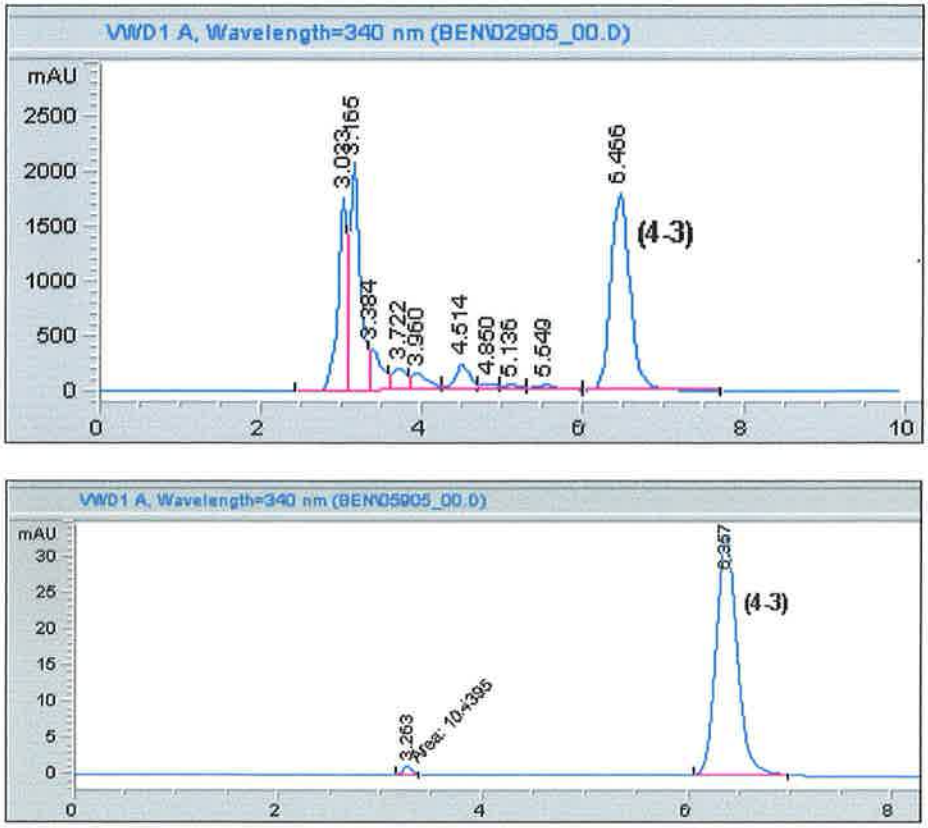


**Figure 6.13**. The semi-preparative HPLC purification of **4-3**: From an initial purity of 37% (top) to a final purity of 98% (bottom). Mobile phase was 100% methanol. Sample solvent was chloroform. Detection was by UV-absorption at 340nm.

Subsequent characterisation of the peak labelled **4-3**, once isolated, indeed confirmed the anticipated identity of **4-3** unambiguously by $^{1}H$ NMR and CHN elemental analysis.

## *6.4 CONCLUSIONS*

Following simple alterations to an analytical LC-MS instrumental setup and synthetic procedure, in 1 hr, quantities of calixarene **5-1** were isolated that are sufficient for characterisation, activity screening and for further synthesis. MS also revealed that **5-1** may be predisposed towards forming complexes with ammonium ions, rather than the more usual sodium ions. Energy minimised complex structures support this.

Complex mixtures of closely related products cannot always be resolved easily by conventional means, particularly where there are subtle changes of connectivity

between species of the same family of compounds with near identical molecular formula. The achievement of effective resolution or separation of a mixture is essential for true characterisation of products and the generation of sufficiently pure material of unambiguous identity and good yield for further synthesis. The use of techniques like LC-UV-MS and LC-DAD is therefore recommended for the synthetic chemist for non-trivial synthesis, complimenting traditional organic workup tools like TLC and conventional column chromatography or replacing these when they are not adequate in terms of characterisation power and separation efficiency.

The identification and partial characterisation (e.g. the ammonium affinity of **5-1**) of products was achieved by the approaches described even prior to any potentially unfruitful effort being made to purify and isolate a target.

The work was extended beyond identification and characterisation by scaling up the LC component of the methods described using the same widely available analytical scale instrumentation to isolate mg quantities of the target host. This constitutes semi-preparative HPLC isolation.

One possible improvement for the SP method described would be the installation of a reliable column thermostat. In this way, the contamination of the product collected from neighbouring impurity peaks due to intermittent temperature induced retention time changes could be avoided. With a thermostat in place, an automated and reliable SP product collection protocol could be set up to achieve reproducible repeat runs and pure product collection without continuous supervision by the analyst.

The approach described was also adopted for the synthesis, characterisation and isolation of **3-1**, **3-2** and **4-3**.

The work presented serves to complement the conventional isolation tools of supramolecular chemists where non-trivial synthesis may yield complex mixtures of

closely related structures. In some circumstances the suggested approach may represent the difference between an aborted and a successful synthesis. The work represents a powerful crossover between analytical and organic chemistry.

## 6.5 EXPERIMENTAL

The following experimental procedures apply unless otherwise stated in the text. HPLC was carried out using a HP1100 with UV detection. For MS work, this was coupled to a Bruker/Hewlard-Packard Esquire system, using a positive ESI source and the software's default 'smart' settings. Mobile phase used was isocratic LC grade Acetonitrile with 0.25% formic acid content. The choice of acetonitrile mobile phase as a starting point was based on a standard calixarene HPLC method described by McMahon and co-workers[100]. This also served as the sample solvent. For analytical LC-MS, a Synergy 150.0 x 2.0mm, 4μm Fusion-RP column was used. Flowrate was 0.2ml/min. Detection wavelength was 210nm. Injections were 5μl of 0.5mg/ml sample.

For semi-preparative HPLC, 100% ACN mobile phase was used and a Synergy 250.0 x 10.0mm, 10μm Fusion-RP chromatographic column. Flowrate was 5.0ml/min. Detection wavelength was 280nm. Injections were 100μl of 300mg/ml sample, filtered before use. Fraction collection was carried out manually or with a Gilson 204 fraction collector in automation mode. Recovery yield was based on % of total peak area.

NaH used was a 60% dispersion in mineral oil. All reactions were carried out under argon. The name *p-tert*-Butylcalix[4]arene was used instead of the IUPAC name for convenience: 5,11,17,23-tetra-*p-tert*-butyl-25,26,27,28-tetrahydroxycalix[4]arene.

Potentiometric membranes were prepared using 250mg 2-Nitrophenyl octyl ether, 125mg PVC, 2.5mg **3** and 0.5mg potassium tetrakis(4-chlorophenyl) borate.

The electrochemical cell used consisted of a double junction reference electrode and a PVC membrane working electrode in the following arrangement:

Ag | AgCl | 3M NaCl || 0.1M LiOAc || sample solution | PVC membrane | 0.1M $NH_4Cl$ | AgCl | Ag.

Membranes were conditioned in 0.1M ammonium chloride for 3 hours and followed by deionised water for half an hour prior to analysing the $10^{-1}$M cation chloride solution of interest. The potentiometric cell was interfaced to a PC using a National Instruments SCB-68 4-channel interface.

**5,11,17,23-Tetra-*p-tert*-butyl-25,27-bis[(cyanomethyl)-oxy]-26-28-dihydroxycalix[4]arene (5-3)**. *p-tert*-Butylcalix[4]arene (5.0g, 7.72mmol), $K_2CO_3$ (1.28g, 9.26mmol) and bromoacetonitrile (1.95g, 16.20mmol) was heated in $CH_3CN$ (80ml) at 50 °C for 5 days. The reaction was monitored by LC-MS. The solvent was evaporated and the residue taken up in $CH_2Cl_2$ (300ml), washed with 1N HCl (100ml), $H_2O$ (50ml) and brine (50ml) and dried with $Mg_2SO_4$. $CH_2Cl_2$ was evaporated and the residue was recrystallised from $CHCl_3$/MeOH yielding a white solid: yield 73%; mp 285-290 °C; UV-vis (ACN) 210nm (ε/L $cm^{-1}$ $mol^{-1}$ 152472), 280nm (25974); IR (KBr) 2250 $cm^{-1}$ (CN), 3515 $cm^{-1}$ (OH) ; $^1$H NMR δ 7.12 (s, 4H), 6.73 (s, 4 H), 4.81 (s, 4H), 4.23 and 3.45 (ABq, 4H, J = 13.6), 1.33 (s, 18H), 0.87 (s, 18H); $^{13}$C NMR δ 150.3 (s), 149.0 (d), 142.9 (d), 135.4 (s), 128.2 (s), 126.6 (s), 125.7 (s), 115.5 (s), 60.8 (s), 34.4 (t), 31.9 (t), 31.5 (s); ESI mass spectrum +m/e 749.6 ([M + $Na^+$], calcd 749.4); HPLC purity: 96.8%. Anal. Calcd for $C_{52}H_{66}N_2O_4$: C, 79.30; H, 8.04; N, 3.85. Found: C, 78.94; H, 7.87; N, 4.00.

**5,11,17,23-Tetra-*p-tert*-butyl-25,27-bis[(cyanopropyl)-oxy]-26-28-bis[(cyanomethyl)-oxy]calix[4]arene (5-1).** Calix[4]arene **5-3** (4.0g, 5.5mmol) and NaH (0.44g, 11.0mmol) was stirred 1 h at room temperature in anhydrous DMF (100ml). 4-Bromobutyronitrile (1.63g, 11.0mmol) was added batch wise and the mixture was stirred at 80 °C for 24 h. The reaction was monitored by HPLC-MS. The mixture was cooled and another equivalent of NaH and 4-Bromobutyronitrile was added and heated as before. After a further 72 h the DMF was evaporated and the residue taken up in $CH_2Cl_2$ (250ml), washed with 1N HCl (100ml), $H_2O$ (50ml), brine (50ml) and saturated $NH_4Cl$ (50ml) and dried with $Mg_2SO_4$. After filtration the $CH_2Cl_2$ was removed to give 4.69g of a beige solid. The solid was purified by semi-preparative HPLC to yield a white solid: Recovery yield 90%; mp 234-236 °C; UV-vis (ACN) 210nm (ε/L $cm^{-1}$ $mol^{-1}$150366), 280nm (28420); IR (KBr) 2248$cm^{-1}$ (CN); $^1$H NMR δ 7.17 (s, 4H), 6.43 (s, 4 H), 4.95 (s, 4H), 4.33 and 3.28 (ABq, 4H, J = 13.0), 3.90 (t, 4H), 2.69 (t, 4H), 2.32 (m, 4H), 1.35 (s, 18H), 0.80 (s, 18H); $^{13}$C NMR δ 152.3 (d), 148.3 (s), 145.8 (s), 135.7 (s), 131.5 (s), 126.7 (s), 125.3 (s), 119.7 (s), 118.0 (s), 74.2 (s), 58.5 (s), 34.7 (s), 34.3 (d), 31.7 (t), 26.3 (s), 15.0 (s); ESI mass spectrum +m/e 878.8 ([M + $NH_4^+$], calcd 878.6); HPLC purity: 97.6%. Anal. Calcd for $C_{56}H_{68}N_4O_4$: C, 78.10; H, 7.96; N, 6.51. Found: C, 77.79; H, 8.13; N, 6.26.

# 7. Conclusions and Future Work

*Conclusions*

The synthesis and properties of a number of calixarene supramolecular hosts was described in this thesis. The ability of these hosts to selectively engage in guest recognition at the molecular level was investigated. In order to fine tune the observed guest selectivity of the host, the most effective strategy was to perform well-rationalised structural changes of the hosts themselves. Changing other sensor parameters also modified observed selectivities (e.g. membrane polarity modifications when ISEs were used) but to a lesser extent.

Besides dramatic changes in observed sensor characteristics, it was found that even subtle structural changes of the host could have profound implications in terms of success or failure of a synthesis and the choice of purification regimes. Where analytical results were generated with relative ease, the burden on the organic chemist was easily underestimated.

Chapters 2 and 3 demonstrated the dual-use functionality of amide and urea based sensors as these functional groups can complex both cations and anions. ISEs can be configured to detect either cations *or* anions using the same host. Chapter 2 is amongst the first attempts at selective anionic guest recognition using amide based ISEs, resulting in the bromide selective host **2-18**. Chapter 3 highlighted an important consideration in aqueous based sensing and a common theme throughout the thesis. Ionic analytes, in particular anions, followed a Hofmesiter order of selectivity whereby selectivity is based on anion size, lipophilicity and degree of hydration. In aqueous based sensing this phenomenon can override the meticulous preorganisation present in

the sensor host, who's purpose is to induce deviation from such a 'default' selectivity pattern. Chapter 4 uses an optical mode of transduction to establish the selectivity of the pyrene-urea host **4-3**. This non-aqueous solution based experiment revealed unambiguous chloride selectivity. Using ISEs this could not be replicated in chapter 3 and a Hofmeister order of response was seen. The use of more than 1 mode of transduction is therefore recommended to thoroughly charaterise a new host system. As most real life sensing applications must take place in an aqueous environment, at least one of these should be water based. In this way the demand for beauty and aesthetics in fundamental reearch and the more pragmatic demands of the real world can be met.

Chapter 5 demonstrated how the selectivity of new sensor hosts is often discovered accidentally. Nitrile calix[4]arene **5-1** was initially intented as an intermediate for a host for tetrahedral anions but due to a failed onward synthesis and some MS observations, ended up as very effective host for spherical mercury (II) ions and amongst the first times the nitrile functional group was reported in soft metal sensing. Such surrendipitous discoveries continually amuse and motivate supermolecular chemists.

Due to the difficulty in the isolation of **5-1**, a new semi-preparative HPLC method was devised and described in chapter 6. The high efficiency of the method spelt the difference between an abandoned synthesis and a successful one. This method will be applied in future to other difficult purification challenges. Critically, it uses commonly available instrumentation and so can complement traditional organic work-up methods in any research group.

*Future work*

There is great potential for the synthesis of new hosts based on the chemistry that was presented here. The work here is amongst the first to use the nitrile functional group to complex soft metal analytes in a sensor capacity. The work can therefore be extended to synthesise improved hosts based on calixarene scaffolds or other formats including other supramolecular platforms or indeed simpler linear or tripodal formats for example. In addition, these systems have yet to be conferred with optical modes of transduction.

The combination of pyrene and urea chemistry in chapter 4 also opens the door to a large variety of new host structures with fluorescent transduction. This is the first time to our knowledge that this combination has yielded truly selective anion recognition. The 2 in 1 precursors **4-1** and **4-2**, on which **4-3** is based, can be applied to other platforms in future, again perhaps including simpler ones than calixarenes. As **4-3** in itself displays remarkable chloride selectivity, the host may be taken as is and applied in a real-life working device. This may include deposition, incorporation into a membrane or covalent attachment to the sensing surface. To benefit from the excellent optical characteristics discovered, a non-electrochemical transduction mode should be considered. This might comprise a miniaturised system incorporating LEDs as a source and detector of the optical signal. In this way the sensor output is based more specifically on an outstanding and selective supramolecular phenomenon rather than additional other sensor parameters such as surface polarity and ion exchange. In this way the dominance of the Hofmeister order of response, particularly associated with anion sensing in aqueous-organic multiphase systems, could perhaps be minimised.

Chapter 2 and 3 serve as a precedent for past and future urea or amide based recognition systems, in that it promotes the opportunity for screening a single host for both cation *and* anion response. This in effect doubles the chance of a selectivity 'hit'. The

bromide selective amide-calix[4]arene **2-18**, serves as an impetus to further investigate anion-amide interactions using ISEs as this approach has virtually never been reported in the past. Urea-calix[4]arene **3-1** shows great potential as an ionophore in nitrate selective electrodes, despite an observed Hofmeister response order. This will be investigated in future. The publications list at the start of this thesis shows the most up to date status of such ongoing research projects at time of printing this thesis.

More than 100 years after their discovery, calixarenes continue to bemuse, bewilder and thoroughly entertain. Due to their unique pre-organisation and potential for attaching various functional group appendages to form well-defined cavities for guest inclusion, they still make appearances at the forefront of supramolecular chemistry.

The divergence from non-aqueous solution based studies of guest recognition sytems will continue. Elegant solution based NMR or spectrophotometric based complexation studies alone will be expanded on. Additional forays into the daring world of aqueous based sensing will become increasingly important as science funding bodies demand more real life results.

The multidisciplinary area of supramolecular chemistry remains both beautiful and challenging, as new receptors are continuously demanded for the assembly line leading to applied sensor devices. The supply chain remains intact, only if the marriage between fundamental organic research and applied analytical chemistry is a happy one.

# 8. References


(1) Steed, W. S., Atwood, J. L. *Supramolecular Chemistry*; Wiley and Sons: Chichester, 2000.
(2) Steed, J. W.; Atwood, J. L. *Supramolecular Chemistry*; Wiley: Chichester, 2000.
(3) Yizhak, M. *Ion Properties*; Marcel Dekker, INC.: New York, 1997.
(4) Beer, P. D.; Gale, P. A.; Smith, D. K. *Supramolecular Chemistry*; Oxford University Press: Oxford, 1999.
(5) Connors, K. A. *Binding Constants*; John Wiley and Sons: New YorK, 1987.
(6) Eatough, D. J. *Analytical Chemistry* **1970**, *42*, 635-&.
(7) Christen.Jj; Wrathall, D. P.; Izatt, R. M. *Analytical Chemistry* **1968**, *40*, 175-&.
(8) Christen.Jj; Wrathall, D. P.; Oscarson, J. O.; Izatt, R. M. *Analytical Chemistry* **1968**, *40*, 1713-&.
(9) Zielenkiewicz, W.; Marcinowicz, A.; Poznanski, J.; Cherenok, S.; Kalchenko, V. *Journal of Molecular Liquids* **2005**, *121*, 8-14.
(10) Arena, G.; Contino, A.; Fujimoto, T.; Sciotto, D.; Aoyama, Y. *Supramolecular Chemistry* **2000**, *11*, 279-288.
(11) Arena, G.; Casnati, A.; Contino, A.; Lombardo, G. G.; Sciotto, D.; Ungaro, R. *Chemistry-a European Journal* **1999**, *5*, 738-744.
(12) Koenig, K. E.; Helgeson, R. C.; Cram, D. J. *Journal of the American Chemical Society* **1976**, *98*, 4018-4020.
(13) Alpaydin, S.; Yilmaz, M.; Ersoz, M. *Separation Science and Technology* **2004**, *39*, 2189-2206.
(14) Alpoguz, H.; Memon, S.; Ersoz, M.; Yilmaz, M. *Separation Science and Technology* **2005**, *40*, 2365-2372.
(15) Alpoguz, H. K.; Kaya, A.; Yilmaz, A.; Yilmaz, M. *Journal of Macromolecular Science, Pure and Applied Chemistry* **2005**, *A42*, 577-586.
(16) Alpoguz, H. K.; Memon, S.; Ersoz, M.; Yilmaz, M. *Separation Science and Technology* **2002**, *37*, 2201-2213.
(17) Alpoguz, H. K.; Memon, S.; Ersoz, M.; Yilmaz, M. *Separation Science and Technology* **2003**, *38*, 1649-1664.
(18) Korkmaz Alpoguz, H.; Kaya, A.; Memon, S.; Yilmaz, M. *Journal of Macromolecular Science, Part A: Pure and Applied Chemistry* **2005**, *A42*, 1159-1168.
(19) Memon, S.; Akceylan, E.; Sap, B.; Tabakci, M.; Roundhill, D. M.; Yilmaz, M. *Journal of Polymers and the Environment* **2003**, *11*, 67-74.
(20) Bakker, E.; Pretsch, E.; Buhlmann, P. *Analytical Chemistry* **2000**, *72*, 1127-1133.
(21) Cattrall, R. W. *Chemical Sensors*; Oxford University Press: Oxford, 1997.
(22) Bakker, E. *Analytical Chemistry* **1997**, *69*, 1061-1069.
(23) Bakker, E.; Willer, M.; Lerchi, M.; Seiler, K.; Pretsch, E. *Analytical Chemistry* **1994**, *66*, 516-521.
(24) Bakker, E.; Simon, W. *Analytical Chemistry* **1992**, *64*, 1805-1812.
(25) Mi, Y. M.; Bakker, E. *Analytical Chemistry* **1999**, *71*, 5279-5287.
(26) Diamond, D.; Nolan, K. *Analytical Chemistry* **2001**, *73*, 22a-29a.
(27) Diamond, D.; McKervey, M. A. *Chemical Society Reviews* **1996**, *25*, 15-24.
(28) O' Connor, K. M.; Arrigan, D. W. M.; Svehla, G. *Electroanalysis* **1995**, *7*, 205-215.
(29) Bakker, E.; Pretsch, E. *TrAC, Trends in Analytical Chemistry* **2005**, *24*, 199-207.

(30) Bakker, E. *Analytical Chemistry* **2004**, *76*, 3285-3298.
(31) Malon, A.; Radu, A.; Qin, W.; Qin, Y.; Ceresa, A.; Maj-Zurawska, M.; Bakker, E.; Pretsch, E. *Analytical Chemistry* **2003**, *75*, 3865-3871.
(32) Bakker, E.; Pretsch, E. *TrAC, Trends in Analytical Chemistry* **2001**, *20*, 11-19.
(33) deSilva, A. P.; Gunaratne, H. Q. N.; Gunnlaugsson, T.; Huxley, A. J. M.; McCoy, C. P.; Rademacher, J. T.; Rice, T. E. *Chemical Reviews* **1997**, *97*, 1515-1566.
(34) Sauer, M. *Angewandte Chemie, International Edition* **2003**, *42*, 1790-1793.
(35) Wolfbeis, O. S. *Journal of Materials Chemistry* **2005**, *15*, 2657-2669.
(36) Bianchi, A., Kristin Bowman, J., Enrique Garcia, E. *Supramolecular Chemistry of Anions*, 1997.
(37) Fayne, D., Dublin City University, 2001.
(38) Cadogan, A.; Gao, Z. Q.; Lewenstam, A.; Ivaska, A.; Diamond, D. *Analytical Chemistry* **1992**, *64*, 2496-2501.
(39) Szigeti, Z.; Bitter, I.; Toth, K.; Latkoczy, C.; Fliegel, D. J.; Gunther, D.; Pretsch, E. *Analytica Chimica Acta* **2005**, *532*, 129-136.
(40) Bakker, E.; Buhlmann, P.; Pretsch, E. *Chemical Reviews* **1997**, *97*, 3083-3132.
(41) Valiyayeettil, S.; Engbersen, J. F. J.; Verboom, W.; Reinhoudt, D. N. *Angewandte Chemie-International Edition in English* **1993**, *32*, 900-901.
(42) Zeng, Z.; He, Y.; Meng, L. *Huaxue Jinzhan* **2005**, *17*, 254-265.
(43) Wang, Y.; Jin, W. *Huaxue Jinzhan* **2003**, *15*, 178-185.
(44) Epstein, J. R.; Walt, D. R. *Chemical Society Reviews* **2003**, *32*, 203-214.
(45) Fabbrizzi, L.; Licchelli, M.; Parodi, L.; Poggi, A.; Taglietti, A. *Journal of Fluorescence* **1998**, *8*, 263-271.
(46) Bren, V. A. *Russian Chemical Reviews* **2001**, *70*, 1017-1036.
(47) Callan, J. F.; de Silva, A. P.; Magri, D. C. *Tetrahedron* **2005**, *61*, 8551-8588.
(48) Bell, J. W.; Hext, N. M. *Chemical Society Reviews* **2004**, *33*, 589-598.
(49) Beer, P. D.; Gale, P. A. *Angewandte Chemie, International Edition* **2001**, *40*, 486-516.
(50) Gale, P. A. *Coordination Chemistry Reviews* **2000**, *199*, 181-233.
(51) Gale, P. A. *Coordination Chemistry Reviews* **2001**, *213*, 79-128.
(52) Gale, P. A. *Coordination Chemistry Reviews* **2003**, *240*, 191-221.
(53) Hay, B. P.; Firman, T. K.; Moyer, B. A. *Journal of the American Chemical Society* **2005**, *127*, 1810-1819.
(54) Bowman-James, K. *Accounts of Chemical Research* **2005**, *38*, 671-678.
(55) Sessler, J. L.; Sansom, P. I.; Andrievsky, A.; Kral, V. *Supramolecular Chemistry of Anions* **1997**, 355-419.
(56) Beer, P. B.; Gale, P. A.; Smith, K. S. *Supramolecular Chemistry*; Oxford University Press: Oxford, 2003.
(57) Schmidtchen, F. P. *Chemische Berichte-Recueil* **1980**, *113*, 864-874.
(58) Schmidtchen, F. P. *Angewandte Chemie-International Edition in English* **1977**, *16*, 720-721.
(59) Luecke, H.; Quiocho, F. A. *Nature* **1990**, *347*, 402-406.
(60) He, J. J.; Quiocho, F. A. *Science* **1991**, *251*, 1479-1481.
(61) Lee, K. H.; Hong, J. I. *Tetrahedron Letters* **2000**, *41*, 6083-6087.
(62) Turner, D. R.; Pastor, A.; Alajarin, M.; Steed, J. W. *Structure and Bonding (Berlin, Germany)* **2004**, *108*, 97-168.
(63) Lang, K.; Curinova, P.; Dudic, M.; Proskova, P.; Stibor, I.; St'astny, V.; Lhotak, P. *Tetrahedron Letters* **2005**, *46*, 4469-4472.
(64) St'astny, V.; Stibor, I.; Petrickova, H.; Sykora, J.; Lhotak, P. *Tetrahedron* **2005**, *61*, 9990-9995.

(65) Nabeshima, T.; Saiki, T.; Iwabuchi, J.; Akine, S. *Journal of the American Chemical Society* **2005**, *127*, 5507-5511.
(66) Stastny, V.; Lhotak, P.; Michlova, V.; Stibor, I.; Sykora, J. *Tetrahedron* **2002**, *58*, 7207-7211.
(67) Budka, J.; Lhotak, P.; Michlova, V.; Stibor, I. *Tetrahedron Letters* **2001**, *42*, 1583-1586.
(68) Nam, K. C.; Kang, S. O.; Jeong, H. S.; Jeon, S. *Tetrahedron Letters* **1999**, *40*, 7343-7346.
(69) Chrisstoffels, L. A. J.; de Jong, F.; Reinhoudt, D. N.; Sivelli, S.; Gazzola, L.; Casnati, A.; Ungaro, R. *Journal of the American Chemical Society* **1999**, *121*, 10142-10151.
(70) Scheerder, J.; vanDuynhoven, J. P. M.; Engbersen, J. F. J.; Reinhoudt, D. N. *Angewandte Chemie-International Edition in English* **1996**, *35*, 1090-1093.
(71) Scheerder, J.; Engbersen, J. F. J.; Casnati, A.; Ungaro, R.; Reinhoudt, D. N. *Journal of Organic Chemistry* **1995**, *60*, 6448-54.
(72) Scheerder, J.; Fochi, M.; Engbersen, J. F. J.; Reinhoudt, D. N. *Journal of Organic Chemistry* **1994**, *59*, 7815-20.
(73) Pelizzi, N.; Casnati, A.; Friggeri, A.; Ungaro, R. *Journal of the Chemical Society-Perkin Transactions 2* **1998**, 1307-1311.
(74) Lee, H. K.; Oh, H.; Nam, K. C.; Jeon, S. *Sensors and Actuators B-Chemical* **2005**, *106*, 207-211.
(75) Fan, E.; Van Arman, S. A.; Kincaid, S.; Hamilton, A. D. *Journal of the American Chemical Society* **1993**, *115*, 369-70.
(76) Albert, J. S.; Hamilton, A. D. *Tetrahedron Letters* **1993**, *34*, 7363-7366.
(77) Hamann, B. C.; Branda, N. R.; Rebek, J. *Tetrahedron Letters* **1993**, *34*, 6837-6840.
(78) Rebek, J., Jr. *Chemical Communications (Cambridge)* **2000**, 637-643.
(79) Cho, Y. L.; Rudkevich, D. M.; Shivanyuk, A.; Rissanen, K.; Rebek, J., Jr. *Chemistry--A European Journal* **2000**, *6*, 3788-3796.
(80) Mogck, O.; Bohmer, V.; Vogt, W. *Tetrahedron* **1996**, *52*, 8489-8496.
(81) Gutsche, C. D. *Calixarenes*; The Royal Society of Chemistry: Cambridge, London, 1989.
(82) Ludwig, R.; Dzung, N. T. K. *Sensors* **2002**, *2*, 397-416.
(83) Ikeda, A.; Shinkai, S. *Chemical Reviews (Washington, D. C.)* **1997**, *97*, 1713-1734.
(84) Arnaud-Neu, F.; Schwing-Weill, M. J. *Synthetic Metals* **1997**, *90*, 157-164.
(85) Bohmer, V. *Angewandte Chemie-International Edition in English* **1995**, *34*, 713-745.
(86) Gutsche, C. D. *Calixarenes Revisited*; The Royal Society of Chemistry: Cambridge, London, 1998.
(87) Mandolini, L.; Ungaro, R.; Editors *Calixarenes in Action*, 2000.
(88) Zinke, A.; Kretz, R.; Leggewie, E.; Hossinger, K. *Monatshefte Fur Chemie* **1952**, *83*, 1213-1227.
(89) Dhawan, B.; Gutsche, C. D. *Journal of Organic Chemistry* **1983**, *48*, 1536-1539.
(90) Gutsche, C. D.; Dhawan, B.; Levine, J. A.; No, K. H.; Bauer, L. J. *Tetrahedron* **1983**, *39*, 409-426.
(91) Gutsche, C. D.; Dhawan, B.; No, K. H.; Muthukrishnan, R. *Journal of the American Chemical Society* **1981**, *103*, 3782-3792.
(92) Helgeson, R. C.; Mazaleyrat, J. P.; Cram, D. J. *Journal of the American Chemical Society* **1981**, *103*, 3929-3931.

(93) Moran, J. R.; Karbach, S.; Cram, D. J. *Journal of the American Chemical Society* **1982**, *104*, 5826-5828.
(94) Rizzoli, C.; Andreetti, G. D.; Ungaro, R.; Pochini, A. *Journal of Molecular Structure* **1982**, *82*, 133-141.
(95) McKervey, M. A.; Seward, E. M.; Ferguson, G.; Ruhl, B. L. *Journal of Organic Chemistry* **1986**, *51*, 3581-3584.
(96) Kammerer, H.; Happel, G.; Mathiasch, B. *Makromolekulare Chemie-Macromolecular Chemistry and Physics* **1981**, *182*, 1685-1694.
(97) Cornfort.Jw; Morgan, E. D.; Potts, K. T.; Rees, R. J. W. *Tetrahedron* **1973**, *29*, 1659-1667.
(98) Iwamoto, K.; Araki, K.; Shinkai, S. *Tetrahedron* **1991**, *47*, 4325-4342.
(99) McMahon, G.; Wall, R.; Nolan, K.; Diamond, D. *Talanta* **2002**, *57*, 1119-1132.
(100) Lynch, A.; Eckhard, K.; McMahon, G.; Wall, R.; Kane, P.; Nolan, K.; Schuhmann, W.; Diamond, D. *Electroanalysis* **2002**, *14*, 1397-1404.
(101) Cadogan, A. M.; Diamond, D.; Smyth, M. R.; Deasy, M.; Mckervey, M. A.; Harris, S. J. *Analyst* **1989**, *114*, 1551-1554.
(102) McKittrick, T.; Diamond, D.; Marrs, D. J.; OHagan, P.; McKervey, M. A. *Talanta* **1996**, *43*, 1145-1148.
(103) Cadogan, F.; Kane, P.; McKervey, M. A.; Diamond, D. *Analytical Chemistry* **1999**, *71*, 5544-5550.
(104) Grady, T.; Maskula, S.; Diamond, D.; Marrs, D. J.; McKervey, M. A.; O'Hagan, P. *Analytical Proceedings* **1995**, *32*, 471-473.
(105) McCarrick, M.; Wu, B.; Harris, S. J.; Diamond, D.; Barrett, G.; McKervey, M. A. *Journal of the Chemical Society-Perkin Transactions 2* **1993**, 1963-1968.
(106) Grady, T.; Harris, S. J.; Smyth, M. R.; Diamond, D.; Hailey, P. *Analytical Chemistry* **1996**, *68*, 3775-3782.
(107) Lynam, C.; Diamond, D. *Journal of Materials Chemistry* **2005**, *15*, 307-314.
(108) Kammerer, H.; Happel, G.; Bohmer, V.; Rathay, D. *Monatshefte Fur Chemie* **1978**, *109*, 767-773.
(109) Gutsche, C. D.; Levine, J. A.; Sujeeth, P. K. *Journal of Organic Chemistry* **1985**, *50*, 5802-5806.
(110) Gutsche, C. D.; Lin, L. G. *Tetrahedron* **1986**, *42*, 1633-1640.
(111) Harris, S. J.; Woods, J. G.; Rooney, J. M.; U.S. Patent 4642362 Loctite, Ireland, Ltd.: Ireland, 1987.
(112) Izatt, R. M.; Lamb, J. D.; Hawkins, R. T.; Brown, P. R.; Izatt, S. R.; Christensen, J. J. *Journal of the American Chemical Society* **1983**, *105*, 1782-1785.
(113) Izatt, S. R.; Hawkins, R. T.; Christensen, J. J.; Izatt, R. M. *Journal of the American Chemical Society* **1985**, *107*, 63-66.
(114) McKervey, M. A.; Seward, E. M.; Ferguson, G.; Ruhl, B.; Harris, S. J. *Journal of the Chemical Society-Chemical Communications* **1985**, 388-390.
(115) Chang, S. K.; Cho, I. *Chemistry Letters* **1984**, 477-478.
(116) Chang, S. K.; Kwon, S. K.; Cho, I. *Chemistry Letters* **1987**, 947-948.
(117) Kimura, K.; Shono, T. *Cation Binding by Macrocycles*; Dekker: New York, 1990.
(118) Diamond, D. *Electrochemistry, Sensors and Analysis*; Elsevier: Amsterdam, 1986.
(119) Kane, P.; Kincaid, K.; Fayne, D.; Diamond, D.; McKervey, M. A. *Journal of Molecular Modeling* **2000**, *6*, 272-281.
(120) Bell, S. E. J.; McKervey, M. A.; Fayne, D.; Kane, P.; Diamond, D. *Journal of Molecular Modeling* **1998**, *4*, 44-52.

(121) Brunink, J. A. J.; Haak, J. R.; Bomer, J. G.; Reinhoudt, D. N.; McKervey, M. A.; Harris, S. J. *Analytica Chimica Acta* **1991**, *254*, 75-80.
(122) Bakker, E.; Buhlmann, P.; Pretsch, E. *Electroanalysis* **1999**, *11*, 1088-1088.
(123) O'Connor, K. M.; Cherry, M.; Svehla, G.; Harris, S. J.; McKervey, M. A. *Talanta* **1994**, *41*, 1207-1217.
(124) Cunningham, K.; Svehla, G.; Harris, S. J.; McKervey, M. A. *Analyst* **1993**, *118*, 341-345.
(125) Brunink, J. A. J.; Bomer, J. G.; Engbersen, J. F. J.; Verboom, W.; Reinhoudt, D. N. *Sensors and Actuators B-Chemical* **1993**, *15*, 195-198.
(126) Kimura, K.; Miura, T.; Matsuo, M.; Shono, T. *Analytical Chemistry* **1990**, *62*, 1510-1513.
(127) Kimura, K.; Matsuo, M.; Shono, T. *Chemistry Letters* **1988**, 615-616.
(128) Arnaudneu, F.; Schwingweill, M. J.; Ziat, K.; Cremin, S.; Harris, S. J.; McKervey, M. A. *New Journal of Chemistry* **1991**, *15*, 33-37.
(129) Bondy, C. R.; Loeb, S. J. *Coordination Chemistry Reviews* **2003**, *240*, 77-99.
(130) Liu, S. Y.; He, Y. B.; Wu, J. L.; Wei, L. H.; Qin, H. J.; Meng, L. Z.; Hu, L. *Organic & Biomolecular Chemistry* **2004**, *2*, 1582-1586.
(131) Casnatia, A.; Bonetti, F.; Sansone, F.; Ugozzoli, F.; Ungaro, R. *Collection of Czechoslovak Chemical Communications* **2004**, *69*, 1063-1079.
(132) Miao, R.; Zheng, Q. Y.; Chen, C. F.; Huang, Z. T. *Tetrahedron Letters* **2005**, *46*, 2155-2158.
(133) Chen, D. H.; Sun, H. W.; Chen, L.; Shen, R. X.; Yuan, J.; Chen, P. Q.; Yuan, M. X.; Lai, C. M. *Chemical Journal of Chinese Universities-Chinese* **2006**, *27*, 153-155.
(134) Cameron, B. R.; Loeb, S. J. *Chemical Communications* **1997**, 573-574.
(135) Casnati, A.; Massera, C.; Pelizzi, N.; Stibor, I.; Pinkassik, E.; Ugozzoli, F.; Ungaro, R. *Tetrahedron Letters* **2002**, *43*, 7311-7314.
(136) Tomapatanaget, B.; Tuntulani, T.; Chailapakul, O. *Organic Letters* **2003**, *5*, 1539-1542.
(137) Liu, S. Y.; Wang, F. J.; Wei, L. H.; Xiao, W.; Meng, L. Z.; He, Y. B. *Science in China Series B-Chemistry* **2004**, *47*, 145-151.
(138) Ben Sdira, S.; Felix, C.; Giudicelli, M. B.; Vocanson, F.; Perrin, M.; Lamartine, R. *Tetrahedron Letters* **2005**, *46*, 5659-5663.
(139) Zhao, B. T.; Blesa, M. J.; Mercier, N.; Le Derf, F.; Salle, M. *New Journal of Chemistry* **2005**, *29*, 1164-1167.
(140) Lee, S. H.; Kim, S. H.; Kim, S. K.; Jung, J. H.; Kim, J. S. *Journal of Organic Chemistry* **2005**, *70*, 9288-9295.
(141) Lee, J. Y.; Kim, S. K.; Jung, J. H.; Kim, J. S. *Journal of Organic Chemistry* **2005**, *70*, 1463-1466.
(142) Liu, S. Y.; Xu, K. X.; He, Y. B.; Qin, H. J.; Meng, L. Z. *Chinese Journal of Chemistry* **2005**, *23*, 321-325.
(143) Tomapatanaget, B.; Tuntulani, T. *Tetrahedron Letters* **2001**, *42*, 8105-8109.
(144) Lynam, C., Dublin City University, 2002.
(145) Emsley, J. *Nature's Building Blocks*; Oxford University Press: Oxford, 2003.
(146) Xiao, K. P.; Buhlmann, P.; Nishizawa, S.; Amemiya, S.; Umezawa, Y. *Analytical Chemistry* **1997**, *69*, 1038-1044.
(147) Berrocal, M. J.; Cruz, A.; Badr, I. H. A.; Bachas, L. G. *Analytical Chemistry* **2000**, *72*, 5295-5299.
(148) Jeon, S. W.; Yeo, H. Y.; Jeong, H. S.; Oh, J. M.; Nam, K. C. *Electroanalysis* **2003**, *15*, 872-877.

(149) Garcia, M. M. R.; Verboom, W.; Reinhoudt, D. N.; Malinowska, E.; Pietrzak, M.; Wojciechowska, D. *Tetrahedron* **2004**, *60*, 11299-11306.
(150) Scheerder, J.; Fochi, M.; Engbersen, J. F. J.; Reinhoudt, D. N. *Journal of Organic Chemistry* **1994**, *59*, 7815-7820.
(151) Wegmann, D.; Weiss, H.; Ammann, D.; Morf, W. E.; Pretsch, E.; Sugahara, K.; Simon, W. *Mikrochimica Acta* **1984**, *3*, 1-16.
(152) Campanella, L.; Colapicchioni, C.; Crescentini, G.; Sammartino, M. P.; Su, Y.; Tomassetti, M. *Sensors and Actuators B-Chemical* **1995**, *27*, 329-335.
(153) Lau, K.-T.; Yerazunis, W. S.; Shepherd, R. L.; Diamond, D. *Sensors and Actuators B: Chemical, In Press, Corrected Proof.*
(154) Lau, K.-T.; Baldwin, S.; O'Toole, M.; Shepherd, R.; Yerazunis, W. J.; Izuo, S.; Ueyama, S.; Diamond, D. *Analytica Chimica Acta*
*Papers presented at the 2nd International Symposium on the Separation and Characterization of Natural and Synthetic Macromolecules - SCM-2 2005* **2006**, *557*, 111-116.
(155) O' Toole, M.; Lau, K. T.; Diamond, D. *Talanta* **2005**, *66*, 1340-1344.
(156) Cho, E. J.; Moon, J. W.; Ko, S. W.; Lee, J. Y.; Kim, S. K.; Yoon, J.; Nam, K. C. *Journal of the American Chemical Society* **2003**, *125*, 12376-12377.
(157) Ren, J.; Wang, Q.; Qu, D.; Zhao, X.; He, T. *Chemistry Letters* **2004**, *33*, 974-975.
(158) Xie, H.; Yi, S.; Yang, X.; Wu, S. *New Journal of Chemistry* **1999**, *23*, 1105-1110.
(159) Esteban-Gomez, D.; Fabbrizzi, L.; Licchelli, M.; Sacchi, D. *Journal of Materials Chemistry* **2005**, *15*, 2670-2675.
(160) Gunnlaugsson, T.; Ali, H. D. P.; Glynn, M.; Kruger, P. E.; Hussey, G. M.; Pfeffer, F. M.; Santos, C. M. G.; Tierney, J. *Journal of Fluorescence* **2005**, *15*, 287-299.
(161) Kim, S. K.; Singh, N. J.; Kim, S. J.; Swamy, K. M. K.; Kim, S. H.; Lee, K.-H.; Kim, K. S.; Yoon, J. *Tetrahedron* **2005**, *61*, 4545-4550.
(162) Gunnlaugsson, T.; Davis, A. P.; O'Brien, J. E.; Glynn, M. *Organic & Biomolecular Chemistry* **2005**, *3*, 48-56.
(163) Przygorzewska, J.; Rakoczy, P.; Rokicki, G. *Wiadomosci Chemiczne* **2003**, *57*, 43-62.
(164) Desilva, A. P.; Desilva, S. A. *Journal of the Chemical Society-Chemical Communications* **1986**, 1709-1710.
(165) Valeur, B.; Pouget, J.; Bourson, J.; Kaschke, M.; Ernsting, N. P. *Journal of Physical Chemistry* **1992**, *96*, 6545-6549.
(166) Descalzo, A. B.; Martinez-Manez, R.; Radeglia, R.; Rurack, K.; Soto, J. *Journal of the American Chemical Society* **2003**, *125*, 3418-3419.
(167) Rettig, W.; Rurack, K.; Sczepan, M.; Brochon, J. C.; Valeur, B. *New Trends in Fluorescence Spectroscopy: Applications to Chemical and Life Sciences*; Springer: Berlin, 2001.
(168) Kirkbright, G. F.; Bishop, E. *Indicators*; Pergamon: Oxford, 1972.
(169) Winnik, M. A. *Chemical Reviews* **1981**, *81*, 491-524.
(170) Forster, T.; Kasper, K. *Zeitschrift Fur Elektrochemie* **1955**, *59*, 976-980.
(171) Birks, J. B. *Reports on Progress in Physics* **1975**, *38*, 903-74.
(172) Ebata, K.; Masuko, M.; Ohtani, H.; Kashiwasakejibu, M. *Photochemistry and Photobiology* **1995**, *62*, 836-839.
(173) Lee, S. H.; Kim, J. Y.; Kim, S. K.; Lee, J. H.; Kim, J. S. *Tetrahedron* **2004**, *60*, 5171-5176.
(174) Jin, T. *Chemical Communications* **1999**, 2491-2492.

(175) Jin, T.; Ichikawa, K.; Koyama, T. *Journal of the Chemical Society-Chemical Communications* **1992**, 499-501.
(176) Kim, J. S.; Shon, O. J.; Rim, J. A.; Kim, S. K.; Yoon, J. *Journal of Organic Chemistry* **2002**, *67*, 2348-2351.
(177) Kim, S. K.; Lee, S. H.; Lee, J. Y.; Lee, J. Y.; Bartsch, R. A.; Kim, J. S. *Journal of the American Chemical Society* **2004**, *126*, 16499-16506.
(178) Saudan, C.; Ceroni, P.; Vicinelli, V.; Maestri, M.; Balzani, V.; Gorka, M.; Lee, S. K.; van Heyst, J.; Vogtle, F. *Dalton Transactions* **2004**, 1597-1600.
(179) Jin, T.; Monde, K. *Chemical Communications* **1998**, 1357-1358.
(180) Kim, S. K.; Kim, S. H.; Kim, H. J.; Lee, S. H.; Lee, S. W.; Ko, J.; Bartsch, R. A.; Kim, J. S. *Inorganic Chemistry* **2005**, *44*, 7866-7875.
(181) Gorbunova, M. G.; Brown, G. M.; Goretzki, G.; Custelcean, R.; Bonnesen, P. V.; Dabestani, R. *Abstracts of Papers, 230th ACS National Meeting, Washington, DC, United States, Aug. 28-Sept. 1, 2005* **2005**, ORGN-014.
(182) Talanova, G. G.; Vedernikova, E. Y.; Staunton, E. A.; Talanov, V. S. *Abstracts of Papers, 230th ACS National Meeting, Washington, DC, United States, Aug. 28-Sept. 1, 2005* **2005**, INOR-110.
(183) Suzuki, Y.; Morozumi, T.; Nakamura, H.; Shimomura, M.; Hayashita, T.; Bartsh, R. A. *Journal of Physical Chemistry B* **1998**, *102*, 7910-7917.
(184) Kim, S. K.; Bok, J. H.; Bartsch, R. A.; Lee, J. Y.; Kim, J. S. *Organic Letters* **2005**, *7*, 4839-4842.
(185) Liao, J. H.; Chen, C. T.; Fang, J. M. *Organic Letters* **2002**, *4*, 561-564.
(186) Lee, J. E.; Kim, J. H.; Choi, S. J.; Han, T. H.; Uhm, D. Y.; Kim, S. J. *Pflugers Archiv-European Journal of Physiology* **2002**, *444*, 619-626.
(187) Sasaki, S.-i.; Citterio, D.; Ozawa, S.; Suzuki, K. *Journal of the Chemical Society, Perkin Transactions 2* **2001**, 2309-2313.
(188) Werner, F.; Schneider, H. J. *Helvetica Chimica Acta* **2000**, *83*, 465-478.
(189) Schazmann, B.; McMahon, G.; Nolan, K.; Diamond, D. *Supramolecular Chemistry* **2005**, *17*, 393-399.
(190) Winnik, F. M. *Chemical Reviews* **1993**, *93*, 587-614.
(191) Yang, J. S.; Lin, C. S.; Hwang, C. Y. *Organic Letters* **2001**, *3*, 889-892.
(192) Lakowicz, J. R. *Topics in Fluorescence Spectroscopy*; Plenum Press: New York, 1994; Vol. 4.
(193) Wolfbeis, O. S. *Analytical Chemistry* **2000**, *72*, 81r-89r.
(194) Wolfbeis, O. S. *Analytical Chemistry* **2002**, *74*, 2663-2677.
(195) Wolfbeis, O. S. *Analytical Chemistry* **2004**, *76*, 3269-3283.
(196) Dasgupta, P. K.; Eom, I.-Y.; Morris, K. J.; Li, J. *Analytica Chimica Acta* **2003**, *500*, 337-364.
(197) Duxbury, A. C.; Duxbury, A. B. *An introduction to the world's oceans*; fifth ed.; WCB Publishers: London, 1997.
(198) Gutsche, C. D.; Levine, J. A. *Journal of the American Chemical Society* **1982**, *104*, 2652-2653.
(199) Kammerer, H.; Happel, G.; Bohmer, V.; Rathay, D. *Monatshefte Fur Chemie* **1978**, *109*, 767-773.
(200) Pearson, R. G. *Chemical hardness*; Wiley-VCH, 1997.
(201) Michelin, R. A.; Mozzon, M.; Bertani, R. *Coordination Chemistry Reviews* **1996**, *147*, 299-338.
(202) Solomos, T. W. G. *Organic Chemistry*; Wiley and Sons: New York, 1992.
(203) Kukushkin, V. Y.; Pombeiro, A. J. L. *Chemical Reviews* **2002**, *102*, 1771-1802.

(204) Yordanov, A. T.; Roundhill, D. M. *New Journal of Chemistry* **1996**, *20*, 447-451.
(205) Sliwa, W. *Journal of Inclusion Phenomena and Macrocyclic Chemistry* **2005**, *52*, 13-37.
(206) Sliwa, W. *Croatica Chemica Acta* **2002**, *75*, 131-153.
(207) Yilmaz, A.; Memon, S.; Yilmaz, M. *Organic Preparations and Procedures International* **2002**, *34*, 417-424.
(208) Memon, S.; Yilmaz, M. *Separation Science and Technology* **2001**, *36*, 473-486.
(209) Uysal, G.; Memon, S.; Yilmaz, M. *Reactive & Functional Polymers* **2001**, *50*, 77-84.
(210) Wall, R., PhD Thesis, Dublin City University, 2003.
(211) Mahajan, R. K.; Kaur, R.; Kaur, I.; Sharma, V.; Kumar, M. *Analytical Sciences* **2004**, *20*, 811-814.
(212) Bagheri, M.; Mashhadizadeh, M. H.; Razee, S.; Momeni, A. *Electroanalysis* **2003**, *15*, 1824-1829.
(213) Fakhari, A. R.; Ganjali, M. R.; Shamsipur, M. *Analytical Chemistry* **1997**, *69*, 3693-3696.
(214) Lue, J.-Q.; Zeng, X.-S.; Ai, J.; Pang, D.-W. *Gaodeng Xuexiao Huaxue Xuebao* **2005**, *26*, 238-240.
(215) Singh, L. P.; Bhatnagar, J. M. *Journal of Applied Electrochemistry* **2004**, *34*, 391-396.
(216) Ruzicka, J.; Tjell, J. C. *Analytica Chimica Acta* **1970**, *51*, 1-&.
(217) Baiulescu, G. E.; Ciocan, N. *Talanta* **1977**, *24*, 37-42.
(218) Baiulescu, G. E.; Cosofret, V. V. *Talanta* **1976**, *23*, 677-678.
(219) Kim, J. H.; Hwang, A.-R.; Chang, S.-K. *Tetrahedron Letters* **2004**, *45*, 7557-7561.
(220) Martinez, R.; Espinosa, A.; Tarraga, A.; Molina, P. *Organic Letters*, ACS ASAP.
(221) Cha, N. R.; Kim, M. Y.; Kim, Y. H.; Choe, J.-I.; Chang, S.-K. *Journal of the Chemical Society, Perkin Transactions 2* **2002**, 1193-1196.
(222) Choi, M. J.; Kim, M. Y.; Chang, S.-K. *Chemical Communications (Cambridge, United Kingdom)* **2001**, 1664-1665.
(223) Kim, Y.-H.; Youk, J. S.; Moon, S. Y.; Choe, J.-I.; Chang, S.-K. *Chemistry Letters* **2004**, *33*, 702-703.
(224) Moon, S. Y.; Cha, N. R.; Kim, Y. H.; Chang, S.-K. *Journal of Organic Chemistry* **2004**, *69*, 181-183.
(225) Moon, S.-Y.; Youn, N. J.; Park, S. M.; Chang, S.-K. *Journal of Organic Chemistry* **2005**, *70*, 2394-2397.
(226) Prodi, L.; Bargossi, C.; Montalti, M.; Zaccheroni, N.; Su, N.; Bradshaw, J. S.; Izatt, R. M.; Savage, P. B. *Journal of the American Chemical Society* **2000**, *122*, 6769-6770.
(227) Youk, J.-S.; Kim, Y. H.; Kim, E.-J.; Youn, N. J.; Chang, S.-K. *Bulletin of the Korean Chemical Society* **2004**, *25*, 869-872.
(228) Youn, N. J.; Chang, S.-K. *Tetrahedron Letters* **2004**, *46*, 125-129.
(229) Youn, N. J.; Kim, J. S.; Song, K. C.; Kim, S. H.; Ahn, S.; Chang, S.-K. *Bulletin of the Korean Chemical Society* **2005**, *26*, 849-851.
(230) Sevdic, D.; Meider, H. *Journal of Inorganic & Nuclear Chemistry* **1981**, *43*, 153-157.
(231) Sevdic, D.; Fekete, L.; Meider, H. *Journal of Inorganic & Nuclear Chemistry* **1980**, *42*, 885-889.

(232) Sevdic, D.; Meider, H. *Journal of Inorganic & Nuclear Chemistry* **1977**, *39*, 1403-1407.
(233) Sevdic, D.; Meider, H. *Journal of Inorganic & Nuclear Chemistry* **1977**, *39*, 1409-1413.
(234) Danil de Namor, A. F.; Chahine, S.; Castellano, E. E.; Piro, O. E. *Journal of Physical Chemistry B* **2004**, *108*, 11384-11392.
(235) Kwon, J. Y.; Soh, J. H.; Yoon, Y. J.; Yoon, J. *Supramolecular Chemistry* **2004**, *16*, 621-624.
(236) Lu, J.-q.; Lu, J.-l.; Zhou, X.-w.; He, X.-w. *Fenxi Kexue Xuebao* **2003**, *19*, 30-32.
(237) Bhalla, V.; Kumar, M.; Katagiri, H.; Hattori, T.; Miyano, S. *Tetrahedron Letters* **2004**, *46*, 121-124.
(238) Mahajan, R. K.; Kaur, I.; Kaur, R.; Bhalla, V.; Kumar, M. *Bulletin of the Chemical Society of Japan* **2005**, *78*, 1635-1640.
(239) Mahajan, R. K.; Kaur, I.; Kumar, M. *Sensors and Actuators, B: Chemical* **2003**, *B91*, 26-31.
(240) Singh, N.; Kumar, M.; Hundal, G. *Tetrahedron* **2004**, *60*, 5393-5405.
(241) Zeng, X.; Weng, L.; Chen, L.; Leng, X.; Ju, H.; He, X.; Zhang, Z.-Z. *Journal of the Chemical Society, Perkin Transactions 2* **2001**, 545-549.
(242) Shriver, D. F.; Atkins, P. W.; Langford, C. H. *Inorganic Chemistry*; Second Edition ed.; Oxford University Press: Oxford, 1994.
(243) Mislin, G.; Graf, E.; Hosseini, M. W.; De Cian, A.; Kyritsakas, N.; Fischer, J. *Chemical Communications (Cambridge)* **1998**, 2545-2546.
(244) Sevdic, D.; Jovanovac, L.; Meider-Gorican, H. *Mikrochimica Acta* **1975**, *2*, 235-242.
(245) Nagele, M.; Mi, Y. M.; Bakker, E.; Pretsch, E. *Analytical Chemistry* **1998**, *70*, 1686-1691.
(246) Buhlmann, P.; Amemiya, S.; Yajima, S.; Umezawa, Y. *Analytical Chemistry* **1998**, *70*, 4291-4303.
(247) Shannon, R. D. *Acta Crystallographica Section A* **1976**, *32*, 751-767.
(248) Atkins, P. W. *Physical Chemistry*; Fifth ed.; Oxford University Press: Oxford, 1994.
(249) O'Malley, S., Dublin City University, 2006.
(250) Bidlingmeyer, B. A. *Practical HPLC Methodology and Applications*; John Wiley and Sons, INC.: New York, 1992.
(251) Scott, R. P. W. *Liquid Chromatography Column Theory*; John Wiley and Sons: Chichester, 1992.
(252) Woodward, R. B. *Pure and Applied Chemistry.* **1973**, *33*.
(253) Ahuja, S. *Chromatography and Separation Science*; Elsevier Science: San Diego, 2003.
(254) Pirkle, W. H.; Anderson, R. W. *Journal of Organic Chemistry* **1974**, *39*, 3901-3903.
(255) Kuhler, T. C.; Lindsten, G. R. *Journal of Organic Chemistry* **1983**, *48*, 3589-3591.
(256) Rodriguez, I.; Li, S. F. Y.; Graham, B. F.; Trengove, R. D. *Journal of Liquid Chromatography & Related Technologies* **1997**, *20*, 1197-1209.
(257) Zetta, L.; Wolff, A.; Vogt, W.; Platt, K. L.; Bohmer, V. *Tetrahedron* **1991**, *47*, 1911-1924.
(258) Knox, J. H.; Pyper, H. M. *Journal of Chromatography* **1986**, *363*, 1-30.
(259) Poole, C. F., Shuette, S. A. *Contemporary Practice of Chromatography*; Elsevier Science Publishers: New York, 1984.